

Homological mirror symmetry for the genus 2 curve in an abelian variety and its
generalized Strominger-Yau-Zaslow mirror

by

Catherine Kendall Asaro Cannizzo

A dissertation submitted in partial satisfaction of the

requirements for the degree of

Doctor of Philosophy

in

Mathematics

in the

Graduate Division

of the

University of California, Berkeley

Committee in charge:

Professor Denis Auroux, Chair

Professor David Nadler

Professor Marjorie Shapiro

Spring 2019

Homological mirror symmetry for the genus 2 curve in an abelian variety and its
generalized Strominger-Yau-Zaslow mirror

Copyright 2019
by
Catherine Kendall Asaro Cannizzo

Abstract

Homological mirror symmetry for the genus 2 curve in an abelian variety and its
generalized Strominger-Yau-Zaslow mirror

by

Catherine Kendall Asaro Cannizzo

Doctor of Philosophy in Mathematics

University of California, Berkeley

Professor Denis Auroux, Chair

Motivated by observations in physics, mirror symmetry is the concept that certain manifolds come in pairs X and Y such that the complex geometry on X mirrors the symplectic geometry on Y . It allows one to deduce symplectic information about Y from known complex properties of X . Strominger-Yau-Zaslow [SYZ96] described how such pairs arise geometrically as torus fibrations with the same base and related fibers, known as SYZ mirror symmetry. Kontsevich [Kon95] conjectured that a complex invariant on X (the bounded derived category of coherent sheaves) should be equivalent to a symplectic invariant of Y (the Fukaya category, see [Aur14], [FOOO09a], [MTFJ19], [cfFc]). This is known as homological mirror symmetry. In this project, we first use the construction of “generalized SYZ mirrors” for hypersurfaces in toric varieties following Abouzaid-Auroux-Katzarkov [AAK16], in order to obtain X and Y as manifolds. The complex manifold is the genus 2 curve Σ_2 (so of general type $c_1 < 0$) as a hypersurface in its Jacobian torus. Its generalized SYZ mirror is a Landau-Ginzburg model (Y, v_0) equipped with a holomorphic function $v_0 : Y \rightarrow \mathbb{C}$ which we put the structure of a symplectic fibration on. We then describe an embedding of a full subcategory of $D^b Coh(\Sigma_2)$ into a cohomological Fukaya-Seidel category of Y as a symplectic fibration. While our fibration is one of the first nonexact, non-Lefschetz fibrations to be equipped with a Fukaya category, the main geometric idea in defining it is the same as in Seidel’s construction for Fukaya categories of Lefschetz fibrations in [Sei08] and in Abouzaid-Seidel [AS].

I dedicate my thesis to my father, John Kendall Cannizzo, with all my love.

Thank you for being the sunlight in my life. May you rest in peace.

Contents

Contents	ii
List of Figures	iv
1 Introduction, background, and set-up	1
1.1 Statement of thesis result and approach	1
1.2 The B-side manifold	3
1.3 Background on toric varieties	14
1.4 The A-side manifold	25
1.5 The definition of the symplectic form	40
2 The symplectic form ω is nondegenerate	47
2.1 Putting bounds on the bump function derivatives	47
2.2 Converting to polar coordinates	50
2.3 Showing ω nondegenerate: \mathbb{C}^3 patch	52
2.4 Showing ω nondegenerate: away from \mathbb{C}^3 patch	69
3 HMS for V and V^\vee abelian varieties	72
3.1 The Fukaya category $Fuk(V^\vee)$	72
3.2 The bounded derived category $D^bCoh(V)$	74
3.3 Towards HMS: fully-faithful embedding $D_{\mathcal{L}}^bCoh(V) \hookrightarrow H^*Fuk(V^\vee)$	76
4 The Fukaya category	84
4.1 The Fukaya-Seidel category of Y : introduction	84
4.2 Monodromy	85
4.3 Background for defining $H^0(FS(Y, v_0))$	97
4.4 Moduli spaces needed to define $H^0(FS(Y, v_0))$	99
4.5 $H^0(FS(Y, v_0))$: definition and independence of choices	113
5 The main theorem	117
5.1 HMS computation	117
5.2 Proof: fully-faithful embedding $D^bCoh_{\mathcal{L}}(H) \hookrightarrow H^0(FS(Y, v_0))$	138

6 Notation	140
Bibliography	142

List of Figures

1.1	Quotient by Γ_B	11
1.2	Moment map gives Lagrangian torus fibration: \mathbb{CP}^2 example	24
1.3	The (0,0) tile delimited by the tropical curve	28
1.4	$\text{Trop}(1 + x_1 + x_2) = 0$	29
1.5	Moment polytope $\subset \mathbb{R}^3$	29
1.6	Moment polytope for central fiber of (Y, v_0) when $H = \Sigma_2$	30
1.7	In one dimension lower, the boundary of $\Delta_{\tilde{Y}}$ is the moment map image of a string of \mathbb{P}^1 's. In the polytope, $ v_0 $ increases in the $(0, 1)$ direction. In the fibration v_0 , $ v_0 $ is the radius of the circle in the base.	31
1.8	Depiction of 3D $\Delta_{\tilde{Y}}$. Coordinates respect Γ_B -action, see below; magenta parallelogram = fundamental domain. Vertices = \mathbb{C}^3 charts. Coordinate transitions, see Lemma 1.4.10. Expressions in the center of tiles indicate e.g. $\eta \geq \varphi(\xi) = -\xi_1 - 1$ over that tile, so $\text{tile}_{(0,0)}$ is given by $(\xi_1, \xi_2) \in \{(\xi_1, \xi_2) \mid -1 \leq \xi_1, \xi_2, -\xi_1 + \xi_2 \leq 1\}$	32
1.9	Delineate regions in $\Delta_{\tilde{Y}}$ around a vertex	38
1.10	Zoom in on region I/II in left/right figures respectively	39
1.11	Interpolate between three potentials: $F = \alpha_1 g_{xy} + \alpha_2 g_{xz} + (1 - \alpha_1 - \alpha_2) g_{yz}$, $0 \leq \alpha_1, \alpha_2 \leq 1$. Region VII is where $\alpha_1 = \alpha_2 = 1/3$ and $F = \frac{1}{3}(g_{xy} + g_{xz} + g_{yz}) \approx \frac{2}{3}((Tr_x)^2 + (Tr_y)^2 + (Tr_z)^2)$ via the log approximation.	41
1.12	How the three angular directions vary	44
2.1	L) Number of potentials interpolated between. R) Zoomed in region about vertex.	52
2.2	The three angular directions	57
3.1	A triangle in the elliptic curve case and representative of the T^4 case	79
4.1	Monodromy in fiber, thought of as a section over the parallelogram $(\xi_1, \xi_2) \mapsto (\theta_1(\xi_1, \xi_2), \theta_2(\xi_1, \xi_2))$	87
4.2	Example of strip-like end	98
4.3	Flow chart for working with moduli spaces in Fukaya categories	101
4.4	L_i = parallel transport ℓ_i around U-shaped curves in base of v_0	114
5.1	Leibniz rule	119
5.2	Diagram illustrating Leibniz rule	119

5.3	Simplified diagram on fibers	120
5.4	The homotopy between ∂ (left) and the count of discs we compute (right)	121
5.5	Plan for computation	122
5.6	Gromov-Witten theory background for mirror symmetry of toric varieties	132

Acknowledgments

This work was partially supported by NSF grants DMS-1264662, DMS-1406274, and DMS-1702049, and by a Simons Foundation grant (# 385573, Simons Collaboration on Homological Mirror Symmetry). I would like to thank my advisor Denis Auroux for the immeasurable academic support and guidance on this thesis project. I would also like to thank Mohammed Abouzaid, Melissa Liu, Katrin Wehrheim, Sheel Ganatra, Heather Lee, Haniya Azam, Roberta Guadagni, Jingyu Zhao, Sara Venkatesh, Wolfgang Schmaltz, Zhengyi Zhou, and Benjamin Filippenko for fruitful mathematical discussions. I thank Jo Nelson, Ailsa Keating, Bahar Acu, Ziva Myer, Yu Pan, Morgan Weiler, and Anastasia Chavez for invaluable advice and support during the application process and in my career trajectory. I also thank the Noetherian Ring and UC Berkeley math department staff. Lastly, I would like to thank my parents for their constant support and being the best role models.

Chapter 1

Introduction, background, and set-up

1.1 Statement of thesis result and approach

In this work, the pronoun “we” is used to denote the author along with the reader.

Theorem 1.1.1 ([Can19]). *Let $\iota : H := \Sigma_2 \hookrightarrow V$ be a genus 2 curve embedded into an abelian variety V of complex dimension 2. It has a mirror (Y, v_0) with symplectic fibration $v_0 : Y \rightarrow \mathbb{C}$ and generic fiber also an abelian variety of complex dimension 2 denoted V^\vee , the mirror to V . Then we have the following commutative diagram, where $D_{\mathcal{L}}^b \text{Coh}$ denotes the full subcategory of $D^b \text{Coh}$ given by objects $\{\mathcal{L}^i[n]\}_{i,n \in \mathbb{Z}}$ for \mathcal{L} an ample line bundle, and vertical arrows are cohomologically fully faithful embedding functors:*

$$\begin{array}{ccc}
 D_{\mathcal{L}}^b \text{Coh}(V) & \xrightarrow{i^*} & D_{\mathcal{L}}^b \text{Coh}(H) \\
 \text{\scriptsize HMS} \downarrow & \curvearrowright & \downarrow \text{\scriptsize HMS (C.)} \\
 H^0(\text{Fuk}(V^\vee)) & \xrightarrow{\cup} & H^0(\text{FS}(Y, v_0))
 \end{array} \tag{1.1}$$

Remark 1.1.2 (Explanation of the diagram). The top row is a restriction functor on line bundles in the bounded derived categories of coherent sheaves. Here we consider full subcategories generated by a certain ample line bundle \mathcal{L} . The bottom row is a functor between cohomological Fukaya categories. It’s given by parallel-transporting Lagrangians in a fiber over U-shapes in the base of v_0 which go around the singularity of v_0 . Morphisms in Fuk and Fukaya-Seidel (FS) are chain complexes, and are not associative but satisfy associativity A_∞ -relations that involve arbitrarily many morphisms as in an A_∞ -category. The statement discussed in this thesis concerns the cohomological Fukaya categories where we pass to cohomology in the morphisms groups, hence obtaining an actual category.

Remark 1.1.3 (Relevance of theorem). This cohomology-level result already gives a lot of information. First, since $\mathcal{L}|_H$ is the canonical bundle of the genus 2 curve, the product structure on the subcategory $D_{\mathcal{L}}^b Coh(V)$ determines the canonical ring of Σ_2 , namely $\bigoplus_{i \geq 0} H^0(\Sigma_2, \mathcal{L}^i)$.

Moreover, recall that one may use sections of a very ample power \mathcal{L}^k of \mathcal{L} to embed H and V into some \mathbb{CP}^N . These projective embeddings are characterized by homogeneous coordinate rings of the projective varieties H and V , which in turn are determined by the product structure that we compute. (This is the ring consisting of restrictions of homogeneous polynomials on the ambient \mathbb{CP}^N , which equivalently correspond to sections of $\mathcal{O}(m) = \mathcal{L}^{mk}$ for all positive integers m).

Remark 1.1.4 (Future directions). The construction of the diagram in the theorem with A_{∞} -functors, namely checking that higher order composition maps match in addition to objects, morphisms and composition, is a future direction. Powers of \mathcal{L} split-generate the derived category so an A_{∞} -enhancement of the result would allow us to extend the functors to iterated mapping cones and hence would give a HMS statement for the whole derived category. (Note that the same method of proof given in this thesis would also apply to other line bundles, but for simplicity we only consider powers of a certain ample line bundle \mathcal{L} .)

Remark 1.1.5 (Previous work on HMS for the genus 2 curve and abelian variety). HMS for abelian varieties of arbitrary dimension and quotient lattice was discussed in [Fuk02] using more advanced machinery. We present a different argument for this particular case in the left vertical arrow.

Seidel proved HMS with the A-model of the genus 2 surface [Sei11], i.e. the symplectic side, so we consider the B-model or complex structure on the genus 2 curve. The complex mirror Seidel constructs is a crepant resolution of $\mathbb{C}^3/\mathbb{Z}_5$, quotienting by the rotation group and then resolving the singularity at zero without a discrepancy in the first Chern class between the singular quotient and the resolution. It is equipped with a superpotential. The critical locus of the superpotential in his paper and the mirror in this paper are the same. One future direction is to further explore how his mirror is related to the mirror considered in this paper. Note: we are not in the exact case as in [Sei08], namely ω is not exact because we have compact fibers in a symplectic fibration with nonzero volume, and we are not in the monotone case, which is discussed later. We are considering a manifold of *general type* ($c_1 < 0$) on the B-side and a Calabi-Yau manifold ($c_1 = 0$) on the mirror Landau-Ginzburg (LG) model.

Outline of proof of Theorem 1.1.1. The approach we take is:

- Embed the genus 2 curve as a hypersurface in an abelian variety V .

- Blow up $V \times \mathbb{C}$ along $\Sigma_2 \times \{0\}$ so Σ_2 is the critical locus of a holomorphic function on the blow-up X , as described in [AAK16] for obtaining SYZ mirrors for hypersurfaces of toric varieties. This comes equipped with a Lagrangian torus fibration.
- Use SYZ to get a complex mirror Y two dimensions higher than Σ_2 and equip that mirror with a holomorphic function v_0 that encodes behavior that is mirror to Σ_2 .
- Both sides are Kähler so instead consider the B-model on the genus 2 curve and construct an A-model on the mirror. Note that involutivity is expected when the pair is Calabi-Yau, so one could have started with the mirror as the A-model and construct X as in [AAK16, §8] or [CLL12].
- Prove the existence of the fully-faithful embedding on the cohomological level for the mirror abelian varieties.
- Prove the same for Σ_2 and (Y, v_0) .
- Future directions: prove the subcategory of Lagrangians considered generates the Fukaya category. Prove an A_∞ -equivalence instead of an equivalence on cohomological categories.

□

Remark 1.1.6. In the general type case of $c_1(\Sigma_2) < 0$, the mirror is a noncompact LG model. Because of the blow-up, we are also in the setting of a non-toric Lagrangian fibration. (A toric fibration arises from a moment map, while here we start with a moment map and then perform operations on the base which still give a Lagrangian torus fibration but no longer from a moment map, see e.g. [Sym03]). In [AAK16] only the last coordinate of the fibration is a moment map.

1.2 The B-side manifold

1.2.1 Complex geometry

Remark 1.2.1 (The input for building an SYZ mirror is a Lagrangian torus fibration). Given a Lagrangian torus fibration on a symplectic manifold, the SYZ construction [SYZ96] produces a candidate mirror complex manifold by prescribing dual fibers over the same base. The points of a dual fiber are parametrized by unitary flat connections on the trivial line bundle on the original fiber. This process is discussed explicitly in [Aur07].

Constructing a suitable Lagrangian torus fibration is a hard problem. Guadagni's thesis [Gua17] finds Lagrangian torus fibrations on central fibers of toric degenerations, which will be the setting of the mirror Y in our case. However there is not an obvious Lagrangian torus fibration on, or toric degeneration to, Σ_2 . Abouzaid-Auroux-Katzarkov [AAK16] construct

Lagrangian torus fibrations on blow-ups of hypersurfaces in toric varieties, which we adapt to the abelian variety case here.

Definition 1.2.2 (Definition of abelian variety). The abelian variety V is topologically T^4 and its complex structure is defined as follows:

$$\begin{aligned} V &:= (\mathbb{C}^*)^2 / \Gamma_B \\ \Gamma_B &:= \mathbb{Z} \langle \gamma', \gamma'' \rangle \subset \mathbb{Z}^2, \quad \gamma' := \begin{pmatrix} 2 \\ 1 \end{pmatrix}, \gamma'' := \begin{pmatrix} 1 \\ 2 \end{pmatrix} \\ \Gamma_B &\curvearrowright (\mathbb{C}^*)^2, \quad \gamma \cdot (x_1, x_2) := (\tau^{-\gamma_1} x_1, \tau^{-\gamma_2} x_2) \end{aligned} \tag{1.2}$$

where $\gamma \in \Gamma_B$ has \mathbb{Z}^2 -coordinates (γ_1, γ_2) and $\tau \in \mathbb{R}$ parametrizes a family of complex structures, which will be mirror to a family of symplectic structures on the mirror. The parameter $\tau \ll 1$ is very small. The complex structure is the Γ_B -quotient of the usual J_0 that is multiplication by i on $(\mathbb{C}^*)^2$ at every point.

Remark 1.2.3 (Additive and multiplicative lattice viewpoints of abelian variety). There are equivalent ways to describe an abelian variety: the lattice can act multiplicatively as above, or equivalently it can act additively as we will describe below. This latter viewpoint allows us to understand the cohomology of V and is described in [BL04] and [Pol03].

The following lattice $\Gamma_B \oplus \Gamma_F$ acts additively on $\mathbb{C}^2 \cong \mathbb{R}^4$ (isomorphic as vector spaces), and the quotient is a product torus denoted $V_+ := T_B \times T_F$.

$$\begin{aligned} \Gamma_B \oplus \Gamma_F &:= \mathbb{Z} \left\langle \begin{pmatrix} 2 \\ 1 \end{pmatrix}, \begin{pmatrix} 1 \\ 2 \end{pmatrix} \right\rangle \oplus \mathbb{Z}^2 \\ V_+ &:= \mathbb{R}_{\xi_1, \xi_2}^2 / \Gamma_B \times \mathbb{R}_{\theta_{x_1}, \theta_{x_2}}^2 / \Gamma_F =: T_B \times T_F \end{aligned} \tag{1.3}$$

The additive structure maps to the multiplicative structure under the exponential map:

$$V_+ \ni (\xi_1, \xi_2, \theta_{x_1}, \theta_{x_2}) \mapsto (\tau^{-\xi_1} e^{2\pi i \theta_{x_1}}, \tau^{-\xi_2} e^{2\pi i \theta_{x_2}}) = (x_1, x_2) \in V \tag{1.4}$$

We see that ξ_1, ξ_2 and $\theta_{x_1}, \theta_{x_2}$ encode the norms and angles, respectively, of the complex coordinates (x_1, x_2) on V . In particular, they are defined modulo Γ_B and Γ_F . The reason for the subscript B is to denote the base of a moment map from the standard T^2 -rotation action $(\alpha_1, \alpha_2) \cdot (x_1, x_2) := (e^{2\pi i \alpha_1} x_1, e^{2\pi i \alpha_2} x_2)$ and F the fiber, i.e. obtained from rotating angles under an orbit for fixed norms $(|x_1|, |x_2|)$. In particular, the Γ_F no longer acts in the multiplicative setting. So in the T_F direction, properties on V_+ should be trivial in order to pass to V under the exponential map.

Claim 1.2.4 (Cohomology of abelian variety V). $H^n(V; \mathbb{Z}) \cong \wedge^n \text{Hom}(\Gamma, \mathbb{Z})$

Sketch, c.f. [BL04, §1.3]. It suffices to work with V_+ since it is homeomorphic to V .

$$\Gamma = \pi_1(V_+) = H_1(V_+; \mathbb{Z}) \therefore H^1(V_+; \mathbb{Z}) = \text{Hom}(\Gamma, \mathbb{Z})$$

The second equality follows because Γ is abelian and H_1 is the abelianization of π_1 . The third equality follows from the universal coefficient theorem and lack of torsion. So using the Künneth formula, its compatibility with the cup product, and the de Rham isomorphism we obtain a map which is an isomorphism of rings by induction:

$$\bigwedge^n \text{Hom}(\Gamma, \mathbb{Z}) \cong \bigwedge^n H^1(V; \mathbb{Z}) \xrightarrow{\cup} H^n(V; \mathbb{Z})$$

□

Corollary 1.2.5 ([Pol03, §1]). *Complex line bundles on V are topologically classified by their first Chern class, which is a skew-symmetric bilinear form $E : \Gamma \times \Gamma \rightarrow \mathbb{Z}$.*

Proof. For a complex line bundle, $c_1(L) \in H^2(V; \mathbb{Z}) \cong \wedge^2 \text{Hom}(\Gamma, \mathbb{Z})$ by the previous claim, and $\wedge^2 \text{Hom}(\Gamma, \mathbb{Z}) \cong \text{Hom}(\wedge^2 \Gamma, \mathbb{Z})$. □

We want to determine which forms E arise as the first Chern class of a *holomorphic* line bundle. These are precisely the L for which $c_1(L) \in H^{1,1}(V)$. So the next step is to consider $\text{Pic}(V)$ and the Hodge decomposition on abelian varieties, then find a description in terms of the lattice Γ as we did above for the topological cohomology.

Claim 1.2.6. Holomorphic line bundles on V are classified by

$$H^1(\pi_1(V_+); H^0(\mathcal{O}_{\tilde{V}_+}^*)) \cong H^1(V_+, \mathcal{O}^*) \quad (1.5)$$

Sketch from [BL04]. This theory is from [BL04, Appendix B], where elements of the left hand side of Equation 1.5 are referred to as *factors of automorphy*. This isomorphism is the analogue of the equivalence of Cartier divisors and line bundles on complex manifolds, but with the addition of Γ -equivariance. In other words, factors of automorphy are functions whose vanishing set, i.e. divisor, is Γ -invariant. The notion of a group action is equivalent to the notion of a cocycle, hence this invariance is encoded in the cohomology group $H^1(\pi_1(V_+); H^0(\mathcal{O}_{\tilde{V}_+}^*))$. The right hand side $H^1(V_+, \mathcal{O}^*) \cong \text{Pic}(V_+)$ consists of holomorphic line bundles on \mathbb{C}^2/Γ . Note that $\tilde{V}_+ = \mathbb{C}^2$.

Let $\pi : \mathbb{C}^2 \rightarrow V_+$ be the universal covering. The isomorphism of Equation 1.5 is constructed as follows, c.f. [BL04, Proposition B.1]. Line bundles over V_+ have a nice description because the cocycle condition on charts over V_+ is equivalent to the condition that Γ has a group action on \mathbb{C}^2 on a collection of charts in the universal cover, each one a lift of an open set on the base. We now describe this.

- Let $\{U_i\}$ be a covering of V_+ . A holomorphic line bundle is defined by gluing $U_i \times \mathbb{C}$ to $U_j \times \mathbb{C}$ by a holomorphic transition function g_{ij} acting on the \mathbb{C} factor. Alternatively, we can lift each U_i to W_i so that $\pi|_{W_i} : W_i \rightarrow U_i$ is a biholomorphism. In particular, $\pi_i^{-1}(x)$ and $\pi_j^{-1}(x)$ are two lifts of the same point, so by definition of the universal cover they differ by some element $\gamma_{ij} \in \Gamma$.

- Thus we can alternatively think of the transition functions as a function f of one of the lifts and the γ_{ij} that records the change between $\pi_i^{-1}(x)$ and $\pi_j^{-1}(x)$. Namely $\pi_j^{-1}(x) = \gamma_{ij}\pi_i^{-1}(x)$ for some $\gamma_{ij} \in \Gamma$. Then define

$$f(\gamma_{ij}, \pi_i^{-1}(x)) := g_{ij}$$

- Because Γ acts on \mathbb{C}^2 , the group action implies $\gamma_{ij}\gamma_{jk} = \gamma_{ik}$. The fact that such a g_{ij} is a cocycle on a line bundle implies

$$\begin{aligned} g_{ij}g_{jk} &= g_{ik} \\ \therefore f(\gamma_{ij}, \pi_i^{-1}(x))f(\gamma_{jk}, \pi_j^{-1}(x)) &= f(\gamma_{ik}, \pi_i^{-1}(x)) \\ \therefore f(\gamma_{ij}, \pi_i^{-1}(x))f(\gamma_{jk}, \gamma_{ij}\pi_i^{-1}(x)) &= f(\gamma_{ij}\gamma_{jk}, \pi_i^{-1}(x)) \\ \iff [f] &\in H^1(\Gamma, H^0(\mathcal{O}_{\mathbb{C}^2}^*)) \end{aligned} \tag{1.6}$$

i.e. f is a factor of automorphy.

- Concretely, by considering what cocycles and coboundaries map to under $g_{ij} \mapsto f(\gamma_{ij}, \pi_i^{-1}(\cdot))$ we obtain Čech cohomology groups with the discrete topology on Γ and taking values in the sheaf $\mathcal{O}_{\mathbb{C}^2}^*$. In particular the image gives a representative of a class in $H^1(\pi_1(V_+); H^0(\mathcal{O}_{V_+}^*))$.
- A trivial line bundle implies transition functions are of the form $g_{ij} = h_j/h_i$. So letting $g_{ij} = f(\gamma_{ij}, \pi_i^{-1}) = h_j/h_i$ we can define a function h on the universal cover by

$$h(\pi_i^{-1}(x)) := h(\pi_j^{-1}(x)) \cdot \frac{h_i}{h_j}$$

- So this corresponds to a coboundary $(\gamma, \tilde{x}) \mapsto h(\gamma \cdot \tilde{x})h(\tilde{x})^{-1}$ for some $h \in H^0(\mathcal{O}_{\mathbb{C}^2}^*)$.
- This correspondence is an isomorphism on cohomology, see [BL04, Proposition B.1].
- Note that there is an analogous result for all higher degree cohomology as well.

□

Claim 1.2.7. $H^{1,1}(V_+) \cong \text{Hom}_{\mathbb{C}}(\mathbb{C}^2, \mathbb{C}) \otimes \text{Hom}_{\overline{\mathbb{C}}}(\mathbb{C}^2, \mathbb{C})$

Proof. On the complex vector space \mathbb{C}^2 , recall we have a decomposition $(\mathbb{C}^2)^{1,0} \oplus (\mathbb{C}^2)^{0,1}$ [Huy05, Lemma 1.2.5]. Then $(T^{1,0}\mathbb{C}^2)^* = \text{Hom}_{\mathbb{C}}(\mathbb{C}^2, \mathbb{C})$ and $(T^{0,1}\mathbb{C}^2)^* = \text{Hom}_{\overline{\mathbb{C}}}(\mathbb{C}^2, \mathbb{C})$ see [BL04, Theorem 1.4.1]. If t_v is translation by v on the torus, we can extend (p, q) forms on \mathbb{C}^2 to all of the torus by pulling back by dt_{-v} . So $H^{1,1}(V_+) \cong \text{Hom}_{\mathbb{C}}(\mathbb{C}^2, \mathbb{C}) \otimes \text{Hom}_{\overline{\mathbb{C}}}(\mathbb{C}^2, \mathbb{C})$.

□

Corollary 1.2.8 (C.f [BL04, Proposition 2.1.6]). *A complex line bundle \mathcal{L} admits a holomorphic structure if and only if the class $c_1(\mathcal{L})$ is a $(1, 1)$ form, i.e. $E(i\cdot, i\cdot) = E(\cdot, \cdot)$, and $E(\Gamma, \Gamma) \subseteq \mathbb{Z}$. In particular, holomorphic line bundles on V_+ correspond with 2×2 hermitian matrices with the same integral property.*

Remark 1.2.9. The exponential short exact sequence of sheaves $0 \rightarrow \mathbb{Z} \rightarrow \mathcal{O} \xrightarrow{\exp} \mathcal{O}^* \rightarrow 1$ gives a long exact sequence containing $H^1(V, \mathcal{O}^*) \cong \text{Pic}(V) \xrightarrow{-c_1} H^2(V; \mathbb{Z}) \subseteq H^2(V; \mathbb{C}) = H^{0,2}(V) \oplus H^{1,1}(V) \oplus H^{2,0}(V)$. In particular, $c_1(\mathcal{L}) \in H^{1,1}(V)$ if and only if taking a wedge product with generators of $H^{0,2}$ and $H^{2,0}$ gives zero.

Note that $H(\cdot, \cdot) := E(i(\cdot), \cdot) + iE(\cdot, \cdot)$ is a Hermitian form, see [Huy05, Lemma 1.2.15]. Define \mathcal{L} by *multiplicators* e_γ (or *factors of automorphy* in [BL04]) i.e. $\Gamma \rightarrow \mathcal{O}^*(V)$ which describe the necessarily Γ -periodic gluing functions of the line as we go around elements of $\pi_1(V)$.

Lemma 1.2.10 (C.f. [Pol03, Theorem 1.3] and [BL04, Appell-Humbert Theorem 2.2.3]). *The Picard group $\text{Pic}(V_+)$ of holomorphic line bundles on V_+ is isomorphic to the set of all pairs (H, α) for Hermitian forms $H : \mathbb{C}^2 \times \mathbb{C}^2 \rightarrow \mathbb{C}$ and $\text{Im } H(\Gamma, \Gamma) \subseteq \mathbb{Z}$ and $\alpha : \Gamma \rightarrow U(1)$ satisfying $\alpha(\gamma + \tilde{\gamma}) = \exp(\pi i E(\gamma, \tilde{\gamma})) \alpha(\gamma) \alpha(\tilde{\gamma})$, where $E = \text{Im } H$.*

Sketch proof from [Pol03, Chapter 2] and [BL04, Chapter 2]. In [Pol03, §2.3] Polishchuk describes how the holomorphic structures are parametrized by an $\alpha : \Gamma \rightarrow U(1)$ that satisfies

$$\alpha(\gamma + \tilde{\gamma}) = \exp(\pi i E(\gamma, \tilde{\gamma})) \alpha(\gamma) \alpha(\tilde{\gamma})$$

as do [BL04, Proposition 2.2.2]. (Note that α in the former is denoted χ in the latter.) Then the factor of automorphy for a choice of (H, α) (where $E = \text{Im } H$) is

$$(\gamma, v) \mapsto \alpha(\gamma) \exp(\pi H(v, \gamma) + \frac{\pi}{2} H(\gamma, \gamma))$$

This factor of automorphy is a natural definition from the perspective of [BD16] where we have the notion of *generalized Heisenberg groups*. In our case the relevant group is the semi-direct product $U(1) \times \mathbb{C}^2$ with group law

$$(\gamma, v) \cdot (\tilde{\gamma}, \tilde{v}) = (\exp(\pi i E(v, \tilde{v})) \gamma \tilde{\gamma}, v + \tilde{v})$$

The key point about Heisenberg groups is a uniqueness of unitary irreducible representations, a theorem due to Stone and von Neumann. The Fock representation gives the factor of automorphy from above.

Conversely, suppose we have a factor of automorphy f for a holomorphic line bundle \mathcal{L} . Because it is nonvanishing we can express $f = \exp(2\pi i g)$ for some holomorphic function g . Then by [BL04, Theorem 2.1.2] the first Chern class corresponds to the alternating form

$$E_{\mathcal{L}}(\gamma, \tilde{\gamma}) = g(\tilde{\gamma}, v + \gamma) + g(\gamma, v) - g(\gamma, v + \tilde{\gamma}) - g(\tilde{\gamma}, v)$$

for all $\gamma, \tilde{\gamma} \in \Gamma = -\log \tau \Gamma_B + 2\pi i \Gamma_F$ and any choice of $v \in \mathbb{C}^2$ (it turns out this expression is independent of v). As we saw above, E corresponds to a Hermitian form when \mathcal{L} is holomorphic, and also $E(\Gamma, \Gamma) \subseteq \mathbb{Z}$. We can also construct an $\alpha : \Gamma \rightarrow U(1)$ as described at the

bottom of [BL04, pg 31].

So this completes the sketch of the isomorphism in the Lemma. \square

Example 1.2.11. Recall that for a complex line bundle on an abelian variety, $c_1(L)$ can be represented by an alternating form $E : \Gamma \times \Gamma \rightarrow \mathbb{Z}$ for $\Gamma \subset \mathbb{C}^2$. Thus taking \mathbb{R} linear combinations we can extend this to an \mathbb{R} -linear form $E : \mathbb{C}^2 \times \mathbb{C}^2 \rightarrow \mathbb{R}$. With respect to the basis given by the generators of Γ_B and Γ_F in Remark 1.3, this gives a 4 by 4 skew-symmetric matrix with respect to $\Gamma_B \times \Gamma_F$.

In the example of our setting here, we want the line bundle to be trivial in the T_F directions. That is, $E(iv, iw) = 0$ for $v, w \in \mathbb{Z}^2$. When L is a holomorphic line bundle, we saw in Corollary 1.2.8 that this implies $E(iv, iw) = E(v, w)$. Hence E is a block matrix

$$\begin{matrix} & \Gamma_B & \Gamma_F \\ \Gamma_B & \begin{pmatrix} 0 & * \\ -* & 0 \end{pmatrix} \\ \Gamma_F & \end{matrix}$$

This produces a corollary of Corollary 1.2.8 above.

Corollary 1.2.12. *Holomorphic line bundles on V_+ that pass under \exp to holomorphic line bundles on V correspond with real integral symmetric 2×2 matrices.*

Proof. On V_+ we can input generic elements of $\Gamma_B + i\Gamma_F$ as $E(\gamma + iw, \tilde{\gamma} + iv)$. By the above, this is $\text{Im } H$ for some hermitian form $H = \begin{pmatrix} a & b \\ \bar{b} & a \end{pmatrix}$ so $a \in \mathbb{R}$.

$$(\gamma_1 + iw_1 \quad \gamma_2 + iw_2) \begin{pmatrix} a & b + ic \\ b - ic & d \end{pmatrix} \begin{pmatrix} \tilde{\gamma}_1 + iv_1 \\ \tilde{\gamma}_2 + iv_2 \end{pmatrix} \quad (1.7)$$

In particular, since $E(iw, iv) = 0$ we find that

$$\begin{aligned} E(iw, iv) &= \text{Im } H(iw, iv) = \text{Im}(aw_1v_1 + bw_1v_2 + icw_1v_2 + bw_2v_1 + dw_2v_2 - icv_1w_2) \\ &= c(w_1v_2 - v_1w_2) = 0 \quad \forall w, v \in \mathbb{Z}^2 \\ \therefore c &= 0 \end{aligned}$$

and H is real hence symmetric. \square

Corollary 1.2.13. *We can express a holomorphic line bundle on V with a factor of automorphy given by*

$$(\gamma, x) \mapsto x^{\lambda(\gamma)} \tau^{\kappa(\gamma)}$$

where $\lambda \in \text{hom}(\Gamma_B, \mathbb{Z}^2) = \text{hom}(\Gamma_B, \Gamma_F^*)$ corresponds to the first Chern class and $\kappa(\gamma)$ is a real degree 2 polynomial whose quadratic part is determined by the first Chern class and whose linear part determines the holomorphic structure.

Proof. The factor of automorphy as described above (or see [Pol03, Equation (1.2.2)] and following discussion) corresponds with a choice of (H, α) and equals

$$(\gamma, v) \mapsto \alpha(\gamma) \exp(\pi H(v, \gamma) + \frac{\pi}{2} H(\gamma, \gamma))$$

We calculate the expression in the exponential (note that an element in the Γ of this particular situation is $\gamma + iw \in \Gamma_B + i\Gamma_F$)

$$\begin{aligned} & \pi H\left(-\frac{1}{\log \tau} \log x, \gamma + iw\right) + \frac{\pi}{2} H(\gamma + iw, \gamma + iw) \\ &= \pi \left[-\frac{1}{\log \tau} (\log x)^t H\gamma + \frac{1}{2} H(\gamma, \gamma) + \frac{1}{2} H(w, w) \right] + i\pi \left(-\frac{1}{\log \tau} \right) [(\log x)^t Hw] \\ &= \pi \left[\left(-\frac{1}{\log \tau} \right) (\log x)^t H\gamma + \frac{1}{2} H(\gamma, \gamma) \right] \end{aligned}$$

where the second line follows because H is real and symmetric, and in the third line we've taken $w = 0$ since the result should not depend on the angle Γ_F directions. So we can set

$$\begin{aligned} (-\log \tau) \lambda(\gamma) &:= H\gamma \\ \kappa(\gamma) &:= \frac{1}{2} H(\gamma, \gamma) + \log(\alpha(\gamma)) \end{aligned} \tag{1.8}$$

for $H(\Gamma_B, \Gamma_B) \subseteq (-\log \tau)\mathbb{Z}$. We will give the choice of H used in this thesis in an example below. □

Example 1.2.14. Recall Example 1.2.11. Let

$$H := (-\log \tau) \begin{pmatrix} 2 & 1 \\ 1 & 2 \end{pmatrix}^{-1}$$

Then this defines

$$\begin{aligned} & \mathcal{L} \rightarrow V \\ & \mathcal{L} = (\mathbb{C}^*)^2 \times \mathbb{C}/\Gamma_B, \quad \gamma \cdot (x_1, x_2, v) := (\tau^{-\gamma_1} x_1, \tau^{-\gamma_2} x_2, \tau^{\kappa(\gamma)} x^{\lambda(\gamma)} v) \\ & \text{Hom}(\Gamma_B, \mathbb{Z}^2) \ni \lambda : \gamma' \mapsto \begin{pmatrix} 1 \\ 0 \end{pmatrix}, \gamma'' \mapsto \begin{pmatrix} 0 \\ 1 \end{pmatrix} \\ & \kappa(n_1 \gamma' + n_2 \gamma'') := -\frac{1}{2} \begin{pmatrix} n_1 & n_2 \end{pmatrix} \begin{pmatrix} 2 & 1 \\ 1 & 2 \end{pmatrix} \begin{pmatrix} n_1 \\ n_2 \end{pmatrix} \end{aligned}$$

Claim 1.2.15. This $\kappa(n_1 \gamma' + n_2 \gamma'') = -\frac{1}{2} n^t \begin{pmatrix} 2 & 1 \\ 1 & 2 \end{pmatrix} n$ satisfies the cocycle condition.

Proof. We want the above definition of κ to satisfy the requirements of a group action $\gamma^2 \cdot (\gamma^1 \cdot (x, v)) = (\gamma^2 \circ \gamma^1) \cdot (x, v)$.

$$\begin{aligned}
(x_1, x_2, v) &\xrightarrow{\gamma^1} (\tau^{-\gamma_1^1} x_1, \tau^{-\gamma_2^1} x_2, \tau^{\kappa(\gamma^1)} x^{\lambda(\gamma^1)} v) \\
(x_{new}, v_{new}) &:= (\tau^{-\gamma_1^1} x_1, \tau^{-\gamma_2^1} x_2, \tau^{\kappa(\gamma^1)} x^{\lambda(\gamma^1)} v) \xrightarrow{\gamma^2} (\tau^{-\gamma_1^2 - \gamma_1^1} x_1, \tau^{-\gamma_2^2 - \gamma_2^1} x_2, \tau^{\kappa(\gamma^2)} x_{new}^{\lambda(\gamma^2)} v_{new}) \\
&= (\tau^{-\gamma_1^2 - \gamma_1^1} x_1, \tau^{-\gamma_2^2 - \gamma_2^1} x_2, \tau^{\kappa(\gamma^2)} (\tau^{-\gamma^1} x)^{\lambda(\gamma^2)} (\tau^{\kappa(\gamma^1)} x^{\lambda(\gamma^1)} v)) \\
&= (\tau^{-\gamma^1 - \gamma^2} x, \tau^{\kappa(\gamma^1) + \kappa(\gamma^2) - \langle \gamma^1, \lambda(\gamma^2) \rangle} x^{\lambda(\gamma^1) + \lambda(\gamma^2)} v)
\end{aligned}$$

On the other hand, applying $\gamma_2 \circ \gamma_1$

$$(x_1, x_2, v) \mapsto (\tau^{-\gamma^1 - \gamma^2} x, \tau^{\kappa(\gamma^1 + \gamma^2)} x^{\lambda(\gamma^1 + \gamma^2)} v)$$

and we know λ is a homomorphism. So to check the two maps agree we need to check that

$$\kappa(\gamma^1) + \kappa(\gamma^2) - \langle \gamma^1, \lambda(\gamma^2) \rangle = \kappa(\gamma^1 + \gamma^2)$$

This is satisfied by a quadratic form, so we make a choice of form $M := \begin{pmatrix} 2 & 1 \\ 1 & 2 \end{pmatrix}$ so that the geometry of the diagrams later on are in a standard form. Define

$$\kappa(n_1 \gamma' + n_2 \gamma'') = -\frac{1}{2} n^t \begin{pmatrix} 2 & 1 \\ 1 & 2 \end{pmatrix} n$$

Then both sides equal $-\frac{1}{2} n^1 M n^1 - \frac{1}{2} n^2 M n^2 - n^1 M n^2$ because $\gamma^1 = M n^1$ and $\lambda(\gamma^2) = n^2$ by definition. □

Claim 1.2.16. Sections of lines bundles on V are functions on $(\mathbb{C}^*)^2$ with the periodicity property

$$s(\gamma \cdot x) = \tau^{\kappa(\gamma)} x^{\lambda(\gamma)} s(x)$$

so have a Fourier expansion.

Proof. A section $s : V \rightarrow \mathcal{L}$ must have the same transition functions as the line bundle, if we consider the Cartier data.

$$s(\gamma \cdot x) / s(x) = \tau^{\kappa(\gamma)} x^{\lambda(\gamma)}$$

□

Corollary 1.2.17. Let \mathcal{L} be the degree $(1, 1)$ line bundle defined above. Then $H^0(V, \mathcal{L}^{\otimes l})$ has the following basis of sections:

$$s_{e,l} := \sum_{\gamma} \tau^{-l\kappa(\gamma + \frac{\gamma_{e,l}}{l})} x^{-l\lambda(\gamma) - \lambda(\gamma_{e,l})}$$

where $\gamma_{e,l} = s\gamma' + t\gamma''$, $0 \leq s, t < l$.

Claim 1.2.18 (Genus 2 curve). $H = \Sigma_2$ is a hypersurface in V defined by the vanishing of the section $s : V \rightarrow \mathcal{L}$:

$$s(x) = \sum_{\gamma \in \Gamma_B} x^{-\lambda(\gamma)} \tau^{-\kappa(\gamma)} \quad (1.9)$$

Proof. By the adjunction formula, $T^*H = K_H \cong (K_V \otimes \mathcal{L})|_H$. Since V is an abelian variety, its tangent bundle is trivializable so $K_H \cong \mathcal{L}|_H$. Recall $\deg(K_H) = \int_H c_1(K_H) = \int_H c_1(\mathcal{L}) = 2g - 2$. Since \mathcal{L} is obtained by winding once in the x_1 and x_2 directions respectively, it has degree 2 and hence $g = 2$. Alternatively, see Figure 1.1 where the solid blue denotes the behavior of the vanishing of $s(x)$ where $|x_i| =: \tau^{-\xi_i}$ is very large or equivalently $\tau \approx 0$ for variables ξ_i defined as $-\log_\tau |x_i|$. In the limit as $\tau \rightarrow 0$ the limit of the vanishing of s is denoted by the dotted line. So identifying opposite ends of the fundamental domain parallelogram and rotating by 2π gives a genus 2 curve. This limiting behavior is described in more detail below using the notion of the *tropicalization of a function*. □

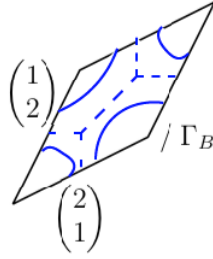


Figure 1.1: Quotient by Γ_B

Remark 1.2.19. The Γ_B lattice chosen above produces the blue curve of horizontal and vertical line segments in Figure 1.1, which we use throughout this thesis. A different choice of generators would give rise to different pictures but the methods used here should be the same.

1.2.2 Relation between invariants on X and H

Theorem 1.2.20 (Construction of Lagrangian torus fibration from [AAK16, §4]). *Recall $x = (x_1, x_2)$ are the periodic coordinates on V . Let $y \in \mathbb{C}$ be the coordinate on the \mathbb{C} factor and $s : V \rightarrow \mathcal{L}$ the function defined above. Then define*

$$\begin{aligned} X &:= Bl_{H \times \{0\}} V \times \mathbb{C} \subset \mathbb{P}(\mathcal{L} \oplus \mathcal{O}) \\ &= \overline{\text{graph}[s(x) : y]} \\ &= \overline{\{(x, y, [s(x) : y]) \in (\mathbb{P}(\mathcal{L} \oplus \mathcal{O}) \rightarrow V \times \mathbb{C})\}} \\ &= \{(x, y, [u : v]) \mid s(x)v = yu\} \end{aligned} \quad (1.10)$$

a subset of the \mathbb{P}^1 -bundle $\mathbb{P}(\mathcal{L} \oplus \mathcal{O})$ on $V \times \mathbb{C}$. The claim is that X admits a Lagrangian torus fibration.

Idea of proof. A toric variety has a natural torus action (with an orbit that is dense in the variety) so this torus action naturally gives a Lagrangian torus fibration from the moment map. There is also an S^1 rotation action on the y -coordinate. Using cut and paste methods on the base of the moment map which correspond to blowing-up the total space, one produces a Lagrangian torus fibration on X . \square

Lemma 1.2.21. $H = \text{Crit}(y)$.

Proof. The zero fiber is the union of the proper transform of V and the exceptional divisor. Let p be the blow-down map:

$$p : X \rightarrow V \times \mathbb{C}, \quad (x, y, (u : v)) \mapsto (x, y)$$

The definition of the proper transform is

$$\tilde{V} := \overline{p^{-1}(V \setminus H \times \{0\})}$$

Geometrically \tilde{V} is a copy of V , i.e. the closure of the part of V away from H in the blow-up which fills in the rest of the V copy. Also define the \mathbb{P}^1 -bundle coming from the blow-down map over H , and a section s^p of that bundle.

$$\begin{aligned} \text{exceptional divisor } E &:= \{(x, 0, (u : v)) \mid x \in H\} = p^{-1}(H \times \{0\}) \\ p|_E : E &\rightarrow H \times \{0\} \\ s^p : H &\rightarrow E, \quad s^p(x) := (x, 0, (1 : 0)) \end{aligned}$$

Now we can see H as the critical locus of the y fibration, as the fixed point set of the S^1 -action that rotates y , namely $(x, e^{i\theta}y, (e^{-i\theta}u : v))$.

$$\begin{aligned} y^{-1}(0) &= \{(x, 0, (u : v)) \mid s(x)v = 0 \cdot u\} \\ &= \{(x, 0, (1 : 0))\} \cup \{(x, 0, (u : v)) \mid s(x) = 0\} \\ &= \tilde{V} \cup E \end{aligned}$$

The claim is that \tilde{V} and E intersect in $s^p(H) \cong H$. Being in E implies $s(x) = 0 \therefore x \in H$. Being in \tilde{V} implies $v = 0$ hence we can scale $u \neq 0$ so that $u = 1$. Thus

$$\tilde{V} \cap E = s^p(H) \cong H = \text{Crit}(y)$$

\square

Symplectic invariants

Remark 1.2.22. If $\dim_{\mathbb{C}} V = 1$, then the zero fiber of $y : X \rightarrow \mathbb{C}$ involves a normal crossings divisor of the form $ab = 0$, which for dimensional reasons produces a Lefschetz singularity. Hence Seidel's Fukaya category of Lefschetz fibrations [Sei08] can be used, and in this case $H = \text{a point}$. We would want an analogue of that Fukaya category with $H = \Sigma_2$ as the critical locus, which requires going up a dimension.

Proposition 1.2.23 (Proposing a Fukaya category of Morse-Bott fibration [AAK16]). *The normal bundle to $H \times 0$ in $V \times \mathbb{C}$ is $\mathcal{L} \oplus \mathcal{O}$. Once we blow up along $H \times \{0\}$, then $H = \Sigma_2$ is the intersection of two divisors in a normal crossing singularity and forms the critical locus of a Morse-Bott fibration given by $y : (x, y, (u : v)) \mapsto y$. Then $\text{Fuk}(H)$ is conjectured by [AAK16, Corollary 7.8] to be equivalent to a Fukaya category $F_s(X, y)$ which AAK describe, because Lagrangians in H can be parallel transported from the central fiber to obtain non-compact Lagrangians in X admissible with respect to the superpotential y .*

Complex invariants

The bounded derived category of coherent sheaves on X and H are related as follows.

Lemma 1.2.24 (Orlov [APS]). *There is a semi-orthogonal decomposition*

$$D^b\text{Coh}(X) = \langle D^b\text{Coh}(H), D^b(V \times \mathbb{C}) \rangle$$

1.2.3 Dependence on choice of genus 2 curve

Claim 1.2.25. Any genus 2 curve can be embedded into an abelian variety of complex dimension 2.

Proof. Fixing a point $x_0 \in \Sigma_2$ the map $\Sigma_2 \ni x \mapsto \mathcal{O}(x - x_0) \in \text{Pic}^0(\Sigma_2)$ is injective [Huy05, Proposition 2.3.34]. Then $\text{Pic}^0(\Sigma_2)$ is isomorphic to the Jacobian of Σ_2 , which is an abelian variety, [For91, §21.7]. Explicitly, let $\{\omega_1, \omega_2\} \in H^{1,0}(\Sigma_2)$ be a basis and take $\alpha_1, \dots, \alpha_4 \in H_1(\Sigma_2; \mathbb{Z})$ to be a basis on homology. Let c be a chain on Σ_2 so that $\partial c = x - x_0$. Then the embedding is

$$\Sigma_2 \ni x \mapsto \left(\int_c \omega_1, \int_c \omega_2 \right) \in \text{Jac}(\Sigma_2) = \mathbb{C}^2 / \text{Per}(\omega_1, \omega_2), \quad \text{Per}(\omega_1, \omega_2) := \mathbb{Z} \left\{ \left\langle \left(\int_{\alpha_i} \omega_1, \int_{\alpha_i} \omega_2 \right) \right\rangle \right\}_i$$

Note that the definition of $\text{Pic}(\Sigma_2)$ as holomorphic line bundles [Huy05] versus as divisors modulo principal divisors [For91, §21.6] are equivalent: any complex curve can be embedded into projective space using sections of a line bundle of suitably high degree [For91, Theorem 17.22], hence the map $\text{Div}(\Sigma_2) \ni D \rightarrow \mathcal{O}(D) \in \text{Pic}(\Sigma_2)$ is surjective [Huy05, Corollary 5.3.7].

□

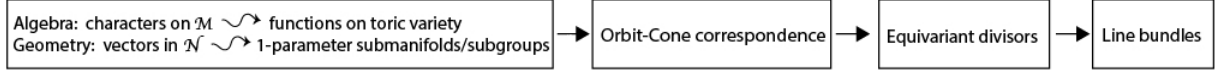
Corollary 1.2.26. *Varying the genus 2 curve corresponds with varying the complex structure parameters of V (and hence of X). The complex structure limit has an enumerative meaning in the mirror map, see [CLL12]. Thus this will also vary the Kähler parameters of Y via the mirror map.*

1.3 Background on toric varieties

The SYZ mirror Y is defined using the machinery of toric varieties to obtain a variety \tilde{Y} and then $Y := \tilde{Y}/\Gamma_B$. Toric varieties are a combinatorial way to produce charts and transitions functions defining a manifold.

We will then define a symplectic form on Y , the first step in equipping Y with a Fukaya category and then proving HMS with that category. Since Y is locally toric, as a quotient of a toric variety \tilde{Y} by a discrete group, and toric varieties constructed from a polytope naturally come with a line bundle, we use sections of that line bundle to define a metric that will give rise to the symplectic form.

We build the theory needed to define that line bundle. Here is the plan of action.



The background here is based on [CLS11, p 59, p128] and [Ful93, Chapter 1].

1.3.1 Characters and 1-parameter subgroups

Let Y_Δ be the toric variety associated to a polytope Δ as will be described. In this thesis we will use the following theory for $Y_\Delta = \mathbb{CP}^2(3)$ i.e. \mathbb{CP}^2 blown up at three points, as well as a related *toric variety of infinite type* [KL19] described later. The Orbit-Cone correspondence explains how combinatorial data (cones) gives geometric data (orbits). The data is encoded in a vector space of characters $M_{\mathbb{R}}$ which are functions on Y_Δ , and a vector space $N_{\mathbb{R}}$ of “co-characters” that generates 1-parameter subgroups (PS) in Y_Δ , respectively. The subscript \mathbb{R} means we tensor a lattice with \mathbb{R} . In particular M is the “algebra” and N is the “geometry” in this algebraic geometry setting of toric varieties.

Definition 1.3.1 (Notation). We fix some notation. We will consider examples of $n = 2$ and $n = 3$ below.

- Geometry: $N := \mathbb{Z}^n$ vectors encode the 1-PS parametrized by \mathbb{C}^* in the torus $T_N := (\mathbb{C}^*)^n$ which is dense in the toric variety. $N \otimes_{\mathbb{Z}} \mathbb{C}^* = T_N$ and $N_{\mathbb{R}} := N \otimes_{\mathbb{Z}} \mathbb{R}$.

- Algebra: $M = \text{Hom}_{\mathbb{Z}}(N, \mathbb{Z})$ encodes both linear functionals on N (combinatorial level) and functions on the toric variety (manifold level). In [AAK16] elements of M are called *weight vectors* because exponentiating them gives *toric monomials* which are *characters* i.e. functions on the toric variety.
- $M_{\mathbb{R}} = \mathbb{R}^n$ and define a nondegenerate pairing $M_{\mathbb{R}} \times N_{\mathbb{R}} \rightarrow \mathbb{R}$ by $\langle e_i, f_j \rangle = f_j(e_i) = \delta_{ij}$.

Definition 1.3.2 (Cone). A *cone* $\sigma \subset N_{\mathbb{R}}$ is an intersection of half spaces $H_u^+ := \{n \in N_{\mathbb{R}} \mid \langle u, n \rangle \geq 0\}$ for a set of normal vectors $u \in M$. For example, take $u_1 = e_1$ and $u_2 = e_2$ to get the first quadrant $e_1, e_2 \geq 0$. Then σ consists of convex linear combinations of lattice vectors called *rays* ρ , the set of which is denoted $\sigma(1)$.

The *dual cone* $\sigma^\vee \subset M_{\mathbb{R}}$ is defined to be the intersection of dual half-spaces as follows.

$$\sigma^\vee := \{m \in M_{\mathbb{R}} \mid \langle m, n \rangle \geq 0 \ \forall n \in \sigma\} = \bigcap_{n \in \sigma(1)} \{m \in M_{\mathbb{R}} \mid \langle m, n \rangle \geq 0\}$$

Definition 1.3.3 (Strongly convex rational polyhedral cone). *Strongly convex* means σ is not generated by $\pm e$ for any direction e (or equivalently $\sigma \cap -\sigma = \{0\}$), and *rational* means σ has integral generators, namely they are in \mathbb{Z}^n .

Remark 1.3.4. If m_1, \dots, m_s generate σ^\vee , then these are the normal vectors of the half-spaces in σ i.e. $\sigma = H_{m_1}^+ \cap \dots \cap H_{m_s}^+$. So the upshot is that σ^\vee encodes the collection of these normal vectors, where its edges are facets of σ . More generally a face τ in σ corresponds to one, call it τ^* , of complementary dimension in σ^\vee namely $\tau^\perp \cap \sigma^\vee$, and conversely.

Definition 1.3.5 (Character). Let $S_\sigma := \sigma^\vee \cap M$ be the lattice points in the dual cone. Then elements of the coordinate ring $\mathbb{C}[S_\sigma]$ are functions locally defined on Y_Δ called *characters* or *toric monomials*. They are \mathbb{C} -linear combinations of elements in the set $\{\chi^u \mid u \in S_\sigma\}$. Define an open set on the toric variety as:

$$U_\sigma := \text{Spec } \mathbb{C}[S_\sigma]$$

In particular, because S_σ is a semi-group, meaning we can add elements and it contains zero, then the set of elements χ^u has a natural ring structure as one expects for the coordinate ring of functions.

Remark 1.3.6 (Notation). We will use the letter u to denote lattice elements in N . We will reserve the letter m to refer to points in $M_{\mathbb{R}}$ or M and n will denote elements of $N_{\mathbb{R}}$. This is to be consistent with [CLS11].

Definition 1.3.7 (Affine charts and functions). An *affine or local chart* on Y_Δ is $\text{Spec } \mathbb{C}[S_\sigma]$. In particular, all local charts contain the dense torus $(\mathbb{C}^*)^n = \text{Spec } \mathbb{C}[\chi^{\pm e_1}, \dots, \chi^{\pm e_n}]$ because

$$M = \text{Span}_{\mathbb{Z}_+} \langle \pm e_1, \dots, \pm e_n \rangle \supset \{u \in \sigma^\vee(1)\}$$

and rays generate the semi-group S_σ . A *local function* is given by characters χ^u as follows. A character is a homomorphism from the dense torus to \mathbb{C}^* :

$$\chi^u : (\mathbb{C}^*)^n \rightarrow \mathbb{C}^*, \quad (t_1, \dots, t_n) \mapsto t^u := t_1^{u_1} \cdot \dots \cdot t_n^{u_n}, \quad u = \sum_{i=1}^n u_i e_i$$

Fix a basis $\{u_1, \dots, u_k\}$ for S_σ in the sense that $\{\pm u_1, \dots, \pm u_l, u_{l+1}, \dots, u_k\}$ generates S_σ over \mathbb{Z}_+ and $\{u_1, \dots, u_k\}$ has no relations (the *minimal generators*). This gives the coordinate chart with *local complex coordinates* $\chi^{u_1}, \dots, \chi^{u_k}$ if σ is a strongly convex cone:

$$(\chi^{u_1}, \dots, \chi^{u_k}) : U_\sigma \rightarrow \mathbb{C}^k$$

Remark 1.3.8. This chart has image given by a potentially singular n -dimensional subvariety of \mathbb{C}^k . In particular for maximal cones, $k = n$, the u_i form a \mathbb{Z} -basis of M , and we obtain a smooth variety and an affine manifold chart in the usual sense, mapping U_σ to the local model \mathbb{C}^n .

In the other case when the u_i are not a \mathbb{Z} -basis for M , we will have some relations among them. In particular,

$$\mathbb{C}[S_\sigma] \cong \mathbb{C}[\chi^{u_1}, \dots, \chi^{u_k}] / I$$

where I is a *toric ideal* that records these relations. In the example of \mathbb{CP}^2 below, Example 1.3.13, we will not need to quotient by toric ideals.

A suitable closure of this chart gives the toric variety. Later we will look at when a character extends to a function on the whole toric variety, i.e. a partial or full compactification of $(\mathbb{C}^*)^n$, meaning we let the coordinates tend to 0 or infinity. This illustrates how M gives rise to functions.

Definition 1.3.9 (Toric variety). Recall that cones σ give affine charts. A fan is a collection of cones arranged in a way that tell us how to glue local charts, namely what the transition functions on the manifold are. A *fan* is a collection of cones $\sigma_i \subset N_{\mathbb{R}}$ so that

- every face of a cone is a cone
- $\tau_{ij} := \sigma_i \cap \sigma_j$ is a face of both σ_i, σ_j hence we glue U_{σ_i} to U_{σ_j} along $U_{\tau_{ij}}$

Suppose σ_1 and σ_2 are two maximal cones so that $\tau = \sigma_1 \cap \sigma_2$ is $(n-1)$ -dimensional.

Claim 1.3.10. $\tau = H_m \cap \sigma_1 = H_m \cap \sigma_2$ for $m \in \sigma_1^\vee \cap (-\sigma_2)^\vee \cap M$.

In particular, the semi-group S_τ now has the $\pm m$ direction whereas σ_1 only had m and σ_2 only had $-m$. This corresponds to inverting the coordinate χ^m in the two charts from $\mathbb{C}[S_{\sigma_1}]$ and $\mathbb{C}[S_{\sigma_2}]$, which will now be required to be nonzero. We glue these two charts along

$$U_\tau = (U_{\sigma_1})_{\chi^m} = (U_{\sigma_2})_{\chi^{-m}}$$

We can see how N gives rise to 1 parameter subgroups.

Definition 1.3.11 (1 parameter-subgroup (PS)). Given $v = \sum_{i=1}^n v_i f_i \in N$, we get a 1-PS λ^v via the multiplicative homomorphism:

$$\lambda^v : \mathbb{C}^* \rightarrow (\mathbb{C}^*)^n, \quad t \mapsto (t^{v_1}, \dots, t^{v_n})$$

For example $v = (1, 1)$ gives the complex 1-PS $(t, t)_{t \in \mathbb{C}^*} \subset (\mathbb{C}^*)^2$. This gives a 1-dimensional submanifold in U_σ by taking the image of $(\chi^{u_1}, \dots, \chi^{u_k})$ on $\{\lambda^v(t)\}_{t \in \mathbb{C}^*}$.

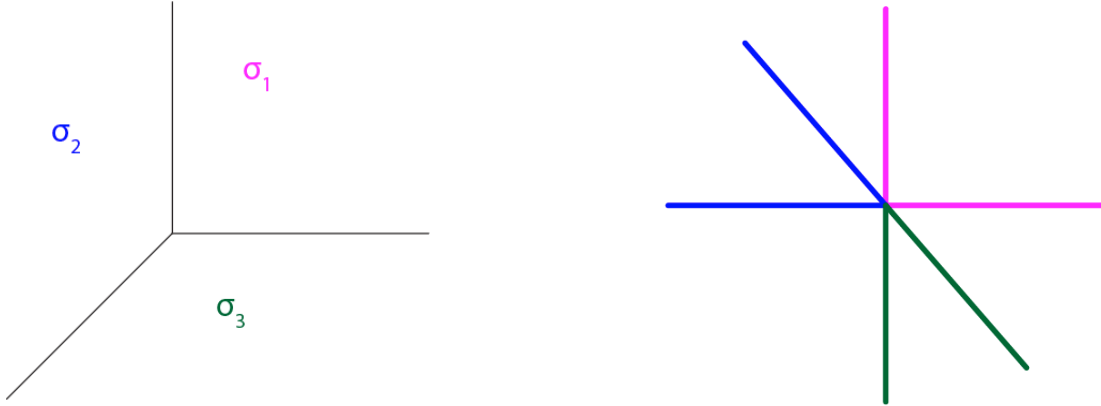
Remark 1.3.12. We can compose characters and 1-PS to get a character of \mathbb{C}^* by

$$\chi^u \circ \lambda^v(t) = t^\ell, \quad \ell = \langle u, v \rangle$$

In particular we can see N geometrically as the dense torus by collecting all the 1-PS via

$$N \otimes_{\mathbb{Z}} \mathbb{C}^* : v \otimes t \mapsto \lambda^v(t)$$

Example 1.3.13 (\mathbb{CP}^2). The fan has three cones, with rays generated by $v_1 = f_1, v_2 = f_2$, and $v_3 = -f_1 - f_2$ in $N_{\mathbb{R}}$.



Dual cones of functionals non-negative on the original cones are

$$\begin{aligned} \sigma_1^\vee &= \text{span}(e_1, e_2) \\ \sigma_2^\vee &= \text{span}(-e_1, -e_1 + e_2) \\ \sigma_3^\vee &= \text{span}(-e_2, e_1 - e_2) \end{aligned}$$

The vectors in these pairs don't have relations between them, so they correspond to variables of an affine chart isomorphic to $\mathbb{C}[x, y]$. In other words, we don't need to quotient by a toric ideal I that would record relations between the generators. The choice of generator in each case gives a complex coordinate on the chart.

$$\begin{aligned} U_{\sigma_1} &= \text{Spec } \mathbb{C}[\chi^{1,0}, \chi^{0,1}] \cong \mathbb{C}^2 \ni (\chi^{1,0}, \chi^{0,1}) \\ U_{\sigma_2} &= \text{Spec } \mathbb{C}[\chi^{-1,0}, \chi^{-1,1}] \cong \mathbb{C}^2 \ni (\chi^{-1,0}, \chi^{-1,1}) \\ U_{\sigma_3} &= \text{Spec } \mathbb{C}[\chi^{0,-1}, \chi^{1,-1}] \cong \mathbb{C}^2 \ni (\chi^{0,-1}, \chi^{1,-1}) \end{aligned}$$

If $\tau = \sigma_1 \cap \sigma_2$, then this corresponds to inverting $\chi^{1,0}$ and τ^\vee is $H_{(1,0)}^+$. A choice of generators gives a choice of coordinates, and the two different natural choices give us the coordinate change.

$$\mathbb{C}[S_{\sigma_1}] = \mathbb{C}[\chi^{(1,0)}, \chi^{(0,1)}] \subset \mathbb{C}[\chi^{\pm(1,0)}, \chi^{(0,1)}] = \mathbb{C}[S_\tau] \rightsquigarrow \text{Spec } \mathbb{C}[\chi^{\pm(1,0)}, \chi^{(0,1)}] \rightarrow \text{Spec } \mathbb{C}[\chi^{(1,0)}, \chi^{(0,1)}]$$

and

$$\mathbb{C}[\chi^{-(1,0)}, \chi^{(-1,1)}] \subset \mathbb{C}[\chi^{\pm(1,0)}, \chi^{(-1,1)}] \rightsquigarrow \text{Spec } \mathbb{C}[\chi^{\pm(1,0)}, \chi^{(-1,1)}] \rightarrow \text{Spec } \mathbb{C}[\chi^{-(1,0)}, \chi^{(-1,1)}]$$

Note that $\mathbb{C}[\chi^{\pm(1,0)}, \chi^{(0,1)}] = \mathbb{C}[\chi^{\pm(1,0)}, \chi^{(-1,1)}]$ and under Spec we get U_τ . The choice of generators give us an identification with $\mathbb{C}^* \times \mathbb{C}$ which then includes, as the identity map, into \mathbb{C}^2 in the two charts. The two different choices of this identification give us the transition map.

$$g_{12}(\chi^{(1,0)}, \chi^{(0,1)}) := \left(\frac{1}{\chi^{(1,0)}}, \frac{\chi^{(0,1)}}{\chi^{(1,0)}} \right)$$

This recovers how we think about $\mathbb{CP}^2 \ni [z_0 : z_1 : z_2]$ with $\chi^{(1,0)} = z_1/z_0$ and $\chi^{(0,1)} = z_2/z_0$.

1.3.2 Orbit-cone correspondence

To understand equivariant divisors, we need to understand how the combinatorial data gives us the geometric data. Divisors correspond to the vanishing of a coordinate on the variety. This can be read off from the fan via the ‘‘Orbit-Cone Correspondence.’’

Lemma 1.3.14 (Orbit-Cone correspondence). *There is a 1-1 correspondence between $n - k$ dimensional $(\mathbb{C}^*)^n$ -orbits of a point in the toric variety, and k dimensional cones of the fan, e.g. between divisors and rays.*

Proof. The idea is ‘‘every 1-parameter subgroup corresponding to a point in the interior of a cone in N limits to the same limit point.’’ (Recall the correspondence between points of N and 1-parameter subgroups in Definition 1.3.11.) That point gives the vector that defines the direction of the 1-PS. By algebraic geometry, a point on a toric variety is a semigroup homomorphism $S_\sigma = \mathbb{C}[\sigma^\vee \cap M] \rightarrow \mathbb{C}$ i.e. a map $\text{Spec } \mathbb{C} \rightarrow U_\sigma$. Recall that M encodes the functions on the toric variety. So such an assignment is determining what all the functions equal at the point; knowing all the functions at a given point is the same information as knowing the point. Given $v \in \sigma \cap N$ we can assign coordinates to the associated point using the following map on a basis of $\sigma^\vee \cap M$:

$$\sigma^\vee \cap M \ni u \mapsto \lim_{t \rightarrow 0} \chi^u(\lambda^v(t)) = t^{\langle u, v \rangle} \in \mathbb{C}$$

Now we use the following claim to see why all vectors of a cone give the same limit point, hence giving the Orbit-Cone correspondence by taking the orbit of that cone’s limit point.

Claim 1.3.15. All 1-PS arising from directions $v \in \text{int}(\sigma) \cap N$ limit to the same point.

Proof. For clarification we will use subscripts u_{bdry}, u_{int} to differentiate between the two cases of functions we need to check on each v (namely u not in the interior of the dual cone $\sigma^\vee \subset M$ and u in the interior). We see that:

1. $u_{bdry} \in \sigma^\vee \cap \sigma^\perp$ implies $\langle u_{bdry}, v \rangle = 0$ for all $v \in \sigma$ hence

$$\lim_{t \rightarrow 0} \chi^u(\lambda^v(t)) = t^{\langle u, v \rangle} = 1$$

2. $u_{int} \in \sigma^\vee \setminus (\sigma^\vee \cap \sigma^\perp)$ implies that, on the one hand $\langle u_{int}, v \rangle \geq 0$ for all $v \in \text{int}(\sigma) \cap N$ by definition of σ^\vee but on the other hand $\langle u_{int}, v \rangle \neq 0$ for v in the interior of σ and $u_{int} \notin \sigma^\perp$. Thus

$$\lim_{t \rightarrow 0} \chi^u(\lambda^v(t)) = t^{\langle u, v \rangle} = 0$$

□

To finish the proof of the Orbit-Cone correspondence, we let the orbit corresponding to the cone σ be $(\mathbb{C}^*)^n \cdot p$ where p is the point $\lim_{t \rightarrow 0} (\chi^{u_1}(\lambda^v(t)), \dots, \chi^{u_k}(\lambda^v(t)))$ for some $v \in \sigma$ and u_1, \dots, u_k generators for S_σ . We can choose any v by the previous claim.

□

Example 1.3.16 (\mathbb{CP}^2). The fan has cones and dual cones:

$$\begin{aligned} \{0\}, \{0\}^\vee &= M_{\mathbb{R}} \cong \mathbb{R}^2 \\ \rho_1 &= \langle (1, 0) \rangle, \rho_2 = \langle (0, 1) \rangle, \rho_3 = \langle -1, -1 \rangle \\ \rho_1^\vee &= \langle \pm(0, 1), (1, 0) \rangle, \rho_2^\vee = \langle \pm(1, 0), (0, 1) \rangle, \rho_3^\vee = \langle \pm(-1, 1), (-1, 0) \rangle \\ \sigma_1 &= \langle (1, 0), (0, 1) \rangle, \sigma_2 = \langle (1, 0), (-1, -1) \rangle, \sigma_3 = \langle (0, 1), (-1, -1) \rangle \\ \sigma_1^\vee &= \langle (1, 0), (0, 1) \rangle, \sigma_2^\vee = \langle (0, 1), (1, -1) \rangle, \sigma_3^\vee = \langle (-1, 0), (-1, 1) \rangle \end{aligned}$$

The limit points γ_σ that generate the orbits corresponding to cones σ are the points sending vectors $m \in \sigma^\perp \cap \sigma^\vee$ to 1 and the rest of σ^\vee to 0. Let $(t_1, t_2) \in (\mathbb{C}^*)^2$ be coordinates on the dense toric orbit. The generators taken for S_{ρ_i} are listed below in the exponents.

$$\begin{aligned} \lambda^{(0,0)}(t) &= (1, 1), & \gamma_{\{0\}} &= \lim_{t \rightarrow 0} (\chi^{(1,0)}(1, 1), \chi^{(0,1)}(1, 1)) = (1, 1) \implies (\mathbb{C}^*)^2 \\ \lambda^{(1,0)}(t) &= (t, 1), & \gamma_{\rho_1} &= \lim_{t \rightarrow 0} (\chi^{(0,1)}(t, 1), \chi^{(1,0)}(t, 1)) = (1, 0) \implies \mathbb{C}^* \times \{0\} \\ \lambda^{(0,1)}(t) &= (1, t), & \gamma_{\rho_2} &= \lim_{t \rightarrow 0} (\chi^{(1,0)}(1, t), \chi^{(0,1)}(1, t)) = (1, 0) \implies \mathbb{C}^* \times \{0\} \\ \lambda^{(-1,-1)}(t) &= (t^{-1}, t^{-1}), & \gamma_{\rho_3} &= \lim_{t \rightarrow 0} (\chi^{(-1,1)}(t^{-1}, t^{-1}), \chi^{(-1,0)}(t^{-1}, t^{-1})) = (1, 0) \implies \mathbb{C}^* \times \{0\} \end{aligned}$$

Taking the closures in the toric variety, we have three toric divisors, i.e. divisors invariant under the $(\mathbb{C}^*)^n$ action.

Claim 1.3.17. Let $O(\sigma)$ denote the orbit corresponding to a cone σ under the Orbit-Cone correspondence. Then the toric divisor given by the closure of an orbit has the following description:

$$\overline{O(\tau)} = \bigcup_{\tau \leq \sigma} O(\sigma)$$

Notation: $N(\sigma)$ is lattice points in N modulo those in $\sigma \cap N =: N_\sigma$.

1.3.3 Divisors, line bundles and polytopes

The divisor-ray correspondence is a special case of the Orbit-Cone correspondence, and by complex geometry [Huy05, §2.3] the defining functions of a divisor give transition functions for line bundles. Below we introduce the notion of a polytope and explain why it determines a line bundle. We'll see that it is constructed so its edges are perpendicular to rays in a fan, and the size of it governs the coefficient on each irreducible toric divisor (corresponding to the rays of a fan). Then this divisor gives the line bundle corresponding to that polytope.

Definition 1.3.18 (Polytope). A *polytope* $P \subset M_{\mathbb{R}}$ is

$$P := \{m \in M_{\mathbb{R}} \mid \langle m, \nu_i \rangle \geq -a_i\} \subset M_{\mathbb{R}}$$

for finitely many i , where the $\nu_i \in N$ generate rays ρ_i of a fan Σ . With infinitely many i we get more generally a *polyhedron*.

Definition 1.3.19 (Faces, facets). Codimension 1 faces in the polytope are called *facets*, $\langle u, \nu_i \rangle = -a_i$ for some i and $\langle u, \nu_j \rangle > -a_j$ for $j \neq i$. Higher codimension faces have $\langle u, \nu_i \rangle = -a_i$ for more than one i .

Definition 1.3.20 (Obtaining fan from P : vertices of full dimensional lattice polytope correspond with toric charts, c.f. [CLS11, p 76]). Given polytope P with vertices \mathbf{v} , we translate each vertex to the origin and take the cone spanned by its edges, namely $C_{\mathbf{v}} := \text{Cone}(P \cap M - \mathbf{v}) \subset M_{\mathbb{R}}$. The corresponding cone of the fan is defined to be

$$\sigma_{\mathbf{v}} := C_{\mathbf{v}}^{\vee} = \text{Cone}(\nu_i \mid i\text{th face contains } \mathbf{v}) \subset N_{\mathbb{R}}$$

Thus the chart $U_{\sigma_{\mathbf{v}}} = \text{Spec } \mathbb{C}[\text{Cone}(P \cap M - \mathbf{v}) \cap M]$. (More generally for a face Q of the polytope, we have σ_Q is the cone on the ν_i of faces containing Q .) So the upshot is “local coordinates of a toric variety can be read off from edges to a vertex of the corresponding polytope.”

The collection of all the cones σ_Q can be checked to give a fan which we define to be Σ_P .

Remark 1.3.21. For a discussion of the analogue of dualizing $\sigma \rightarrow \sigma^{\vee}$ on the level of polytopes (polytope \rightarrow polar polytope), see [Ful93, §1.5, p 26]. One can pass between a polytope P in $M_{\mathbb{R}}$ to a cone given by $\text{Cone}(P \times \{1\}) \subset M_{\mathbb{R}} \times \mathbb{R}$, then take the dual $^{\vee}$ on

cones to get a cone in $N_{\mathbb{R}} \times \mathbb{R}$, and show that this is a cone on the *polar* P^0 of P , i.e. of the form $\text{Cone}(P^0 \times \{1\})$ for the dual polytope $P^0 \subset N_{\mathbb{R}}$.

Definition 1.3.22 (Equivariant divisor). An *equivariant or T -divisor* is a linear combination of closures of toric orbits.

Claim 1.3.23. A T -divisor is a linear combination of divisors corresponding to facets.

Proof. Rays of a fan correspond to equivariant divisors. Indeed, given a ray ρ its orthogonal ρ^\perp has codimension 1, which means the distinguished point γ_ρ has $n - 1$ ones and 1 zero (from the one direction generated by ρ sending the codimension 1 space ρ^\perp to zero). So the $(\mathbb{C}^*)^n$ -orbit is dimension $n - 1$. Taking the closure of this gets the divisor D_ρ . Namely

$$D_\rho = \overline{O(\rho)} = \bigcup_{\rho \leq \sigma} O(\sigma)$$

We get a divisor from the vanishing of a coordinate. □

Remark 1.3.24 (Notation). Since we now know that the i in ν_i and a_i are indexed by facets F of the polytope, we can use F to index them.

Definition 1.3.25 (A distinguished divisor). Let $P := \{m \in M_{\mathbb{R}} \mid \langle m, \nu_i \rangle \geq -a_i\} \subset M_{\mathbb{R}}$ be an integral polytope, namely $a_i \in \mathbb{Z}$. By the Orbit-Cone correspondence we can take the closure of the corresponding orbit of each ray ν_F in Σ_P to obtain the toric divisor D_F . We may then construct a toric variety Y_P from this fan. Finally we define the distinguished divisor in Y_P to be

$$D := \sum_F a_F D_F$$

Remark 1.3.26. The integral condition allows us to define the divisor and later embed Y_P into projective space since D will correspond to an ample line bundle.

Claim 1.3.27 (Sections of $\mathcal{O}(D)$, [CLS11][Proposition 4.3.3]). The sections of $\mathcal{O}(D)$ are given by

$$\Gamma(Y_P, \mathcal{O}(D)) = \bigoplus_{m \in P \cap M} \mathbb{C} \cdot \chi^m$$

where $P := \{m \in M_{\mathbb{R}} \mid \langle m, \nu_F \rangle \geq -a_F\} \subset M_{\mathbb{R}}$ and $D = \sum_F \text{facet} a_F D_F$.

Proof. By definition

$$\Gamma(Y_P, \mathcal{O}(D)) = \{f \in \mathbb{C}(Y_P)^* \mid \text{div}(f) + D \geq 0\} \cup \{0\}$$

where $\mathbb{C}(Y_P)^*$ consists of invertible rational functions on Y_P . Note that

$$\text{Supp}(D) \cap T_N = \emptyset$$

because T_N is the orbit where all coordinates are nonzero and $\text{Supp}(D)$ consists of D_F , which contain orbits where at least one coordinate is zero. Hence $D|_{T_N} = 0$ and $\text{div}(f)|_{T_N} \geq 0$ i.e. f is a regular function on $T_N = \text{Spec } \mathbb{C}[M]$. We deduce that $f \in \mathbb{C}[M]$ and thus

$$\Gamma(Y_P, \mathcal{O}(D)) \subset \mathbb{C}[M]$$

Write $f = \sum_{m \in \mathcal{A}} c_m \chi^m$ over some subset $\mathcal{A} \subset M$ and complex coefficients c_m . Note that $\Gamma(Y_P, \mathcal{O}(D))$ is a T_N -invariant subset, under the action

$$\begin{aligned} T_N \curvearrowright \Gamma(Y_P, \mathcal{O}(D)) : t \cdot f &:= f \circ t^{-1} \\ T_N \curvearrowright T_N : t \cdot p &:= (t_1 p_1, \dots, t_n p_n) \end{aligned}$$

because D_F are T_N -invariant and f and $f \circ t^{-1}$ have the same vanishing set. In particular, let

$$B = \text{span}\{\chi^m \mid m \in \mathcal{A}\}$$

Since $\chi^m : T_N \rightarrow \mathbb{C}^*$ is a homomorphism, we see that T_N preserves the space spanned by χ^m because

$$t \cdot \chi^m(p) = \chi^m(t^{-1} \cdot p) = \chi^m(t^{-1}) \chi^m(p) \therefore t \cdot \chi^m = \chi^m(t^{-1}) \chi^m$$

so $W := B \cap \Gamma(Y_P, \mathcal{O}(D))$ (which is finite dimensional because f is a finite sum), as an intersection of T_N -invariant subspaces is also T_N -invariant. Now we apply some results of linear algebra. Note that the T_N -action consists of linear maps on the finite-dimensional space W , so gives rise to commuting finite-dimensional matrices (as T_N is a commutative group) so the matrices can all be simultaneously diagonalized, i.e. we can find a basis of eigenvectors for W . In particular, by representation theory we can write the representation $T_N \rightarrow \text{GL}(W)$ as a direct sum of 1-dimensional representations, namely characters χ^m . So the upshot is that, $f \in W$ is expressed as a sum of characters in $\mathbb{C}[M]$ and also as a sum of characters in W , but by uniqueness those two expressions are the same. So $\chi^m \in W$ for $m \in \mathcal{A}$ and $f \in \bigoplus_{\chi^m \in \Gamma(Y_P, \mathcal{O}(D))} \mathbb{C} \cdot \chi^m$ thus

$$\Gamma(Y_P, \mathcal{O}(D)) = \bigoplus_{\chi^m \in \Gamma(Y_P, \mathcal{O}(D))} \mathbb{C} \cdot \chi^m$$

The final step is as follows. Pick a global section χ^m . The condition $\text{div}(\chi^m) + D \geq 0$, looking at coefficients, is equivalent to the statement

$$\langle m, \nu_F \rangle + a_F \geq 0$$

In other words, this is equivalent to $m \in P$. But since χ^m is a character that means $m \in M$ hence this is equivalent to $m \in P \cap M$ and we get the final result

$$\Gamma(Y_P, \mathcal{O}(D)) = \bigoplus_{m \in P \cap M} \mathbb{C} \cdot \chi^m$$

□

Claim 1.3.28 (Basepoint free, [CLS11][Proposition 6.1.1].) There does not exist a point $p \in Y_P$ where $\chi^{m_i}(p) = 0$ for all $m_i \in P \cap M$. In other words, $\mathcal{O}(D)$ is *basepoint free*, because $\Gamma(Y_P, \mathcal{O}(D)) = \bigoplus_{m_i \in P \cap M} \chi^{m_i}$.

Proof. Recall that faces $Q \subset P$ give cones σ_Q that describe the fan of the polytope Σ_P . We show that for each affine piece U_{σ_Q} , there is a global section which does not vanish on that piece. Since the U_{σ_Q} cover the toric variety, that will suffice.

Write the face $Q = \bigcap_{F \supset Q} F$ as an intersection of facets. Hence

$$Q := \{m \in M_{\mathbb{R}} \mid \langle m, \nu_F \rangle = -a_F, \quad \forall F \supset Q\} \subset M_{\mathbb{R}}$$

Pick a lattice point $m_Q \in Q$, e.g. a vertex. Then χ^{m_Q} is a global section of $\mathcal{O}(D)$ by Claim 1.3.27. Furthermore $\langle m_Q, \nu_F \rangle + a_F = 0$ for $F \supset Q$ means that the order of vanishing of $\chi^{m_Q} + D$ along U_{σ_Q} is zero.

$$(div(\chi^{m_Q}) + D)|_{U_{\sigma_Q}} = \sum_{F \supset Q} (\langle m_Q, \nu_F \rangle + a_F) D_F = 0$$

In other words, $\chi^{m_Q}(U_{\sigma_Q}) \neq 0$. □

Corollary 1.3.29 (Definition of a symplectic form, [Huy05][Example 4.1.2]). *Recall by Claim 1.3.27 that*

$$\Gamma(Y_P, \mathcal{O}(D)) = \bigoplus_{m_i \in P \cap M} \chi^{m_i}$$

Because $\mathcal{O}(D)$ is basepoint free by Claim 1.3.28, these basis elements do not simultaneously vanish at any point $p \in Y_P$. Hence we can define a Kähler form by

$$\omega_P := \frac{i}{2\pi} \bar{\partial} \partial h, \quad h = \frac{1}{\sum_{i=1}^s |\chi^{m_i}|^2}$$

where $|\cdot|$ refers to the standard norm in \mathbb{C} since χ^{m_i} are complex coordinates.

Remark 1.3.30. $\mathcal{O}(D)$ is an ample line bundle, which implies that Y_{Δ} can be viewed as a variety in a projective space. The reason it is ample can be found in [CLS11], and is because of the combinatorics of the polytope. Some multiple kP of the polytope is normal (Chapter 2) which implies the polytope is ample (definition in Chapter 2) which is seen later to be equivalent to the line bundle being ample (Chapter 6). A very ample polytope intuitively has enough lattice points, corresponding to there being enough sections to define an embedding.

Example 1.3.31. Consider the complex projective plane with the standard Fubini-Study form:

$$(\mathbb{CP}^2, \omega_{FS} = \frac{i}{2\pi} \partial \bar{\partial} \log(\sum_{i=0}^2 |z_i|^2))$$

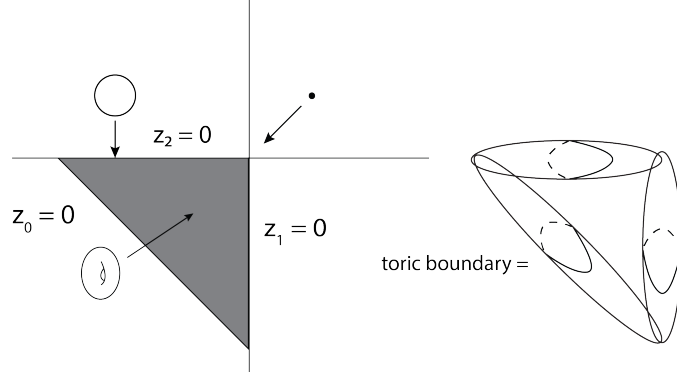


Figure 1.2: Moment map gives Lagrangian torus fibration: \mathbb{CP}^2 example

with points denoted $[z_0 : z_1 : z_2]$. There is a well-defined Hamiltonian T^2 -action as follows:

$$\begin{aligned} (\theta_1, \theta_2) &\in \mathbb{R}^2 / 2\pi\mathbb{Z}^2 = T^2 \curvearrowright \mathbb{CP}^2 \\ \rho(\alpha_1, \alpha_2)[z_0 : z_1 : z_2] &= [z_0 : e^{i\alpha_1} z_1 : e^{i\alpha_2} z_2] \end{aligned} \quad (1.11)$$

This is Hamiltonian:

$$\begin{aligned} X_j &= d\rho \left(\frac{\partial}{\partial \alpha_j} \right) = iz_j \frac{\partial}{\partial z_j} \implies \iota_{X_i} \omega_{FS} = d\mu_i, \quad \mu_i := -\frac{|z_i|^2}{|z_0|^2 + |z_1|^2 + |z_2|^2} \\ \therefore \theta_i &:= \arg(x_i), \quad x_i \text{ local } \mathbb{C}^2 \text{ coordinates} \implies \omega_{FS} = d\mu_1 \wedge d\theta_1 + d\mu_2 \wedge d\theta_2 \end{aligned} \quad (1.12)$$

Thus the moment map $\mu := (\mu_1, \mu_2) : \mathbb{CP}^2 \rightarrow \mathbb{R}^2$ (which is $Lie(T^2), [,] = 0$) given by

$$\mu = \left(-\frac{|z_1|^2}{|z_0|^2 + |z_1|^2 + |z_2|^2}, -\frac{|z_2|^2}{|z_0|^2 + |z_1|^2 + |z_2|^2} \right)$$

can be seen as follows, where the diagonal edge follows from adding $\mu_1 + \mu_2$ and allowing the coordinates to vary:

The moment map gives a Lagrangian torus fibration because the moment map is a function of the norms, so in the preimage of a point in the polytope above we can rotate by the T^2 -action on the angles to obtain a fiber, which is Lagrangian because ω_{FS} is invariant under rotating the complex coordinates.

We can also read off the geometry of the fibration from Figure 1.2. When both local complex coordinates are non-zero, the preimage is T^2 . When one coordinate goes to zero, we only have the other coordinate to rotate, so the fiber is an S^1 . And when both coordinates are zero in each of the three local \mathbb{C}^2 charts we obtain a point.

There are three toric divisors D_0, D_1, D_2 from $z_0 = 0$, $z_1 = 0$, and $z_2 = 0$. This polytope has edges described by the two coordinate axes (say $m_1 = 0, m_2 = 0$) and $m_1 + m_2 = -1$. Two of the facets go through the origin so $a_F = 0$ for those. The equation of the third facet is $\left\langle m, \begin{pmatrix} 1 \\ 1 \end{pmatrix} \right\rangle + 1 = 0$. Hence the line bundle described by this polytope is $\mathcal{O}(\{z_0 = 0\})$ with sections given by the integral vertices of the polytope $\chi^{(0,0)} = 1, \chi^{(-1,0)}, \chi^{(0,-1)}$ and dividing the expression $\sum_{i=0}^2 |z_i|^2$ by the harmonic function $|z_0|^2$ we do find that the expression inside the $\partial\bar{\partial}\log$ (note $\partial\bar{\partial} = -\bar{\partial}\partial$) for the corresponding symplectic form is 1 plus the norm squared of the two sections with simple poles on the divisor $\{z_0\} = 0$, namely z_1/z_0 and z_2/z_0 .

1.4 The A-side manifold

We have the toric background, so the next step is to describe the tools we use to construct the polytope for \tilde{Y} . Since (Y, v_0) for a suitable holomorphic function v_0 should be mirror to $H = \Sigma_2 \subset V$, we would expect that the polytope is built from information about the genus 2 curve. We can glean combinatorial data from the defining section s by taking its tropicalization.

1.4.1 Tropicalization of theta function

Definition 1.4.1 (Tropicalization). Let $f(x) = \sum_{a \in A \subset \mathbb{Z}^n} c_a x^a \tau^{\rho(a)}$. Let $\xi = (\xi_1, \dots, \xi_n)$ be Log coordinates so defined by

$$|x_i| = \tau^{-\xi_i}$$

as earlier. Then

$$f = \sum_a c_a \left(\frac{x}{|x|} \right)^a \tau^{\rho(a) - \langle a, \xi \rangle}$$

In particular, the *tropical limit* corresponds to $\tau^{-1} \rightarrow \infty$, i.e. rescaling $|x_i|$ so that ξ_i remains constant. As $\tau^{-1} \rightarrow \infty$ we see that the leading order term in f is the one with the largest exponent on τ^{-1} , namely

$$\text{Trop}(f) := \max_{a \in A} \langle a, \xi \rangle - \rho(a)$$

Claim 1.4.2. Let s be the theta function above. The tropicalization $\varphi := \text{Trop } s$ satisfies the following periodicity property

$$\varphi(\xi + \tilde{\gamma}) = \varphi(\xi) - \kappa(\tilde{\gamma}) + \langle \xi, \lambda(\tilde{\gamma}) \rangle \quad (1.13)$$

Proof. Recall

$$s(x) = \sum_{\gamma \in \Gamma_B} \tau^{-\kappa(\gamma)} x^{-\lambda(\gamma)}$$

where

$$\begin{aligned}\kappa(\gamma) &= -\frac{1}{2}\lambda(\gamma)^t M \lambda(\gamma), & M &= \begin{pmatrix} 2 & 1 \\ 1 & 2 \end{pmatrix} \\ \lambda(\gamma') &= \begin{pmatrix} 1 \\ 0 \end{pmatrix}, & \lambda(\gamma'') &= \begin{pmatrix} 0 \\ 1 \end{pmatrix}\end{aligned}$$

Here let $|x| = \tau^\xi$. Then this becomes

$$s(x) = \sum_{\gamma \in \Gamma_B} \tau^{-\kappa(\gamma) - \langle \xi, \lambda(\gamma) \rangle}$$

So letting $\tau \rightarrow 0$ we see that the leading term is the minimum exponent or the maximum of its negative, namely

$$\varphi(\xi) := \text{Trop}(s)(\xi) := \max_{\gamma} \kappa(\gamma) + \langle \xi, \lambda(\gamma) \rangle \quad (1.14)$$

Since κ is negative definite of degree 2 and λ is positive of degree 1, this should have a maximum. We have the following periodicity property:

$$\begin{aligned}\varphi(\xi + \tilde{\gamma}) &= \max_{\gamma} \kappa(\gamma) + \langle \xi + \tilde{\gamma}, \lambda(\gamma) \rangle \\ &= \max_{\gamma} \kappa(\gamma) + \langle \xi, \lambda(\gamma) \rangle + \langle \tilde{\gamma}, \lambda(\gamma) \rangle\end{aligned}$$

We know that

$$\kappa(\gamma - \tilde{\gamma}) = \kappa(\gamma) + \kappa(\tilde{\gamma}) + \lambda(\gamma)^t M \lambda(\tilde{\gamma})$$

and

$$M \lambda(\tilde{\gamma}) = \tilde{\gamma}$$

by the above convention for $\lambda(\gamma)$. So we can rewrite the expression for the tropicalization as

$$\begin{aligned}\varphi(\xi + \tilde{\gamma}) &= \max_{\gamma} \langle \xi, \lambda(\gamma) \rangle + [\kappa(\gamma - \tilde{\gamma}) - \kappa(\tilde{\gamma})] \\ &= \left(\max_{\gamma} \kappa(\gamma - \tilde{\gamma}) + \langle \xi, \lambda(\gamma - \tilde{\gamma}) \rangle \right) - \kappa(\tilde{\gamma}) + \langle \xi, \lambda(\tilde{\gamma}) \rangle\end{aligned}$$

This implies that

$$\varphi(\xi + \tilde{\gamma}) = \varphi(\xi) - \kappa(\tilde{\gamma}) + \langle \xi, \lambda(\tilde{\gamma}) \rangle$$

□

Definition 1.4.3 (Vanishing set of tropicalization). The *vanishing of* $\text{Trop}(f)$, denoted $V(\text{Trop}(f))$, is defined to be where two leading order exponents are equal because they can cancel each other out in the limit to get zero.

Claim 1.4.4. $V(\text{Trop } s) \subset \mathbb{R}^2$ is a honeycomb shape that is a tiling by hexagons.

Proof. Let $\xi = 0$. Then $\text{Trop}(s)(0)$ is the maximum over γ of $\kappa(\gamma)$. Note that $\kappa(\gamma)$ is a negative definite form so at most it can be zero. Hence $\varphi(0) = 0$, and since the maximum continues to be achieved by $\gamma = 0$ for ξ in a neighborhood of the origin, the function φ is identically zero in a neighborhood of the origin, which we call the $(0,0)$ tile. We let the (m,n) tile be obtained by moving m times in the γ' direction and n times in the γ'' direction from the $(0,0)$ tile. Now we want to know what happens when we change tiles in order to find the vanishing of the tropicalization.

In what follows in this section ξ is always in the $(0,0)$ tile, and we translate by elements of Γ_B and use the periodicity property of φ to see how its value changes. Let $\tilde{\gamma} = \gamma' := (2,1)$. Then the above equation tells us that for ξ in the $(0,0)$ tile

$$\varphi(\xi + \gamma') = 0 + \frac{1}{2}(1,0)M(1,0)^t + \xi_1 = \xi_1 + 1$$

So setting this equal to 0 we should find where the two piecewise linear components meet. $\xi_1 + 1 = 0 \implies \xi_1 = -1$. Since $\xi_1 = -1$ exactly when the first component of $\xi + \gamma'$ is equal to $-1 + 2 = 1$, we find that the $(0,0)$ and $(1,0)$ tiles meet along the line $\xi_1 = 1$.

Similarly we see what happens when we move in the $\gamma'' = (1,2)$ direction. For ξ in the $(0,0)$ tile

$$\varphi(\xi + \gamma'') = 0 + \frac{1}{2}(0,1)M(0,1)^t + \xi_2 = \xi_2 + 1$$

and similarly we find that the $(0,0)$ tile and $(0,1)$ tile intersect along $\xi_2 = 1$.

Next we consider moving in the negative γ' and γ'' directions. Then

$$\varphi(\xi - \gamma') = 0 + \frac{1}{2}(-1,0)M(-1,0)^t - \xi_1 = -\xi_1 + 1$$

so $-\xi_1 + 1 = 0 \implies \xi_1 = 1$ so the two tiles intersect along the line $\xi_1 = -1$. And similarly along $\xi_2 = -1$ for the $(0,0)$ and $(0,-1)$ tile.

We almost have the hexagonal shape of \mathbb{CP}^2 blown up in three points. We just check $\gamma'' - \gamma'$ and $\gamma' - \gamma''$ when ξ is again in the $(0,0)$ tile.

$$\varphi(\xi + \gamma'' - \gamma') = \varphi(\xi + \gamma'') + \frac{1}{2}(-1,0)M(-1,0)^t + \langle \xi + \gamma'', \lambda(-\gamma') \rangle = \xi_2 + 1 + 1 - \xi_1 - 1 = -\xi_1 + \xi_2 + 1$$

which, setting equal to 0 we get $\xi_1 - \xi_2 = 1$. This line is parametrized as $(t+1, t)$ which means the vanishing of the tropicalization there is $(t+1, t) + \gamma'' - \gamma' = (t+1, t) + (1, 2) - (2, 1) = (t+1, t) + (-1, 1) = (t, t+1)$. This intersects the line $\xi_1 = -1$ when $t = -1$ and the line $\xi_2 = 1$ when $t = 0$ so those are the bounds i.e. the line segment from $(-1, 0)$ to $(0, 1)$.

Final edge:

$$\varphi(\xi + \gamma' - \gamma'') = \varphi(\xi + \gamma') + \frac{1}{2}(0, -1)M(0, -1)^t + \langle \xi, \lambda(-\gamma'') \rangle = \xi_1 + 1 + 1 - \xi_2 - 1 = \xi_1 - \xi_2 + 1$$

so $(t, t+1) + (2, 1) - (1, 2) = (t, t+1) + (1, -1) = (t+1, t)$ which intersects $\xi_1 = 1$ at $t = 0$ and $\xi_2 = -1$ at $t = -1$ so we get the line segment from $(0, -1)$ to $(1, 0)$.

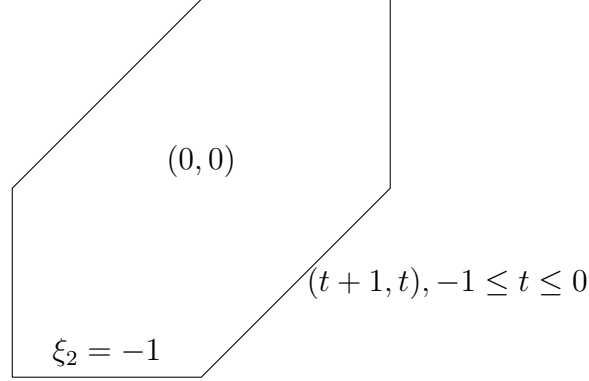


Figure 1.3: The $(0,0)$ tile delimited by the tropical curve

So by periodicity, this picture tiles the plane, and the slope of the (m, n) tile is going to be $m\xi_1 + n\xi_2 + \kappa(m\gamma' + n\gamma'')$ by Equation 1.14. \square

1.4.2 Outline: definition of (Y, v_0) and ω

The smooth manifold Y is constructed as a portion of a toric variety \tilde{Y} quotiented by Γ_B acting properly discontinuously via holomorphic maps. The defining polytope is

$$\begin{aligned} \Delta_{\tilde{Y}} &:= \{(\xi_1, \xi_2, \eta) \in \mathbb{R}^3 \mid \eta \geq \text{Trop}(s)(\xi)\} \\ \Delta_Y &:= (\Delta_{\tilde{Y}})|_{\eta \leq T^l} / \Gamma_B \text{ where} \\ \text{Trop}(s)(\xi) &:= \max_{\gamma} \kappa(\gamma) + \langle \xi, \lambda(\gamma) \rangle \\ \gamma \cdot (\xi_1, \xi_2, \eta) &:= (\xi_1 + \gamma_1, \xi_2 + \gamma_2, \eta - \kappa(\gamma) + \langle \xi, \lambda(\gamma) \rangle) \\ \therefore \text{Trop}(s)(\xi + \gamma) &= \text{Trop}(s)(\xi) - \kappa(\gamma) + \langle \xi, \lambda(\gamma) \rangle \end{aligned} \tag{1.15}$$

The polytope $\Delta_{\tilde{Y}}$ is illustrated in Figure 1.8, where η is bounded below by the expression in the center of the tile, and comes out of the page. We discuss the complex coordinates on Y below. For now we give a definition.

Definition 1.4.5 ([AAK16][Definition 1.2]). (Y, v_0) is a *generalized SYZ mirror* for $H = \Sigma_2$.

Remark 1.4.6. Note that one can apply SYZ in the reverse direction by starting with a Lagrangian torus fibration on Y minus a divisor to recover X as its complex mirror, see [AAK16, §8] or [CLL12].

1.4.3 Pair of pants: the local model

We describe an illustrative example of generalized SYZ that is the local model of our setting.

Example 1.4.7 ([AAK16][§9.1]). Suppose $H \subset V$ is the pair of pants $f(x_1, x_2) := 1 + x_1 + x_2 = 0$ in $V = (\mathbb{C}^*)^2$. This is a pair of pants because $x_1 \in \mathbb{C}^* \setminus \{-1\}$ and a cylinder minus a point is a pair of pants. Recall the definition of $\text{Trop}(f)$ in Definition 1.4.1.

So in the pair of pants example, $\rho \equiv 0$ and $A = \{(0, 0), (1, 0), (0, 1)\}$ hence $\text{Trop}(f)(\xi_1, \xi_2) = \max\{0, \xi_1, \xi_2\}$. If $\xi_1, \xi_2 < 0$ then 0 is the maximum, if $\xi_1 > \xi_2 > 0$ then ξ_1 is the maximum and if $\xi_2 > \xi_1 > 0$ then ξ_2 is the maximum. So the zero set (Definition 1.4.3) of $\text{Trop}(f)$ is the following picture

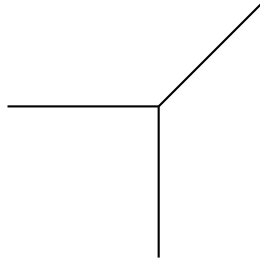


Figure 1.4: $\text{Trop}(1 + x_1 + x_2) = 0$

and the moment polytope is $\Delta := \{(\xi, \eta) \mid \eta \geq \text{Trop}(f)(\xi)\} \subset \mathbb{R}^{n+1}$ which gives

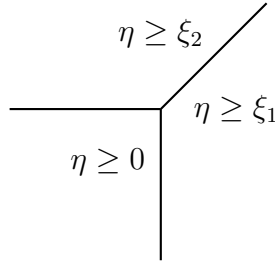


Figure 1.5: Moment polytope $\subset \mathbb{R}^3$

Under a linear transformation on (ξ_1, ξ_2, η) this polytope becomes $\mathbb{R}_{\geq 0}^3$. Then the corresponding toric variety is $\text{Spec } \mathbb{C}[x, y, z] = \mathbb{C}^3$. The superpotential is $v_0 = xyz$ and we get the expected mirror to the pair of pants, (\mathbb{C}^3, xyz) .

1.4.4 ω determines Γ_B -action on complex coordinates

We want to construct a symplectic form ω so that 1) it is Kähler i.e. compatible with the complex structure inherited from the complex toric coordinates, 2) $v_0 := xyz$ is a symplectic

fibration and 3) it is toric, i.e. invariant under the torus action.

Because of 3), it suffices to define the symplectic form in terms of the norms of the complex coordinates. To ensure 1), we define ω locally as $\frac{i}{2\pi}\partial\bar{\partial}$ of a suitable Kähler potential, where $\partial\bar{\partial}$ is taken with respect to the local complex toric coordinates. To ensure 2) we need all fibers to be symplectic when we restrict the symplectic form. The central fiber is the toric variety with moment polytope given by the hexagon in Figure 1.6, quotiented by Γ_B . This comes equipped with a symplectic form as described in the theory of Section 1.3 with the toric variety $\mathbb{CP}^2(3 \text{ points})$. As we move away from $v_0 = 0$ but still near a vertex of the polytope, the toric variety is locally modelled on the (\mathbb{C}^3, xyz) picture that was the local model of Example 1.4.7. So we will use bump functions to interpolate between the toric symplectic form of $\mathbb{CP}^2(3 \text{ points})$ and the standard form on \mathbb{C}^3 .

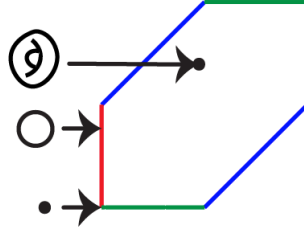


Figure 1.6: Moment polytope for central fiber of (Y, v_0) when $H = \Sigma_2$.

We explain the pictorial motivation for how the symplectic form is constructed in the one dimension down case.

Example 1.4.8 ($H = pt$). Let H be a point inside an elliptic curve. Then the polytope $\Delta_{\tilde{Y}}$ is two-dimensional, so we can draw it.

A fiber of $v_0 : \tilde{Y} \rightarrow \mathbb{C}$ is topologically a cylinder with necks increasingly pinched, \mathbb{Z} -periodically, as $|v_0| \rightarrow 0$, degenerating to a string of \mathbb{P}^1 's over the central fiber. Around the widest parts of the cylinder, it looks like a portion of a sphere, and \mathbb{P}^1 comes canonically equipped with the Fubini-Study form. On the other hand, neighborhoods of the vertices of the polytope give charts \mathbb{C}^2 and the local picture of the Lefschetz fibration $\mathbb{C}^2 \rightarrow \mathbb{C}$, $(x, y) \mapsto xy$ where cylinders degenerate to a cone over zero. In particular, \mathbb{C}^2 comes canonically equipped with the standard form ω_{std} . When the toric coordinates are very small, the Fubini-Study form and the standard form are approximately the same by a Taylor expansion of \log . For example when Tr_x is very small, we have $\log(1 + (Tr_x)^2) \approx (Tr_x)^2$.

So a symplectic form can be constructed by interpolating between these two Kähler forms.

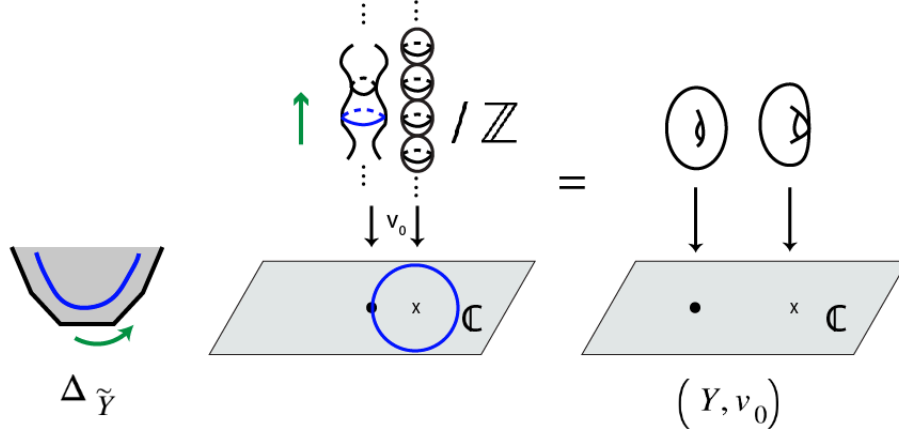


Figure 1.7: In one dimension lower, the boundary of $\Delta_{\tilde{Y}}$ is the moment map image of a string of \mathbb{P}^1 's. In the polytope, $|v_0|$ increases in the $(0, 1)$ direction. In the fibration v_0 , $|v_0|$ is the radius of the circle in the base.

Example 1.4.9 ($H = \Sigma_2$). Let $r_x = |x|$ etc and $0 < T \ll 1$ be a constant. In the case of $H = \Sigma_2$, the symplectic form will interpolate between $(\mathbb{C}^3, \omega_{std})$ with Kähler potential $\frac{1}{3}T^2(r_x^2 + r_y^2 + r_z^2)$ from charts locally around the vertices, and the toric Kähler form induced by the hexagon as $\mathbb{CP}^2(3 \text{ points})$, the blow-up at three points. The Kähler potential is the logarithm of the sum of squares of suitably scaled sections corresponding to lattice points, as described in Corollary 1.3.29.

Lemma 1.4.10. *Set $g_{xy} := \log(1 + |T^a x|^2)(1 + |T^b y|^2)(1 + |T^c xy|^2)$ for some (a, b, c) . Then $(a, b, c) = (1, 1, 2)$ has the correct symmetries for ω to be compatible with the Γ_B -action and define a symplectic form on the quotient \tilde{Y}/Γ_B .*

Proof. Consider Figure 1.8, depicting the three dimensional $\Delta_{\tilde{Y}}$ of this thesis. By toric geometry we know (x, y) must map to some scaling of (y^{-1}, xy) as drawn in that figure. We will define a suitable (α, β) in what follows so that the scaling is $(x, y) \mapsto (T^\alpha y^{-1}, T^\beta xy)$.

Definition 1.4.11. Define $G = \mathbb{Z}/6 \curvearrowright \tilde{Y}$ to rotate the hexagon clockwise as follows, where g is the generator of G :

$$g \cdot (x, y) = (T^\alpha y^{-1}, T^\beta xy) \quad (1.16)$$

More specifically, this action on (x, y) determines an action on \tilde{Y} by prescribing it to restrict to an action on a fiber of v_0 , either a generic one or the degenerate central one. In other words, the action on the z coordinate is $g \cdot z = T^{-\alpha-\beta} yz$ so that $v_0 = xyz \mapsto T^{\alpha+\beta-\alpha-\beta} y^{-1} \cdot xy \cdot yz = xyz$ is preserved.

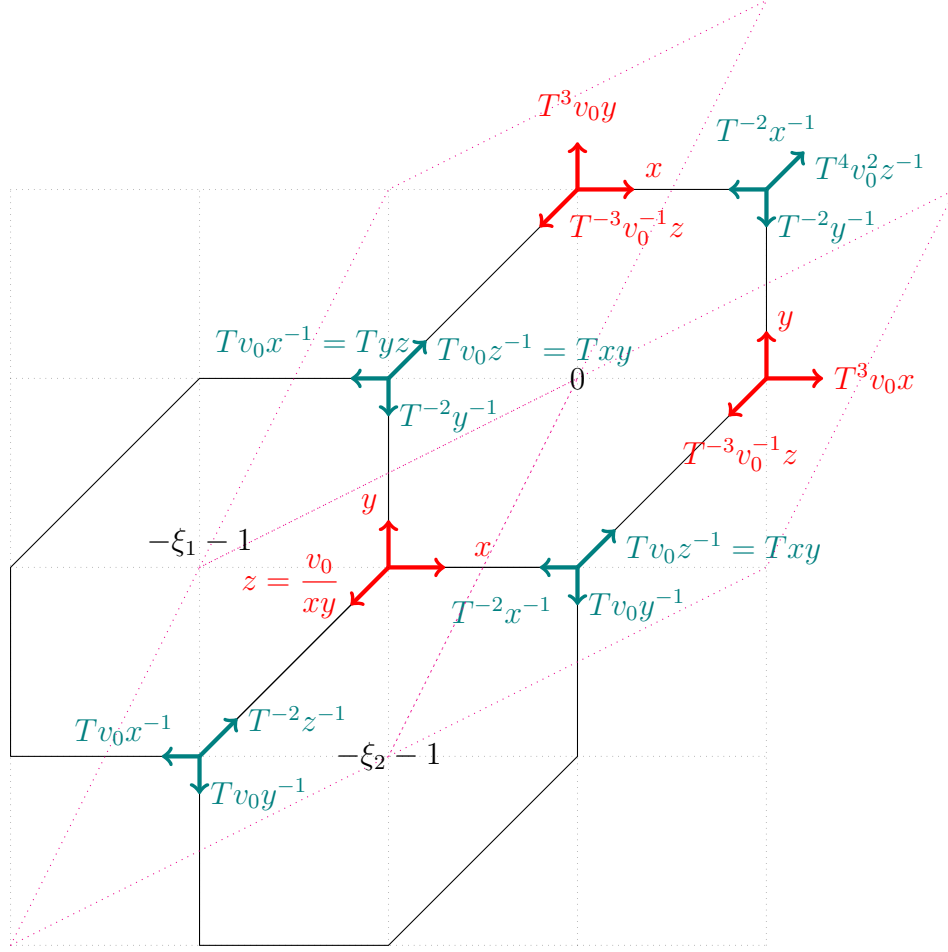


Figure 1.8: Depiction of 3D $\Delta_{\tilde{\gamma}}$. Coordinates respect Γ_B -action, see below; magenta parallelogram = fundamental domain. Vertices = \mathbb{C}^3 charts. Coordinate transitions, see Lemma 1.4.10. Expressions in the center of tiles indicate e.g. $\eta \geq \varphi(\xi) = -\xi_1 - 1$ over that tile, so $\text{tile}_{(0,0)}$ is given by $(\xi_1, \xi_2) \in \{(\xi_1, \xi_2) \mid -1 \leq \xi_1, \xi_2, -\xi_1 + \xi_2 \leq 1\}$.

$$g^* \log(1 + |T^a x|^2)(1 + |T^b y|^2)(1 + |T^c xy|^2) = \log(1 + |T^{a+\alpha} y^{-1}|^2)(1 + |T^{b+\beta} xy|^2)(1 + |T^{c+\alpha+\beta} x|^2)$$

$$g_{xy} = \log(1 + |T^a x|^2)(1 + |T^b y|^2)(1 + |T^c xy|^2)$$

We expect the two potentials to differ by $\log |T^b y|^2$ because y becomes y^{-1} under g . So

comparing exponents we obtain:

$$\begin{aligned} b &= -a - \alpha \\ a &= c + \alpha + \beta \\ c &= b + \beta \end{aligned}$$

We have 5 unknowns and 3 equations so should be able to reduce to 2 unknowns. Namely write (a, b, c) in terms of (α, β) and then, requiring $x \leftrightarrow y$ symmetry, we impose $a = b$ and determine α in terms of β .

$$\begin{aligned} a &= c + \alpha + \beta = (b + \beta) + \alpha + \beta = (-a - \alpha) + \alpha + 2\beta \\ \implies a &= \beta \\ \implies b &= -\alpha - \beta \\ a = b &\therefore \alpha = -2\beta \\ \implies c &= b + \beta = 2\beta \\ \therefore g_{xy} &= \log(1 + |T^\beta x|^2)(1 + |T^\beta y|^2)(1 + |T^{2\beta} xy|^2) \\ \text{Choose } \beta = 1 &\implies g_{xy} = \log(1 + |Tx|^2)(1 + |Ty|^2)(1 + |T^2 xy|^2) \end{aligned}$$

Since we set $\beta = 1$, we see that along the x axis (so y and z axes by symmetry), the complex modulus changes by T^{-2} . So the value of y becomes large when we apply g , but the new coordinate system there denoted (x'', y'', z'') , will have the same small values as at (x, y, z) . \square

Note that the \mathbb{P}^1 -edges have symplectic area 1, for this particular choice of symplectic form.

Claim 1.4.12. Under G , if g_{xy} maps to a Kähler potential that differs by a harmonic function, namely by $\log |T^{\alpha/2} y|^2$, then the symplectic area of the \mathbb{P}^1 along the y -axis is 1.

Proof. We consider the calculation along the z -axis, which suffices because that along the y -axis is analogous once we have the symmetries. Note that the symplectic area of the \mathbb{P}^1 along the z -axis is 1, by Stokes' theorem. Recall \mathbb{P}^1 has an open covering U_0, U_∞ and charts ϕ_0 and ϕ_1 sending $[z_0 : z_1]$ to z_1/z_0 and z_0/z_1 respectively. We want to split up the integration over \mathbb{P}^1 into these two charts, but only the portion of the chart up to where they intersect (else we integrate over too much). So we have z is the coordinate on $\phi_0(U_0) \cong \mathbb{C}$ then it is $1/(T^\alpha z)$ on $\phi_\infty(U_\infty)$ and $|z| = |1/T^\alpha z| \implies |z| = 1/T^{\alpha/2}$. Then let D_0 be the disc in $\phi_0(U_0)$ and D_∞ the corresponding in the other one. Let F_0, F_∞ be the Kähler potential in the two charts.

$$\begin{aligned}
\int_{\mathbb{P}^1} \frac{i}{2\pi} \partial \bar{\partial} F &= \frac{i}{2\pi} \left[\int_{\phi_0^{-1}(D_0)} d(\bar{\partial} F) + \int_{-\phi_\infty^{-1}(D_\infty)} d(\bar{\partial} F) \right] \\
&= \frac{i}{2\pi} \left[\int_{\partial D_0} \bar{\partial}(\phi_0^{-1})^* F - \int_{\partial D_\infty} \bar{\partial}(\phi_\infty^{-1})^* F \right] \\
&= \frac{i}{2\pi} \int_{C_{1/T^{\alpha/2}}} \bar{\partial}(F_0 - F_\infty) \\
&= \frac{i}{2\pi} \int_{C_{1/T^{\alpha/2}}} \bar{\partial} \log(|T^{\alpha/2} z|^2) = \frac{i}{2\pi} \int_{C_{1/T^{\alpha/2}}} \frac{T^\alpha z d\bar{z}}{|T^{\alpha/2} z|^2} \\
&= \frac{i}{2\pi} \int_0^{2\pi} e^{i\theta} (-i) e^{-i\theta} d\theta = 1
\end{aligned}$$

□

We see in the next section why $(\alpha, \beta) = (-2, 1)$ and $g \cdot (x, y) = (T^{-2}y^{-1}, Txy)$ determine the Γ_B -action depicted in Figure 1.8. Then this allows us to define Y as the quotient \tilde{Y}/Γ_B where \tilde{Y} is constructed from $\Delta_{\tilde{Y}}$ as explained in Section 1.3.

1.4.5 The definition of Y

Remark 1.4.13 (Convention). The convention is that moving up and right in Figure 1.8 is negative since the powers of $T \ll 1$ are positive, hence decreasing values in the coordinates corresponds with moving in the negative direction of the group action. That is, the actions of γ' and γ'' map the coordinates (x, y, z) to the charts centered at $(-2, -1)$ and $(-1, -2)$ respectively in Figure 1.8.

Definition 1.4.14 (Definition of the Γ_B -action). The Γ_B -action on (x, y, z) can be read off from the $\mathbb{Z}/6$ -action defined above in Definition 1.4.11 as follows. Namely, g^2 maps (x, y, z) to the coordinate system centered at $(\xi_1, \xi_2) = (1, 2)$ as $-\gamma''$ would, but it permutes the coordinate directions by a rotation. Indeed, g sends $(x, y, z) \mapsto (T^{-2}y^{-1}, Txy, Tyz)$. After undoing this permutation in g so the directions are preserved, i.e. $(x, y, z) \mapsto (Tyz, T^{-2}y^{-1}, Txy) = (Tv_0x^{-1}, T^{-2}y^{-1}, Tv_0z^{-1})$, we can define the Γ_B -action by similarly permuting the resulting coordinates from applying g^2 :

$$(-\gamma'') \cdot (x, y, z) := (x, T^3v_0y, T^{-3}v_0^{-1}z)$$

Definition 1.4.15 (Definition of Y). Now we may define Y via the quotient \tilde{Y}/Γ_B :

$$\begin{aligned}
\Delta_{\tilde{Y}} &:= \{(\xi_1, \xi_2, \eta) \in \mathbb{R}^3 \mid \eta \geq \text{Trop}(s)(\xi)\} \\
\Delta_Y &:= (\Delta_{\tilde{Y}})|_{\eta \leq T^l} / \Gamma_B \text{ where Equation 1.13 implies} \\
\gamma \cdot (\xi_1, \xi_2, \eta) &:= (\xi_1 + \gamma_1, \xi_2 + \gamma_2, \eta - \kappa(\gamma) + \langle \xi, \lambda(\gamma) \rangle)
\end{aligned} \tag{1.17}$$

Every vertex of $\Delta_{\tilde{Y}}$ corresponds to three complex coordinates which we can write in terms of (x, y, z) (and $v_0 = xyz$). Figure 1.8 lists these coordinates, which we gather here for clarity as charts U_{n,g^k} where $\gamma = n_1\gamma' + n_2\gamma''$ denotes the center of the tile in $\Delta_{\tilde{Y}}$ we are looking at, when projected to the first two coordinates, and g^k denotes how far around the hexagon we are. The g^k allows us to index the charts, but as noted in Definition 1.4.14 the coordinates are a permutation of the coordinates $g^k \cdot (x, y, z)$ so the subscript is mainly for indexing. The transition maps are

$$(x, y, z) \mapsto \sigma_{g^n} \cdot (g^n \circ \gamma) \cdot (x, y, z), \quad n \in \mathbb{Z}/6, \gamma \in \Gamma_B$$

for a suitable permutation σ_{g^n} on the coordinates that depends on n , see Definition 1.4.14. Going clockwise around on the $(0, 0)$ tile from (x, y, z) :

- $U_{\underline{0},g^0} : (x, y, z)$
- $U_{\underline{0},g} : (Tv_0x^{-1}, T^{-2}y^{-1}, Tv_0z^{-1}) =: (x'', y'', z'')$
- $U_{\underline{0},g^2} : (x, T^3v_0y, T^{-3}v_0^{-1}z) =: (-\gamma'') \cdot (x, y, z)$
- $U_{\underline{0},g^3} : (T^{-2}x^{-1}, T^{-2}y^{-1}, T^4v_0^2z^{-1})$
- $U_{\underline{0},g^4} : (T^3v_0x, y, T^{-3}v_0^{-1}z) =: (-\gamma') \cdot (x, y, z)$
- $U_{\underline{0},g^5} : (T^{-2}x^{-1}, Tv_0y^{-1}, Tv_0z^{-1}) =: (x', y', z')$
- Going along the z axis we get to the g^{-1} vertex in the $(-1, 0)$ tile:
- $U_{(-1,0),g^{-1}} : (Tv_0x^{-1}, Tv_0y^{-1}, T^{-2}z^{-1}) =: (x''', y''', z''')$

The upshot is that for $|v_0| = T^l$ with $T \ll 1$ and l sufficiently small, Γ_B acts properly discontinuously and holomorphically so the quotient is a well-defined complex manifold Y .

Calculation of coordinates from $\mathbb{Z}/6$ action. Since $g \cdot (x, y) = (T^{-2}y^{-1}, Txy)$, applying the group action twice we find

$$(x, y) \sim (T^{-2}y^{-1}, Txy) \sim (T^{-2}(T^{-1}x^{-1}y^{-1}), T(T^{-2}T^{-1})(Txy)) = (T^{-3}x^{-1}y^{-1}, x)$$

In particular Γ_B fixes $v_0 = xyz$ so we may rewrite the transformed y -coordinate as T^3v_0y to obtain the γ'' action, after suitable permutation σ_{g^2} :

$$\sigma_{g^2} \cdot g^2 \cdot (x, y, z) =: -\gamma'' \cdot (x, y, z) = (x, T^3v_0y, T^{-3}v_0^{-1}z)$$

The γ' calculation is similar. To find the coordinate system (x''', y''', z''') , we first move down and left by γ' action to be in the $(0, -1)$ tile, then rotate by g^{-1} and finally apply a suitable permutation. Since $g^{-1} \cdot (x, y) = (Txy, T^{-2}x^{-1})$ we obtain $g^{-1} \cdot (x, y, z) =$

$(Tv_0z^{-1}, T^{-2}x^{-1}, Tv_0y^{-1})$. Then:

$$\begin{aligned}\gamma' \cdot (x, y, z) &= (T^{-3}v_0^{-1}x, y, T^3v_0z) \\ g^{-1} \cdot (T^{-3}v_0^{-1}x, y, T^3v_0z) &= (Tv_0(T^3v_0z)^{-1}, T^{-2}(T^{-3}v_0^{-1}x)^{-1}, Tv_0y^{-1}) \\ &= (T^{-2}z^{-1}, Tv_0x^{-1}, Tv_0y^{-1}) \\ \therefore (x''', y''', z''') &:= \sigma_{g^{-1}} \cdot g^{-1} \cdot \gamma' \cdot (x, y, z) = (Tv_0x^{-1}, Tv_0y^{-1}, T^{-2}z^{-1})\end{aligned}$$

The calculations to obtain the remaining coordinates in the charts listed above are similar. \square

Remark 1.4.16. Note that the symmetry properties required for ω told us what complex structure was needed (it produces a product complex structure), which by mirror symmetry will correspond to a specific symplectic form on A-model of X . We label some of the green chart coordinates of Figure 1.8 with new primed-variables in the list in Definition 1.4.15 above.

Corollary 1.4.17 (Complex structure on Y). *The complex structure is obtained by first identifying toric charts for each vertex of the polytope $\Delta_{\tilde{Y}}$ by gluing (x, y, z) to the new coordinate system of each of the other vertices. Then we quotient by the action of Γ_B , which rescales the coordinates while preserving $v_0 = xyz$, so that the fibers of v_0 on the quotient are abelian varieties. In terms of the complex coordinates the Γ_B -action is:*

$$\begin{aligned}(x, y, z) &\sim (T^3v_0x, y, T^{-3}v_0^{-1}z) \\ (x, y, z) &\sim (x, T^3v_0y, T^{-3}v_0^{-1}z)\end{aligned}$$

Remark 1.4.18. Note that before the Γ_B -action quotient the fibers would be $(\mathbb{C}^*)^2$ after gluing all the toric charts together. The Γ_B -action in complex coordinates corresponds to passing from $\Delta_{\tilde{Y}}$ to $\Delta_Y = \Delta_{\tilde{Y}}/\Gamma_B$. We still glue toric charts by identifying monomials according to the polytope, but we allow rescaling to happen when gluing the complex coordinates. (E.g. in a lower dimension for $\mathbb{C}^* \ni x \mapsto Tx$ we glue a unit circle with a radius T circle, giving a torus.)

Remark 1.4.19 (Terminology). The toric variety \tilde{Y} is referred to as a toric variety of “infinite-type” by [KL19], because of the infinitely many facets, where the neighborhood of the toric divisor there is the same as our restriction to $|v_0|$ small, i.e. η small.

Definition 1.4.20 (Superpotential). The *superpotential* v_0 is the holomorphic function $Y \rightarrow \mathbb{C}$ defined to be

$$v_0(x, y, z) := xyz \tag{1.18}$$

which is well-defined as a global function on Y because it is invariant under the Γ_B action.

Remark 1.4.21. We will equip v_0 with the structure of a symplectic fibration in Section 2, which we then equip with a Fukaya-Seidel category in Section 4.1.

Remark 1.4.22. The Γ_B -action on complex coordinates here is different than that described in [AAK16, §10.2]. That means that Y is mirror to X with a different symplectic form than the one considered in their paper. The complex structure there is

$$\mathbf{v}^m \sim v_0^{\langle \lambda(\gamma), m \rangle} T^{\langle \gamma, m \rangle} \mathbf{v}^m \quad (1.19)$$

where they use complex coordinates $\mathbf{v} = (v_1, v_2)$. Thus setting $(x, y, z) = (v_1^{-1}, v_2^{-1}, v_0 v_1 v_2)$, their complex structure arises from the following Γ_B -action:

$$\begin{aligned} \gamma' \cdot (x, y, z) &= (T^{-2} v_0^{-1} x, T^{-1} y, T^3 v_0 z) \\ \gamma'' \cdot (x, y, z) &= (T^{-1} x, T^{-2} v_0^{-1} y, T^3 v_0 z) \end{aligned}$$

1.4.6 Delineating polytope into regions

Recall the polytope $\Delta_{\tilde{Y}}$ of Figure 1.8. We will start by defining ω in a neighborhood of a vertex. It will be defined in terms of a new set of local real radial and angular coordinates d and θ on \tilde{Y} in each delineated region of Figure 1.10.

The delineations are defined in terms of the following variables. We fix $|v_0| (= |xyz|) = T^l$ for $T \ll 1$ and l a large positive constant. In the support of Figure 1.10, we have $r_x, r_y, r_z \ll 1$ so the approximations of Equation 1.21 are valid.

We define functions ϕ_x, ϕ_y, ϕ_z which will be crucial in understanding calculations to follow.

$$\begin{aligned} \phi_x(x, y, z) &:= \log_T \frac{1 + |Tx|^2}{1 + |T^2 yz|^2} \\ \phi_y(x, y, z) &:= \log_T \frac{1 + |Ty|^2}{1 + |T^2 xz|^2} \\ \phi_z(x, y, z) &:= \log_T \frac{1 + |Tz|^2}{1 + |T^2 xy|^2} \end{aligned} \quad (1.20)$$

Now we can define the the local radial and angular coordinates we'll do calculations with. Their subscripts indicate which region of Figure 1.4.6 they are defined in:

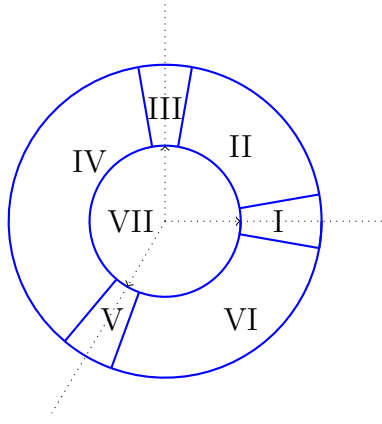


Figure 1.9: Delineate regions in $\Delta_{\tilde{\gamma}}$ around a vertex

$$\begin{aligned}
 d_I &:= \phi_x - \frac{1}{2}(\phi_y + \phi_z) \\
 &= \log_T \left(\frac{1 + |Tx|^2}{1 + |T^2 v_0 x^{-1}|^2} / \sqrt{\frac{1 + |Ty|^2}{1 + |T^2 v_0 y^{-1}|^2} \cdot \frac{1 + |Tz|^2}{1 + |T^2 v_0 z^{-1}|^2}} \right) \\
 &\approx (Tr_x)^2 - \frac{1}{2}((Tr_y)^2 + (Tr_z)^2) \text{ for } r_x, r_y, r_z \ll 1
 \end{aligned} \tag{1.21}$$

$$\begin{aligned}
 \theta_I &:= \phi_y - \phi_z \\
 &= \log_T \left(\frac{1 + |Ty|^2}{1 + |Tz|^2} \cdot \frac{1 + |T^2 xy|^2}{1 + |T^2 xz|^2} \right) \approx (Tr_y)^2 - (Tr_z)^2
 \end{aligned}$$

$$\begin{aligned}
 d_{IIA} &:= \phi_x - \frac{1}{2}(\phi_y + \phi_z) + \frac{3}{2}\alpha_6(\theta_{II}) \cdot \phi_y \approx T^2[r_x^2 - \frac{1}{2}(r_y^2 + r_z^2) + \frac{3}{2}\alpha_6(\theta_{II}) \cdot r_y^2] \\
 d_{IIB} &:= \phi_x + \phi_y - \frac{1}{2}\phi_z \\
 d_{IIC} &:= \phi_y - \frac{1}{2}(\phi_x + \phi_z) + \frac{3}{2}\alpha_6(-\theta_{II}) \cdot \phi_x \\
 \theta_{II} &:= \log_T r_y - \log_T r_x
 \end{aligned} \tag{1.22}$$

where α_6 is a cut-off function in the angular direction that we define below. Lastly, we define

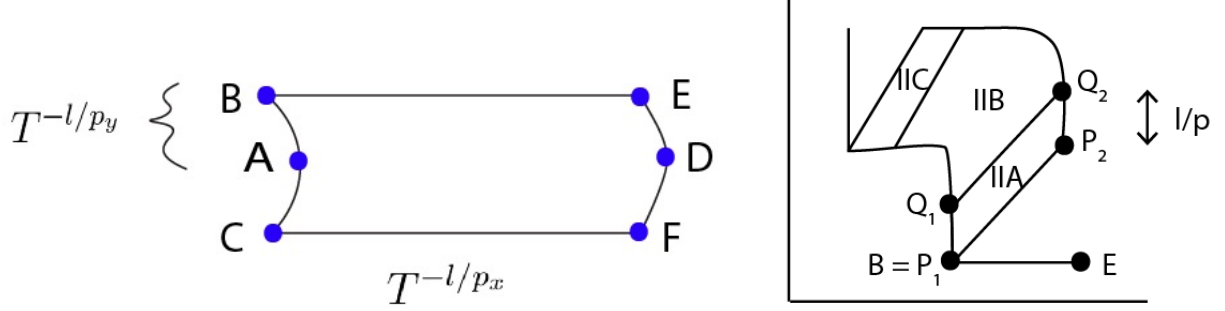


Figure 1.10: Zoom in on region I/II in left/right figures respectively

$$\begin{aligned}
 d_{III} &:= \phi_y - \frac{1}{2}(\phi_x + \phi_z) \\
 \theta_{III} &:= \phi_z - \phi_x
 \end{aligned}
 \tag{1.23}$$

$$\begin{aligned}
 d_V &:= \phi_z - \frac{1}{2}(\phi_x + \phi_y) \\
 \theta_V &:= \phi_x - \phi_y
 \end{aligned}$$

Along the axes in the top diagram of Figure 1.10 we have $r_y = r_z < r_x$ for the $(1, 0)$ direction, $r_x = r_z < r_y$ for the $(0, 1)$ direction and $r_x = r_y < r_z$ for the $(-1, -1)$ direction.

Definition 1.4.23 (Definition of regions in Figure 1.10). The curves delineating region I are: on the left and right d_I is constant and on the top and bottom θ_I is constant. We can approximate these as r_x constant and r_y constant respectively, letting the other two variables vary while $|xyz| = T^l$ remains constant. Over the origin in region VII $|x| = |y| = |z| = T^{l/3}$ because the three coordinates are equal and their product is $|v_0| = T^l$. We define the following, for a value of p sufficiently large.

Region I

- $A(r_x, r_y, r_z) = (T^{l/4}, T^{3l/8}, T^{3l/8})$
- $B(r_x, r_y, r_z) \approx (T^{l/4}, T^{3l/8-l/p}, T^{3l/8+l/p})$.
- $C(r_x, r_y, r_z) \approx (T^{l/4}, T^{3l/8+l/p}, T^{3l/8-l/p})$
- $D(r_x, r_y, r_z) = (T^{l/4-l/p}, T^{3l/8+l/2p}, T^{3l/8+l/2p})$.
Here r_x has increased while maintaining $r_y = r_z$.
- $E(r_x, r_y, r_z) \approx (T^{l/4-l/p}, T^{3l/8-l/p}, T^{3l/8+2l/p})$.

- $F(r_x, r_y, r_z) \approx (T^{l/4-l/p}, T^{3l/8+2l/p}, T^{3l/8-l/p})$

The curves delineating region II are θ_{II} constant for the radially outward lines, and d_{IIA} or d_{IIB} constant along angular curves. Note that d_{IIA} constant here is approximately r_x constant.

Region II

- $P_1 = B \approx (T^{l/4}, T^{3l/8-l/p}, T^{3l/8+l/p})$

- $P_2 \approx (T^{l/4-l/p}, T^{3l/8-2l/p}, T^{3l/8+3l/p})$.

This follows because the sliver from P_1 to P_2 is $\theta_{II} = \log_T r_y - \log_T r_x$ constant, while P_2 is obtained by moving E up along constant $d_I \approx (Tr_x)^2$ so $r_x(P_2) \approx T^{l/4-l/p}$. Then constant θ_{II} implies:

$$\begin{aligned} \theta_{II}(P_1) &\approx 3l/8 - l/p - l/4 = l/8 - l/p \\ &= \theta_{II}(P_2) \approx \log_T r_y - (l/4 - l/p) \\ \implies \log_T r_y &\approx 3l/8 - 2l/p \end{aligned}$$

- $Q_1 \approx (T^{l/4}, T^{3l/8-2l/p}, T^{3l/8+2l/p})$

From P_1 to Q_1 along d_{IIA} constant we increase r_y by a factor of $T^{-l/p}$ keeping r_x approximately constant.

- $Q_2 \approx (T^{l/4-l/p}, T^{3l/8-3l/p}, T^{3l/8+4l/p})$

From Q_1 to Q_2 we have θ_{II} is constant and at Q_1 we have $\theta_{II}(Q_1) \approx 3l/8 - 2l/p - l/4 = l/8 - 2l/p$. From P_2 to Q_2 we have r_x approximately constant hence $\log_T r_x$ at Q_2 is approximately $l/4 - l/p$ so

$$\log_T r_y \approx (l/8 - 2l/p) + (l/4 - l/p) = 3l/8 - 3l/p$$

The r_z coordinate is determined by $r_x r_y r_z = T^l$.

Now finally we get a condition on p . We want $r_x \gg r_y$ everywhere in region IIA so that contour lines for d_{IIA} look roughly as they are drawn and approximations for d_{IIA} are valid. Looking at Q_1 this means $T^{l/4} \gg T^{3l/8-2l/p}$ and Q_2 gives the same constraint. Hence we need $1/8 - 2/p > 0$ or $p > 16$. E.g. take $p = 17$.

The rest of the regions are defined by symmetry.

1.5 The definition of the symplectic form

Now we define the symplectic form in the case of $H = \Sigma_2$.

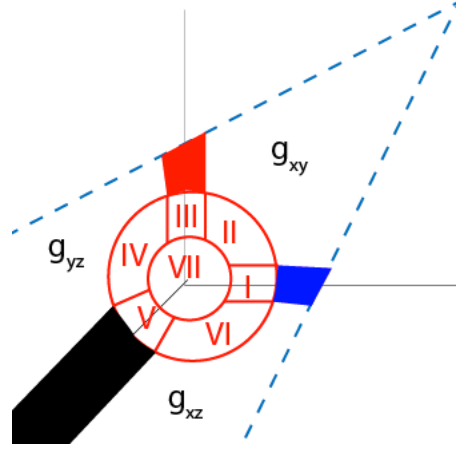


Figure 1.11: Interpolate between three potentials: $F = \alpha_1 g_{xy} + \alpha_2 g_{xz} + (1 - \alpha_1 - \alpha_2) g_{yz}$, $0 \leq \alpha_1, \alpha_2 \leq 1$. Region VII is where $\alpha_1 = \alpha_2 = 1/3$ and $F = \frac{1}{3}(g_{xy} + g_{xz} + g_{yz}) \approx \frac{2}{3}((Tr_x)^2 + (Tr_y)^2 + (Tr_z)^2)$ via the log approximation.

Definition 1.5.1 (Definition of symplectic form). We set $\omega = \frac{i}{2\pi} F$ where F is defined locally as follows in terms of the coordinates in Equation 1.21 and

$$\begin{aligned} g_{yz} &= \log(1 + |Ty|^2)(1 + |Tz|^2)(1 + |T^2 yz|^2) \\ g_{xz} &= \log(1 + |Tx|^2)(1 + |Tz|^2)(1 + |T^2 xz|^2) \\ g_{xy} &= \log(1 + |Tx|^2)(1 + |Ty|^2)(1 + |T^2 xy|^2) \end{aligned} \tag{1.24}$$

We introduce new bump functions $\alpha_3, \dots, \alpha_6$ as follows:

$$\frac{2}{3} \leq \alpha_3(d_I) = \alpha_1 + \alpha_2 \leq 1, \quad -\frac{1}{2} \leq \alpha_4(\theta_I) \leq \frac{1}{2}, \quad 0 \leq \alpha_5(d_I) \leq 1, \quad 0 \leq \alpha_6(\theta_{II}) \leq 1$$

$$\alpha_4(\theta_I) \cdot \alpha_5(d_I) = \frac{1}{2}(\alpha_1 - \alpha_2)$$

These bump functions are smooth, increasing as functions of the specified variable, and near the ends of their domain of definition they are constant at the bounds given. We also require that α_4 is an odd function. See the subsection below “Motivating the definition” for an explanation of the properties of these bump functions. Now the definition is as follows, noting that $g_{xz} - g_{yz} = \phi_x - \phi_y$ and similarly permuting (x, y, z) :

Regions $g_{*\bullet}$ in Fig 1.11: $F = g_{xy}, F = g_{yz}, F = g_{xz}$ respectively

$$\text{Region I: } F = g_{yz} + \alpha_3(d_I)d_I + \alpha_4(\theta_I)\alpha_5(d_I)\theta_I$$

$$\text{Region IIA: } F = g_{yz} - \alpha_6(\theta_{II})\phi_y + \alpha_3(d_{IIA})d_{IIA} + \frac{1}{2}\alpha_5(d_{IIA})(\phi_y - \phi_z - \alpha_6(\theta_{II})\phi_y)$$

$$\text{Region IIB: } F = (g_{yz} - \phi_y) + \alpha_3(d_{IIB})d_{IIB} - \frac{1}{2}\alpha_5(d_{IIB})\phi_z$$

$$\text{Region IIC: } F = g_{xz} - \alpha_6(-\theta_{II})\phi_x + \alpha_3(d_{IIC})d_{IIC} + \frac{1}{2}\alpha_5(d_{IIC})(\phi_x - \phi_z - \alpha_6(-\theta_{II})\phi_x) \quad (1.25)$$

$$\text{Region I to Region IIA: } F = g_{yz} + \alpha_3(d_I) \cdot d_I + \frac{1}{2}\alpha_5(d_I) \cdot \theta_I$$

$$= g_{yz} + \alpha_3(d_{IIA})d_{IIA} + \frac{1}{2}\alpha_5(d_{IIA}) \cdot \theta_I$$

$$\text{Region VII: } F = \frac{1}{3}(g_{xy} + g_{xz} + g_{yz})$$

These formulas match at the boundaries, which allows us to define the rest of the regions III – VI similarly to I and II by symmetry, via permuting the coordinates (x, y, z) . For example, one can check that the formula for region IIA agrees with that for region VII when $\alpha_3 = \frac{2}{3}$ and $\alpha_5 = 0$; with that for region I when $\alpha_6 = 0$ and $\alpha_4 = \frac{1}{2}$; with that for region IIB when $\alpha_6 = 1$; and with g_{xy} when $\alpha_3 = \alpha_5 = 1$. The calculation is similar for the other regions.

Along the coordinate axes (namely the regions shaded red, blue, and black) we interpolate between the relevant $g_{*\bullet}$'s using the same formulas as in regions I, III, and V, with $\alpha_3 \equiv 1$. E.g. along the r_x -axis (blue region) the formula is $F = \frac{1}{2}(g_{xy} + g_{xz}) + \alpha_4(\theta_I)(g_{xy} - g_{xz})$ and similarly for the other edges.

Since we have defined the Kähler potential locally, and it is symmetric in (x, y, z) over a neighborhood of the origin in (ξ_1, ξ_2) coordinates, we may define the Kähler form everywhere by requiring it to be invariant under both the $\mathbb{Z}/6$ action described earlier, and the Γ_B -action. The consistency condition for this to happen is verified in Claim 1.5.2 below.

This completes the definition of the symplectic form.

1.5.1 Motivating the definition

We can rearrange terms of the initial expression of F depending on α_1 and α_2 to motivate the definitions of α_3 and $\alpha_4 \cdot \alpha_5$, as well as of the d and θ in each region. The choice of α_6 and the variables in region II are chosen to interpolate between the definition of F in either

side, namely in regions I and III.

$$\begin{aligned}
F &= \alpha_1 g_{xy} + \alpha_2 g_{xz} + (1 - \alpha_1 - \alpha_2) g_{yz} \\
&= \alpha_1 \log(1 + |Tx|^2)(1 + |Ty|^2)(1 + |T^2 xy|^2) + \alpha_2 \log(1 + |Tz|^2)(1 + |Tx|^2)(1 + |T^2 xz|^2) \\
&\quad + (1 - \alpha_1 - \alpha_2) \log(1 + |Tz|^2)(1 + |Ty|^2)(1 + |T^2 yz|^2) \\
&= g_{yz} + (\alpha_1 + \alpha_2) \phi_x - \left(\frac{\alpha_1 + \alpha_2}{2} - \frac{\alpha_1 - \alpha_2}{2} \right) \cdot \phi_y - \left(\frac{\alpha_1 + \alpha_2}{2} + \frac{\alpha_1 - \alpha_2}{2} \right) \cdot \phi_z \\
&= g_{yz} + (\alpha_1 + \alpha_2) \left(\phi_x - \frac{1}{2}(\phi_y + \phi_z) \right) + \frac{1}{2}(\alpha_1 - \alpha_2)(\phi_y - \phi_z)
\end{aligned}$$

Note that $\alpha_1, \alpha_2, 1 - \alpha_1 - \alpha_2$ is asymmetric but all three should be treated symmetrically, hence we collect them as done above. In other words, if we rotate (α_1, α_2) thought of as a vector by $\pi/4$, we get something proportional to

$$\begin{pmatrix} 1 & -1 \\ 1 & 1 \end{pmatrix} \begin{pmatrix} \alpha_1 \\ \alpha_2 \end{pmatrix} = \begin{pmatrix} \alpha_1 - \alpha_2 \\ \alpha_1 + \alpha_2 \end{pmatrix}$$

Define $\alpha_3 = \alpha_1 + \alpha_2$. To obtain its bounds, we consider the geometry and how α_1, α_2 vary. In the center region VII, $\alpha_1 = \alpha_2 = 1/3$. As we move through region I and reach the end along the r_x direction, there should not be a g_{yz} contribution, meaning that $\alpha_3 = \alpha_1 + \alpha_2 = 1$ there. Hence α_3 goes from $2/3$ to 1 in region I.

We use $\alpha_1 - \alpha_2$ to define a bump function α_4 that varies in the angular direction, which we'll denote θ_I and define below. There is a caveat. Note that at the start of region I, $\alpha_1 = \alpha_2 = 1/3$ so $\alpha_1 - \alpha_2$ goes from 0 to 0 as we trace out the angle θ_I , but at the end of region I we go from $(\alpha_1, \alpha_2) = (0, 1)$ at the bottom to $(\alpha_1, \alpha_2) = (1, 0)$ at the top, so that $\alpha_1 - \alpha_2$ goes between -1 and 1 . Thus we need to multiply $\alpha_4(\theta_I)$ by another bump function $\alpha_5(d_I)$ that goes from 0 to 1 and depends on a variable d_I that increases along increasing r_x , which we'll define next. Hence we scale the interval that α_4 varies in. We require α_4 to be an odd function for symmetry reasons. Let $\alpha_4 \cdot \alpha_5 = \frac{1}{2}(\alpha_1 - \alpha_2)$ so that:

$$F = g_{yz} + \alpha_3 \left(\phi_x - \frac{1}{2}(\phi_y + \phi_z) \right) + \alpha_4 \cdot \alpha_5 (\phi_y - \phi_z)$$

The crux of the calculation that follows is that bump functions will be multiplied by the variable they are a function of. The α_i vary according to “how far around the circle” we are, an angular direction, and “how far out from center” we are, a radial direction. So we will introduce a set of coordinates d and θ which can be read off from the expression for F above: $d_I = \phi_x - \frac{1}{2}(\phi_y + \phi_z)$ and $\theta_I = \phi_y - \phi_z$. We motivate geometrically why they make sense.

We are trying to construct a symplectic form whose moment polytope is the same as the toric polytope by Delzant's theorem. What we can read off from the picture is how r_x, r_y

and r_z compare to each other; even if we can't specify their values we can observe how they compare to one another. In particular, in Figure 1.12 we see that e.g. $T^2(r_y^2 - r_z^2)$ increases in the upward vertical direction and $(Tr_x)^2$ increases in the rightward horizontal direction. This motivates our choices for the angular and radial variables, which we can approximate using leading order terms.

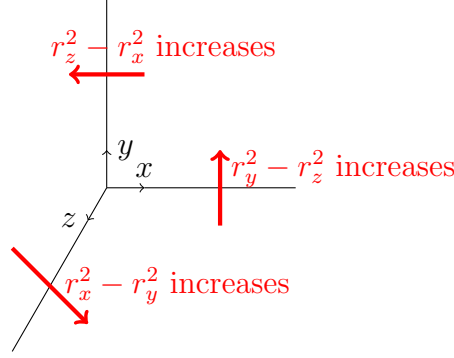


Figure 1.12: How the three angular directions vary

In region I, d should increase with x . In particular $d_I := \phi_x - \frac{1}{2}(\phi_y + \phi_z)$ will still be increasing with x because $r_x \gg r_y, r_z$ when Region I starts. (Since $v_0 = xyz$, if we fix a fiber then $|x|$ increasing means that $|yz|$ decreases accordingly.)

For the angle directions, note that in the expression $\phi_x := \log(1 + |Tx|^2)/(1 + |T^2yz|^2)$, the leading order term is $|Tx|^2$. Thus $\theta_I = \phi_y - \phi_z$ should be the angle coordinate as we saw above and we obtain:

$$F = g_{yz} + \alpha_3(d_I) \cdot d_I + \alpha_4(\theta_I) \cdot \alpha_5(d_I) \cdot \theta_I$$

We've now defined the Kähler potential in region I. This will define it in the corresponding regions of III and V, by symmetry in (x, y, z) . Then region II will interpolate between these.

1.5.2 ω extends over the central fiber and descends to Y

Because of the construction of ω , the form extends to one on the total space including the zero fiber. If we draw a disc around a vertex and consider all $|v_0|$ values over that disc, we get a patch in \mathbb{C}^3 with a Kähler form which approximates the standard symplectic form for r_x, r_y, r_z small, i.e. we've transplanted part of the (\mathbb{C}^3, xyz) model fibration, which we know is a smooth manifold and has a well-defined symplectic form. If we take a disc shape centered in the middle of the hexagon where only one Kähler potential is at play, and then consider all $|v_0|$ above that, we obtain the model toric Kähler form in the fiber. Then we add a term from the base of the fibration v_0 , namely $K|xyz|^2$ for sufficiently large K , so that ω is

positive-definite and we obtain a product symplectic form in an open region corresponding to the middle of the hexagonal tiles in the moment polytope.

In the regions interpolating between these two, we get a convex linear combination of two positive-definite Kähler potentials. In particular, we can pick ϵ sufficiently small that adding ϵ to either of these two metrics will not affect positive-definiteness. Then fix a value of l , for some $|v_0| = T^l$ so that all bump function derivatives described below are less than epsilon. Then we can let $|v_0| = T^{l'}$ tend to zero, and the bounds will still hold because if they hold for l they will only get smaller as $l' \rightarrow \infty$. In other words, once we have enough space for the bump function derivatives, we can define them to have the same support for all $v_0 \rightarrow 0$ fibers and be constant on the rest.

Furthermore, ω extends to all of \tilde{Y} in a Γ_B invariant manner (and also in a $\mathbb{Z}/6$ -invariant manner) – by using the group actions to define it in the other coordinate charts U_{n,g^k} introduced in Definition 1.4.15. Then these formulas match on the overlaps of the charts and give a well-defined 2-form on \tilde{Y} . Moreover it descends to a well-defined 2-form on the quotient Y as follows.

Claim 1.5.2. The form ω descends to a well-defined 2-form on the quotient $Y = \tilde{Y}/\Gamma_B$.

Proof. We saw above that the local model for ω is well-defined because all local definitions agree on the boundaries. This is noted at the end of Definition 1.5.1. Furthermore, when we glue coordinate charts U_{n,g^k} (see Definition 1.4.15) at each vertex of $\Delta_{\tilde{Y}}$ and in the center of the hexagon tiles, the formulas agree. E.g. in Lemma 1.4.10 we show g_{xy} is symmetric under the $\mathbb{Z}/6$ -action. Lastly, the definitions along the edges must be compatible. In other words, extending beyond regions I, III and V into the shaded black, red, and blue regions of Figure 1.11 after setting $\alpha_3 = \alpha_5 = 1$, we check that the transformation is consistent. By symmetry, it suffices to check along the r_z -axis. In the notation of Definition 1.4.15, this is a transformation between the main chart U_{0,g^0} with coordinates (x, y, z) and the chart $U_{(-1,0),g^{-1}}$ with coordinates $(x''', y''', z''') = (Tyz, Txz, T^{-2}z^{-1})$.

Let F denote the Kähler potential for the symplectic form in the unprimed coordinates and F''' that in the triple-primed coordinates. In the region we consider, F is given by the formula for region V after setting $\alpha_3 = \alpha_5 = 1$.

$$\begin{aligned}
F_V &= g_{xy} + d_V + \alpha_4(\theta_V) \cdot \theta_V \\
g_{xy} + d_V &= \log_T(1 + |Tx|^2)(1 + |Ty|^2)(1 + |T^2xy|^2) \cdot \left(\frac{1 + |Tz|^2}{1 + |T^2xy|^2} \cdot \sqrt{\frac{1 + |T^2xz|^2}{1 + |Ty|^2} \cdot \frac{1 + |T^2yz|^2}{1 + |Tx|^2}} \right) \\
&= \frac{1}{2} \log_T(1 + |Tx|^2)(1 + |Ty|^2)(1 + |T^2xz|^2)(1 + |T^2yz|^2) + \log_T(1 + |Tz|^2) \\
\theta_V &= \phi_x - \phi_y \\
\therefore g_{xy}''' &= \left(\frac{1}{2} \log_T(1 + |T^2yz|^2)(1 + |T^2xz|^2)(1 + |Ty|^2)(1 + |Tx|^2) + \log_T(1 + |T^{-1}z^{-1}|^2) \right) \\
&\quad + \alpha_4(-\theta_V) \cdot (-\theta_V) \\
&= F_V - \log_T(|Tz|^2)
\end{aligned}$$

where the last equality follows because in the first term, pulling back by the coordinate change between (x, y, z) and (x''', y''', z''') just amounts to permuting the factors, and in the second term we use that $\alpha_4(-\theta) = -\alpha_4(\theta)$. Also note that θ_V''' corresponds to $-\theta_V$ under the coordinate chart. Thus to go from one chart to the other we add $\log_T(|Tz|^2)$ which is harmonic because $\log(Tz)$ is holomorphic and its conjugate is antiholomorphic. \square

Lemma 1.5.3. *The definition of ω produces a well-defined symplectic form on Y .*

The full proof of this is in the next chapter, showing positive-definiteness.

Chapter 2

The symplectic form ω is nondegenerate

The goal of this chapter is to show:

Lemma 2.0.1. *The ω defined in Section 1.5 is non-degenerate on fibers of the Landau-Ginzburg model given by $v_0 : Y \rightarrow \mathbb{C}$.*

The proof is technical and is the content of this chapter. The reader may wish to skip this chapter and refer back to it as needed.

Corollary 2.0.2. *By adding a term proportional to $|xyz|^2$ on the base, with sufficiently large constant of proportionality, we obtain a non-degenerate form ω on Y .*

This particular symplectic form is used because it is straightforward to compute parallel transport. However, there are other symplectic forms one can equip (Y, v_0) with.

2.1 Putting bounds on the bump function derivatives

Claim 2.1.1 (Logarithmic derivatives facilitate finding estimates). Let α be any of $\alpha_3, \dots, \alpha_5$ and let μ be the appropriate d or θ variable. Then one can ensure that the logarithmic derivative $\alpha'^{\log} = \mu\alpha'(\mu)$ is bounded by a constant over $\log(T^l)$, and similarly for the second derivative. The argument for α_6 is different because its argument is already a function of \log of the norms of the complex coordinates, so we can control the regular derivative.

In particular, Log_T derivatives can be made small. This is the power of writing the Kähler potential in the form $\alpha(\mu) \cdot \mu$ for suitable α and μ . In this section we consider derivatives of the bump functions. So the first order derivatives will pick up terms of the form

$$\alpha'(\mu) \cdot \mu_* \cdot \mu = \mu_* d\alpha / d(\log_T \mu) \approx (\text{small}) \cdot \Delta\alpha / \Delta \log_T \mu$$

where μ_* is some derivative of μ with respect to one of the coordinates. Recall that μ will be approximated by a sum of squares of T times a norm. The norms are very small, on the order of T^l . However $\log_T T^l = l$ so that both the numerator and the denominator change by $O(1)$ terms, which is then multiplied by something that can be made very small. In particular, we divide by l which we can make as large as we like.

Remark 2.1.2 (Checking enough space to make derivatives small, see Figure 1.10). In region I, $d \approx T^2[r_x^2 - \frac{1}{2}(r_y^2 + r_z^2)] > 0$ because r_x is many orders of magnitude bigger than r_y and r_z get in that region. However, in the calculation for α_4 , we end up dividing by θ . So α_4 will need to be constant for a short while in the middle, so we don't divide by zero. This will be detailed below.

Also, there is enough space in θ_{II} and $\log d_{IIA}$ for α_6 and α_3, α_5 respectively. Recall

$$d_{IIA} \approx T^2[r_x^2 - \frac{1}{2}(r_y^2 + r_z^2) + \frac{3}{2}\alpha_6 \cdot r_y^2]$$

Since everywhere in region IIA we have $r_x \gg r_y$, the leading order term in d_{II} is $(Tr_x)^2$. Likewise since θ_{II} is linear in $\log_T r_y - \log_T r_x$, for it to stay constant we find that both $\log_T r_y$ and $\log_T r_x$ increase the same amount along contour lines. At P_1 and P_2 , $\theta_{II} \approx \log_T(T^{l/8-l/p})$. At Q_1 and Q_2 , $\theta_{II} \approx \log_T(T^{l/8-2l/p})$. Thus the change is l/p and $\alpha'_6 \approx \Delta\alpha_6/\Delta\theta_{II} \approx p/l$. This can be made small by taking l large.

Now we check d_{IIA} for α_3 and α_5 . At the smaller value we have $d_{IIA} \approx (Tr_x)^2$ at P_1 where r_x^2 has exponent $l/2$. At the larger value we get $l/2 - 2l/p$. So the change is $2l/p$ and the derivatives in α_3 and α_5 are approximately $p/2l$ times whatever the full range of α_i is. Again this can be made small.

Second-order derivatives also have enough space. In the bump functions $\alpha_3, \dots, \alpha_6$ the variable we're taking the derivative with respect to has space $k \cdot l$ for some $k > 0$ to move while each of the bump functions moves through an amount $1/3$ or 1 . By making l really big, we can ensure that while this is happening, the second derivative doesn't get too big. The graph of the bump functions won't be linear because they have to level off at the endpoints of their support. But with enough space, we can make sure they don't turn too quickly from horizontal to linear.

The argument that there is enough space in IIC follows from IIA by swapping r_x and r_y in the calculations. The only variable in region IIB is d_{IIB} and we take the two radial curves to be where d_{IIB} is constant, with the same amount of change in the variable as in d_{IIA} . Note that when $r_x \gg r_y$ we see that $d_{IIB} \approx T^2[r_x^2 + r_y^2 - \frac{1}{2}r_z^2] \approx (Tr_x)^2$. So initially, constant d_{IIB} is approximately the same thing as constant r_x . At some point we increase r_y enough to equal r_x . Likewise, coming from region IIC we have that constant d_{IIB} means, initially, approximately the same thing as constant r_y . So in the middle the curve interpolates between vertical (constant r_x) and horizontal (constant r_y). The derivatives for functions of

d_{IIB} have enough space because d_{IIB} goes through the same amount as d_{IIA} and d_{IIC} .

Checking enough space for $\alpha_3^{\prime \log}$ and $\alpha_5^{\prime \log}$ sufficiently small. Since α_3 is a function of $d_I \approx T^2[r_x^2 - \frac{1}{2}(r_y^2 + r_z^2)] \approx (Tr_x)^2$ in region I, we need to see how $\log_T(Tr_x)^2$ changes. Recall that r_x changed by l/p orders of magnitude, so $\log_T(Tr_x)^2$ changes by approximately $2l/p$. Thus the log derivative can be made as small as possible, as explained above.

For $\alpha_3^{\prime \prime \log}$ we want to know the change in slope over $\log d$ time. The derivative goes from 0 to $\frac{1}{3l}$ in approximately $l \log$ time. Think of a bump function from $2/3$ to 1. Hence all terms involving a derivative of α_3 are bounded by a constant times T^2/l .

Checking enough space for log derivatives across axes. Recall Figure 1.10 and that from A to B r_y moves through l/p orders of T magnitude while from D to E it moves through $3l/2p$ which is a lot more for small T .

In the calculations above, we have cut out a region where $T < (r_y/r_z)^2 < T^{-1}$. In this region $\alpha_4 \equiv 0$. To do this, we need to make sure that we have at least one order of magnitude difference between r_y and r_z . This is fine in region I because we have r_y and r_z many orders of magnitude apart at B and C , with even more discrepancy as we move out to E and F . (Note however, the reverse would have happened in region II. In other words, r_z gets smaller as we move out, so r_x and r_y get bigger, and constant $r_y^2 - r_x^2$ means they will get closer and closer together as we move out.)

Checking $\alpha_4^{\prime \log}$, function of θ_I . This one is a function of $\theta_I \approx T^2[r_y^2 - r_z^2]$ or its negative. Furthermore, we're taking out a sliver around the axis where $T < (r_y/r_z)^2 < 1/T$. So we need to check there's enough space left. At the bottom where C and F are, $\theta_I \approx -(Tr_z)^2$ which is on the order of $-T^{2(\frac{3l}{8} - \frac{l}{p} + 1)}$ as seen above. Then we stop when $r_z/r_y = 1/\sqrt{T}$. At this point r_z and r_y are basically equal, since they are only about one T -order of magnitude apart and both really small. At some fixed d_I , we have $r_x \approx T^{l/4 - tl/p}$ where t is fixed at some number between 0 and 1. So $r_z = \sqrt{T^{-1}}r_y$ and:

$$r_x r_y r_z = T^l \implies T^{l/4 - tl/p} \cdot r_y \cdot \sqrt{T^{-1}}r_y = T^l \implies r_y^2 = \sqrt{T} \cdot T^{3l/4 + tl/p}$$

Hence

$$\begin{aligned} \theta_I \approx T^2[r_y^2 - r_z^2] &= T^2 r_y^2 \left(1 - \left(\frac{r_z}{r_y}\right)^2\right) \approx T^2 \sqrt{T} \cdot T^{3l/4 + tl/p} (1 - T^{-1}) \\ &\approx -T^{3l/4 + tl/p + 3/2} \cdot T << 1 \end{aligned}$$

We are checking how θ_I changes when we cut out this sliver to make sure α_4 has enough space for the log derivatives. We find θ_I decreases from order of magnitude $3l/4 - 2l/p + 2$

to order of magnitude $3l/4 + tl/p + 3/2$. This means a net change of

$$(3l/4 - 2l/p + 2) - (3l/4 + tl/p + 3/2) = -l \left(\frac{2}{p} + \frac{t}{p} \right) + 1/2$$

with a multiple of l , so we're still okay for the log derivative of α_4 because this is the denominator of the log derivative which can be made very large because of the l . Note that we only care about α_4 in region I since it's constant at $1/2$ when we exit the region and move into region II.

2.2 Converting to polar coordinates

To define the metric, we will convert to polar coordinates where it is easier. Locally the symplectic form is $\frac{i}{2\pi} \partial \bar{\partial} F$ where F is a function of $|x|$ and $|y|$. So we want to transform the derivatives in $\partial \bar{\partial}$ using the real transformation $(r_x, \theta_x) \leftrightarrow (x_1, x_2)$ where $x = x_1 + ix_2 = r_x e^{i\theta_x}$, and similarly for y . Recall $\partial_x = \frac{1}{2}(\partial_{x_1} - i\partial_{x_2})$. Hence $\partial_{x_i} = \partial_{x_i}(r_x)\partial_{r_x} + \partial_{x_i}(\theta_x)\partial_{\theta_x}$ implies that

$$\begin{aligned} \frac{\partial}{\partial x} &= \frac{1}{2} \left(\frac{\partial}{\partial x_1} - i \frac{\partial}{\partial x_2} \right) \\ &= \frac{1}{2} \left(\left[\frac{\partial r_x}{\partial x_1} - i \frac{\partial r_x}{\partial x_2} \right] \frac{\partial}{\partial r_x} + \left[\frac{\partial \theta_x}{\partial x_1} - i \frac{\partial \theta_x}{\partial x_2} \right] \frac{\partial}{\partial \theta_x} \right) \end{aligned}$$

We next re-express each real partial derivatives in terms of polar coordinates $r_x^2 = x_1^2 + x_2^2$ and $\theta_x = \tan^{-1}(x_2/x_1)$, and similarly for y . Recall that the derivative of $\arctan(t) = 1/(1+t^2)$.

$$\begin{aligned} \frac{\partial}{\partial x_1} &= \frac{\partial r_x}{\partial x_1} \frac{\partial}{\partial r_x} + \frac{\partial \theta_x}{\partial x_1} \frac{\partial}{\partial \theta_x} \\ r_x \frac{\partial r_x}{\partial x_i} &= x_i \implies \frac{\partial r_x}{\partial x_i} = \frac{x_i}{r_x} \\ \frac{\partial \theta_x}{\partial x_1} &= -\frac{x_2}{r_x^2}, \quad \frac{\partial \theta_x}{\partial x_2} = \frac{x_1}{r_x^2} \\ \implies \frac{\partial}{\partial x} &= \frac{1}{2} [e^{-i\theta_x} \partial_{r_x} - i e^{-i\theta_x} / r_x \partial_{\theta_x}] \\ \frac{\partial}{\partial \bar{x}} &= \frac{1}{2} [e^{i\theta_x} \partial_{r_x} + i e^{i\theta_x} / r_x \partial_{\theta_x}] \end{aligned}$$

Similarly for y . We also need to rewrite the differentials $dx = dx_1 + i dx_2$ and $d\bar{x}$. Use

$$\begin{aligned} x_1 &= r_x \cos \theta_x \\ x_2 &= r_x \sin \theta_x \\ \therefore dx &= e^{i\theta_x} dr_x + i r_x e^{i\theta_x} d\theta_x \\ d\bar{x} &= e^{-i\theta_x} dr_x - i r_x e^{-i\theta_x} d\theta_x \end{aligned}$$

Now we can convert $\partial\bar{\partial}F$ into polar coordinates.

$$\begin{aligned}
i\partial\bar{\partial}F &= \sum_{i,j=1}^3 \frac{\partial^2 F}{\partial z_i \partial \bar{z}_j} dz_i \wedge d\bar{z}_j \\
&= i \sum_{i,j} \left(\frac{1}{2} e^{-i\theta_{z_i}} \left[\partial_{r_{z_i}} - i/r_{z_i} \partial_{\theta_{z_i}} \right] \right) \left(\frac{1}{2} e^{i\theta_{z_j}} \left[\partial_{r_{z_j}} + i/r_{z_j} \partial_{\theta_{z_j}} \right] \right) (F) (e^{i\theta_i} (dr_i + ir_i d\theta_i)) \\
&\quad \wedge (e^{-i\theta_j} (dr_j - ir_j d\theta_j)) \\
&= i \frac{1}{4} \sum_{i,j} e^{-i\theta_i} \left[e^{i\theta_j} \partial_{r_i r_j}^2 F - \frac{i}{r_i} \partial_{r_j} F \delta_{ij} e^{i\theta_j} \right] (e^{i\theta_i} (dr_i + ir_i d\theta_i)) \wedge (e^{-i\theta_j} (dr_j - ir_j d\theta_j)) \\
&= \frac{i}{4} \left[\sum_i (\partial_{r_i}^2 F + \frac{1}{r_i} \partial_{r_i} F) (dr_i + ir_i d\theta_i) \wedge (dr_i - ir_i d\theta_i) \right] \\
&\quad + \frac{i}{4} \left[\sum_{i \neq j} (\partial_{r_i r_j}^2 F) (dr_i + ir_i d\theta_i) \wedge (dr_j - ir_j d\theta_j) \right]
\end{aligned}$$

In order for this to arise from a metric, we need compatibility with J_0 where J_0 is induced from multiplication by i on the complex coordinates (x, y, z) in the toric chart where they are defined. But ω is compatible with J because it comes from a Kähler potential. J is multiplication by i , which commutes with $\partial\bar{\partial}$.

Next we need positive-definiteness, namely $\omega(v, Jv) > 0$ for all $v \neq 0$.

$$\begin{aligned}
\partial_{r_1} &= \frac{\partial x_1}{\partial r_1} \partial_{x_1} + \frac{\partial x_2}{\partial r_1} \partial_{x_2} \\
&= \cos \theta_1 \partial_{x_1} + \sin \theta_1 \partial_{x_2} \\
\partial_{\theta_1} &= -r_1 \sin \theta_1 \partial_{x_1} + r_1 \cos \theta_1 \partial_{x_2} \\
J(\partial_{x_1}) &= \partial_{x_2}, \quad J(\partial_{x_2}) = -\partial_{x_1} \\
\implies J(\partial_{r_1}) &= \frac{1}{r_1} \partial_{\theta_1} \\
J(\partial_{\theta_1}) &= -r_1 \partial_{r_1}
\end{aligned}$$

We want $g(u, v) := \omega(u, Jv)$ to be a metric, so positive definite. In the 3d case, this gives a 6 by 6 matrix which we want to be positive definite. It'll be block diagonal with the r block and the θ block. The entries along the diagonal in the r block will be

$$g_{ii} = \omega(\partial_{r_i}, J\partial_{r_i}) = \omega(\partial_{r_i}, \frac{1}{r_i} \partial_{\theta_i}) = \frac{1}{r_i} \omega(\partial_{r_i}, \partial_{\theta_i}) = \frac{1}{2} (\partial_{r_i}^2 F + \frac{1}{r_i} \partial_{r_i} F)$$

which will pick up the $dr_i \wedge d\theta_i$ term, which looking back at $\partial\bar{\partial}F$ above is $\frac{2}{4}r_i dr_i \wedge d\theta_i$ times the F derivative term. Similarly

$$\begin{aligned} g_{ij} &= \omega(\partial_{r_i}, J\partial_{r_j}) = \frac{1}{r_j} \omega(\partial_{r_i}, \partial_{\theta_j}) \\ &= \frac{1}{2}(\partial_{r_i r_j}^2 F) \end{aligned}$$

2.3 Showing ω nondegenerate: \mathbb{C}^3 patch

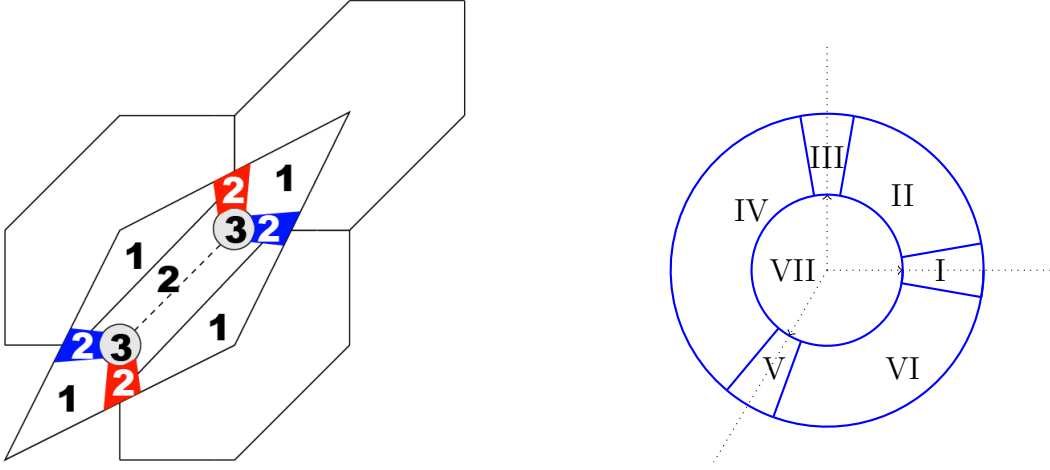


Figure 2.1: L) Number of potentials interpolated between. R) Zoomed in region about vertex.

Leading order Region I terms

First we look at the terms with no derivatives of the bump functions. This should give us a positive definite matrix so we get a metric. Then it will be enough to show that all the remaining terms can be expressed in terms of (log-derivatives of the bump functions) · (bounded terms), which can be made as small as we like by making l as large as we like. First, recall that this is the metric in polar coordinates:

$$\begin{pmatrix} \partial_{r_x}^2 F + \frac{1}{r_x} \partial_{r_x} F & \partial_{r_x r_y}^2 F & \partial_{r_x r_z}^2 F \\ \partial_{r_x r_y}^2 F & \partial_{r_y}^2 F + \frac{1}{r_y} \partial_{r_y} F & \partial_{r_y r_z}^2 F \\ \partial_{r_x r_z}^2 F & \partial_{r_y r_z}^2 F & \partial_{r_z}^2 F + \frac{1}{r_z} \partial_{r_z} F \end{pmatrix}$$

$$\begin{aligned}
F &= f + \alpha_3 d + \alpha_4 \cdot \alpha_5 \theta \\
d &\approx T^2[r_x^2 - \frac{1}{2}(r_y^2 + r_z^2)] \\
\theta &\approx T^2[r_y^2 - r_z^2] \\
f &\approx T^2[r_y^2 + r_z^2]
\end{aligned}$$

Note that because everywhere r_x appears is as r_x^2 , applying $\partial_{r_x r_x}^2$ is the same as applying ∂_{r_x}/r_x . Here are the terms that do not involve derivatives of the α_i , where for ease of notation subscript x means ∂_{r_x} :

$$\begin{aligned}
&\begin{pmatrix} 2(f_{xx} + \alpha_3 d_{xx} + \alpha_4 \alpha_5 \theta_{xx}) & f_{xy} + \alpha_3 d_{xy} + \alpha_4 \alpha_5 \theta_{xy} & f_{xz} + \alpha_3 d_{xz} + \alpha_4 \alpha_5 \theta_{xz} \\ & \text{"} & \text{"} \\ & 2(f_{yy} + \alpha_3 d_{yy} + \alpha_4 \alpha_5 \theta_{yy}) & f_{yz} + \alpha_3 d_{yz} + \alpha_4 \alpha_5 \theta_{yz} \\ & \text{"} & \text{"} \\ & & 2(f_{zz} + \alpha_3 d_{zz} + \alpha_4 \alpha_5 \theta_{zz}) \end{pmatrix} \\
&\approx T^2 \begin{pmatrix} 4\alpha_3 & 0 & 0 \\ 0 & 4 - 2\alpha_3 + 4\alpha_4 \alpha_5 & 0 \\ 0 & 0 & 4 - 2\alpha_3 - 4\alpha_4 \alpha_5 \end{pmatrix}
\end{aligned}$$

Derivatives of the higher order terms in the expansions above will have variables Tr_* so will be negligible. This is bounded below assuming we restrict the region a little, each entry is bounded below. One of the coordinates does go to zero as the bump functions reach their bounds. However, the one that goes to zero in the xy -plane is the z term and similarly in the xz -plane it's the y term. Since we add a term $|xyz|^2$ for the base, this will ensure positive definiteness away from the zero fiber.

Terms with derivatives of bump functions in Region I

The terms that produce derivatives of the bump functions are $\alpha_3(d_I)d_I$ and $\alpha_4(\theta_I)\alpha_5(d_I)\theta_I$. Note that d in region I close to where $r_x = r_y = r_z$ is approximately linear in $(Tr_x)^2, (Tr_y)^2$, and $(Tr_z)^2$.

Some notation: Let $d \equiv d_I$ in this section. We want to allow the variable we're taking the derivative with respect to to vary among $\{r_x, r_y, r_z\}$. So we denote those variables to be $\{r_\star, r_\bullet\} \in \{r_x, r_y, r_z\}$. Furthermore, $'\log$ means we take the log derivative $d\alpha_3/d(\log(d_I)) = \alpha_3' \cdot d$. The following calculation for the second derivative applies to α_5 as well, and α_4 if we

replace d with θ .

$$\begin{aligned}\frac{d^2\alpha_3}{d(\log d)^2} &= (\alpha'_3 \cdot d)' \cdot d = (\alpha''_3 \cdot d + \alpha'_3)d \\ \Rightarrow \alpha''_3 \cdot d + \alpha'_3 &= \frac{1}{d} \cdot \frac{d^2\alpha_3}{d(\log d)^2} \\ \Rightarrow \alpha''_3 &= \frac{1}{d^2} \cdot \left(\frac{d^2\alpha_3}{d(\log d)^2} - \frac{d\alpha_3}{d(\log d)} \right)\end{aligned}$$

Derivatives of $\alpha_3 d$

First order derivative $\frac{1}{r_*} \partial_{r_*}(\alpha_3 d)$: the term involving α'_3 is $\frac{1}{r_*} \partial_{r_*}(d) \alpha'_3 d$, in which $\frac{1}{r_*} \partial_{r_*}(d)$ is approximately a constant times T^2 , and $\alpha'_3 d = \alpha_3'^{\log}$ is a log derivative so can be made arbitrarily small.

Second order derivatives:

A second order derivative of $\alpha_3 d$ involves a first order derivative of $(\partial_{r_*} d) \alpha'_3 d$, which involves terms like $\alpha'_3 d$ from before, as well as $(\partial_{r_*} d)(\partial_{\bullet} d)(\alpha''_3 d + \alpha'_3)$ up to powers of T i.e. proportional to $T^2 r_{\star} r_{\bullet} (\alpha''_3 d + \alpha'_3)$ because d is approximately linear in $(Tr_x)^2, (Tr_y)^2, (Tr_z)^2$. Thus we get

$$T^2 \frac{r_{\star} r_{\bullet}}{d} \alpha_3''^{\log}$$

If we divide numerator and denominator by r_x^2 we get $\frac{(r_{\star} r_{\bullet})/(r_x)^2}{1 - \frac{1}{2}((r_y/r_x)^2 + (r_z/r_x)^2)}$ which is close to 1 on the bottom, and small or 1 on the top, because $r_x \gg r_y, r_z$. So we get something bounded times something small. Thus all derivatives involving α_3 lead to small terms for a fixed sufficiently large l . Here are the calculations.

Diagonal terms for $\alpha_3(d) \cdot d$:

$$\begin{aligned}
d &\approx T^2[r_x^2 - \frac{1}{2}(r_y^2 + r_z^2)] \\
d_{r_*} &\approx \lambda T^2 r_*, \quad d_{r_* r_*} \approx \lambda T^2, \quad \lambda \in \{2, -1\} \\
\left(\frac{1}{r_*} \partial_{r_*} + \partial_{r_* r_*}^2\right)(\alpha_3(d) \cdot d) &= \frac{1}{r_*}(\alpha'_3 d_{r_*} d + \alpha_3(d) \cdot d_{r_*}) \\
&+ (\alpha''_3 d_{r_*}^2 d + \alpha'_3 d_{r_* r_*} d + 2\alpha'_3(d) d_{r_*}^2 + \alpha_3(d) \cdot d_{r_* r_*}) \\
&\approx \frac{1}{r_*}(\alpha'_3 \lambda T^2 r_* d + \alpha_3(d) \cdot \lambda T^2 r_*) \\
&+ (\alpha''_3 (\lambda T^2 r_*)^2 d + \alpha'_3 \lambda T^2 d + 2\alpha'_3(d) (\lambda T^2 r_*)^2 + \alpha_3(d) \cdot \lambda T^2) \\
&= \lambda T^2[\alpha'_3 d + \alpha_3 + \lambda T^2 \alpha''_3 r_*^2 \cdot d + \alpha'_3 d + 2\lambda T^2 \alpha'_3 r_*^2 + \alpha_3(d)] \\
&= \lambda T^2[\alpha'_3(2d + \lambda T^2 r_*^2) + \lambda T^2 r_*^2(\alpha''_3 d + \alpha'_3)] + 2\lambda T^2 \alpha_3 \\
&= \lambda T^2[\alpha'_3{}^{\log}(2 + \frac{\lambda T^2 r_*^2}{d}) + \lambda \frac{T^2 r_*^2}{d} \alpha''_3{}^{\log}] + 2\lambda T^2 \alpha_3
\end{aligned}$$

$$\begin{aligned}
\alpha'_3{}^{\log} &\approx \frac{\Delta \alpha_3}{\Delta \log d} \approx \propto \frac{1}{l} \\
\frac{T^2 r_*^2}{d} &\approx \frac{T^2 r_*^2}{T^2[r_x^2 - \frac{1}{2}(r_y^2 + r_z^2)]} = \frac{r_*^2}{r_x^2 - \frac{1}{2}(r_y^2 + r_z^2)} = \frac{r_*^2/r_x^2}{1 - \frac{1}{2}(\frac{r_y^2}{r_x^2} + \frac{r_z^2}{r_x^2})} \approx 1 \text{ or } 0 : r_x \gg r_y, r_z \\
\alpha''_3{}^{\log} &\approx \propto \frac{1}{l^2}
\end{aligned}$$

Off-diagonal terms for $\alpha_3(d) \cdot d$ where $*$ \neq \star :

$$\begin{aligned}
d_{r_* r_*} &= 0 \\
\partial_{r_* r_*}^2(\alpha_3 \cdot d) &= \partial_{r_*}(\alpha'_3 d_{r_*} d + \alpha_3(d) \cdot d_{r_*}) \\
&= \alpha''_3 d_{r_*} d_{r_*} d + \alpha'_3 d_{r_* r_*} d + 2\alpha'_3 d_{r_*} d_{r_*} + \alpha_3 \cdot d_{r_* r_*} \\
&\approx T^4 \lambda \mu r_* r_* \alpha''_3 d + 0 + 2T^4 \lambda \mu r_* r_* \alpha'_3 + 0, \quad \lambda, \mu \in \{2, -1\} \\
&= T^4 \lambda \mu \frac{r_* r_*}{d} d(\alpha''_3 d + \alpha'_3 + \alpha'_3) \\
&= T^4 \lambda \mu \frac{r_* r_*}{d} (\alpha''_3{}^{\log} + \alpha'_3{}^{\log}) \\
\frac{T^2 r_* r_*}{d} &\approx \frac{r_* r_* / r_x^2}{1 - \frac{1}{2}((r_y/r_x)^2 + (r_z/r_x)^2)} \approx 0 \text{ or } 1
\end{aligned}$$

Again we see that all the derivatives of the bump functions are log derivatives and all the terms are bounded by a constant times T^2/l .

Derivatives of $\alpha_4 \alpha_5 \theta$

For $\alpha_4\alpha_5\theta$, the first order derivative terms (dividing by whatever variable we take the derivative with respect to) involve $\alpha_5(\alpha'_4\theta)$, which is an $O(1)$ term (recall α_5 goes from 0 to 1) times a log derivative, as well as $\alpha_4(\alpha'_5\theta) = \alpha_4(\alpha_5'^{\log} \cdot \frac{\theta}{d})$ because α_5 is a function of d . So we need to check that θ/d is bounded, independent of l . Dividing by r_x^2 gets a small expression on top and close to 1 on the bottom. So these are both bounded by $O(1/l)$.

From first derivatives we have $r_\star\alpha_5(\alpha'_4\theta)$ and $r_\star\alpha_4(\alpha'_5\theta)$. Differentiating the r_\star with respect to r_\bullet gives terms we already know are small from the previous paragraph, or zero if $\bullet \neq \star$. So we put it out front and differentiate the remaining expression. Keep in mind α_4 is a function of θ and α_5 is a function of d . Using again the quadratic approximations for d and θ , we now obtain terms such as:

- $r_\star r_\bullet \alpha'_4 \alpha'_5 \theta = \frac{r_\star r_\bullet}{d} \alpha_4'^{\log} \alpha_5'^{\log}$

We multiplied and divided by a d to get the α_5 log derivative.

- $r_\star r_\bullet \alpha_5(\alpha''_4\theta + \alpha'_4) = \alpha_5 \cdot \frac{r_\star r_\bullet}{\theta} \alpha_4''^{\log}$

The r_\bullet comes from $\partial_\bullet \theta$. In particular, if $r_\bullet = r_x$ then we get zero because $\theta \approx T^2[r_y^2 - r_z^2]$ which means that $\theta_{r_x} \approx 0$.

- $r_\star r_\bullet \alpha_4(\alpha''_5\theta) = \alpha_4 \cdot \frac{r_\star r_\bullet}{d} (\alpha_5''^{\log} - \alpha_5'^{\log}) \cdot \frac{\theta}{d}$

- $r_\star r_\bullet \alpha_4(\alpha'_5) = \frac{r_\star r_\bullet}{d} \cdot \alpha_4 \alpha_5'^{\log}$

We've already seen above that $T^2 \frac{r_\star r_\bullet}{d}$ and hence $\frac{\theta}{d}$ are bounded. So it remains to check that $T^2 \frac{r_\star r_\bullet}{\theta}$ is bounded. Also, we only need to consider the cases where the numerator does not involve r_x by the comment above that we get zero otherwise and that second-order partial derivatives are symmetric. So we have to bound the following expressions:

$$\frac{r_y^2}{r_y^2 - r_z^2}, \frac{r_z^2}{r_y^2 - r_z^2}, \frac{r_y r_z}{r_y^2 - r_z^2}$$

We are considering the top half of region I, where $r_y > r_z$. We declare that α_4 is constant in the region $1 < \left(\frac{r_y}{r_z}\right)^2 < \frac{1}{T}$. So the support of α_4 is where $\left(\frac{r_y}{r_z}\right)^2 > \frac{1}{T}$. In particular, we see that

$$\frac{1}{\left(\frac{r_y}{r_z}\right)^2 - 1} < \frac{1}{T^{-1} - 1} = \frac{T}{1 - T} \approx T$$

So these terms are bounded, which can be seen dividing top and bottom by r_z^2 . Here is the explicit calculation.

Diagonal terms $\frac{1}{r_\bullet} \partial_{r_\bullet} + \partial_{r_\bullet r_\bullet}^2$ and off-diagonal terms $\partial_{r_\bullet r_\star}^2$.

$$\begin{aligned}
\theta &\approx T^2(r_y^2 - r_z^2) \\
d &\approx T^2(r_x^2 - \frac{1}{2}(r_y^2 + r_z^2)) \\
\theta_{r_\bullet} &\approx \lambda_\bullet T^2 r_\bullet, \quad \lambda_\bullet \in \{0, \pm 2\} \\
d_{r_\bullet} &\approx \mu_\bullet T^2 r_\bullet, \quad \mu_\bullet \in \{2, -1\} \\
\frac{1}{r_\bullet} \partial_{r_\bullet} (\alpha_4 \alpha_5 \theta) &= \frac{1}{r_\bullet} (\alpha'_4 \theta_{r_\bullet} \alpha_5 \theta + \alpha_4 \alpha'_5 d_{r_\bullet} \theta + \alpha_4 \alpha_5 \theta_{r_\bullet}) \\
&\approx T^2 (\lambda_\bullet \alpha_4'^{\log} \alpha_5 + \mu_\bullet \alpha_4 \alpha_5'^{\log} \frac{\theta}{d} + \lambda_\bullet \alpha_4 \alpha_5)
\end{aligned}$$

$$\begin{aligned}
\partial_{r_\star r_\bullet}^2 (\alpha_4 \alpha_5 \theta) &\approx T^2 \partial_{r_\star} [r_\bullet \lambda_\bullet \alpha'_4 \theta \alpha_5 + r_\bullet \mu_\bullet \alpha_4 \alpha'_5 \theta + r_\bullet \lambda_\bullet \alpha_4 \alpha_5] \\
&= T^2 [\partial_{r_\star} (r_\bullet) \lambda_\bullet \alpha'_4 \theta \alpha_5 + r_\bullet \lambda_\bullet \alpha_4' \theta_{r_\star} \alpha_5 + r_\bullet \lambda_\bullet \alpha_4' \theta_{r_\star} \alpha_5 + r_\bullet \lambda_\bullet \alpha_4' \theta \alpha_5' d_{r_\star} \\
&\quad + \partial_{r_\star} (r_\bullet) \alpha_4 \alpha'_5 \theta + r_\bullet \mu_\bullet \alpha_4' \theta_{r_\star} \alpha_5 \theta + r_\bullet \mu_\bullet \alpha_4 \alpha_5'' d_{r_\star} \theta + r_\bullet \mu_\bullet \alpha_4 \alpha_5' \theta_{r_\star} \\
&\quad + \partial_{r_\star} (r_\bullet) \lambda_\bullet \alpha_4 \alpha_5 + r_\bullet \lambda_\bullet \alpha_4' \theta_{r_\star} \alpha_5 + r_\bullet \lambda_\bullet \alpha_4 \alpha_5' d_{r_\star}] \\
&\approx T^2 [\delta_{\bullet\star} \lambda_\bullet \alpha_4'^{\log} \alpha_5 + T^2 [\lambda_\bullet \lambda_\star \frac{r_\bullet r_\star}{\theta} (\alpha_4''^{\log} - \alpha_4'^{\log}) \alpha_5 + \lambda_\bullet \lambda_\star \frac{r_\bullet r_\star}{\theta} \alpha_4'^{\log} \alpha_5 + \lambda_\bullet \mu_\star \frac{r_\bullet r_\star}{d} \alpha_4'^{\log} \alpha_5'^{\log}] \\
&\quad + \delta_{\bullet\star} \frac{\theta}{d} \alpha_4 \alpha_5'^{\log} + \mu_\bullet \lambda_\star \frac{T^2 r_\bullet r_\star}{d} \alpha_4'^{\log} \alpha_5'^{\log} + \mu_\bullet \mu_\star \frac{T^2 r_\bullet r_\star \theta}{d^2} \alpha_4 (\alpha_5''^{\log} - \alpha_5'^{\log}) + \mu_\bullet \lambda_\star \frac{T^2 r_\bullet r_\star}{d} \alpha_5'^{\log} \alpha_4 \\
&\quad + \delta_{\bullet\star} \lambda_\bullet \alpha_4 \alpha_5 + \lambda_\bullet \lambda_\star \frac{T^2 r_\bullet r_\star}{\theta} \alpha_4'^{\log} \alpha_5 + \lambda_\bullet \mu_\star \frac{T^2 r_\bullet r_\star}{d} \alpha_4 \alpha_5'^{\log}]
\end{aligned}$$

We see $\lambda_\bullet \lambda_\star \frac{T^2 r_\bullet r_\star}{\theta}$, $\frac{T^2 r_\bullet r_\star}{d}$, $\frac{\theta}{d}$ are bounded, as before, and the derivatives are log derivatives.

Setting up region III and V to match Region I

In region I, r_x was the dominating coordinate. In region III, r_y will dominate and in region V, r_z will dominate. So we take the analogous data for half regions of III and V, by modeling I.

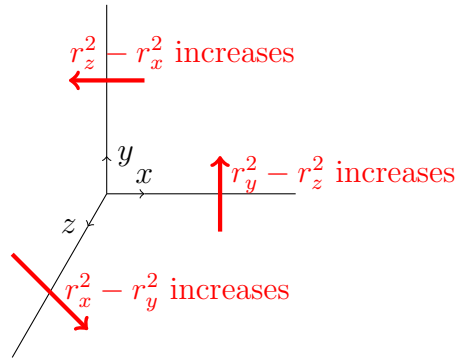


Figure 2.2: The three angular directions

$$\begin{aligned}
F_I &= g_{yz} + \alpha_3(d_I) \cdot d_I + \alpha_4(\theta_I)\alpha_5(d_I) \cdot \theta_I \\
g_{yz} &\approx T^2[r_y^2 + r_z^2] \\
\theta_I &\approx T^2[r_y^2 - r_z^2] \\
d_I &\approx T^2[r_x^2 - \frac{1}{2}(r_y^2 + r_z^2)]
\end{aligned}$$

$$\begin{aligned}
F_{III} &= g_{xz} + \alpha_3(d_{III}) \cdot d_{III} + \alpha_4(\theta_{III})\alpha_5(d_{III}) \cdot \theta_{III} \\
g_{xz} &\approx T^2[r_x^2 + r_z^2] \\
\theta_{III} &\approx T^2[r_z^2 - r_x^2] \\
d_{III} &\approx T^2[r_y^2 - \frac{1}{2}(r_x^2 + r_z^2)]
\end{aligned}$$

$$\begin{aligned}
F_V &= g_{xy} + \alpha_3(d_V) \cdot d_V + \alpha_4(\theta_V)\alpha_5(d_V) \cdot \theta_V \\
g_{xy} &\approx T^2[r_x^2 + r_y^2] \\
\theta_V &\approx T^2[r_x^2 - r_y^2] \\
d_V &\approx T^2[r_z^2 - \frac{1}{2}(r_x^2 + r_y^2)]
\end{aligned}$$

The expressions for the Kähler potentials in regions III and V thus differ from that in region I by a permutation of the coordinates x, y, z . In particular, these potentials are still convex combinations of g_{xy}, g_{yz}, g_{xz} (with coefficients determined by α_3 and $\alpha_4\alpha_5$). Again in both cases, α_3 goes from $2/3$ to 1 and α_4 goes from $-1/2$ to $1/2$ while α_5 scales it by going from 0 to 1 . All the calculations carry through as before with $f + \alpha_3 d + \alpha_4 \alpha_5 \theta$ since we've set up everything to be symmetric in (r_x, r_y, r_z) . The issue now is that $\alpha_{\geq 3}$ are functions of d and θ , and these two variables have different definitions in each of the three regions. So we will patch together the d coordinate across regions II, IV and VI.

The reason we only care about patching together the d is because at the boundaries of the odd-numbered regions, α_4 has leveled out to either $1/2$ or $-1/2$, and α_3, α_5 only depend on d . So we take another bump function α_6 , going from 0 to 1 , that allows us to interpolate between the two definitions of d by adding increasing amounts of the θ -coordinate in the even-numbered regions. So just to recap in regions II, IV, VI: α_3 and α_5 are functions of d , which in turn is a function of $\alpha_6(\theta_{\text{even}}) \cdot \theta_{\text{even}}$. So we're going to need to apply two levels in the chain rule when taking derivatives with respect to r_x, r_y, r_z .

Leading order Region IIA terms

First we find the terms not involving derivatives of the bump functions. These will form the nondegenerate part of the metric on region II and we will show the rest of the terms can

be made sufficiently small. Since everything not a bump function is approximately linear in $(Tr_x)^2, (Tr_y)^2$ and $(Tr_z)^2$, we again have that $\frac{1}{r_x}\partial_{r_x} = \partial_{r_x r_x}^2$. Recall $2/3 \leq \alpha_3 \leq 1$ and $0 \leq \alpha_5, \alpha_6 \leq 1$.

$$\begin{aligned} F \approx & T^2[(r_y^2 + r_z^2 - \alpha_6(\theta_{II}) \cdot r_y^2) + \alpha_3(d_{IIA}) \cdot (r_x^2 - \frac{1}{2}(r_y^2 + r_z^2) + \frac{3}{2}\alpha_6(\theta_{II}) \cdot r_y^2) \\ & + \frac{1}{2}\alpha_5(d_{IIA}) \cdot (r_y^2 - r_z^2 - \alpha_6(\theta_{II}) \cdot r_y^2)] \end{aligned}$$

Off-diagonal terms $\partial_{r_\bullet r_\star}^2$ for $\star \neq \bullet$ are zero because derivatives of non-bump functions means differentiating r_\star^2 for some \star . Diagonal terms we get $\frac{1}{r_\star}\partial_{r_\star} + \partial_{r_\star r_\star}^2 = 2\partial_{r_\star r_\star}^2$ which, applied to $(Tr_\star)^2$ is $4T^2$. So in the (\star, \star) entry of the matrix, the leading terms are $4T^2$ times the coefficients on r_\star^2 .

$$\begin{aligned} x : & T^2(4\alpha_3) \geq T^2 8/3 \\ y : & T^2(4 - 4\alpha_6 - 2\alpha_3 + 6\alpha_3\alpha_6 + 2\alpha_5 - 2\alpha_5\alpha_6) = T^2[4 + (2 - 2\alpha_6)(\alpha_5 - \alpha_3) + 4\alpha_6(\alpha_3 - 1)] \\ & \geq T^2[4 + 2(0 - 2/3) + 4(-1/3)] = T^2 \cdot \frac{4}{3} \\ z : & T^2(4 - 2\alpha_3 - 2\alpha_5) \end{aligned}$$

Note that when $\alpha_3 = \alpha_5 = 1$ the z term goes to zero. However, it is bounded below in a region where α_3, α_5 are bounded away from 1. In the region where it goes to 1, we add a term to F from the base, i.e. $|xyz|^2$, to maintain nondegeneracy. Because xyz is bounded below in the region where we add it, we can take the partial derivatives and get something positive definite.

Terms with derivatives of bump functions in Region IIA

Now we show that the bump function derivative terms can be made small. For reference:

$$\begin{aligned} F \approx & (g_{yz} - \alpha_6 \cdot (Tr_y)^2) + \alpha_3(d_{IIA})d_{IIA} + \frac{1}{2}\alpha_5(d_{IIA}) \cdot ((Tr_y)^2 - (Tr_z)^2 - \alpha_6(Tr_y)^2) \\ g_{yz} \approx & T^2[r_y^2 + r_z^2] \\ d_{IIA} \approx & T^2[r_x^2 - \frac{1}{2}(r_y^2 + r_z^2)] + \frac{3}{2}\alpha_6(\log r_y - \log r_x) \cdot (Tr_y)^2 \\ \theta_{II} = & \log(r_y/r_x) \end{aligned}$$

Bump function terms in F are: $\alpha_6 \cdot (Tr_y)^2$, $\alpha_3 \cdot d_{IIA}$, $\{\alpha_5(Tr_\star)^2\}_{\star=y,z}$, $\alpha_5\alpha_6 \cdot (Tr_y)^2$

1st term for region IIA: $\alpha_6(\log(r_y/r_x)) \cdot (Tr_y)^2$

First derivative divided by r_* :

$$\begin{aligned}\frac{1}{r_x} \partial_{r_x} [\alpha_6 (\log r_y - \log r_x) (Tr_y)^2] &= -\frac{1}{r_x^2} \alpha'_6 \cdot (Tr_y)^2 = -T^2 \cdot \frac{r_y^2}{r_x^2} \alpha'_6, \quad \left| \frac{r_y^2}{r_x^2} \right| < 1 \\ \frac{1}{r_y} \partial_{r_y} [\alpha_6 (\log r_y - \log r_x) (Tr_y)^2] &= \frac{1}{r_y^2} \alpha'_6 \cdot (Tr_y)^2 + \alpha_6 \cdot (2T^2) = T^2 \alpha'_6 + 2T^2 \alpha_6 \\ \frac{1}{r_z} \partial_{r_z} [\alpha_6 (\log r_y - \log r_x) (Tr_y)^2] &= 0 \\ \alpha'_6 &\approx \propto \frac{1}{l}\end{aligned}$$

So all bump function derivative terms from first order derivatives of this term can be made small.

Second derivative $\partial_{\star\bullet}^2$:

$$\begin{aligned}\partial_{r_x r_x}^2 (\alpha_6 (Tr_y)^2) &= \partial_{r_x} \left(-\frac{(Tr_y)^2}{r_x} \alpha'_6 \right) = \frac{(Tr_y)^2}{r_x^2} (\alpha'_6 + \alpha''_6) < T^2 (\alpha'_6 + \alpha''_6) \approx \propto T^2 \left(\frac{1}{l} + \frac{1}{l^2} \right), \quad \text{small} \\ \partial_{r_x r_y}^2 (\alpha_6 (Tr_y)^2) &= \partial_{r_y} \left(-\frac{(Tr_y)^2}{r_x} \alpha'_6 \right) = \frac{-T^2 r_y}{r_x} (2\alpha'_6 + \alpha''_6), \quad \text{norm} < T^2 (2\alpha'_6 + \alpha''_6) \\ \partial_{r_y r_y}^2 (\alpha_6 (Tr_y)^2) &= \partial_{r_y} (T^2 \alpha'_6 r_y + 2T^2 \alpha_6 r_y) = T^2 (3\alpha'_6 + \alpha''_6 + 2\alpha_6)\end{aligned}$$

Note the first derivative α'_6 goes from 0 to a maximum of $1/l + \epsilon$ at the half way point of $l/2$ so the change in slope is roughly $1/l^2$, still small. (Strictly speaking, $(1/l + \epsilon)(2/l)$.) Thus the derivatives of $\alpha_6 r_y^2$ can be made small by taking l sufficiently large.

2nd term for region IIA: $\alpha_3(d_{IIA})d_{IIA}$

First derivative. $\frac{1}{r_*} \partial_{r_*} (\alpha_3 d_{IIA}) = (\alpha'_3 d_{IIA} + \alpha_3) \cdot \frac{d_{IIA\star}}{r_*}$.

Here are the partial derivatives of d_{IIA} .

$$\begin{aligned}d_{IIA} &\approx T^2 [r_x^2 - \frac{1}{2}(r_y^2 + r_z^2)] + \frac{3}{2} \alpha_6 (\log r_y - \log r_x) \cdot (Tr_y)^2 \\ \frac{(d_{IIA})_x}{r_x} &= \frac{T^2}{r_x} [2r_x + \frac{3}{2} (\alpha'_6 \cdot \frac{-1}{r_x} \cdot r_y^2)] = T^2 [2 + \frac{3}{2} (\alpha'_6 \cdot \frac{-r_y^2}{r_x^2})] \\ \frac{(d_{IIA})_y}{r_y} &= \frac{T^2}{r_y} [-r_y + \frac{3}{2} (\alpha'_6 \cdot \frac{1}{r_y} \cdot r_y^2 + 2r_y \alpha_6)] = T^2 [-1 + \frac{3}{2} (\alpha'_6 + 2\alpha_6)] \\ \frac{(d_{IIA})_z}{r_z} &= \frac{T^2}{r_z} [-r_z] = -T^2\end{aligned} \tag{2.1}$$

Hence the terms in $\frac{1}{r_*} \partial_{r_*} (\alpha_3 d_{IIA}) = (\alpha'_3 d_{IIA} + \alpha_3) \cdot \frac{d_{IIA\star}}{r_*}$ are as follows:

- Multiplying $\alpha'_3 d_{IIA}$ by possible terms in $\frac{d_{IIA\star}}{r_\star}$:
 - $\alpha'_3 d_{IIA}$: \star anything, from constant terms in each $\frac{d_{IIA\star}}{r_\star}$
 - $\alpha'_3 d_{IIA} \alpha_6$: $\star = y$, since α_6 only shows up in $\star = y$ derivative
 - $\alpha'_3 d_{IIA} \alpha'_6$: $\star = y$, ”
 - $\alpha'_3 d_{IIA} \alpha'_6 \cdot \left(\frac{r_y}{r_x}\right)^2$: $\star = x$ only
- Multiplying α_3 by $\frac{d_{IIA\star}}{r_\star}$:
 - α_3 : \star anything
 - $\alpha_3 \alpha_6$: $\star = y$
 - $\alpha_3 \alpha'_6$: $\star = y$
 - $\alpha_3 \alpha'_6 \cdot \left(\frac{r_y}{r_x}\right)^2$: $\star = x$

Thus we have terms which are either $\alpha_3'^{\log} = \alpha'_3 d_{IIA}$ or a regular derivative of α_6 , which may be multiplied by $(r_y/r_x)^2$ but $r_x > r_y$ in region IIA. So derivative terms of $\alpha_3(d_{IIA})d_{IIA}$ can be made small for l sufficiently large.

Second derivative terms. We differentiate each of the first derivative terms. Let's say P is a term in the list above. Then we want to differentiate $r_\star P$ because above we divided by r_\star . Thus using the product rule with a differential operator $D = \partial_{r_\bullet}$ we get $D(r_\star)P + r_\star D(P)$. The first term gives 0 or 1 times P , which we already know is small by the above item for each P on the list. So we'll only need to consider $r_\star D(P)$ for the 8 choices of P listed above.

1. $P = \alpha'_3 d_{IIA}$

Then this term contributes to $\partial_{r_\star r_\bullet}^2(F)$ via $r_\star \partial_{r_\bullet}(P)$ i.e.

$$\begin{aligned}
 r_\star \partial_{r_\bullet}(\alpha'_3 d_{IIA}) &= r_\star \alpha_3'' \cdot (d_{IIA})_\bullet \cdot d_{IIA} + r_\star \alpha'_3 (d_{IIA})_\bullet = \frac{r_\star (d_{IIA})_\bullet}{d_{IIA}} \alpha_3''^{\log} \\
 (d_{IIA})_\bullet \text{ terms : } \{T^2 r_\bullet, T^2 \alpha_6 r_y, T^2 \alpha'_6 r_y, T^2 \alpha'_6 \frac{r_y^2}{r_x}\} &< T^2 r_\bullet, \because \alpha_6 \leq 1, \alpha'_6 \approx \alpha \frac{1}{l}, \frac{r_y}{r_x} < 1 \\
 \frac{T^2 r_\star r_\bullet}{d_{IIA}} &\approx \frac{r_\star r_\bullet}{r_x^2 - \frac{1}{2}(r_y^2 + r_z^2) + \frac{3}{2}\alpha_6 r_y^2} = \frac{r_\star r_\bullet / r_x^2}{1 - \frac{1}{2}((r_y/r_x)^2 + (r_z/r_x)^2) + \frac{3}{2}\alpha_6 (r_y/r_x)^2} \quad (2.2) \\
 &\approx \frac{r_\star r_\bullet}{r_x^2} \approx \in \{0, 1\} \because r_x \gg r_y, r_z \text{ in region IIA} \\
 \therefore r_\star \partial_{r_\bullet}(P) &= \frac{r_\star (d_{IIA})_\bullet}{d_{IIA}} \alpha_3''^{\log} \approx (\text{bounded}) \cdot \frac{1}{l^2}
 \end{aligned}$$

2. $P = \alpha'_3 d_{IIA} \alpha_6$ term from differentiating F first wrt y , i.e. $\partial_{r_y}(F)$

$$\begin{aligned} r_y \partial_{r_\bullet}(\alpha'_3 d_{IIA} \alpha_6) &= r_y \partial_{r_\bullet}(\alpha'_3 d_{IIA}) \cdot \alpha_6 + r_y(\alpha'_3 d_{IIA}) \cdot \partial_{r_\bullet}(\alpha_6) \\ &= (\text{above case}) \cdot \alpha_6 \pm \alpha_3'^{\log} \alpha'_6 \cdot c r_y, \quad c \in \left\{ \frac{1}{r_x}, \frac{1}{r_y}, 0 \right\} \\ &= \text{small} + \text{small} \end{aligned}$$

3. $\alpha'_3 d_{II} \alpha'_6$ term from differentiating first wrt y . Same as 2, replacing α_6 with α'_6 .

4. $\alpha'_3 d_{II} \alpha'_6 \cdot \left(\frac{r_y}{r_x}\right)^2$ from differentiating first wrt x

$$\begin{aligned} r_x \partial_{r_\bullet}(\alpha'_3 d_{II} \alpha'_6 \cdot \left(\frac{r_y}{r_x}\right)^2) &= r_x \partial_{r_\bullet}(\alpha'_3 d_{II} \alpha'_6) \cdot \left(\frac{r_y}{r_x}\right)^2 + r_x(\alpha'_3 d_{II} \alpha'_6) \cdot \partial_{r_\bullet} \left(\frac{r_y}{r_x}\right)^2 \\ &= \frac{r_y}{r_x} \cdot r_y \partial_{r_\bullet}(\alpha'_3 d_{II} \alpha'_6) \pm (\alpha_3'^{\log} \alpha'_6) \cdot c r_x, \quad c \in \{2r_y^2/r_x^3, 2r_y/r_x^2, 0\} \\ &= (\text{small})(\text{previous case}) + (\text{small})(r_y/r_x)^i, \quad i \in \{1, 2\} \\ &= \text{small} \because r_x \gg r_y \end{aligned}$$

5. $P = \alpha_3$: shows up in first derivative of F wrt any variable

Taking another derivative gives $r_\star \partial_{r_\bullet} \alpha_3 = r_\star \alpha'_3 (d_{IIA})_\bullet = \alpha_3'^{\log} \cdot (r_\star (d_{IIA})_\bullet) / d_{IIA}$. So we want $(r_\star (d_{IIA})_\bullet) / d_{IIA}$ to be bounded. This was checked in Equation (2.2).

6. $P = \alpha_3 \alpha_6$: shows up in first derivatives of F wrt y

$$r_y \partial_{r_\bullet}(\alpha_3 \alpha_6) = r_y((\alpha_3)_\bullet \alpha_6 + \alpha_3 (\alpha_6)_\bullet)$$

The term involving the derivative of α_3 is included in the previous case. The second term gives $\alpha_3 \alpha'_6$ times one or zero, since $r_y/r_x \ll 1$ or 1, so that term is a bounded term times a small term hence also small.

7. $P = \alpha_3 \alpha'_6$: $\star = y$. Replace α_6 with α'_6 in the previous case.

8. $P = \alpha_3 \alpha'_6 (r_y/r_x)^2$: $\star = x$. The calculation for this is identical to 4, where now the “already-checked” part is $\alpha_3 \alpha'_6$ instead of $\alpha'_3 d_{II} \alpha'_6$.

This concludes our check of the first and second order derivatives of $\alpha_3(d_{IIA})d_{IIA}$.

3rd term for region IIA: $\alpha_5 \cdot (Tr_\star)^2$ for $\star \in \{y, z\}$

We run through the same argument as with $\alpha_3 \cdot d_{IIA}$ above, replacing d_{IIA} with $(Tr_*)^2$ in the second term.

First derivative. $\frac{1}{r_*} \partial_{r_*} (\alpha_5 (Tr_*)^2) = \frac{1}{r_*} \alpha'_5 (d_{IIA})_* (Tr_*)^2 + \alpha_5 \cdot \frac{((Tr_*)^2)_*}{r_*}$.

The partial derivatives of $(Tr_*)^2$ are $\frac{1}{r_*} \partial_{r_*} ((Tr_*)^2) = 2T^2$ or 0.

Hence the nonzero terms in $\frac{1}{r_*} \partial_{r_*} (\alpha_5 (Tr_*)^2)$ are $2T^2 \alpha_5$ and

$$\frac{1}{r_*} \alpha'_5 (d_{IIA})_* (Tr_*)^2 = \alpha'_5 \log \frac{T^2 r_*^2 (d_{IIA})_*}{d_{IIA} r_*}$$

Note that $\frac{T^2 r_*^2}{d_{IIA}}$ and $\frac{(d_{IIA})_*}{r_*}$ are bounded. The latter was already checked in Equation (2.1). For the former:

$$\frac{r_*^2}{r_x^2 - \frac{1}{2}(r_y^2 + r_z^2) + \frac{3}{2}\alpha_6 r_y^2} = \frac{r_*^2/r_x^2}{1 - \frac{1}{2}((r_y/r_x)^2 + (r_z/r_x)^2) + \frac{3}{2}\alpha_6 (r_y/r_x)^2} \ll 1 \because r_x \gg r_y, r_z \quad (2.3)$$

Note that $* \in \{y, z\}$. So first derivatives are bounded for sufficiently large l in $\alpha_5 \cdot (Tr_*)^2$ since they are either non-bump function derivatives or a bounded quantity multiplied by a small log derivative.

Second derivative terms. We differentiate each of the first derivative terms. They are $\alpha'_5 (d_{IIA})_* (Tr_*)^2$ and $2T^2 r_* \alpha_5$. Let's say Pr_* is one of these terms, i.e. P was considered in the previous item. Thus using the product rule with a differential operator $D = \partial_{r_\bullet}$ we get $D(r_*)P + r_* D(P)$. The first term gives 0 or 1 times P , which we already know is small by the above item for each P on the list. So we'll only need to consider $r_* D(P)$ for these 2 choices of P .

1. $P = \alpha'_5 (Tr_*)^2 \frac{(d_{IIA})_*}{r_*}$. This involves the following terms, where we multiply $\alpha'_5 (Tr_*)^2$ by the four possible types of terms showing up in $\frac{(d_{IIA})_*}{r_*}$, and check second derivatives arising from each.

(i) $\alpha'_5 (Tr_*)^2$: this term contributes to $\partial_{r_* r_\bullet}^2 (F)$ via $r_* \partial_{r_\bullet} (P)$ i.e.

$$\begin{aligned} r_* \partial_{r_\bullet} (\alpha'_5 (Tr_*)^2) &= r_* \alpha''_5 \cdot (d_{IIA})_\bullet \cdot (Tr_*)^2 + r_* \alpha'_5 ((Tr_*)^2)_\bullet \\ &= (\alpha''_5 \log - \alpha'_5 \log) \frac{r_* \cdot (d_{IIA})_\bullet \cdot (Tr_*)^2}{d_{IIA}^2} + \alpha'_5 \log \frac{2T^2 r_\bullet r_*}{d_{IIA}} \end{aligned}$$

$$\text{Already checked bounded: } \frac{r_* (d_{IIA})_\bullet}{d_{IIA}} \because (2.2), \frac{(Tr_*)^2}{d_{IIA}} \because (2.3), \frac{T^2 r_\bullet r_*}{d_{IIA}} \because (2.2)$$

$$\therefore r_* \partial_{r_\bullet} (\alpha'_5 (Tr_*)^2) = (\text{small})(\text{bounded}) + (\text{small})(\text{bounded})$$

(ii) $\alpha'_5(Tr_*)^2\alpha_6$: term from differentiating F first wrt y , i.e. $\partial_{r_y}(F)$

$$\begin{aligned} r_y \partial_{r_\bullet}(\alpha'_5(Tr_*)^2\alpha_6) &= r_y \partial_{r_\bullet}(\alpha'_5(Tr_*)^2) \cdot \alpha_6 + r_y(\alpha'_5(Tr_*)^2) \cdot \partial_{r_\bullet}(\alpha_6) \\ &= (\text{above case}) \cdot \alpha_6 \pm \alpha'_5 \log \frac{(Tr_*)^2}{d_{IIA}} \alpha'_6 \cdot cr_y, \quad c \in \left\{ \frac{1}{r_x}, \frac{1}{r_y}, 0 \right\} \\ &= (\text{small})(\text{bounded}) + (\text{small})(\text{bounded}) \end{aligned}$$

(iii) $\alpha'_5(Tr_*)^2\alpha'_6$: term from differentiating first wrt y . Same as previous, replacing α_6 with α'_6 .

(iv) $\alpha'_5(Tr_*)^2\alpha'_6 \cdot \left(\frac{r_y}{r_x}\right)^2$: from differentiating first wrt x

$$\begin{aligned} r_x \partial_{r_\bullet}(\alpha'_5(Tr_*)^2\alpha'_6 \cdot \left(\frac{r_y}{r_x}\right)^2) &= r_x \partial_{r_\bullet}(\alpha'_5(Tr_*)^2\alpha'_6) \cdot \left(\frac{r_y}{r_x}\right)^2 + r_x(\alpha'_5(Tr_*)^2\alpha'_6) \cdot \partial_{r_\bullet} \left(\frac{r_y}{r_x}\right)^2 \\ &= \frac{r_y}{r_x} \cdot r_y \partial_{r_\bullet}(\alpha'_5(Tr_*)^2\alpha'_6) \pm (\alpha'_5 \log \frac{(Tr_*)^2}{d_{IIA}} \alpha'_6) \cdot cr_x, \quad c \in \left\{ \frac{2r_y^2}{r_x^3}, \frac{2r_y}{r_x^2}, 0 \right\} \\ &= (\text{small})(\text{previous case}) + (\text{small})(r_y/r_x)^i, \quad i \in \{1, 2\} \\ &= \text{small} \because r_x \gg r_y \end{aligned}$$

2. $P = 2T^2\alpha_5$: shows up in first derivative of F wrt any variable

Taking another derivative gives $r_\star \partial_{r_\bullet} 2T^2\alpha_5 = r_\star 2T^2\alpha'_5(d_{IIA})_\bullet = 2T^2\alpha'_5 \log \cdot (r_\star(d_{IIA})_\bullet)/d_{IIA}$. So we want $(r_\star(d_{IIA})_\bullet)/d_{IIA}$ to be bounded. This was checked in Equation (2.2).

This concludes our check of the first and second order derivatives of $\alpha_5(d_{IIA})(Tr_*)^2$ for $\star \in \{y, z\}$. We have one more remaining type of term showing up in F that we have to check first and second order derivatives of.

4th term for region IIA: $\alpha_5\alpha_6 \cdot (Tr_y)^2$

$$\begin{aligned} \frac{1}{r_\star} \partial_{r_\star}(\alpha_5(Tr_y)^2) \cdot \alpha_6 + \alpha_5(Tr_y)^2 \cdot \frac{1}{r_\star} \partial_{r_\star} \alpha_6 &= (\text{previous}) \cdot \alpha_6 \pm \alpha_5(Tr_y)^2 \cdot \frac{c}{r_\star^2} \alpha'_6 \\ \text{2nd term: } \star = z &\implies c = 0, \quad \star = x \implies \approx 0 \because r_x \gg r_y, \quad \star = y \implies \frac{r_y^2}{r_\star^2} = 1 \end{aligned}$$

So again first derivatives may be made small by taking l sufficiently large. Finally, we check second order derivatives.

$$\begin{aligned} \partial_{r_\bullet}[\partial_{r_\star}(\alpha_5(Tr_y)^2) \cdot \alpha_6 + \alpha_5(Tr_y)^2 \cdot \partial_{r_\star}(\alpha_6)] &= \partial_{r_\bullet r_\star}^2(\alpha_5(Tr_y)^2) \cdot \alpha_6 + \partial_{r_\star}(\alpha_5(Tr_y)^2) \partial_{r_\bullet} \alpha_6 \\ &\quad + \partial_{r_\bullet}(\alpha_5(Tr_y)^2) \partial_{r_\star} \alpha_6 + \alpha_5(Tr_y)^2 \cdot \partial_{r_\bullet} \partial_{r_\star}(\alpha_6) \end{aligned}$$

1st term ok by previous check on $\alpha_5(Tr_y)^2$

$$\begin{aligned} \text{Terms 2 \& 3: } \partial_{r_*}(\alpha_5(Tr_y)^2) \cdot \partial_{r_*}\alpha_6 &= (\alpha_5' \log \frac{(d_{IIA})^*}{d_{IIA}}(Tr_y)^2 + 2\alpha_5 T^2 \delta_{y*} r_y) \cdot \frac{\pm 1}{r_x \text{ or } r_y} \cdot \alpha_6' \\ &= \pm [T^2 \alpha_5' \log \frac{(d_{IIA})^* r_y}{d_{IIA}} \cdot \frac{r_y}{r_x \text{ or } r_y} \cdot \alpha_6' + 2\alpha_5 T^2 \frac{r_y}{r_x \text{ or } r_y} \cdot \alpha_6'] \end{aligned}$$

$$\begin{aligned} \text{4th term: } \alpha_5(Tr_y)^2 \partial_{r_*} \left(\frac{\alpha_6'}{r_x \text{ or } r_y} \right) &= \alpha_5(Tr_y)^2 \left[\alpha_6'' \cdot \frac{\pm 1}{r_x \text{ or } r_y} \cdot \frac{1}{r_x \text{ or } r_y} - \alpha_6' \frac{1}{r_x^2 \text{ or } r_y^2} \right] \\ &= T^2 \alpha_5 \alpha_6'' \frac{\pm r_y^2}{r_x^2, r_x r_y, \text{ or } r_y^2} - T^2 \alpha_5 \alpha_6' \frac{r_y^2}{r_x^2 \text{ or } r_y^2} \\ &= \text{small,} \quad \because r_x \gg r_y \\ \implies \partial_{r_*} \partial_{r_*} (\alpha_5 \alpha_6 \cdot (Tr_y)^2) &= (\text{small}) \end{aligned}$$

where the final line follows from the calculations for the 1st term of region IIA, which was $\alpha_6(Tr_y)^2$, and the third term of region IIA, which was $\alpha_5(Tr_y)^2$. So the upshot is: all terms involving derivatives of bump functions can be made arbitrarily small because they are multiplied by expressions which are bounded (taking either log derivatives of α_3, α_5 or regular derivatives of α_6 .) So we get a positive-definite form for l sufficiently large, because the terms not involving derivatives of bump functions are $O(1)$ so they dominate, and we already showed they give something positive-definite.

Region IIB

We just checked in region IIA hence by symmetry region IIC, and similarly IVA, IVC and VIA, VIC by symmetry. Swap $r_x \leftrightarrow r_y$ to get to IIC and subscripts I become III.

The characteristics in region IIB which we did not have in regions IIA and C are 1) r_x and r_y go from $r_x \gg r_y$ to $r_y \gg r_x$, passing through $r_x = r_y$ and 2) $\alpha_6 \equiv 1$. All of r_x, r_y, r_z are still small so we still have an approximation for the Kähler potential:

$$\begin{aligned} F &\approx T^2 r_z^2 + \alpha_3(d_{IIB})d_{IIB} + \frac{1}{2}\alpha_5(d_{IIB}) \cdot (-(Tr_z)^2) \\ d_{IIB} &\approx T^2[r_x^2 + r_y^2 - \frac{1}{2}r_z^2] \end{aligned}$$

Let's repeat the calculations above for $\alpha_3(d_{IIA}) \cdot d_{IIA}$ and $\alpha_5 \cdot (Tr_z)^2$ with region IIB, and see if they relied on $r_x \gg r_y$. What we know in region IIB is that $r_x, r_y \gg r_z$.

1st term for region IIB: $\alpha_3(d_{IIB})d_{IIB}$

First derivative. $\frac{1}{r_\star} \partial_{r_\star} (\alpha_3 d_{IIB}) = (\alpha'_3 d_{IIB} + \alpha_3) \cdot \frac{d_{IIB\star}}{r_\star}$.
Here are the partial derivatives of d_{IIB} .

$$\begin{aligned} d_{IIB} &\approx T^2 [r_x^2 + r_y^2 - \frac{1}{2} r_z^2] \\ \frac{(d_{IIB})_x}{r_x} &\approx \frac{T^2}{r_x} (2r_x) = \frac{T^2}{2} \\ \frac{(d_{IIB})_y}{r_y} &\approx \frac{T^2}{2} \\ \frac{(d_{IIB})_z}{r_z} &\approx -\frac{T^2}{4} \end{aligned}$$

Hence the terms in $\frac{1}{r_\star} \partial_{r_\star} (\alpha_3 d_{IIB}) = (\alpha'_3 d_{IIB} + \alpha_3) \cdot \frac{d_{IIB\star}}{r_\star}$ are proportional to $\alpha'_3 d_{IIB}$ (a log derivative, so small) and α_3 (not a derivative). So first derivatives of $\alpha_3(d_{IIB})d_{IIB}$ may be made small for l sufficiently large.

Second derivative terms. We differentiate each of the first derivative terms. Let's say P is a term in the list above. Then we want to differentiate $r_\star P$ because above we divided by r_\star . Thus using the product rule with a differential operator $D = \partial_{r_\bullet}$ we get $D(r_\star)P + r_\star D(P)$. The first term gives 0 or 1 times P , which we already know is small by the above item for each P on the list. So we'll only need to consider $r_\star D(P)$ for the 2 choices of P listed above.

$$1. P = \alpha'_3 d_{IIB}$$

Then this term contributes to $\partial_{r_\star r_\bullet}^2(F)$ via $r_\star \partial_{r_\bullet}(P)$ i.e.

$$\begin{aligned} r_\star \partial_{r_\bullet} (\alpha'_3 d_{IIB}) &= r_\star \alpha''_3 \cdot (d_{IIB})_\bullet \cdot d_{IIB} + r_\star \alpha'_3 (d_{IIB})_\bullet = \frac{r_\star (d_{IIB})_\bullet}{d_{IIB}} \alpha''_3 \log \\ (d_{IIB})_\bullet \text{ terms : } T^2 r_\bullet \\ \frac{T^2 r_\star r_\bullet}{d_{IIB}} &\approx \frac{r_\star r_\bullet}{r_x^2 + r_y^2 - \frac{1}{2} r_z^2} = \frac{r_\star r_\bullet / r_x^2}{1 + (r_y/r_x)^2 - \frac{1}{2} (r_z/r_x)^2} \approx \frac{r_\star r_\bullet / r_x^2}{1 + (r_y/r_x)^2} \\ (\star, \bullet) \in \{(r_x, r_x), (r_x, r_z), (r_z, r_z)\} &\implies \frac{r_\star r_\bullet}{r_x^2} \in \{1, \text{small}\} \because r_x \gg r_z \\ (\star, \bullet) = (r_y, r_z) &\implies \frac{r_y r_z}{r_x^2} < \frac{r_y}{r_x} \end{aligned}$$

$$(\star, \bullet) \in \{(r_x, r_y), (r_y, r_y)\} \text{ suffices to bound: } \frac{a}{1+a^2}, \frac{a^2}{1+a^2}, \quad a = r_y/r_x$$

$$\frac{a^2}{1+a^2} \leq 1, \quad a < 1 \implies \frac{a}{1+a^2} < 1, \quad a \geq 1 \implies \frac{a}{1+a^2} \leq \frac{a^2}{1+a^2} \leq 1$$

$$\therefore r_\star \partial_{r_\bullet} (\alpha'_3 d_{IIB}) = (\text{bounded})(\text{small})$$

2. $P = \alpha_3$

Taking another derivative gives $r_\star \partial_{r_\bullet} \alpha_3 = r_\star \alpha'_3 (d_{IIB})_\bullet = \alpha_3^{\prime \log} \cdot (r_\star (d_{IIB})_\bullet) / d_{IIB}$. So we want $(r_\star (d_{IIB})_\bullet) / d_{IIB}$ to be bounded. This was just checked above.

2nd term for region IIB: $\alpha_5 \cdot (Tr_z)^2$

We run through the same argument as with $\alpha_3 \cdot d_{IIB}$ above, replacing d_{IIB} with $(Tr_z)^2$ in the second term.

First derivative. $\frac{1}{r_\star} \partial_{r_\star} (\alpha_5 (Tr_z)^2) = \frac{1}{r_\star} \alpha'_5 (d_{IIB})_\star (Tr_z)^2 + \alpha_5 \cdot \frac{(Tr_z)^2_\star}{r_\star}$.

The partial derivatives of $(Tr_z)^2$ are $\frac{1}{r_\star} \partial_{r_\star} ((Tr_z)^2) = 2T^2$ or 0.

Hence the nonzero terms in $\frac{1}{r_\star} \partial_{r_\star} (\alpha_5 (Tr_z)^2)$ are $2T^2 \alpha_5$ and

$$\frac{1}{r_\star} \alpha'_5 (d_{IIB})_\star (Tr_z)^2 = \alpha_5^{\prime \log} \frac{T^2 r_z^2 (d_{IIB})_\star}{d_{IIB} \cdot r_\star}$$

Note that $\frac{T^2 r_z^2}{d_{IIB}}$ and $\frac{(d_{IIB})_\star}{r_\star}$ are bounded. The latter is approximately constant because d_{IIB} is approximately linear in r_x^2, r_y^2 and r_z^2 . For the former:

$$\frac{r_z^2}{r_x^2 + r_y^2 - \frac{1}{2} r_z^2} = \frac{r_z^2 / r_x^2}{1 + \frac{r_y^2}{r_x^2} - \frac{1}{2} ((r_z / r_x)^2)} \approx \frac{r_z^2 / r_x^2}{1 + \frac{r_y^2}{r_x^2}} \approx 0 \because r_x \gg r_z$$

So first derivatives of $\alpha_5 \cdot (Tr_z)^2$ may be made small by taking l sufficiently large.

Second derivative terms. We differentiate each of the first derivative terms. They are $\alpha'_5 (d_{IIB})_\star (Tr_z)^2$ and $2T^2 r_\star \alpha_5$. Let's say Pr_\star is one of these terms, i.e. P was considered in the previous item. Thus using the product rule with a differential operator $D = \partial_{r_\bullet}$ we get $D(r_\star)P + r_\star D(P)$. The first term gives 0 or 1 times P , which we already know is small by the above item for each P on the list. So we'll only need to consider $r_\star D(P)$ for these 2 choices of P .

1. $P = \alpha'_5(T r_z)^2 \frac{(d_{IIB})_\star}{r_\star}$. It suffices to consider $\alpha'_5(T r_z)^2$ because $\frac{(d_{IIB})_\star}{r_\star}$ is a constant.

$$\begin{aligned} r_\star \partial_{r_\bullet} (\alpha'_5(T r_z)^2) &= r_\star \alpha''_5 \cdot (d_{IIB})_\bullet \cdot (T r_z)^2 + r_\star \alpha'_5 ((T r_z)^2)_\bullet \\ &= (\alpha''_5{}^{\log} - \alpha'_5{}^{\log}) \frac{r_\star \cdot (d_{IIB})_\bullet \cdot (T r_z)^2}{d_{IIB}^2} + \alpha'_5{}^{\log} \frac{2T^2 r_z r_\star}{d_{IIB}} \end{aligned}$$

Already checked bounded: $\frac{r_\star (d_{IIB})_\bullet}{d_{IIB}}, \frac{(T r_z)^2}{d_{IIB}} \therefore$ (above)

$$\frac{T^2 r_z r_\star}{d_{IIB}} \approx \frac{r_z r_\star / r_x^2}{1 + (r_y/r_x)^2 - \frac{1}{2}(r_z/r_x)^2} \approx \frac{r_z r_\star / r_x^2}{1 + (r_y/r_x)^2} < \frac{r_\star / r_x}{1 + (r_y/r_x)^2}$$

$\star = x \implies$ bounded

$\star = y \implies a/(1 + a^2)$ bounded as above

$\star = z \implies$ small

$$\therefore r_\star \partial_{r_\bullet} (\alpha'_5(T r_z)^2) = (\text{small})(\text{bounded}) + (\text{small})(\text{bounded})$$

2. $P = 2T^2 \alpha_5$: shows up in first derivative of F wrt any variable

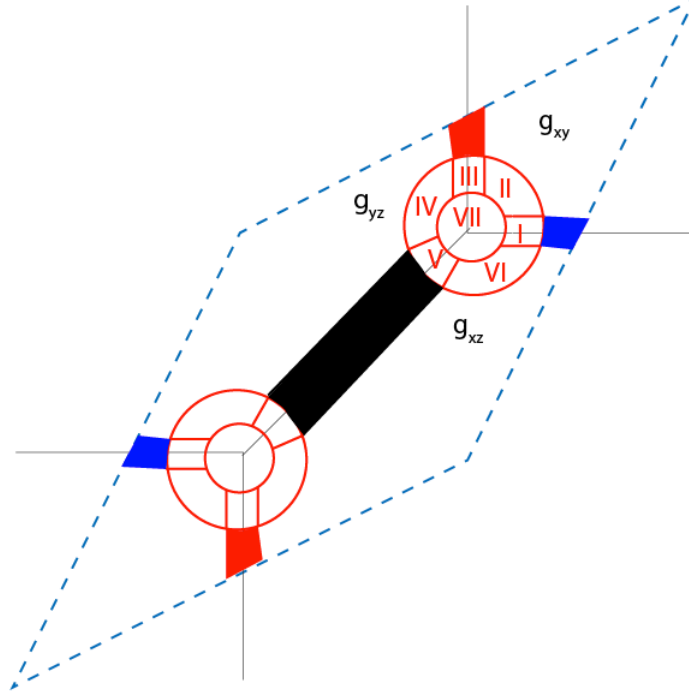
Taking another derivative gives $r_\star \partial_{r_\bullet} 2T^2 \alpha_5 = r_\star 2T^2 \alpha'_5 (d_{IIB})_\bullet = 2T^2 \alpha'_5{}^{\log} \cdot (r_\star (d_{IIB})_\bullet) / d_{IIB}$.
So we want $(r_\star (d_{IIB})_\bullet) / d_{IIB}$ to be bounded, which was already checked above.

This completes the calculation of positive definiteness in region IIB.

The remainder of \mathbb{C}^3 patch

In the region between region I and region IIA the only bump functions at play are α_3 and α_5 and they are allowed to vary in the same amount of space as checked above, and still $r_x \gg r_y, r_z$ so all the previous estimates apply.

2.4 Showing ω nondegenerate: away from \mathbb{C}^3 patch



All the calculations above involved approximations because r_x, r_y, r_z are all very small near the \mathbb{C}^3 patch. Around each vertex in the unbounded polytope we have some coordinate system with very small coordinates, so we define a symplectic form locally around all the vertices. (An analogue to think about are the coordinates z around 0 and $w = 1/z$ around ∞ in \mathbb{P}^1 . It is true that z gets very large in the w chart, but z and w are both small in the same way so one could take $\log(1 + |\text{coord}|^2)$ which would look the same in each chart.) So what remains to be checked is that the symplectic form glues positive-definitely along e.g. the z axis. Namely, recall that the same properties will hold along the other axes by symmetry, and in the remaining regions ω agrees with the standard Kähler form of the blowup $\mathbb{CP}^2(3)$.

In the black region along the z -axis we no longer have any dependence the d_V coordinate because the bump functions α_3, α_5 depending on them are constant and equal to 1. However we still have an angular coordinate to allow us to interpolate between g_{xz} and g_{yz} in the unprimed coordinates, or $g_{x'''z'''}$ and $g_{y'''z'''}$ in the tripled primed coordinates at the lower left vertex. So we need to check we have positive definiteness when only α_4 is at play and r_z is large. Note that when there are no bump functions we have positive definite-ness because either we are in region VII where we have the standard Kähler potential or we are in the center of a $\mathbb{CP}^2(3)$ of the toric variety of \mathbb{CP}^2 blown up at three points, which has a natural potential that can be read off from its lattice points.

Recall from the construction of coordinate charts on Y (Definition 1.17) that the charts U_{0,g^0} with coordinates (x, y, z) and $U_{(-1,0),g^{-1}}$ with coordinates (x''', y''', z''') are glued to each other via $(x''', y''', z''') = (Tv_0x^{-1}, Tv_0y^{-1}, T^{-2}z^{-1})$. Also recall from section 1.5 that along the z -axis, where $\alpha_3 = \alpha_5 = 1$, ω is defined by the Kähler potentials

$$F = \frac{1}{2}(g_{xz} + g_{yz}) + \alpha_4(\theta_V)\theta_V,$$

where $\theta_V = \phi_x - \phi_y$, and

$$F''' = \frac{1}{2}(g'''_{xz} + g'''_{yz}) + \alpha_4(\theta_V''')\theta_V''',$$

which differs from F by a harmonic term (see proof of Claim 1.5.2).

Using the symmetry between these two charts, it suffices to check that ω is positive definite on just half of the z -axis. Namely, we can assume that $|z| \leq T^{-1}$, since otherwise $|z'''| = |T^{-2}z^{-1}| \leq T^{-1}$.

Given this, we check that the bump function derivatives are bounded. The Kähler potential is of the form $(f + d) + \alpha_4(\theta) \cdot \theta$. So we just check derivatives of $\alpha_4(\theta) \cdot \theta$. We can use the above calculations for this term by the following reasoning. Although $|z| \leq T^{-1}$, we may assume that $|x|$ and $|y|$ are very small. They are at most of the order of $T^{3l/8-l/p}$, see Definition 1.4.23; otherwise α_4 is constant and equal to $\pm 1/2$, so F agrees with either g_{xz} or g_{yz} . Thus $|T^2xz| \leq |Tx|$ and $|T^2yz| \leq |Ty|$ hence these quantities are very small and we have again small scale approximations for their logarithms.

$$\begin{aligned} \theta &= \phi_x - \phi_y = \log_T(1 + |Tx|^2) - \log_T(1 + |T^2yz|^2) - \log_T(1 + |Ty|^2) + \log_T(1 + |T^2xz|^2) \\ &\approx (1 + |Tz|^2)(|Tx|^2 - |Ty|^2) \end{aligned}$$

$$\begin{aligned} \frac{1}{r_*} \frac{\partial}{\partial r_*}(\alpha_4 \theta) &= (\alpha'_4 \theta + \alpha_4) \frac{\theta_*}{r_*} \\ \frac{\partial}{\partial r_\bullet}(\alpha'_4 \theta \theta_*) &= \alpha''_4 \theta_\bullet \theta \theta_* + \alpha'_4 \theta_\bullet \theta_* + \alpha'_4 \theta \theta_{*\bullet} = (\alpha''_4 \theta^2 + \alpha'_4 \theta) \cdot \frac{\theta_\bullet \theta_*}{\theta} + \alpha'_4 \log \theta_{*\bullet} \\ \frac{\partial}{\partial r_\bullet}(\alpha_4 \theta_*) &= \alpha'_4 \theta_\bullet \theta_* + \alpha_4 \theta_{*\bullet} = \alpha'_4 \log \frac{\theta_\bullet \theta_*}{\theta} + \alpha_4 \theta_{*\bullet} \end{aligned}$$

Thus we'll need to bound the following three terms, and then check we have enough space for the log derivatives:

- $\frac{\theta_*}{r_*}$ has estimates $2(1 + |Tz|^2)T^2$ for $* \in \{x, y\}$ and for $* = z$ we have the estimate

$$\frac{\theta_z}{r_z} \approx T^4(r_x^2 - r_y^2) \approx 0$$

(using the fact that $r_x, r_y \ll r_z$.)

- $\frac{\theta_{\bullet}\theta_{*}}{\theta}$ implies we'll need to consider $\frac{r_{\bullet}r_{*}}{r_x^2-r_y^2}$ so we need to know size constraints so that the support of α_4 is away from a region where $r_x = r_y$. Recall from above that we make α_4 constant equal to zero on a sliver $T < (r_x/r_y)^2 < 1/T$. Also we get approximately zero unless both $*$ and \bullet are not z , because θ is approximately $(1 + T^2 r_z^2)T^2(r_x^2 - r_y^2)$ and $r_x, r_y \ll r_z$. As above, we divide top and bottom by r_x^2 or r_y^2 depending on which variable is larger, and then the numerator is at most 1 while the denominator is bounded below from the constraint $T < (r_x/r_y)^2 < 1/T$.
- $\theta_{*\bullet}$ is approximately zero unless $* = \bullet$ in which case it's a constant, so bounded.

Note that we will have enough space for log derivatives because $\theta \approx (1 + |Tz|^2)T^2(r_x^2 - r_y^2)$ for r_x, r_y very small and this was already checked earlier when $\theta \approx T^2(r_x^2 - r_y^2)$.

Chapter 3

HMS for V and V^\vee abelian varieties

Homological mirror symmetry for tori can be derived from SYZ mirror symmetry using Family Floer Theory, [Fuk02]. In particular, Family Floer theory implies that line bundles should mirror the behavior of Lagrangian sections of the SYZ fibration. This is because by Serre duality $\text{Ext}^n(\mathcal{O}_{p_0}, \mathcal{O}) \cong \mathcal{O}_{p_0}$, while the intersection of the vertical linear Lagrangian on a torus with any other linear Lagrangian of integer slope will have one intersection point. In dimension > 1 , the notion of “integer slope” means that the matrix describing the Lagrangian maps the base lattice Γ_B to the fiber lattice $\Gamma_F = \mathbb{Z}^2$, so that along loops in the base torus T_B the vertical coordinates change by an integer number of turns around the fiber torus T_F .

Said another way, we can define a line bundle at each point to correspond to the 1-dimensional vector space generated by that intersection point of a linear integer-slope Lagrangian with L_{pt} on the Floer theory side, and put a holomorphic structure on the result to obtain a holomorphic line bundle, c.f. [Fuk02].

3.1 The Fukaya category $Fuk(V^\vee)$

We consider the following full subcategory of the Fukaya category $Fuk(V^\vee)$, an A_∞ -category.

- Objects: Let $M = \begin{pmatrix} 2 & 1 \\ 1 & 2 \end{pmatrix}$ and $\Gamma_B := M(\mathbb{Z}^2)$. We have affine action-angle coordinates $(\xi_1, \xi_2, \theta_1, \theta_2)$ on a fiber V^\vee of $v_0 : Y \rightarrow \mathbb{C}$, where ξ_i are monotonic in the norms of the complex coordinates and θ_i are their angles. The symplectic form on the fiber in these coordinates is $\omega = d\xi \wedge d\theta$. We consider the subcategory with objects given by the following linear Lagrangians:

$$\ell_i = \{(\xi_1, \xi_2, -i \cdot M^{-1}(\xi))\}_{\xi \in T_B = \mathbb{R}^2 / M(\mathbb{Z}^2)}$$

These are the analogue of the lines of slope i considered on an elliptic curve in [PZ98].

- Morphisms: $|i - j| \geq 1$, then $\text{Hom}(\ell_i, \ell_j) := \oplus_{p \in \ell_i \cap \ell_j} \mathbb{C} \cdot \{p\} \cong \mathbb{C}^{(i-j)^2}$ by a modular arithmetic argument. Note that this is the same as $h^0(V, \mathcal{L}^{\otimes(j-i)})$ for $j > i$ and $h^2(V, \mathcal{L}^{\otimes(j-i)})$ for $i > j$ which will tell us the morphism groups are isomorphic. If ξ corresponds to the coordinates on ℓ_i and $\tilde{\xi}$ on ℓ_j then they can only intersect at points where

$$\begin{aligned}
& 1) \xi \equiv \tilde{\xi} \pmod{M(\mathbb{Z}^2)} \\
& 2) i \cdot M^{-1}(\xi) \equiv j \cdot M^{-1}(\tilde{\xi}) \pmod{\mathbb{Z}^2} \\
& \implies i \cdot \xi \equiv j \cdot \tilde{\xi} \equiv j \cdot \xi \pmod{M(\mathbb{Z}^2)} \\
& \implies \xi \in \frac{1}{i-j} M(\mathbb{Z}^2)
\end{aligned} \tag{3.1}$$

So let $\xi = s(2, 1) + t(1, 2)$. Then $(i-j)s$ and $(i-j)t$ can be anything from 0 up to $i-j-1$ and we get $(i-j)^2$ intersection points.

- μ^1 on homs: the differential counts holomorphic bigons between intersection points.

Claim 3.1.1. There are no bigons on T^4 between any two intersection points of the linear Lagrangian submanifolds $\ell_i \cap \ell_j$, for $i \neq j$, so $\mu^1 = 0$.

Proof. Suppose we have a bigon $u : \mathbb{D}^2 \setminus \{\pm 1\} \rightarrow T^4$ between two intersection points p, q with boundary on $\ell_i \cup \ell_j$. Pick lifts $\tilde{\ell}_i = \{(\xi_1, \xi_2, i \cdot M^{-1}(\xi))\}_{\xi \in \mathbb{R}^2}$ and $\tilde{\ell}_j$ to the universal cover \mathbb{R}^4 , and translate the lift of the original intersection point p to $\tilde{p} = 0$.

Let ∂_1 and ∂_2 denote the boundary components of $\mathbb{D}^2 \setminus \{\pm 1\}$ which map to ℓ_i and ℓ_j respectively under u . Select lifts γ_1, γ_2 of $u(\partial_i)$ to \mathbb{R}^4 such that $\gamma_i(0) = \tilde{p}$ and set $\tilde{q}_i := \gamma_i(1)$. Then by contractibility of the disk domain \mathbb{D}^2 , the map $\mathbb{D}^2 \rightarrow T^4$ lifts to the universal cover \mathbb{R}^4 and hence $\tilde{q}_1 = \tilde{q}_2$. However, an intersection point of $\tilde{\ell}_i \cap \tilde{\ell}_j$ must have first two coordinates $\xi^{(i)} = \xi^{(j)}$. So if we denote this by ξ , we have $i\xi = j\xi \therefore \xi = 0$ since $|i-j| \geq 1$.

So there can only be one intersection point. I.e. observing that $\tilde{\ell}_i$ and $\tilde{\ell}_j$ are linear subspaces of \mathbb{R}^4 intersecting transversely at the origin, we see that any disc in \mathbb{R}^4 with boundary on $\tilde{\ell}_i \cup \tilde{\ell}_j$ must be homotopically trivial with all its corners at the origin. \square

The hom spaces are dimension $(i-j)^2$ for i and j distinct, matching $h^0(V, L^{j-i})$ only when $j > i$, otherwise they live in Floer degree 2 and match $h^2(V, L^{j-i})$ (a negative line bundle). Meanwhile, for $i = j$, there typically *are* bigons between ℓ_i and a slight Hamiltonian perturbation of it. However it is still true that $HF(\ell_i, \ell_i) = H^*(T^2)$ from the PSS and Morse isomorphisms, and the key geometric fact this relies on is that ℓ_i does not bound any discs in the torus, so self-HF reduces to classical cohomology. Since $HF^*(\ell_i, \ell_i) \cong H^*(\ell_i) = H^*(T^2)$, in all cases we find that $HF^*(\ell_i, \ell_j) \cong \text{Ext}_V^*(\mathcal{L}^{\otimes i}, \mathcal{L}^{\otimes j})$.

- Composition, or μ^2 , on homs (by analogy with the [PZ98] picture for the elliptic curve): we consider lifts $\tilde{\ell}_0, \tilde{\ell}_1, \tilde{\ell}_2$ and look at the possible triangles that can occur. One obtains a sum indexed by elements of Γ , which matches the expansions for multi-theta functions as we shall see below.
- The isomorphism $HF^*(\ell_i, \ell_i) \cong H^*(\ell_i)$ mentioned above is in fact well-known to be a ring isomorphism. The Donaldson-Fukaya category is unital, with identity morphisms given by the generator of $HF^0(\ell_i, \ell_i) \cong H^0(\ell_i)$. A reference for this is [Sei08, §(8c)].

Note: when it comes to the *ring* isomorphism between $HF^*(\ell_i, \ell_i)$ and $H^*(\ell_i)$, which in particular implies that the unit for the Floer product corresponds to the unit in $H^0(\ell_i)$, the isomorphism can also be checked by comparing Floer homology, with its product, to Morse cohomology, with its product. This first appears as a special case of a result of Fukaya-Oh [FO97], which includes a more general A_∞ -algebra statement. In the specific case of just the product, see also [KMS11].

3.2 The bounded derived category $D^bCoh(V)$

Definition 3.2.1. The *bounded derived category* is defined as follows. Let \mathcal{A} be the category of coherent sheaves on V . Note that V is an abelian variety, hence a projective variety.

Claim 3.2.2. \mathcal{A} is an abelian category, in particular has kernels and cokernels, so we can define chain complexes of objects.

Definition 3.2.3. Define $Kom(\mathcal{A})$ to be the category of chain complexes in $Coh(V)$, where morphisms are chain maps and composition is composition of chain maps.

Definition 3.2.4. Define $K(\mathcal{A})$ to have objects given by chain complexes as above, and morphisms are identified under an equivalence relation \sim which is homotopy equivalence.

Definition 3.2.5. The derived category $D(\mathcal{A})$ has the same objects as $K(\mathcal{A})$ and a morphism $A^\bullet \rightarrow B^\bullet$ is a roof $A^\bullet \leftarrow C^\bullet \rightarrow B^\bullet$ where $C^\bullet \rightarrow A^\bullet$ is a quasi-isomorphism, i.e. a chain map inducing an isomorphism on homology. Two morphisms are equivalent if they are dominated in $K(\mathcal{A})$ by a third object of the same sort.

Then the bounded derived category is obtained by carrying out this process after starting with $Kom^b(\mathcal{A})$, where we take only bounded chain complexes (zero outside a finite sequence of objects).

Claim 3.2.6. $D^bCoh(V)$ can be enhanced to a dg-category, namely an A_∞ -category where $\mu^{\geq 3} = 0$.

We will not need this here because we only consider cohomology.

Remark 3.2.7 (Notation). Consider a power \mathcal{L}^k of the ample line bundle \mathcal{L} on V which is very ample, and so it determines a projective embedding such that the restriction of $\mathcal{O}(1)$ to the image is \mathcal{L}^k . Hence we may use $\mathcal{O}(-n)$ to denote \mathcal{L}^{-kn} .

Claim 3.2.8. Recall $\mathcal{L} \rightarrow V$ defined earlier. Then we claim $\mathcal{O}, \mathcal{L}, \mathcal{L}^2$ split-generate $D^bCoh(V)$.

Remark 3.2.9. While this allows us to reduce to considering only these objects, it comes at the expense of requiring more information about higher A_∞ -products. This is because other objects will come up as complexes built from $\mathcal{O}, \mathcal{L}, \mathcal{L}^2$, but the calculation of cohomology level hom's between these complexes requires knowledge of some chain-level higher compositions among $\mathcal{O}, \mathcal{L}, \mathcal{L}^2$. In particular we would in principle need to know all μ^k 's involving an arbitrary sequence of objects taken from $\mathcal{O}, \mathcal{L}, \mathcal{L}^2$, with as many repetitions as desired among these.

Claim 3.2.10. \mathcal{L} as defined above is an ample line bundle.

Proof. Line bundles on complex tori are characterized by hermitian forms H (see Polishchuk book on Abelian Varieties, [Pol03]). Ample line bundles are equivalently those with $H^0(V, \mathcal{L}^i) \neq 0$ for some i , as is the case in this setting because \mathcal{L}^i for $i > 0$ has i^2 sections, and also the kernel of the map $V \ni x \mapsto t_x^* \mathcal{L} \otimes \mathcal{L}$ is finite, which is equivalent to H being non-degenerate (see [Pol03, Chapter 8.5–8.6]). But here

$$H = \begin{pmatrix} 2 & 1 \\ 1 & 2 \end{pmatrix}$$

has nonzero determinant, i.e. is nondegenerate, so that \mathcal{L} is ample and the claim applies. \square

Corollary 3.2.11. *The abelian variety V is projective.*

For the definition of split-generate, we need some preliminary definitions.

Definition 3.2.12. A category \mathcal{C} is *triangulated* if it contains all mapping cones, i.e. given any morphism f the object $Cone(f)$ is an object in \mathcal{C} . Rather, it contains the shift functor, the auto-equivalence $A \mapsto A[1]$ and it has a class of distinguished triangles.

Definition 3.2.13. A triangulated subcategory $\mathcal{D} \subset \mathcal{C}$ is *thick* if it closed under taking direct summands, i.e. $E \oplus F \in Ob(\mathcal{D}) \implies E, F \in Ob(\mathcal{D})$.

Definition 3.2.14. We say a set of objects $\{G_i\}_{i \in I} \in Ob(\mathcal{C})$ *split-generate* \mathcal{C} if their thick envelope is \mathcal{C} , namely if we take the smallest triangulated category containing the G_i which is closed under taking direct summands, we get all of \mathcal{C} .

Proof of Claim 3.2.8. The following uses background learned in [APS] and relies on induction. Recall that $\mathcal{L} = \mathcal{O}(H)$ defines the hypersurface $H \subset V$ as the zero set of a section $s : V \rightarrow \mathcal{L}$. Consider $\mathcal{O}_H(kH) = i_* i^* \mathcal{L}^k \equiv i_* \mathcal{L}^k|_H$ where i is the inclusion of H in V ; this is a restriction of \mathcal{L}^k to H followed by pushforward under the inclusion map to obtain a sheaf

on V supported on H . The defining section s gives rise to the classical short exact sequence $\mathcal{O}(-H) \rightarrow \mathcal{O} \rightarrow \iota_* \mathcal{O}_H$, where the first map is multiplication by s , since functions vanishing on H are the image of the first map and kernel of the second. Twisting by \mathcal{L}^k gives the short exact sequence $0 \rightarrow \mathcal{L}^{k-1} \xrightarrow{\otimes s} \mathcal{L}^k \rightarrow i_* \mathcal{L}^k|_H \rightarrow 0$ of sheaves on V . A s. e. s. gives rise to an exact triangle in the derived category, by standard theory, so we obtain the exact triangle:

$$\mathcal{L}^{k-1} \rightarrow \mathcal{L}^k \rightarrow i_* \mathcal{L}^k|_H$$

Although $s|_H$ vanishes on H , the restriction $\mathcal{L}|_H \cong K_H$ (by the adjunction formula) has other sections as $h^0(K_H) = g(H) = 2$. Let s' be a nontrivial section and $P := s'^{-1}(0)$, i.e. two points on H . Let \mathcal{O}_P denote the skyscraper sheaf for this set, a direct sum of two skyscraper sheaves each at a point. The crucial fact is that a line bundle over a finite set of points is trivial. Thus restricting the classical sequence to H , twisting by the k th power of K_H , and pushing forward to V we obtain a second exact triangle:

$$i_* \mathcal{L}^{k-1}|_H \rightarrow i_* \mathcal{L}^k|_H \rightarrow \mathcal{O}_P$$

The first exact triangle involving the powers of \mathcal{L} tells us that \mathcal{O}, \mathcal{L} , and \mathcal{L}^2 generate $i_* \mathcal{L}|_H$ and $i_* \mathcal{L}^2|_H$ as mapping cones $\mathcal{O} \rightarrow \mathcal{L}$ and $\mathcal{L} \rightarrow \mathcal{L}^2$. The second exact triangle implies $i_* \mathcal{L}|_H$ and $i_* \mathcal{L}^2|_H$ generate \mathcal{O}_P .

The second exact triangle then tells us, by induction, that given $i_* \mathcal{L}|_H$ and \mathcal{O}_P we can obtain all the $i_* \mathcal{L}^k|_H$'s. We go in the forward direction for positive k so $i_* \mathcal{L}^k|_H$ is a mapping cone $\mathcal{O}_P \rightarrow i_* \mathcal{L}^{k-1}|_H$, and in the backward direction for negative k , i.e. $i_* \mathcal{L}^{k-1}|_H$ is a mapping cone $i_* \mathcal{L}^k|_H \rightarrow \mathcal{O}_P$.

The first exact triangle, by induction, now implies that given \mathcal{O} and all the $i_* \mathcal{L}^k|_H$'s we can obtain all the \mathcal{L}^k 's, again in the forward for positive k , \mathcal{L}^k is a mapping cone $i_* \mathcal{L}^k|_H \rightarrow \mathcal{L}^{k-1}$, and in the backward direction for negative k , \mathcal{L}^{k-1} is a mapping cone $\mathcal{L}^k \rightarrow i_* \mathcal{L}^k|_H$. So we've split-generated all the \mathcal{L}^k 's as claimed. \square

So it would be enough to prove the fully-faithful embedding of categories by looking at the functor on $\mathcal{O}, \mathcal{L}, \mathcal{L}^2$, though at the expense of needing to know about higher A_∞ -products.

3.3 Towards HMS: fully-faithful embedding

$$D_{\mathcal{L}}^b Coh(V) \hookrightarrow H^* Fuk(V^\vee)$$

The functor $D_{\mathcal{L}}^b Coh(V) \rightarrow H^* Fuk(V^\vee)$ is as follows. On objects we map $\mathcal{L}^{\otimes k} \mapsto \ell_k$. Recall Corollary 1.2.17 that $H^0(V, \mathcal{L}^{\otimes l})$ has the following basis of sections:

$$s_{e,l} := \sum_{\gamma} \tau^{-l\kappa(\gamma + \frac{\gamma_{e,l}}{l})} x^{-l\lambda(\gamma) - \lambda(\gamma_{e,l})}$$

where $\gamma_{e,l} = s\gamma' + t\gamma''$, $0 \leq s, t < l$. Recall that the l^2 intersection points of ℓ_i and ℓ_{i+l} have ξ coordinates which are l -torsion elements of $\mathbb{R}^2 \bmod \Gamma_B$. Thus they may also be indexed by the $\gamma_{e,l}$'s, namely set $p_{e,l}$ to be the intersection point with ξ coordinate given by $\gamma_{e,l}/l$.

So on morphisms the functor does the following (where s_i denotes the choices for $\gamma_{e,l}$): the section $s_{e,l}$ of \mathcal{L}^l corresponding to the choice of a given $\gamma_{e,l}$, viewed as a generator of $\text{hom}(\mathcal{L}^i, \mathcal{L}^{i+l})$, is mapped to the intersection point $p_{e,l}$ of ℓ_i and ℓ_{i+l} whose ξ coordinate is equal to $\gamma_{e,l}/l \bmod \Gamma_B$. We denote the four choices of $\gamma_{e,l}$ for $l = 2$ by indices $i \in \{1, \dots, 4\}$, and then we may write this mathematically:

$$\begin{aligned} \text{hom}(\mathcal{O}, \mathcal{L}) &= H^0(V, \mathcal{L}) \ni s \mapsto p \in \text{hom}(\ell_0, \ell_1) = \bigoplus_{p \in \ell_0 \cap \ell_1} \mathbb{C} \cdot p = \mathbb{C} \cdot p \\ \text{hom}(\mathcal{O}, \mathcal{L}^2) &= H^0(V, \mathcal{L}^2) \ni (s_1, s_2, s_3, s_4) \mapsto (p_1, p_2, p_3, p_4) \in \bigoplus_{p \in \ell_0 \cap \ell_2} \mathbb{C} \cdot p, \quad |\ell_0 \cap \ell_2| = 4 \\ \text{hom}(\mathcal{L}, \mathcal{L}^2) &\cong \text{hom}(\mathcal{O}, \mathcal{L}^* \otimes \mathcal{L}^2) \cong \text{hom}(\mathcal{O}, \mathcal{L}) = H^0(V, \mathcal{L}) \ni s \mapsto p' \in \text{hom}(\ell_1, \ell_2) = \mathbb{C} \cdot p' \end{aligned}$$

Compatible with composition, namely:

$$\begin{aligned} s(x) &= \sum_{\gamma} \tau^{-\kappa(\gamma)} x^{-\lambda(\gamma)} \\ s^2(x) &= \sum_{\tilde{\gamma}, \tilde{\tilde{\gamma}}} \tau^{-\kappa(\tilde{\gamma}) - \kappa(\tilde{\tilde{\gamma}})} x^{-\lambda(\tilde{\gamma}) - \lambda(\tilde{\tilde{\gamma}})} \\ \text{hom}(\mathcal{L}, \mathcal{L}^2) \otimes \text{hom}(\mathcal{O}, \mathcal{L}) &\ni s^2(x) = c_1 s_1 + c_2 s_2 + c_3 s_3 + c_4 s_4 \\ &\leftrightarrow \mu^2(p, p') = c_1 p_1 + c_2 p_2 + c_3 p_3 + c_4 p_4 \end{aligned}$$

In particular, we expect the coefficients c_i to be theta functions $s(x)$ for a particular value of x , analogous to the calculation in [PZ98]. We wish to express $s^2(x)$ in terms of this basis for $H^0(V, \mathcal{L}^2)$. We split the sum above for $s^2(x)$ into four sums, corresponding to the four possible parities of the coefficients on the pair γ', γ'' in $\tilde{\gamma} + \tilde{\tilde{\gamma}}$. We then do a coordinate change

$$\begin{aligned} \gamma &= \frac{1}{2}(\tilde{\gamma} + \tilde{\tilde{\gamma}} - \gamma_e), \eta = \frac{1}{2}(\tilde{\tilde{\gamma}} - \tilde{\gamma} - \gamma_e) \\ \gamma_e &\in \{0, \gamma', \gamma'', \gamma' + \gamma''\} \end{aligned}$$

For example, if $\tilde{\gamma} + \tilde{\tilde{\gamma}} = (n_1 + m_1)\gamma' + (n_2 + m_2)\gamma''$ and $n_1 + m_1$ and $n_2 + m_2$ are both even, that means we can write $\tilde{\gamma} + \tilde{\tilde{\gamma}}$ as 2γ for some $\gamma \in \Gamma_B$. If they are odd and even then we must subtract off γ' , etc. That's how we get the four choices for γ_e . Now we can write $s^2(x)$ in terms of the $s_i(x)$ by separating into four sums corresponding to the four parity choices.

Also recall that the quadratic form κ satisfies $\kappa(\gamma + \eta) = \kappa(\gamma) + \kappa(\eta) - \langle \gamma, \lambda(\eta) \rangle$.

$$\begin{aligned}
s^2(x) &= \sum_{\tilde{\gamma}, \tilde{\tilde{\gamma}}} \tau^{-\kappa(\tilde{\gamma}) - \kappa(\tilde{\tilde{\gamma}})} x^{-\lambda(\tilde{\gamma} + \tilde{\tilde{\gamma}})} \\
&= \sum_{\gamma, \eta} \tau^{-\kappa(\gamma - \eta) - \kappa(\gamma + \eta)} x^{-2\lambda(\gamma)} + \tau^{-\kappa(\gamma + \gamma'/2 - \eta - \gamma'/2) - \kappa(\gamma + \gamma'/2 + \eta + \gamma'/2)} x^{-2\lambda(\gamma)} x_1^{-1} \\
&\quad + \tau^{-\kappa(\gamma + \gamma''/2 - \eta - \gamma''/2) - \kappa(\gamma + \gamma''/2 + \eta + \gamma''/2)} x^{-2\lambda(\gamma)} x_2^{-1} \\
&\quad + \tau^{-\kappa(\gamma + (\gamma' + \gamma'')/2 - \eta - (\gamma' + \gamma'')/2) - \kappa(\gamma + (\gamma' + \gamma'')/2 + \eta + (\gamma' + \gamma'')/2)} x^{-2\lambda(\gamma)} (x_1 x_2)^{-1} \\
&= \sum_{\eta} \tau^{-2\kappa(\eta)} \sum_{\gamma} \tau^{-2\kappa(\gamma)} x^{-2\lambda(\gamma)} + \sum_{\eta} \tau^{-2\kappa(\eta + \gamma'/2)} \sum_{\gamma} \tau^{-2\kappa(\gamma + \gamma'/2)} x^{-2\lambda(\gamma)} x_1^{-1} \\
&\quad + \sum_{\eta} \tau^{-2\kappa(\eta + \gamma''/2)} \sum_{\gamma} \tau^{-2\kappa(\gamma + \gamma''/2)} x^{-2\lambda(\gamma)} x_2^{-1} \\
&\quad + \sum_{\eta} \tau^{-2\kappa(\eta + (\gamma' + \gamma'')/2)} \sum_{\gamma} \tau^{-2\kappa(\gamma + (\gamma' + \gamma'')/2)} x^{-2\lambda(\gamma)} (x_1 x_2)^{-1} \\
&= \sum_{\eta} \tau^{-2\kappa(\eta)} s_1 + \sum_{\eta} \tau^{-2\kappa(\eta + \gamma'/2)} s_2 + \sum_{\eta} \tau^{-2\kappa(\eta + \gamma''/2)} s_3 + \sum_{\eta} \tau^{-2\kappa(\eta + (\gamma' + \gamma'')/2)} s_4
\end{aligned}$$

Claim 3.3.1. The coefficients on the s_i match up with the triangle counts, i.e. μ^2 in the Fukaya category.

Proof. Let $\tilde{\cdot}$ denote lifts to the universal cover \mathbb{R}^4 . There are four choices for where to place $\tilde{\ell}_0 \cap \tilde{\ell}_2$ in the triangle (the other choices producing the same triangles on the abelian variety). From the calculation in Equation 3.1, we take these to be $(\gamma_e/2, 2M^{-1}(\gamma_e/2)) = (\gamma_e/2, \lambda(\gamma_e))$ because λ is the linear map M^{-1} .

$$\tilde{p}_e = (\gamma_e/2, \lambda(\gamma_e))$$

We know the lift \tilde{p} of $p = \ell_0 \cap \ell_1$ must lie on $\tilde{\ell}_0$ which goes through \tilde{p}_e . Since there is no change in the second two coordinates along $\tilde{\ell}_0$ this means $\lambda(\gamma_e)$ is the angular coordinates. And \tilde{p} lies above $(0, 0)$ so the first coordinate is some $\eta \in \Gamma_B$.

$$\tilde{p} = (\eta, \lambda(\gamma_e))$$

If \tilde{p} is at $(0, 0)$, then the lift of $p' = \ell_1 \cap \ell_2$ is some $(\xi, M^{-1}(\xi)) = (\xi, \lambda(\xi))$ because $\tilde{\ell}_2$ would go through the origin (assume clockwise ordering of the Lagrangians). Since it is shifted by $(\eta, \lambda(\gamma_e))$, we get that $\tilde{p}' = (\eta, \lambda(\gamma_e)) + (\xi, \lambda(\xi))$ for some ξ . This ξ is determined by the fact that $\tilde{p}'\tilde{p}_e$ lies on $\tilde{\ell}_2$ i.e. the angle changes by 2λ .

$$\begin{aligned}
\tilde{p}'\tilde{p}_e &= \langle \eta + \xi - \gamma_e/2, \lambda(\gamma_e + \xi) - \lambda(\gamma_e) \rangle \\
\implies 2\lambda(\eta + \xi - \gamma_e/2) &= \lambda(\xi) \therefore \xi = \gamma_e - 2\eta \\
\therefore \tilde{p}' &= (\gamma_e - \eta, 2\lambda(\gamma_e - \eta))
\end{aligned}$$

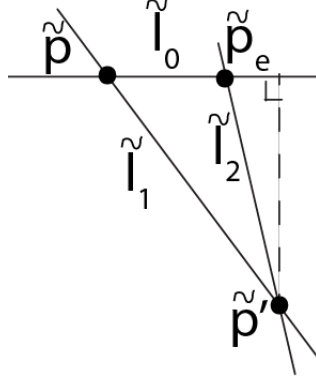


Figure 3.1: A triangle in the elliptic curve case and representative of the T^4 case

Now that we have three points of the triangle, we want to find the area. We calculate the symplectic area of the triangle by pairing the base of the triangle (the edge contained in $\tilde{\ell}_0$) with its height (in the angular directions):

$$\int_{\Delta} d\xi \wedge d\theta = \langle (\eta - \gamma_e/2), \lambda(\eta - \gamma_e/2) \rangle = -2\kappa(\eta - \gamma_e/2)$$

This agrees with the exponents on τ on the complex side. We will show below (Claim 3.3.4) that, even though the “straight” affine triangles with these vertices are not holomorphic for the standard complex structure, there exists an almost-complex structure for which they are J -holomorphic and are the only J -holomorphic triangles contributing to the Floer product μ^2 . Hence this completes the proof of the claim. \square

Now we want to prove that multiplication matches up in the more general setting for $i < j < k$. First we consider the line bundles. We have $\text{Hom}(\mathcal{L}^i, \mathcal{L}^j) \cong H^0(V, \mathcal{L}^{j-i})$ so let $l := j - i$ and $l' := k - j$. We take the following basis for \mathcal{L}^l :

$$s_{e,l} := \sum_{\gamma} \tau^{-l\kappa(\gamma + \frac{\gamma_{e,l}}{l})} x^{-\lambda(l\gamma + \gamma_{e,l})}$$

In particular, $\gamma_{e,l} = s\gamma' + t\gamma''$ for some $0 \leq s, t < l$, which gives us l^2 basis elements for $H^0(V, \mathcal{L}^l)$. We want to write the product of two such sections in terms of the basis for $H^0(V, \mathcal{L}^{l+l'})$, and compare coefficients with the triangle count on the other side.

$$s_{e,l} \cdot s_{e,l'} = \sum_{\tilde{\gamma}, \tilde{\gamma}'} \tau^{-l\kappa(\tilde{\gamma} + \frac{\gamma_{e,l}}{l}) - l'\kappa(\tilde{\gamma}' + \frac{\gamma_{e,l'}}{l'})} x^{-\lambda(l\tilde{\gamma} + \gamma_{e,l} + l'\tilde{\gamma}' + \gamma_{e,l'})}$$

We want to write this in terms of the similar basis for $H^0(V, \mathcal{L}^{l+l'})$:

$$s_e := \sum_{\gamma} \tau^{-(l+l')\kappa(\gamma + \frac{\gamma_e}{l+l'})} x^{-(l+l')\lambda(\gamma + \frac{\gamma_e}{l+l'})}$$

Comparing with the powers of x in the product, we define γ by considering the sum $l\tilde{\gamma} + \gamma_{e,l} + l'\tilde{\tilde{\gamma}} + \gamma_{e,l'}$ as an element in $(l+l')\Gamma_B$ plus a remainder γ_e . Namely define this element to be $\gamma \in \Gamma_B$ and denote the remainder as γ_e :

$$(l+l')\gamma + \gamma_e := l\tilde{\gamma} + \gamma_{e,l} + l'\tilde{\tilde{\gamma}} + \gamma_{e,l'}$$

Analogous to the $(i, j, k) = (0, 1, 2)$ case above, we want to find a change of coordinates in terms of new variables A, B satisfying the following equality, as exponents of τ :

$$(\tilde{\gamma} + \frac{\gamma_{e,l}}{l}, \tilde{\tilde{\gamma}} + \frac{\gamma_{e,l'}}{l'}) = (A + \frac{B}{l}, A - \frac{B}{l'})$$

because $-l\kappa(A + \frac{B}{l}) - l'\kappa(A - \frac{B}{l'}) = -(l+l')\kappa(A) - (\frac{1}{l} + \frac{1}{l'})\kappa(B)$. We will want $A = \gamma + \frac{\gamma_e}{l+l'}$, which does hold. And B should be a function of a variable η and a remainder term, so that $\eta \in \Gamma_B$. We make the following definition for which this is true, and the motivation will become clear when counting triangles below.

$$B = \frac{ll'}{l+l'} \left(\tilde{\gamma} + \frac{\gamma_{e,l}}{l} - \tilde{\tilde{\gamma}} - \frac{\gamma_{e,l'}}{l'} \right) =: \eta - \frac{l\gamma_e}{l+l'}$$

Claim 3.3.2. $\eta \in \Gamma_B$.

Proof.

$$\begin{aligned} \eta &= \frac{ll'}{l+l'} \left(\tilde{\gamma} + \frac{\gamma_{e,l}}{l} - \tilde{\tilde{\gamma}} - \frac{\gamma_{e,l'}}{l'} \right) + \frac{l\gamma_e}{l+l'} \\ &= \frac{1}{l+l'} (ll'\tilde{\gamma} + l'\gamma_{e,l} - ll'\tilde{\tilde{\gamma}} - l\gamma_{e,l'} - l(l+l')\gamma + l^2\tilde{\gamma} + l\gamma_{e,l} + ll'\tilde{\tilde{\gamma}} + l\gamma_{e,l'}) \\ &= l\tilde{\gamma} + \gamma_{e,l} - l\gamma \in \Gamma_B \end{aligned}$$

□

Corollary 3.3.3.

$$\begin{aligned} s_{e,l} \cdot s_{e,l'} &= \sum_{\tilde{\gamma}, \tilde{\tilde{\gamma}}} \tau^{-l\kappa(\tilde{\gamma} + \frac{\gamma_{e,l}}{l}) - l'\kappa(\tilde{\tilde{\gamma}} + \frac{\gamma_{e,l'}}{l'})} x^{-\lambda(l\tilde{\gamma} + \gamma_{e,l} + l'\tilde{\tilde{\gamma}} + \gamma_{e,l'})} \\ &= \sum_{\gamma, \eta} \tau^{-l\kappa(\gamma + \frac{\gamma_e}{l+l'} + \frac{1}{l}(\eta - \frac{l\gamma_e}{l+l'})) - l'\kappa(\gamma + \frac{\gamma_e}{l+l'} - \frac{1}{l'}(\eta - \frac{l\gamma_e}{l+l'}))} x^{-(l+l')\lambda(\gamma) - \lambda(\gamma_e)} \\ &= \sum_{\eta} \tau^{-(\frac{1}{l} + \frac{1}{l'})\kappa(\eta - \frac{l\gamma_e}{l+l'})} \sum_{\gamma} \tau^{-(l+l')\kappa(\gamma + \frac{\gamma_e}{l+l'})} x^{-(l+l')\lambda(\gamma) - \lambda(\gamma_e)} \end{aligned}$$

Claim 3.3.4. The left vertical functor $D_{\mathcal{L}}^b \text{Coh}(V) \rightarrow \text{Fuk}(V^\vee)$ respects composition.

Proof. We compare the coefficients in the expression for the product of two sections with the triangle count. Take p_1, p_2, p_3 for $\ell_i \cap \ell_k$, $\ell_i \cap \ell_j$ and $\ell_j \cap \ell_k$ respectively. We have $(l + l')^2$ choices for $\ell_i \cap \ell_k$ as follows:

$$p_1 = \left(\frac{\gamma_e}{k-i}, -\frac{k}{k-i} \lambda(\gamma_e) \right)$$

Then $p_2 \vec{p}_1$ lies on $\tilde{\ell}_i$ so takes the form $(\xi, -i\lambda(\xi))$. Also, p_2 lies on a lift of ℓ_i so is also of this form (we use η/l so $\eta \in \Gamma_B$ will ultimately agree with the η used above in the multi-theta functions), up to a shift by a lattice element, which turns out to be $(0, \lambda(\gamma_e))$.

$$\begin{aligned} p_2 &= \left(\frac{\eta}{l}, -i\lambda\left(\frac{\eta}{l}\right) - \lambda(\gamma_e) \right) \\ p_2 \vec{p}_1 &= \left(\frac{\gamma_e}{k-i} - \frac{\eta}{l}, -\frac{k}{k-i} \lambda(\gamma_e) + i\lambda\left(\frac{\eta}{l}\right) + \lambda(\gamma_e) \right) = (\xi, -i\lambda(\xi)) \end{aligned}$$

Then $p_3(A, B)$ has two conditions as follows.

$$\begin{aligned} p_2 \vec{p}_3 &= \left(A - \frac{\eta}{l}, B + i\lambda\left(\frac{\eta}{l}\right) + \lambda(\gamma_e) \right) \\ \therefore B + i\lambda\left(\frac{\eta}{l}\right) + \lambda(\gamma_e) &= -j\lambda\left(A - \frac{\eta}{l}\right) \\ p_1 \vec{p}_3 &= \left(A - \frac{\gamma_e}{k-i}, B + \frac{k}{k-i} \lambda(\gamma_e) \right) \\ \therefore B + \frac{k}{k-i} \lambda(\gamma_e) &= -k\lambda\left(A - \frac{\gamma_e}{k-i}\right) \\ \implies B &= -k\lambda(A) \\ \implies -k\lambda(A) &= -j\lambda(A) + (j-i)\lambda\left(\frac{\eta}{l}\right) - \lambda(\gamma_e) \\ \implies (k-j)A &= (i-j)\frac{\eta}{l} + \gamma_e \\ \therefore A &= \frac{i-j}{k-j} \frac{\eta}{l} + \frac{1}{k-j} \gamma_e = -\frac{1}{l'} \eta + \frac{1}{l'} \gamma_e \\ B &= -k\lambda(A) \end{aligned}$$

We set $\zeta := -\frac{\eta}{l} + \frac{\gamma_e}{l+l'}$ since the expression shows up in multiple places. To get the symplectic area of the triangle (which is the same under homotopy invariance, i.e. for any holomorphic triangle with these corners), we take $\frac{1}{2} \int_P d\xi \wedge d\theta$ where P is the parallelogram spanned by

$$\vec{a} := p_2 \vec{p}_1 = \left(\frac{\gamma_e}{l+l'} - \frac{\eta}{l}, -i\lambda\left(\frac{\gamma_e}{l+l'} - \frac{\eta}{l}\right) \right) = (\zeta, -i\lambda(\zeta))$$

and to define the other vector $\vec{b} := p_1 \vec{p}_3$ we will consider the following expression, so we simplify it first:

$$-\frac{1}{l'} \eta + \frac{1}{l'} \gamma_e - \frac{\gamma_e}{l+l'} = \frac{l}{l'} \left(-\frac{\eta}{l} + \frac{\gamma_e}{l+l'} \right) = \frac{l}{l'} \zeta$$

hence we define

$$\vec{b} := p_1 \vec{p}_3 = \left(\frac{l}{l'} \zeta, -k\lambda\left(\frac{l}{l'} \zeta\right) \right)$$

because we've set \tilde{l}_k to go through the origin hence points on \tilde{l}_k and vectors parallel to it are both of the form $(\xi, -k\lambda(\xi))$. Finally we can compute the symplectic area.

$$\begin{aligned} \frac{1}{2} \int_P d\xi \wedge d\theta &= \frac{1}{2} (a_\xi \cdot b_\theta - a_\theta \cdot b_\xi) = \frac{1}{2} \left\langle \zeta, -k\lambda\left(\frac{l}{l'} \zeta\right) \right\rangle - \frac{1}{2} \left\langle -i\lambda(\zeta), \frac{l}{l'} \zeta \right\rangle \\ &= \left(\frac{kl}{l'} - \frac{il}{l'} \right) \kappa(\zeta) = \frac{l+l'}{ll'} \kappa \left(-\eta + \frac{l\gamma_e}{l+l'} \right) \end{aligned}$$

We obtain the same exponent as on τ above, namely $-\left(\frac{1}{l} + \frac{1}{l'}\right) \kappa\left(\eta - \frac{l\gamma_e}{l+l'}\right)$, since κ is an even function. □

Claim 3.3.5. There exists an ω -compatible almost-complex structure J on V^\vee for which the triangles described above bounded by ℓ_i, ℓ_j, ℓ_k are J -holomorphic, regular, and are the only J -holomorphic triangles bounded by these Lagrangians.

Before we prove this, we recall that Lagrangian Floer theory in the setting of the example of this paper is independent of *regular* or *generic* J , as follows.

Lemma 3.3.6. *There exists a dense set $\mathcal{J}_{reg} \subset \mathcal{J}(V^\vee, \omega)$ of ω -compatible almost complex structures J such that, for all J -holomorphic maps $u : \mathbb{D} \rightarrow V^\vee$ with suitable Lagrangian boundary condition, the linearized $\bar{\partial}$ -operator D_u is surjective.*

We postpone the proof to our discussion of regularity below in more generality.

Lemma 3.3.7. *The counts μ_2 for any two regular almost-complex structures J_1 and J_2 on V^\vee are equal.*

Sketch. This will rely on arguments from the proof of the previous statement. The argument will be the same, but our Fredholm problem will have an additional $[0, 1]$ factor in the Banach bundle setup. So we will obtain a 1-dimensional manifold. There is no other boundary expected because 1) sphere bubbling cannot happen as $\pi_2(T^4) = 0$, furthermore 2) strip breaking would break off a bigon but there are no bigons on a torus by parameter translation considerations and dimensional/index reasons (namely all intersection points have the same index and a broken strip would have indices differing by 2, c.f. the Morse analogue with flow lines) and 3) disc bubbling doesn't occur because Lagrangians don't bound discs on a torus (since π_2 is preserved upon taking the universal cover of the torus which has no π_2). Since the signed boundary of a 1-dimensional manifold is zero, we get $\mathcal{M}(p_1, p_2, p_3, [u], J_1) = \mathcal{M}(p_1, p_2, p_3, [u], J_2)$ for regular J_1 and J_2 . The existence of a dense set of regular paths is similar to the proof for the existence of regular J , which we'll see below. □

Now we can prove that the triangles counted above are J -holomorphic for a particular suitable regular J , and are the only J -holomorphic triangles for this almost-complex structure.

Proof of Claim 3.3.5. To count the triangles, we pick the most convenient J . Take the J that is block off-diagonal with blocks $\lambda = \begin{pmatrix} 2 & 1 \\ 1 & 2 \end{pmatrix}^{-1}$, $-\lambda^{-1}$ in lower left and upper right respectively, with respect to the ξ, θ coordinates. This squares to $-\mathbf{1}$ and is ω -compatible because multiplying the standard symplectic form (which we have here, namely $d\xi \wedge d\theta$) with this J to compute $\omega(\cdot, J\cdot)$, we do indeed get a metric, i.e. it is positive definite. Taking the universal cover of V^\vee , we split up the resulting linear space into a product of two 2-planes, $P := \langle(\zeta, 0), J(\zeta, 0) = (0, \lambda(\zeta))\rangle$ and P^ω the symplectic orthogonal complement. In particular, P and P^ω are J -holomorphic planes, by definition of J .

We then show that the triangles above, spanned by $\vec{a}, \vec{b} \in \langle(\zeta, 0), (0, \lambda(\zeta))\rangle = P$, are holomorphic with respect to this J . First note that the Lagrangians $\tilde{\ell}_i, \tilde{\ell}_j, \tilde{\ell}_k$ decompose as products of a straight line of slope $-i$ (respectively $-j, -k$) in P , and a straight line of the same slope in P^ω . However, by definition of ζ and of the plane P , in P the straight lines form a triangle, whereas in P^ω they all meet in a single point. Therefore, the maps $u : \mathbb{D}^2 \rightarrow V^\vee$ have a triangle image in P , and in P^ω they are constant maps at the triple intersection point of the three Lagrangians. Namely, the boundary condition of the projection of the 3-punctured disc to the latter plane must be constant.

Now that we can work in components P and P^ω , we have a holomorphic disc in P where J is a complex structure (as every almost complex structure is integrable in two dimensions) with a specified Lagrangian boundary condition so by the Riemann mapping theorem it's unique. A further corollary is that the discs are regular by standard regularity arguments in the plane.

□

Remark 3.3.8. This J is a bit unusual compared to the standard J_0 that is multiplication by i in each component. For J_0 , the holomorphic triangle would be area-minimizing for the Euclidean metric but wouldn't be planar, whereas for this J the area-minimizing triangles are linear.

Chapter 4

The Fukaya category

4.1 The Fukaya-Seidel category of Y : introduction

The Fukaya category for symplectic manifolds, and the Fukaya-Seidel category for symplectic fibrations, are A_∞ -categories. In what follows, we consider a subcategory of the Fukaya-Seidel category of $v_0 : Y \rightarrow \mathbb{C}$. We then prove, passing to the cohomology level where the A_∞ -category becomes a category, that this subcategory is equivalent to the bounded derived category of coherent sheaves on the hypersurface $H = \Sigma_2$.

Remark 4.1.1 (Not exact, not compact, Hamiltonian perturbation method not used). In [Sei08] the Fukaya category of a Lefschetz fibration has Lagrangians given by thimbles obtained by parallel transporting a sphere to the singular point in the Morse singular fiber where it gets pinched to a point. In our situation, the degenerate fiber over 0 is not a Lefschetz singularity (i.e. modeled on $\sum_i z_i^2$) but instead the fiber T^4 degenerates by collapsing a family of S^1 's, and also collapsing a T^2 in two points. So instead, we will consider Lagrangians that go around this singular fiber, with suitable behavior at infinity governed by the superpotential v_0 . This is because it is a smoothing of two fiber Lagrangians parallel transported to the central fiber. This is the notion of a U-shaped curve from [AS].

One difference of our set-up to that in [Sei08] is that we are in the non-exact case so there are sphere bubbles. Also the manifold is non-compact in the base of the fibration v_0 , or equivalently we can restrict to a neighborhood of the origin and then it will have boundary. Another difference is that although Seidel in some later papers defines the Fukaya category on U-shaped curves, he uses Hamiltonian perturbations where the symplectic form used is a product on the base and fiber. Since the symplectic form is not a product here, we instead use the notion of *categorical localization* of [AS] and Ganatra's notes.

Example 4.1.2 (Not monotone). A compact symplectic manifold (P, ω) is *monotone* if $\int c_1(P) = \alpha \int \omega : \pi_2(P) \rightarrow \mathbb{R}$ for some $\alpha > 0$. Our setting is not monotone: taking $P := Y$, which is Calabi-Yau, we have $c_1(Y) = 0$ however $[\omega] \neq 0$ so α would have to be zero, contradiction.

Definition 4.1.3 (Maslov index of a map). Given $u : (\mathbb{D}, \partial\mathbb{D}) \rightarrow (M, L)$ we first trivialize u^*TM over the disc. Then the Maslov index counts the rotation of u^*TL around the boundary in this trivialized pullback.

Definition 4.1.4. A *monotone* Lagrangian L in symplectic manifold (M, ω) is such that $[\omega] = k \cdot [\mu(u)]$ for all $u \in \pi_2(M, L)$, for some constant k . Namely, the areas of discs are proportional to the Maslov indices of those discs.

Example 4.1.5. An example can be found in Oh [Oh93], who shows the Clifford torus in $(\mathbb{CP}^n, \omega_{FS})$ is a monotone Lagrangian submanifold. In this thesis, all discs considered have Maslov index 2, but the areas vary as prescribed by a formula of [CO06] which we will elaborate on later.

Now that we've indicated how this set-up differs from those currently in the literature, we give an outline of the sections below that first define the Fukaya-Seidel category and then prove the HMS statement. In Section 4.2 we discuss monodromy around the central fiber in $v_0 : Y \rightarrow \mathbb{C}$ because it will be needed to define the Lagrangians in the subcategory of $FS(Y, v_0)$ we will consider. Then Section 4.3 sets up the background needed to define the structure maps in $H^0FS(Y, v_0)$, and Section 4.4 proves the moduli spaces involved in these structure maps have the required conditions to be put into the definition. Finally we give the definition in Section 4.5 and show it's well-defined for regular choices of data.

4.2 Monodromy

4.2.1 Monodromy background

We define monodromy. This is how we will obtain Lagrangians in the total space, by parallel transporting Lagrangians in the fiber. We will define Darboux coordinates in local charts, also called action-angle coordinates. This will enable us to do symplectic geometry calculations in the Fukaya category.

Definition 4.2.1. A *symplectic fibration* is a symplectic manifold (Y, ω) with a fibration such that fibers of the fibration are symplectic with respect to ω .

Example 4.2.2. In this paper, we've constructed (Y, ω) so that $v_0 : Y \rightarrow \mathbb{C}$ is a symplectic fibration.

Definition 4.2.3. The *symplectic horizontal distribution* of a symplectic fibration $\pi : Y \rightarrow C$ to a base manifold C is $H \subset TY$ such that if F is a generic fiber of π then $H = TF^\omega$ is the ω -complement, i.e.

$$\omega(H, TF) = 0$$

Definition 4.2.4. Given two points $p_0, p_1 \in C$ and a path $\gamma : I \rightarrow C$ between them (i.e. $\gamma(0) = p_0$ and $\gamma(1) = p_1$), the *parallel transport map* is a symplectomorphism $\Phi : F_{p_0} \rightarrow$

F_{p_1} defined as follows: given $x \in F_{p_0}$, we set $\Phi(x)$ to be $\tilde{\gamma}(1)$ where $\tilde{\gamma} : I \rightarrow Y$ such that $\pi \circ \tilde{\gamma} = \gamma$, $d\pi(\tilde{\gamma}') = \gamma'$ and $\tilde{\gamma}'$ is in the horizontal distribution.

Claim 4.2.5. By standard theory, this last condition implies Φ is a symplectomorphism.

Proof. There is a unique horizontal vector field X_H on $\pi^{-1}(\gamma(I))$ with flow ϕ^H by existence and uniqueness of differential equation solutions, and that horizontal implies there is no component of the vector field in the fiber direction. Then since $d\Phi$ is the identity on vectors in H we have $\omega(d\Phi(X_H), d\Phi(v)) = \omega(X_H, v)$ for $v \in H$. Also, H is ω -perpendicular to TF , which is a condition also preserved under parallel transport: when $v \in TF$ is transported infinitesimally in the parallel direction, it must still be in TF , otherwise any component in H could be reverse parallel-transported to a vector component in H at the original fiber, contradiction. So $\omega(X_H, v) = 0 = \omega(d\Phi(X_H), d\Phi(v))$ and $\Phi^*\omega = \omega$ since $TY = TF \oplus H$ in regions where we parallel transport. \square

Claim 4.2.6. $\Phi(\ell_i)$ is Lagrangian in V^\vee with respect to $\omega|_{V^\vee}$, also a symplectic form as v_0 is a symplectic fibration with respect to ω .

Proof. Parallel transport is defined by taking $H := (TF)^\omega$, the symplectic complement of the fiber. Thus the monodromy is a symplectomorphism, e.g. see [MS17], and so preserves Lagrangians. \square

Definition 4.2.7. *Monodromy* is parallel transport around a loop going once around a singularity in the base.

Remark 4.2.8 (Notation). Hereafter F will refer to the Kähler potential function defining the symplectic form, and a fiber of v_0 will be denoted V^\vee .

The main result of this section is the following, illustrated in Figure 4.1:

Lemma 4.2.9. *The monodromy of the symplectic fibration $v_0 : Y \mapsto \mathbb{C}$ is of the form $(\xi_1, \xi_2, \theta_1, \theta_2) \mapsto (\xi_1, \xi_2, \theta_1 + f(\xi), \theta_2 + g(\xi))$. Over the parallelogram-shaped fundamental domain of the torus T_B , the functions (f, g) vary as follows between the different regions delimited by the tropical curve: away from the tropical curve we obtain $(0, 0)$ in the upper right corner where $r_z^{-1} \gg r_x^{-1}, r_y^{-1}$, then $(0, 1)$ on the right where r_y^{-1} is the largest, $(1, 0)$ on the left where r_x^{-1} largest and thus $(1, 1)$ in the bottom left corner.*

The proof will be given in the following sections. First we show the result holds in the \mathbb{C}^3 patch. Then we show it holds away from the \mathbb{C}^3 patch.

Remark 4.2.10. We say a few words to illuminate the geometry depicted in Figure 4.1. A v_0 -fiber V^\vee can be described in action-angle coordinates $(\xi_1, \xi_2, \theta_1, \theta_2)$. A linear Lagrangian ℓ_i is a graph of a linear function on $\xi := (\xi_1, \xi_2) \in T_B$ (where T_B can be pictured as the quotient of a hexagon tile in the projection of $\Delta_{\tilde{Y}}$ to the first two coordinates). When we parallel transport V^\vee about the origin, $\Phi(\ell_i)$ is still the graph of a function of ξ but the angles have rotated according to the monodromy. This is calculated below.

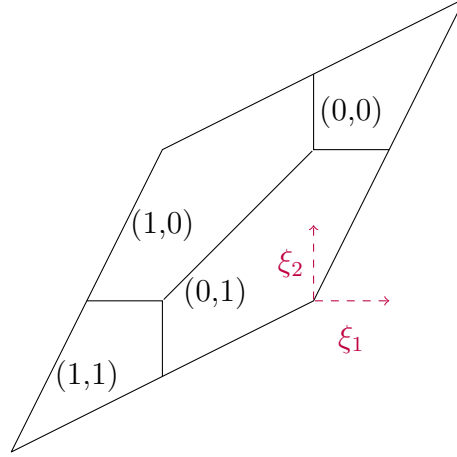


Figure 4.1: Monodromy in fiber, thought of as a section over the parallelogram $(\xi_1, \xi_2) \mapsto (\theta_1(\xi_1, \xi_2), \theta_2(\xi_1, \xi_2))$.

Remark 4.2.11 (Caveat). We next define the action-angle coordinates arising from the symplectic form. We will find that the image of the moment map is the same as the toric polytope, an instance of Delzant's theorem e.g. see [MS17]. Note that a usual moment map would land in \mathbb{R}^n where n is the dimension of the torus, but here the moment map will land in \mathbb{R}^3/Γ_B instead. This is known as a *quasi-Hamiltonian* action.

Claim 4.2.12 (Definition of action-angle coordinates). Let $\theta_1 := \arg(x)$, $\theta_2 := \arg(y)$, $\theta_\eta = \arg(v_0) = \arg(xyz)$, where x, y, z are the complex toric coordinates. They are defined in the following region: $|v_0| = |xyz| \leq T^\ell$ for sufficiently large ℓ and $x, y \in (\mathbb{C}^*)^2/\Gamma_B$. When $v_0 \notin \mathbb{R}_+$ the angle variables θ_1 and θ_2 on V^\vee are only well-defined up to additive constants, as they jump by $\arg(v_0) = \theta_\eta$ under the action of the generators of Γ_B due to the transformation rules for the complex coordinates x and y , see Corollary 1.4.17.

Then there exist coordinates ξ_1, ξ_2 so that $\omega|_{V^\vee} = d\xi_1 \wedge d\theta_1 + d\xi_2 \wedge d\theta_2$, which we may abbreviate as $d\xi \wedge d\theta$. The coordinates (ξ_1, ξ_2) are Γ_B -periodic; namely under the action of $\gamma \in \Gamma_B$ we find that ξ maps to $\xi + \gamma$. We have a third coordinate pair $\eta, \theta_\eta := \arg(v_0)$, where the angle variable θ_η is globally defined on Y but the action variable η transforms non-trivially under Γ_B , namely $(\xi, \eta) \sim (\xi + \gamma, \eta - \kappa(\gamma) + \langle \xi, \lambda(\gamma) \rangle)$ for $\gamma \in \Gamma_B$.

Proof. We define a T^3 action that rotates x and y but preserves the fiber in the first two infinitesimal directions in $\text{Lie}(T^3) = \mathfrak{t}^3$, and the third direction of the T^3 -action rotates v_0 fixing x and y , in other words it rotates z . Hence $(\alpha_1, \alpha_2, \alpha_\eta) \in T^3$ acts on \tilde{Y} by:

$$\rho : T^3 \times Y \rightarrow Y, \quad (\alpha_1, \alpha_2, \alpha_\eta) \cdot (x, y, z) = (e^{2i\pi\alpha_1}x, e^{2i\pi\alpha_2}y, e^{2i\pi(\alpha_\eta - \alpha_1 - \alpha_2)}z) \quad (4.1)$$

In other words, we get an action that passes to the quotient Y . The infinitesimal action of α_1 and α_2 on Y is expressed by the pushforwards $d\rho(\partial_{\alpha_i})$ for $i \in \{1, 2, \eta\}$. These vector fields are

$$\frac{\partial}{\partial\theta_1} = (ix, 0, -iz), \quad \frac{\partial}{\partial\theta_2} = (0, iy, -iz), \quad \frac{\partial}{\partial\theta_\eta} = (0, 0, iz) \quad (4.2)$$

where we can see the first two actions preserve the fibers of v_0 and are globally defined on the quotient Y because they commute with the Γ_B -action. However the last one isn't global as it transforms non-trivially under Γ_B , hence the infinitesimal vector field $\eta := d\rho\left(\frac{\partial}{\partial v_0}\right)$ will too.

We now justify why we claimed above that $d\rho(\partial_{\alpha_i}) = \frac{\partial}{\partial\theta_i}$ above. Let $X_i := d\rho(\partial_{\alpha_i})$. If $\iota_{X_i}\omega|_{V^\vee}$ were exact, say dH_i for some function H_i (known as the Hamiltonian), then the torus action would be called a *Hamiltonian group action* and (H_1, H_2) would be the moment map. This leads us to the caveat in Remark 4.2.11. In the setting here, ω is complicated so computing $\iota_{X_i}\omega|_{V^\vee}$ is involved. However, the 1-forms $\iota_{X_i}\omega$ are closed, and hence locally exact, so there exist locally defined functions ξ_1, ξ_2 so that $\iota_{X_i}\omega = d\xi_i$. Notationally we are assuming $\xi_\eta \equiv \eta$. Globally, as seen above, the first two ξ_i are Γ_B -periodic and their differentials pass to 1-forms on a torus fiber \mathbb{R}^4/Λ . Action-angle coordinates $\{(\xi_i, \theta_i)\}_{i \in \{1, 2\}}$ are useful because their definition implies that

$$\omega|_{V^\vee} = d\xi_1 \wedge d\theta_1 + d\xi_2 \wedge d\theta_2$$

The action coordinates can be expressed locally in terms of the Kähler potential:

$$\begin{aligned} \iota_{X_i}\omega|_{V^\vee} = d\xi_i &\implies \omega|_{V^\vee} = d\xi \wedge d\theta \\ \implies \iota_{X_i} \left(\frac{i}{2\pi} \partial\bar{\partial}F \right) &= \frac{i}{2\pi} d\iota_{X_i} \partial F = d\xi_i \\ \therefore \xi_1 &:= i/2\pi \partial F (2\pi i x \partial_x - 2\pi i z \partial_z) + \text{const} \\ \therefore \xi_1 &= -\frac{1}{2} \left(\frac{\partial F}{\partial \log |x|} - \frac{\partial F}{\partial \log |z|} \right) + \text{const} \\ \therefore \xi_2 &= -\frac{1}{2} \left(\frac{\partial F}{\partial \log |y|} - \frac{\partial F}{\partial \log |z|} \right) + \text{const} \\ \eta &= \frac{1}{2} \cdot \frac{\partial F}{\partial \log |z|} + \text{const} \end{aligned}$$

using $\partial\bar{\partial} = -\bar{\partial}\partial = -d\partial$, the conversion to polar coordinates from §2.2 and that F is preserved by rotating x, y, z as it is a function of their norms, hence the Lie derivative $\mathcal{L}_{X_i}\bar{\partial}F = 0$ and also $\partial_{\rho_x}F = 0$. The calculation for ξ_2 is similar. This calculation of ξ_i is up to additive constants. The upshot is that the moment map (ξ_1, ξ_2) provides periodic action-coordinates which are monotonic increasing in $|x|$ and $|y|$ for fixed v_0 because of how we defined F . (But recall the caveat, we are calling it a moment map but it takes values in a torus instead of affine space, so we are expanding the definition of moment map here to allow the ξ_i

to be periodic multivalued functions.) We see that V^\vee is symplectomorphic to $(T_B \times T_F, \omega_{std})$.

Note that an orbit is precisely the kernel of $(d\xi_1, d\xi_2)$ so that a preimage of a moment map value is a T^2 -orbit. Said another way, the torus action preserves the moment map. Or said yet another way, the tangent space to a fiber of the moment map is $\partial_{\theta_1}, \partial_{\theta_2}$.

Now we prove the final statements about how ξ_1, ξ_2, η transform under the Γ_B -action.

Claim 4.2.13. We claim that $\gamma \in \Gamma_B$ acts by $\gamma \cdot (\xi, \eta) = (\xi + \gamma, \eta - \kappa(\gamma) + \langle \xi, \lambda(\gamma) \rangle)$.

Proof. This follows from the gluing behavior of the local Kähler potentials for ω along the x, y, z coordinate axes. We can see this by combining two gluings that together give the action of the generator $\gamma' \in \Gamma_B$.

Namely, we have seen in the proof of Claim 1.5.2 that, when gluing across the z -axis the coordinate chart $U_{(-1,0),g^{-1}}$ with coordinates (x''', y''', z''') to the main coordinate chart U_{0,g^0} with coordinates (x, y, z) , the Kähler potential transforms by $F_V''' = F_V - \log(|Tz|^2)$. Thus this discrepancy between the local Kähler potentials implies that the value of $\xi_1 = -1/2(\partial F/\partial \log|x| - \partial F/\partial \log|z|)$ is modified by adding the constant -1 , and similarly for ξ_2 . Similarly, when gluing across the x -axis the main chart to the chart U_{0,g^5} with coordinates (x', y', z') the local Kähler potentials differ by $-\log(|Tx|^2)$, which modifies (ξ_1, ξ_2) by $(1, 0)$.

Combining the two transformations amounts to the action of γ' , namely changing coordinates from (x''', y''', z''') to (x', y', z') . This action modifies (ξ_1, ξ_2) by adding $(2, 1)$, which is exactly γ' . Similarly for γ'' .

For the statement about η , recall that η takes values $\eta \geq \varphi(\xi)$, so since $\varphi(\xi + \gamma) = \varphi(\xi) - \kappa(\gamma) + \langle \xi, \lambda(\gamma) \rangle$

$$\gamma \cdot \eta = \eta - \kappa(\gamma) + \langle \xi, \lambda(\gamma) \rangle$$

when $\gamma \in \Gamma_B$. □

Corollary 4.2.14. *The ℓ_k are Lagrangian in a fiber.* □

Proof. We have ℓ_k is the graph $\Gamma_{kM^{-1}(\xi)}$. So

$$T\ell_k = \langle \partial_{\xi_i} + kM^{-1}(\partial_{\xi_i}) \rangle_{i=1,2}$$

and the condition

$$\omega(\partial_{\xi_1} + kM^{-1}(\partial_{\xi_1}), \partial_{\xi_2} + kM^{-1}(\partial_{\xi_2})) = 0$$

follows from M being a symmetric matrix. Namely,

$$\partial_{\xi_1} + kM^{-1}(\partial_{\xi_1}) = \partial_{\xi_1} + (2k/3)\partial_{\theta_1} - (k/3)\partial_{\theta_2}$$

and similarly for the other generator of $T\ell_k$. So when pairing these with ω , the nontrivial terms cancel out because the coefficient of ∂_{θ_2} in $M^{-1}(\partial_{\xi_1})$ and the coefficient of ∂_{θ_1} in $M^{-1}(\partial_{\xi_2})$ are equal to each other, i.e. the matrices M and M^{-1} are symmetric. \square

Remark 4.2.15. The action coordinates (ξ_1, ξ_2, η) are globally well-defined on the universal cover \tilde{Y} , on which the T^3 -action discussed above is well-defined and Hamiltonian. It is useful to recall the following characterization of moment map coordinates in terms of symplectic areas of discs.

Claim 4.2.16. Consider a disc $D \subset Y$, whose lift $\tilde{D} \subset \tilde{Y}$ is invariant under the action of an S^1 subgroup of T^3 . Denote the corresponding moment map by μ . In particular the boundary of \tilde{D} is an S^1 -orbit $S^1 \cdot (x, y, z)$, while its center is a fixed point (x_0, y_0, z_0) .

Then the symplectic area of the disc D is equal to $\mu(x, y, z) - \mu(x_0, y_0, z_0)$.

Proof. We claim $\mu(x, y, z) - \mu(x_0, y_0, z_0) = \int_{\tilde{D}} \omega$. The \mathbb{CP}^1 moment map image is a segment over which we can draw an elongated sphere and map a value in the segment to the area of the part traced out in the sphere. The lift \tilde{D} has boundary component given by an orbit, which we can think of as the integral flow of the vector field generated by the infinitesimal action, call it $X^\#$. Then the integral over \tilde{D} involves integrating over this $X^\#$ and the line from (x, y, z) to (x_0, y_0, z_0) . Call this line C . Then we can write the integral as

$$\int_C \iota_{X^\#} \omega = \int_C d\mu = \mu(x, y, z) - \mu(x_0, y_0, z_0)$$

\square

Remark 4.2.17. We are starting with a polytope, which we want to be the moment map image with respect to some symplectic form that we construct. In particular, we have found a symplectic form so that the boundary \mathbb{P}^1 's of the hexagon have length 1 i.e. symplectic area 1. This follows from the change in Kähler potential under gluing across coordinate axes, see Claim 4.2.13.

4.2.2 Monodromy computations

Example 4.2.18 (One dimension down, 2D local case). The case of \mathbb{C}^2 with symplectic fibration $(x, y) \mapsto xy$ is the setting of a Lefschetz fibration, with singular fiber given by two copies of \mathbb{C} from $x = 0$ or $y = 0$, and monodromy is a Dehn twist about the S^1 around the belt of the cylindrical fibers.

$f(x, y) = xy$ and S^1 -action is $(e^{i\theta}x, e^{-i\theta}y)$. The holomorphic vector field corresponding to this is $iz_1\partial_{z_1} - iz_2\partial_{z_2}$, whose contraction with $\omega = \frac{i}{2}(dz_1 \wedge d\bar{z}_1 + dz_2 \wedge d\bar{z}_2)$ gives Hamiltonian vector field $-\frac{1}{2}(|z_1|^2 - |z_2|^2)$. We have a new set of coordinates on the two dimensional fiber:

the moment map coordinate μ and the angle coordinate of the action θ . As we approach $xy = 0$, the orbit at μ -height 0, namely $|x| = |y|$, goes to zero. That's one way to see how we get the picture of a cylinder with the neck pinching to zero.

Example 4.2.19 (3D local case). We do this in steps.

- **Parallel transport for holomorphic fibration.**

$$\begin{aligned} f &= xyz, & |f|^2 &= (x_1^2 + x_2^2)(y_1^2 + y_2^2)(z_1^2 + z_2^2) \\ \nabla_{\omega_0} f &= 2 \langle x|yz|^2, y|xz|^2, z|xy|^2 \rangle \perp (|f|^2)^{-1}(c^2) = \{|xyz| = c\} \end{aligned} \quad (4.3)$$

So the projection of the gradient vector field of $|f|^2$ will be perpendicular to circle in case. In particular, multiplying by i we get something tangent to the circle. The fact that multiplying by i on top gives the correct horizontal lift follows because f is holomorphic so the symplectic orthogonal to its level set is a complex subspace. Also we will see that the gradient is a linear combination of elements in the horizontal subspace.

- **Finding horizontal subspace.**

Claim 4.2.20. $X_{\Re(f)}, X_{\Im(f)} \in H$ where H is the horizontal distribution.

Proof. A fiber is precisely a level set of f .

$$\begin{aligned} \ker(d_p f) &= T_p(f^{-1}(c)), & p &\in f^{-1}(c) \\ \ker(df) &= \ker(d\Re(f)) \cap \ker(d\Im(f)) \\ \ker(d\Re(f)) &= \ker(\omega_0(X_{\Re(f)}, \cdot)) = (\mathbb{R} \cdot X_{\Re(f)})^\omega \\ \ker(d\Im(f)) &= \ker(\omega_0(X_{\Im(f)}, \cdot)) = (\mathbb{R} \cdot X_{\Im(f)})^\omega \\ \therefore H &:= (\ker(df))^\omega = (\ker(d\Re(f)) \cap \ker(d\Im(f)))^\omega \\ &= \ker(d\Re(f))^\omega + \ker(d\Im(f))^\omega \\ &= \mathbb{R} \cdot X_{\Re(f)} + \mathbb{R} \cdot X_{\Im(f)} \end{aligned} \quad (4.4)$$

□

Remark 4.2.21. Note that f holomorphic implies that

$$\begin{aligned} \nabla(\Re(f)) &= -J \nabla(\Im(f)) \\ \therefore \nabla(\Re(f)) &= -J X_{\Re(f)} = X_{\Im(f)} \\ \therefore H &= \langle X_{\Re(f)}, X_{\Im(f)} \rangle = \langle \nabla(\Re(f)), \nabla(\Im(f)) \rangle \end{aligned} \quad (4.5)$$

where \langle, \rangle denotes \mathbb{R} -span, so H is preserved under J , i.e. a complex subspace.

- **Calculations for parallel transport.** To find the parallel transport around the singularity, we first take a vector tangent to a circle in the base. Then we find the horizontal lift of $i\nabla|f|^2$ which we suitably scale first. In complex notation:

$$i\nabla(|f|^2) = \langle 2ix|y|^2|z|^2, 2iy|x|^2|z|^2, 2iz|x|^2|y|^2 \rangle \quad (4.6)$$

Integrating, we find that the time- θ flow of this vector field is

$$\rho^{i\nabla(|f|^2)}(\theta) = (e^{2i\theta|y|^2|z|^2}x, e^{2i\theta|x|^2|z|^2}y, e^{2i\theta|x|^2|y|^2}z) \quad (4.7)$$

We want to find a horizontal lift of the angular vector field $\partial/\partial\theta$, i.e. the vector field on the complex plane whose value at w is iw . Namely $df(i(\nabla|f|^2)/g) = iw$ for a suitable scalar function g .

$$\begin{aligned} df &= yzdx + xzdy + xydz \\ \nabla_{g_0}|f|^2 &= 2\langle x|yz|^2, y|xz|^2, z|xy|^2 \rangle \\ X_H &= \frac{2i}{g} \langle x|yz|^2, y|xz|^2, z|xy|^2 \rangle \text{ s.t. } df(X_H) = iw \\ \therefore \frac{2i}{g}xyz(|yz|^2 + |xz|^2 + |xy|^2) &= iw = i(xyz) \implies g = 2(|yz|^2 + |xz|^2 + |xy|^2) \\ \therefore X_H &= \frac{i}{|yz|^2 + |xz|^2 + |xy|^2} \langle x|yz|^2, y|xz|^2, z|xy|^2 \rangle \\ \therefore \rho^{X_H}(x, y, z, \theta) &= (e^{i\theta \frac{|y|^2|z|^2}{|y|^2|z|^2 + |x|^2|z|^2 + |x|^2|y|^2}}x, e^{i\theta \frac{|x|^2|z|^2}{|y|^2|z|^2 + |x|^2|z|^2 + |x|^2|y|^2}}y, e^{i\theta \frac{|x|^2|y|^2}{|y|^2|z|^2 + |x|^2|z|^2 + |x|^2|y|^2}}z) \\ &= (e^{i\theta \frac{|x|^{-2}}{|x|^{-2} + |y|^{-2} + |z|^{-2}}}x, e^{i\theta \frac{|y|^{-2}}{|x|^{-2} + |y|^{-2} + |z|^{-2}}}y, e^{i\theta \frac{|z|^{-2}}{|x|^{-2} + |y|^{-2} + |z|^{-2}}}z) \end{aligned} \quad (4.8)$$

because recall $w = xyz$ on the circle and in the last step we divide by $|f|^2$ to make it easier to see Dehn twisting behavior. This gives the monodromy result, Lemma 4.2.9 at the start of this section, in the local model near the origin of \mathbb{C}^3 .

Example 4.2.22 (In the setting $v_0 : Y \rightarrow \mathbb{C}$ of this paper).

Claim 4.2.23. If $\gamma(t)(v_0) = e^{2\pi it}v_0$ then the horizontal lift of γ' is of the form

$$X_{hor} = \partial/\partial\theta_{v_0} + f(\xi, \eta)\partial/\partial\theta_1 + g(\xi, \eta)\partial/\partial\theta_2$$

where f and g are functions of ξ_1, ξ_2, η only, and not of the angular coordinates.

Proof. **Part 1) General form.** Note that the Lie bracket on $\text{Lie } T^3$ is zero, so standard theory implies

$$\omega(X_{\zeta_1}, X_{\zeta_2}) = X_{[\zeta_1, \zeta_2]} = 0$$

In particular, if we take $\zeta_1 = (1, 0, 0)$ or $(0, 1, 0)$, namely the angular tangent directions of TF for F a fiber of v_0 , and ζ_2 anything, then we get zero. Furthermore, since $\omega(X_{(1,0,0)}, -) = d\xi_1$ we see that X_{ζ_2} does not have a $\partial/\partial\xi_1$ term, in other words its flow preserves the moment map coordinates ξ_1 and ξ_2 .

Part 1') General form in this case. In particular, let X_{hor} be the horizontal lift in the statement of the claim. Let $X_{(1,0,0)}$ be the vector field generated by the infinitesimal action of rotating the x coordinate, keeping y and v_0 fixed. Then X_{hor} being horizontal implies (by definition of the moment map ξ_1)

$$d\xi_1(X_{hor}) = \omega(X_{(1,0,0)}, X_{hor}) = 0$$

Thus if ϕ_t is the flow of X_{hor} we see by the Chain rule

$$\frac{d}{dt}(\xi_1 \circ \phi_t) = 0 \therefore \xi_1 \circ \phi_t = \xi_1$$

and similarly with ξ_2 . So parallel transport preserves the moment map coordinates ξ_1, ξ_2 . It also preserves η because we are considering angular parallel transport, so in coordinates $\pi : (\xi_1, \xi_2, \eta, \theta_x, \theta_y, \theta_{v_0}) \rightarrow (|w|, \theta_w) := (|v_0|, \theta_{v_0})$ for w the coordinate on the base \mathbb{C} of $v_0 : Y \rightarrow \mathbb{C}$

$$\begin{aligned} d\pi(X_{hor}) &= \partial/\partial\theta_{v_0} \\ \implies \begin{pmatrix} \partial|v_0|/\partial\xi_1 & \partial|v_0|/\partial\xi_2 & \partial|v_0|/\partial\eta & 0 & 0 & 0 \\ 0 & 0 & 0 & 0 & 0 & 1 \end{pmatrix} \begin{pmatrix} 0 \\ 0 \\ h \\ f \\ g \\ a \end{pmatrix} &= \begin{pmatrix} h\partial|v_0|/\partial\eta \\ a \end{pmatrix} = (0, 1) \end{aligned}$$

thus $a = 1$ and $h = 0$ because η depends on $|v_0|$. So we get the following form for the horizontal lift:

$$X_{hor} = \partial/\partial\theta_{v_0} + f\partial/\partial\theta_1 + g\partial/\partial\theta_2$$

Part 2) f and g are independent of angular coordinates. Let ρ^t be the flow of the horizontal vector field X_{hor} from angular parallel transport:

$$\rho^t(\xi_1, \xi_2, \eta, \theta_1, \theta_2, \theta_{v_0}) = (\xi_1, \xi_2, \eta, \theta_1 + tf, \theta_2 + tg, \theta_{v_0} + t)$$

Let ϕ_α be the action of T^2 by fiber-preserving symplectomorphisms given by $\phi_\alpha(x, y, v_0) =$

$(e^{2\pi i \alpha_1} x, e^{2\pi i \alpha_2} y, v_0)$. So we have:

$$\begin{aligned}
0 &= \phi_\alpha^* \omega(TF, H) = \omega((\phi_\alpha)_* TF, (\phi_\alpha)_* H) = \omega(TF, (\phi_\alpha)_* H) \\
&\quad \therefore (\phi_\alpha)_* H = H \\
d\pi((\phi_\alpha)_* X_{hor}) &= d(\pi \circ \phi_\alpha)(X_{hor}) = d\pi(X_{hor}) \\
\therefore (\phi_\alpha)_*(X_{hor}) \circ \phi_\alpha^{-1} &= X_{hor} \\
\implies d\phi_\alpha\left(\frac{d}{dt}\rho^t\right) \circ \phi_\alpha^{-1} &= \frac{d}{dt}(\phi_\alpha \circ \rho^t) \circ \phi_\alpha^{-1} = \frac{d}{dt}(\rho^t) \\
\implies \phi_\alpha \circ \rho^t &= \rho^t \circ \phi_\alpha \\
&\implies (\xi_1, \xi_2, \eta, \theta_1 + \alpha_1 + tf(\xi, \theta + \alpha), \theta_2 + \alpha_2 + tg(\xi, \theta + \alpha), \theta_{v_0} + t) \\
&\quad = (\xi_1, \xi_2, \eta, \theta_1 + \alpha_1 + tf(\xi, \theta), \theta_2 + \alpha_2 + tg(\xi, \theta), \theta_{v_0} + t) \\
&\implies f(\xi, \theta + \alpha) = f(\xi, \theta), \quad g(\xi, \theta + \alpha) = g(\xi, \theta) \quad \forall \alpha
\end{aligned}$$

where we integrate the terms with $\frac{d}{dt}$ to get to the next expression. Thus we find that f and g are independent of θ_1, θ_2 . A similar argument shows they are independent of θ_{v_0} , i.e. $\phi_\lambda \circ \rho^t = \rho^t \circ \phi_\lambda$ for $\lambda \in S^1$ the action on the v_0 coordinate. \square

Proof of Lemma 4.2.9. To arrive at the statement of monodromy at the start, we need to consider what happens away from the \mathbb{C}^3 -patch. Recall that in the upper right corner of the fundamental domain parallelogram where $r_z \ll r_x, r_y$, the Kähler form ω is the sum of a term ω_{xy} given by the potential g_{xy} , which only involves the complex coordinates x and y and does not involve z , and a term ω_{v_0} which only involves the coordinate $v_0 = xyz$. Hence horizontal vectors are those whose x and y components vanish, namely

$$H = \text{span} \left(\frac{\partial}{\partial \Re z}, \frac{\partial}{\partial \Im z} \right)$$

Specifically, if we consider vectors $u_1 \in TF = \ker(dv_0)$ and u_2 with no x and y components, then $\omega_{xy}(u_2, \cdot) = 0$ as u_2 has only a z component while ω_{xy} only involves the x and y variables. Also $\omega_{v_0}(u_1, \cdot) = 0$ as $u_1 \in \ker dv_0$. Thus in this upper right corner region, parallel transport varies z while fixing x and y . It follows that the monodromy preserves θ_1 and θ_2 , so $(f, g) = (0, 0)$.

By the same argument, in the region where the fiberwise potential is g_{yz} , the horizontal distribution is parallel to the x coordinate axis, so parallel transport varies x while keeping y and z constant. In particular the angular parallel transport vector field is $(ix, 0, 0)$ so the monodromy increases θ_1 at unit rate while keeping θ_2 constant, and $(f, g) = (1, 0)$. Similarly where we have g_{xz} , angular parallel transport is $(0, iy, 0)$, monodromy increases θ_2 while keeping θ_1 constant, and $(f, g) = (0, 1)$.

Finally, in the other hexagonal tiles, the values of (f, g) are again integer constants, determined by using the change of coordinate transformations described in section 1.4. In particular at the lower-left corner of the parallelogram, in terms of the coordinates (x''', y''', z''')

the parallel transport only varies z''' while keeping $\arg(x''')$ and $\arg(y''')$ constant. However, because $x''' = Tv_0x^{-1}$, fixing $\arg(x''')$ implies $\arg(v_0) - \arg(x)$ remains constant. Thus varying $\arg(v_0)$ around the unit circle also varies $\arg(x)$ and so θ_1 increases by 1. Similarly for y , and we find $(f, g) = (1, 1)$. □

4.2.3 Fiber Lagrangians Hamiltonian isotopic to linear Lagrangians

Definition 4.2.24. Let L_i be the parallel transport over a U-shape of the ℓ_i in the fiber.

Claim 4.2.25. The parallel transported ℓ_i is Hamiltonian isotopic to ℓ_{i+1} .

Proof. We construct an isotopy $\psi_t : F \rightarrow F$ in the fiber $F = V^\vee$ in coordinates $(\xi_1, \xi_2, \theta_1, \theta_2)$. In particular, on a fiber, η is a function of ξ_1, ξ_2 so it doesn't show up in the notation until the end of the proof, when we consider maps on the total space Y . It maps ℓ_1 to $\phi(\ell_0)$ where ϕ is the monodromy. To prove ψ_t is a Hamiltonian isotopy, i.e. $\iota_{\frac{d}{dt}\psi_t}\omega = dH_t$ for some H_t , a classical result of Banyaga (cf [MS17, Theorem 3.3.2] or [Pas14, Equation (6)]) implies that it suffices to show that the flux of ω through cylinders traced out by generators of $H_1(F)$ is zero.

$$\left\langle \int_t \iota_{X_t} \omega, [\gamma] \right\rangle = \langle \text{Flux}(\psi_t), [\gamma] \rangle = \int_{\psi_t(\gamma)} \omega = \text{area of cylinder traced out by } \gamma \text{ over time}$$

First we define the isotopy, and set $A := M^{-1}$.

$$\psi_t(\xi_1, \xi_2, \theta_1, \theta_2) := (\xi_1, \xi_2, \theta_1 + t(f(\xi) - A_1\xi), \theta_2 + t(g(\xi) - A_2\xi))$$

This is well-defined modulo Γ_B in the first two coordinates and modulo \mathbb{Z}^2 in the second two coordinates. The latter is true by the following reasoning. Recall that $(f, g)(\xi + \gamma) = (f, g)(\gamma) - M^{-1}\gamma$ for $\gamma \in \Gamma_B$ by the argument in the proof of Lemma 4.2.9 on page 94. Thus since A has the same periodicity by linearity, subtracting we find that $(f, g)(\xi + \gamma) - A(\xi + \gamma) = (f, g)(\xi) - A(\xi)$.

We note that $H_1(F)$ has rank four since $F \cong T_B \times T_F$. If we let γ be the loop generated by $(0, 0, 1, 0)$ or $(0, 0, 0, 1)$ the two angular directions, then $\{\psi_t(\gamma)\}_t$ is one dimensional because ξ is constant thus the integral is zero. Now we let

$$\gamma(t) = (2t, t, 0, 0), \quad -\frac{1}{2} \leq t \leq \frac{1}{2}$$

The case of $\gamma(t) = (t, 2t, 0, 0)$ is similar.

$$\begin{aligned}
flux &= \int_{\psi_t(\gamma)} \omega = \int_{\gamma} \iota_{X_t} \omega = \int_{\gamma} (d\xi_1 \wedge d\theta_1 + d\xi_2 \wedge d\theta_2)((f - A_1)\partial_{\theta_1} + (g - A_2)\partial_{\theta_2}, -) \\
&= \int_{\gamma} (f - A_1)d\xi_1 + (g - A_2)d\xi_2 \\
&= \int_{-1/2}^{1/2} 2f(2t, t)dt + g(2t, t)dt
\end{aligned}$$

where we used that A being a linear map implies symmetry across zero, and it remains to show that the above is zero, namely symmetry across zero in f and g . It suffices to show that $f(-\xi) = -f(\xi)$ and similarly with g .

To do this we recall that f and g are defined by

$$X_{hor} = \frac{\partial}{\partial \theta_{v_0}} + f(\xi, \eta) \frac{\partial}{\partial \theta_1} + g(\xi, \eta) \frac{\partial}{\partial \theta_2}$$

Also recall that X_{hor} will be preserved by any fiber-preserving symplectomorphism of Y , as we saw above in the example of the T^2 -action. Another fiber-preserving symplectomorphism is $\phi_- : (\xi, \eta, \theta, \theta_\eta) \mapsto (-\xi, \eta, -\theta, \theta_\eta)$. It is a symplectomorphism because $d\xi \wedge d\theta + d\eta \wedge d\theta_\eta \mapsto d(-\xi) \wedge d(-\theta) + d\eta \wedge d\theta_\eta = d\xi \wedge d\theta + d\eta \wedge d\theta_\eta$. It remains to prove that it preserves a fiber.

Recall that varying η corresponds with varying $|z|$. If we fix a fiber, then varying $|z|$ but preserving $|xyz|$ means that $|x|$ and/or $|y|$ will also vary. In particular, η will be a function of ξ_1, ξ_2 on a fiber. Recall the coordinates from Figure 1.8. The map $\Delta_{\tilde{Y}} \rightarrow \Delta_{\tilde{Y}}$ given by

$$(x, y, z) \rightarrow (T^{-2}x^{-1}, T^{-2}y^{-1}, T^4v_0^2z^{-1})$$

is the result of applying the symplectomorphism ϕ_- , in particular preserving the polytope. This squares to the identity and preserves the fiber. On action-angle coordinates this map negates $\theta_1, \theta_2, \theta_\eta$ since rotating x, y, z will rotate the new coordinates in the other direction. More specifically, the T^3 action on the new coordinates will be:

$$\begin{aligned}
T^{-2}x^{-1} &\mapsto e^{-2i\pi\alpha_1}T^{-2}x^{-1} \\
T^{-2}y^{-1} &\mapsto e^{-2i\pi\alpha_2}T^{-2}y^{-1} \\
T^4v_0^2z^{-1} &\mapsto e^{4i\pi\alpha_\eta}e^{-2i\pi(\alpha_\eta - \alpha_1 - \alpha_2)}T^4v_0^2z^{-1}
\end{aligned} \tag{4.9}$$

i.e. the last coordinate gets rotated by $\alpha_\eta + \alpha_1 + \alpha_2$. That is, the action of $(\alpha_1, \alpha_2, \alpha_3)$ becomes the action of $(-\alpha_1, -\alpha_2, \alpha_\eta)$ on the new coordinates, hence ξ_1, ξ_2 are negated while η stays the same. This is up to additive constants so suppose ϕ_- is defined by:

$$(\xi_1, \xi_2, \eta) \mapsto (-\xi_1 + c_1, -\xi_2 + c_2, \eta + c)$$

where the constants are such that the origin maps to itself. Thus the constants are zero. So

$$\begin{aligned} (\phi_-)_*(X_{hor}) &= X_{hor} \circ \phi_- \\ \implies f(-\xi) &= -f(\xi), \quad g(-\xi) = -g(\xi) \end{aligned}$$

and this completes the proof. \square

4.3 Background for defining $H^0(FS(Y, v_0))$

The following background is from [Sei08].

Remark 4.3.1 (Notation). We start with the symplectic fibration $v_0 : Y \rightarrow \mathbb{C}$, which is not exact because fibers are compact tori. Although Y does not have boundary, we will restrict to a small disc around the origin, which does have boundary. In particular, in the terminology of [Sei08], we do not have a *horizontal boundary* since fibers are tori, but we do have a *vertical boundary* by taking the preimage of a compact neighborhood in the base.

The class of almost complex structures we consider are 1) compatible with the ω defined above and 2) are equal to the standard J_0 induced from the complex toric coordinates near the boundary. We will denote this set as $\mathcal{J}(Y, \partial Y)$. This set is non-empty, because it contains J_0 , and contractible by the same argument as for the set of all ω -compatible almost complex structures.

Definition 4.3.2 (Domains). A *punctured boundary Riemann surface* S is the data of a compact, connected, nonempty boundary Riemann surface with punctures removed on its boundary, and the assignment of a Lagrangian to each component of ∂S . We further “*rigidify*” by adding extra structure to S ; denote punctures as “positive” or “negative” and define *strip-like ends* via embeddings $\epsilon : (-\infty, 0]_s \times [0, 1]_t \rightarrow \mathbb{D}$ or $\epsilon : [0, \infty)_s \times [0, 1]_t \rightarrow \mathbb{D}$ for the negative and positive punctures ζ^\pm respectively, such that $\lim_{s \rightarrow \pm\infty} \epsilon(s, t) = \zeta^\pm$. This is called a *Riemann surface with strip-like ends*.

Example 4.3.3. In this thesis, S will be one of the unit disc \mathbb{D} , two discs glued together at a point on their boundary, or a disc union a configuration of spheres, in each case with potentially some punctures. One example of a strip-like end we use later on to glue two discs is $(-\infty, 0] \times [0, 1] \ni (s, t) \mapsto \epsilon^-(s, t) := \frac{e^{-\pi(s+it)} + i}{e^{-\pi(s+it)} - i} = \frac{z+i}{z-i} \circ e^{-z} \circ \pi \cdot (s+it) \in \mathbb{D} \setminus \{1\}$. Note that $-\infty$ is the puncture which would map to $\zeta^- := 1$ in the disc. See Figure 4.2.

Remark 4.3.4. This “rigidifies” because any operation on S must preserve the additional data of strip-like ends, thus placing further restrictions. The strips provide a nice set of coordinates near the punctures (namely s and t) and give a straightforward way to glue two sections by gluing linearly in the (s, t) coordinates. See [Sei08, §(8i) and §(9k)].

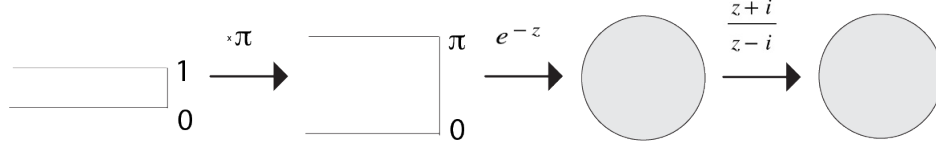


Figure 4.2: Example of strip-like end

Definition 4.3.5 (Maps). Let $J \in \mathcal{J}(Y, \partial Y)$. A *pseudo-holomorphic map* is a J -holomorphic map $u : (S, \partial S) \rightarrow (Y, \sqcup_{i \in \pi_0(\partial S)} L_i)$. A J -*pseudo-holomorphic curve* is the image of such a map. We require

$$\lim_{s \rightarrow \pm\infty} u(\epsilon_{ij}(s, t)) \in L_i \cap L_j$$

for strip-like end ϵ_{ij} limiting to an intersection point of $L_i \cap L_j$.

Remark 4.3.6 (With data of a symplectic fibration, can look at sections). We can think of the above as a section of a trivial fibration with fixed Lagrangian boundary condition. Now we generalize to non-trivial fibrations. Consider a holomorphic polygon in the total space of a fibration with boundary in fiber Lagrangians parallel transported around polygon in the base. If we project to the base of a holomorphic fibration, we obtain a holomorphic polygon. This indicates we should look at holomorphic sections.

Definition 4.3.7 (Sections). A pseudo-holomorphic section of a fibration is a pseudo-holomorphic map to the total space (equipped with an almost-complex structure which makes the projection map holomorphic) whose projection down to the base is an embedded holomorphic polygon.

Definition 4.3.8 (Perturbed sections). When the boundary conditions are fibered Lagrangians obtained by parallel transport over arcs, one could use the base polygon determined by these arcs as the domain for the map u . Or we may view sections as maps $S \rightarrow Y$ such that composing with projection $v_0 \circ u : S \rightarrow \mathbb{C}$ gives a biholomorphism onto its image. In the latter case we could take the domain S to be this subset of \mathbb{C} , so that $v_0 \circ u = \mathbf{1}_S$.

When we perturb J , the fibers of v_0 are not necessarily almost-complex submanifolds so we won't consider sections anymore. In other words, J_0 -holomorphic sections are deformed to J -holomorphic maps which are sections in a region U where $J|_U = J_0|_U$ and have algebraic intersection number 1 with fibers of v_0 in the region where J has been perturbed.

Remark 4.3.9. The above assumes that Lagrangians intersect transversely. Since Lagrangians are half-dimensional, if they intersect transversely then their intersection is 0-dimensional and we have a discrete set of points. There are several ways that have been invented to account for non-transverse intersections. One is by introducing a Hamiltonian function and flowing one Lagrangian along the symplectically dual vector field to the derivative

of that Hamiltonian function, until the two Lagrangians intersect transversely, c.f. [Sei08]. Sometimes it is possible for the Hamiltonian vector field to be tangent to the fibers, which preserves the feature that the projection of a perturbed holomorphic curve under v_0 is a holomorphic polygon.

We have a Hamiltonian function H defined on the fiber and 1-form γ defined on the base of S , vanishing on the boundary. In particular, we define γ to be zero near punctures where there is no problem and nonzero near punctures where the Lagrangians do not intersect transversally. Then maps u should satisfy the modified Cauchy-Riemann equation

$$(du - X_H \circ \gamma)^{0,1} = 0$$

with a modified asymptotic condition: at a puncture the map u converges to a trajectory of X_H from L_i to L_j . Alternatively we can reformulate by considering the image of u under a suitable amount of flow of X_H , dependent on the point of S , which satisfies a Cauchy-Riemann equation for a different J and boundary conditions: the new map limits to an intersection point of the Lagrangian and the time-1 flow under X_H of the other Lagrangian intersecting non-transversely. We can use this to compute self-homs of Lagrangians ℓ_i in the fiber.

Here since the symplectic form is not a product of the base and fiber, we will use the categorical localization method of [AS], see also [Gan16b], instead of Hamiltonian perturbation.

Example 4.3.10. Let t_z be the preimage of a moment map value $(c_1, c_2) \in T_B$, intersected with a fiber. So $t_z = \{c_1, c_2, \theta_1, \theta_2\}_{\theta_i \in [0, 2\pi)}$ which in particular is invariant under parallel transport because that map rotates the angles. Since $\ell_i \cap t_z$ is the one point of ℓ_i with $(\xi_1, \xi_2) = (c_1, c_2)$, any pseudo-holomorphic section u must limit to that one point over the corresponding puncture in the base.

Example 4.3.11. The intersection in $t_z \cap t_z$ is not transverse, so we'll need to introduce an inhomogeneous Hamiltonian term as above. This is a smooth function on the fiber. In our case the time-1 flow of X_H is an automorphism of the fiber that is a graph on the real norms of the coordinates $|x|, |y|, |z|$, chosen so that it descends to a map from the torus to itself. The PSS isomorphism implies $HF^*(t_z, t_z) \cong H^*(t_z; \mathbb{C})$, the cohomology of a 2-torus.

4.4 Moduli spaces needed to define $H^0(FS(Y, v_0))$

Remark 4.4.1 (Reason for moduli spaces in the Fukaya category). The Fukaya category is an A_∞ -category. This means we have objects, morphisms, and structure maps on k morphisms for any natural number k that satisfy A_∞ -relations, which can be thought of as higher order associativity relations on the morphisms. Objects are Lagrangians, morphisms are intersection points, and structure maps count pseudo-holomorphic maps with boundary

punctures limiting to k input intersection points and 1 output intersection point. For the Fukaya-Seidel category, the input is a symplectic fibration and we consider non-compact Lagrangians in the total space Y which fiber over arcs, so that the pseudo-holomorphic discs which determine the structure maps will turn out to be sections of the fibration over polygons in the base.

To ensure we can make these counts, we first collect pseudo-holomorphic maps into a set modulo reparametrization. Gromov equipped this quotient set with a topology so it is a topological space, known as a moduli space because we mod out by automorphisms of the Riemann surface S . Using his result of Gromov compactness we can compactify this topological space by analyzing what behavior can happen to a limit of pseudo-holomorphic curves, via results from complex analysis that still hold in the pseudo-holomorphic setting such as unique continuation. However, moduli spaces are expected to be manifolds whose dimension is determined by an index formula, and the structure maps of the Fukaya category aim to count solutions when this expected dimension is equal to 0. So we use differential geometry on function spaces to put the structure of a compact zero-dimensional smooth manifold on the moduli space, which is a finite set of points that can be counted. Here is the plan for defining the moduli spaces, fitting them into the framework of the Fukaya-Seidel category, and then working out the HMS computation:

- Immediately below: determine **homology classes in Y** where curves map to.
- Section §4.4 (current): Prove **existence of regular J** , for which the moduli spaces in the Fukaya category are compact 0-dimensional manifolds. This will adapt [MS12] from the $S = \mathbb{CP}^1$ setting to the $S = \mathbb{D}$ setting with Lagrangian boundary conditions, and is also discussed in [Sei08] and [Gan16b].
- Section §4.5: **Define the category** following [AS] and **prove independence of choice of regular J and Hamiltonian isotopy class of the Lagrangian** in $FS(Y, v_0)$, up to quasi-isomorphism, by a standard continuation map argument.
- Chapter §5: **Embed fully faithfully** the full subcategory $D^bCoh_{\mathcal{L}}(H)$ of the bounded derived category of coherent sheaves to a full subcategory of $H^0(FS(Y, v_0))$.

The last three steps involve moduli spaces. Figure 4.3 is a flow chart for how to define them and what we hope to do with them.

Lemma 4.4.2 (Homology of Y).

$$H_2(Y) \cong H_2(\mathbb{CP}^2(3)/\Gamma_B) \cong \mathbb{Z}^4$$

where all homology classes will be over \mathbb{Z} .

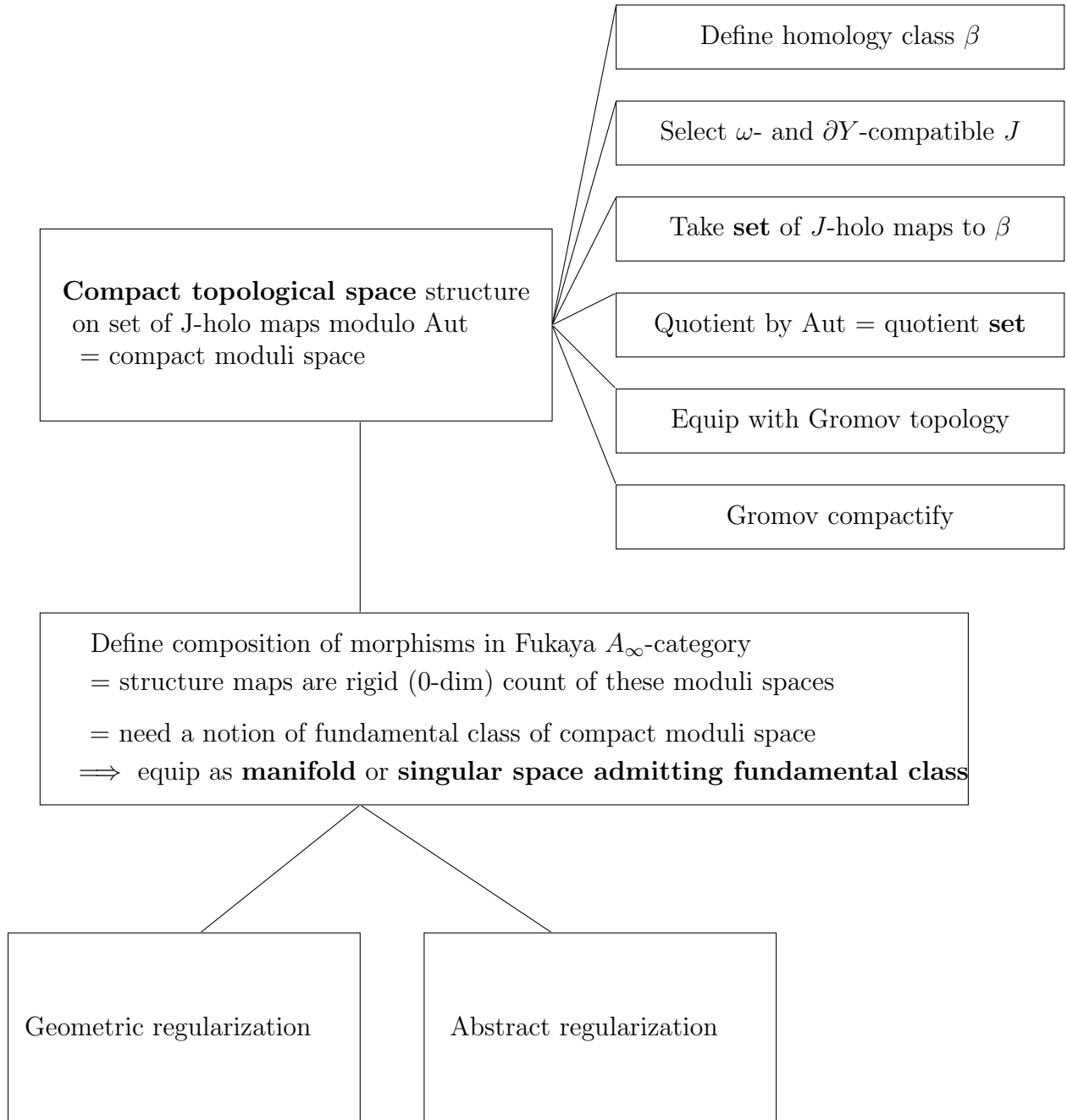


Figure 4.3: Flow chart for working with moduli spaces in Fukaya categories

Proof. Note that Y deformation retracts onto the central fiber over the contractible base, determined by parallel transport in the inward radial direction. Therefore the homology of Y is the homology of the central fiber, a degeneration of a T^4 fiber.

To get $H_2(\mathbb{CP}^2(3)/\sim)$ we may use Mayer-Vietoris as follows. Cut out an open set projecting to a disc at the center of the hexagon in the hexagonal picture, which then retracts onto the boundary. This gives two open sets, which in the moment map picture are a disc and its complement, intersecting in an S^1 .

Let $B := D^2 \times T^2$ correspond to the disc in the moment polytope. Let \tilde{A} be the complement, a string of 6 \mathbb{CP}^1 's in a circle and $A := \tilde{A}/\Gamma_B$ the banana manifold. In particular, $\tilde{A} \cap B$ retracts onto $S^1 \times T^2 = T^3$. Then we have

$$\begin{aligned} 0 &= H_3(\tilde{A}) \oplus H_3(B) \rightarrow H_3(Z) = 0 \\ &\rightarrow H_2(\tilde{A} \cap B) = \mathbb{Z}^3 \xrightarrow{(*)} H_2(\tilde{A}) \oplus H_2(B) = \mathbb{Z}^6 \oplus \mathbb{Z} \rightarrow H_2(\mathbb{CP}^2(3)) \rightarrow 0 \\ H_1(\tilde{A} \cap B) &= \mathbb{Z}^3 \xrightarrow{\cong} H_1(\tilde{A}) \oplus H_1(B) = \mathbb{Z} \oplus \mathbb{Z}^2 \rightarrow H_1(\mathbb{CP}^2(3)) = 0 \end{aligned}$$

where $(*) = \begin{pmatrix} 1 & 0 & 0 \\ 0 & 1 & 0 \\ -1 & 1 & 0 \\ -1 & 0 & 0 \\ 0 & -1 & 0 \\ 1 & -1 & 0 \\ 0 & 0 & 1 \end{pmatrix}$ and the second to last map is the 3-by-3 identity matrix with

respect to the three generators of $H_1(\tilde{A} \cap B) = H_1(S^1 \times T^2)$ (call them b for the S^1 in the moment polytope and T_1, T_2 for the two loops in the 2-torus fiber). Then passing to the quotient $\mathbb{CP}^2(3)/\sim$ we find that

$$\begin{aligned} 0 &= H_3(A) \oplus H_3(B) \rightarrow H_3(\mathbb{CP}^2(3)/\sim) \\ &\rightarrow H_2(A \cap B) = \mathbb{Z}^3 \xrightarrow{(**)} H_2(A) \oplus H_2(B) = \mathbb{Z}^3 \oplus \mathbb{Z} \\ &\rightarrow \textcolor{red}{H_2(\mathbb{CP}^2(3)/\sim) = \mathbb{Z}^4} \rightarrow \mathbb{Z} \cdot b \subset H_1(A \cap B) = \mathbb{Z}^3 \\ &\xrightarrow{(***)} H_1(A) \oplus H_1(B) = \mathbb{Z}^2 \oplus \mathbb{Z}^2 \rightarrow H_1(\mathbb{CP}^2(3)/\sim) = \mathbb{Z}^2 \end{aligned}$$

where $(**) = \begin{pmatrix} 0 & 0 & 0 \\ 0 & 0 & 0 \\ 0 & 0 & 0 \\ 0 & 0 & 1 \end{pmatrix}$ and $(***) = \begin{pmatrix} 0 & 0 & 0 \\ 0 & 0 & 0 \\ 0 & 1 & 0 \\ 0 & 0 & 1 \end{pmatrix}$. Note that the final term is consistent

with Y being the quotient of its universal cover \tilde{Y} by $\Gamma_B = \mathbb{Z}^2$, where $\pi_1(Y) = \pi_1(\mathbb{CP}^2(3)/\sim)$

should be \mathbb{Z}^2 . So ultimately we look at the projection of the 6 \mathbb{P}^1 's mapping to the three glued \mathbb{P}^1 's. Again we find that the homology is \mathbb{Z}^4 . □

Now we have the homology classes of Y where images of sphere bubbles may exist. We also want to know relative H_2 for discs with boundary in a given Lagrangian. Recall our discussion of maps and sections above in the background section. We now define the discs we will consider in this thesis. The homology classes in $\pi_2(Y, L)$ that we consider cover a disc in the base around 0, and pass through the central fiber in one point. Varying this point using the toric geometry of the central fiber allows one to enumerate all the homology classes, done in [CO06]. We will discuss this below when we do the computation of the disc count for a particular J . Here we will just show existence of moduli spaces for a given homology class β in $H_2(Y, L)$.

We give a more precise definition of the perturbed section maps defined above.

Definition 4.4.3 (Section-like maps). We select an open set around the origin, call it U . Then we restrict ourselves to look at almost complex structures that are identically J_0 outside of U . In particular, discs will be sections there. If $J = J_0$ everywhere, then the Riemann mapping theorem implies that composing the J_0 -holomorphic map on the disc with the J_0 -holomorphic map v_0 to the base is unique. To allow enough regularity, we will need to consider J which can vary away from J_0 inside the set U . In particular, we will define all our Lagrangians below to be required to go through the point -1 in the base so if we choose U to be a disc of radius smaller than 1 and require our Lagrangian submanifolds of Y to lie entirely outside of U , this allows us to conclude there are no multiply-covered discs because they cannot wrap around the boundary. Take U to be the disc of radius $1/2$ centered at the origin.

The geometry of this set-up allows us to conclude some results about disc bubbling and strip-breaking. Because the Lagrangians we consider lie outside of U , the projection of a hypothetical disc bubble under v_0 , if non-constant, would satisfy the open mapping principle outside of U , which immediately gives a contradiction since the Lagrangian projects to a U-shaped curve which does not enclose any bounded region of the complex plane. And disc bubbles inside the fibers of v_0 cannot exist either because linear Lagrangians in tori have zero relative π_2 i.e. they don't bound discs. Likewise, because of the section-like behavior outside of U (hence everywhere along the boundary of the disc), degenerations of the domain or strip-breaking can be controlled by considering the projection to v_0 . Any component that breaks off must either lie entirely within a fiber of v_0 , or the degeneration must be visible in the projection to v_0 . Namely, the polygonal region of the complex plane over which the section-like map projects also decomposes into a union of polygons with boundary on the given arcs.

If we did have multiple covers, we may require that J depend on $z \in S$, in which case we replace J with J_z . The text [MS12] lays this foundation for Lagrangian boundary conditions

case which is described in [Aur14] and will involve an \mathbb{R} -family of J 's on a strip. But we don't need to do that here since we are considering section-like discs, which are injective near their boundary.

Remark 4.4.4. J -curves have some analogous properties as complex curves. For example, the Carleman similarity principle and unique continuation (if two J -holomorphic maps agree on an open set, or all derivatives agree at a point, then the maps are equal). Also, there are only finitely many points in a preimage and only finitely many critical points, and simple curves have an open dense set of injective points.

Now that we've discussed the homology classes where the curves have their image in Y , we next move to proving existence of regular J , which will allow us to construct a Fredholm problem where the Cauchy-Riemann operator $\bar{\partial}_J$ will cut out the moduli spaces as a section of a Banach bundle, and the implicit function theorem will tell us the preimage of zero is a manifold, which will allow us to put a smooth structure on our moduli spaces.

Example 4.4.5. This is an infinite-dimensional Banach analogue to Sard's theorem asserting the regularity of generic level sets of smooth maps between finite-dimensional manifolds (e.g. a sphere is smooth as a level set of a smooth function with surjective derivative). In the Banach-bundle setting, regular means not only surjective but also a continuous right inverse exists.

The difference here is that the differential operator inputs functions, which lands us in the world of infinite-dimensional Banach spaces. The following theory follows the arguments of [MS12, Chapters 3–10] but for curves with boundary, also discussed in [Sei08]. An example of the geometric regularization theory is implemented in [Weh13] for Gromov non-squeezing, which involves illustrating how to show a family of moduli spaces varying J_t is 1 dimensional (Fredholm), a manifold (transversality/regularity), compact (Gromov compactness) and has boundary. A nice reference for abstract regularization theories is [Weh14].

We now proceed to prove existence of a regular J .

Lemma 4.4.6 (Geometric regularization). *There exists a dense set $\mathcal{J}_{reg}^1 \subset \mathcal{J}(Y, \omega)$ of ω -compatible almost complex structures J that are identically J_0 outside of U such that, for all J -holomorphic maps $u : (\mathbb{D}, \partial\mathbb{D}) \rightarrow (Y, L|_\gamma)$ with boundary condition $L|_\gamma := \cup L_i|_{\gamma_i}$ given by a union of fibered Lagrangians in Y given by parallel transporting fiber Lagrangians around U -shaped arcs γ_i in the base from -1 , the linearized $\bar{\partial}$ -operator D_u is surjective.*

Remark 4.4.7. We use the superscript 1 because later we will want existence of slightly smaller sets \mathcal{J}_{reg}^2 and \mathcal{J}_{reg}^3 which are regular for a disc attached to a disc and a disc attached to a sphere, with similar Lagrangian boundary conditions. These will be labelled 2 and 3 and will require not only surjectivity of the linearized operator but also compatible behavior when evaluating at the intersection point.

Sketch adapting the 2nd edition book [MS12, pg 55, proof of Theorem 3.1.6 (ii)]. We give a road map adapting McDuff-Salamon to the setting with Lagrangian boundary conditions. The background for this was also learned from [Weh14, Lecture 9]. Note Theorem C.1.10 in [MS12] proves we have a Fredholm problem for the case of boundary.

Introduction. “Regularization” refers to perturbing the $\bar{\partial}_J$ operator to be equivariantly transverse to the zero section of a Fredholm bundle which we can build so that the operator is a section of the bundle. “Geometric regularization” means the perturbations are obtained by perturbing the almost complex structure J , so are geometric in nature. Namely the perturbations of $\bar{\partial}_J$ are $\bar{\partial}_{J'} - \bar{\partial}_J$ as J' varies. In this setting equivariance will be automatic, as described below. Note that later on, we will need to use a non-regular J for computations and in that case we will use “abstract regularization” by adding abstract perturbations ν which are sections of the same Fredholm bundle but are not necessarily of the form $\bar{\partial}_{J'} - \bar{\partial}_J$.

To prove existence of regular J for discs with boundary mapping to fiber Lagrangians parallel-transported over U-shaped curves (so all curves considered must intersect the central fiber), we show that there is a dense set of them in $\mathcal{J}_\omega^\ell(Y, U) := \{J \in \Gamma(TY) \mid J^2 = -\mathbf{1}, J_{Y \setminus U} \equiv J_0, J \in C^\ell\}$. (This set of J is what’s needed in the boundary case, see [MS12, Remark 3.2.3].) First, we define the set of all $W^{k,p}$ maps u and geometric perturbations encoded by varying J :

$$\mathcal{M}_{\mathcal{J}} := \{(u, J) \mid J \in \mathcal{J}_\omega^\ell(Y, U), W^{k,p} \ni u : (\mathbb{D}, \partial D) \rightarrow (Y, L)\}$$

For sufficiently large k , $W^{k,p} \subset C^\ell$. Then elliptic bootstrapping will imply that J -holomorphic maps u are in C^ℓ . This moduli space is called “universal” because we allow J to vary. We use $W^{k,p}$ because it is complete, i.e. a Banach space, which will be needed to invoke Sard-Smale and elliptic regularity in the infinite dimensional setting of function spaces. In particular, we want $\mathcal{M}_{\mathcal{J}}$ to be a $C^{\ell-1}$ separable Banach manifold. Then we can use Sard-Smale on the projection map $(u, J) \rightarrow J$ to prove existence of a dense set of regular J for the disc.

Banach bundle set-up. We want to view $\mathcal{M}_{\mathcal{J}} \subset \mathcal{B}^{k,p} \times \mathcal{J}_\omega^\ell(Y, U) \ni (u, J) \rightarrow J$ as the zero set of a Fredholm section of a Banach bundle in order to invoke Sard-Smale to get a dense set of regular values. Since a *Fredholm* operator (e.g. the linearization D_u of the section $u \mapsto \bar{\partial}_J u$) is defined to have finite dimensional kernel and cokernel as well as closed image, a trivial cokernel for such an operator implies the operator is surjective. For regularity we also need the existence of a continuous right inverse, which is a requirement in the infinite-dimensional setting. Then an implicit function theorem will imply the set of (u, J) cut out by the zero set of this section is a Banach submanifold of the base and not just a subset. Note that the zero-set consists of (u, J) so that u is J -holomorphic.

Banach manifold structure on $\mathcal{B}^{k,p} \ni u$: we construct a local Banach chart about an arbitrary map u . The local model is $T\Gamma(u^*TY, u^*TL) \ni \xi$ via $u \mapsto \exp_u \xi$. This is well-defined: we always have existence of a metric so that one Lagrangian is totally geodesic [MS12, Lemma

4.3.4] and so one Lagrangian, or two, are totally geodesic from some metric. And at any point considered there are at most two Lagrangians intersecting so this suffices. We need totally geodesic for this to provide a chart in the case of Lagrangian boundary condition: given a point in $\partial\mathbb{D}$, move along the vector ξ planted at that point and the result will be tangent to L so that geodesic remains in L .

Now we put a Banach manifold structure on $\mathcal{J}_\omega^\ell(Y, U) \ni J$, the second factor of the base of the Banach bundle we are constructing, cf [MS12, §3.2]. We linearize to obtain the equations for the tangent space \dot{J} , and local charts can then be recovered from the tangent space by exponentiating. Three conditions on J become linearized: 1) $J|_{Y \setminus U} \equiv J_0$ implies $\dot{J}|_{Y \setminus U} \equiv 0$ (this is specific to the setup where J varies only in U), 2) $J^2 = -\mathbf{1}$ implies $\dot{J}J + J\dot{J} = 0$, and 3) $\omega(\cdot, J\cdot) > 0$ and symmetric also gets linearized. A chart is constructed via $\dot{J} \mapsto J \exp(-\dot{J}J)$. C.f. [Sei08].

A fiber of the bundle will not have boundary conditions because it is given by the space where $(du)^{0,1} = \frac{1}{2}(du + J \circ du \circ j)$ lands in, namely $W^{k-1,p}(S, \Lambda^{0,1} \otimes u^*TY)$, and that doesn't concern the boundary. Note that $J \circ du \circ j$ does not a priori have the same behavior as du in the direction tangent to the boundary, so $(du)^{0,1}$ does not satisfy any particular boundary condition.

Now we describe how to put the structure of a Banach bundle over open sets in the base. This will mimic the case of [MS12] because there are no boundary conditions on the fiber. We use the exponential map to trivialize the bundle over a neighborhood $\mathcal{N}(u)$ in the first factor of $\mathcal{B}^{k,p} \times \mathcal{J}_\omega^\ell(Y, U)$, and we use parallel transport to trivialize over a neighborhood $\mathcal{N}(J)$. This trivializes the bundle over a neighborhood in the base, and a composition of these gives transition maps that satisfy conditions for a Banach bundle, [MS12] and [Sei08].

Fredholm problem. A *Fredholm problem* concerns the zero set of a *Fredholm section* of a Banach bundle. I.e. a section whose linearization is a Fredholm operator, namely $\dim \ker - \dim \operatorname{coker}$ is finite and whose image is closed. More generally it's a set-up of the moduli spaces (main part and Gromov compactifying components that are fiber products) as the zero sets of Fredholm sections. We claim that the section $(u, J) \mapsto \bar{\partial}_J(u)$ is Fredholm. To take the linearization of the $\bar{\partial}$ operator at some map u , we have to see what happens as we vary u infinitesimally by a tangent vector ξ . That is, we differentiate the $\bar{\partial}$ operator in a family and take the derivative at zero. See [MS12, Proposition 3.1.1]. Similarly we will vary J infinitesimally by tangent vector \dot{J} .

$$D_u : W^{k,p}(S, \partial S; u^*TY, u^*TL) \rightarrow W^{k-1,p}(S, \Lambda^{1,0} \otimes_j u^*TY)$$

We define D_u as follows: for a nearby u' in the exp neighborhood of u , we parallel transport back to the origin of the chart at u , take $\bar{\partial}_J$, then map forward again on the fiber under parallel transport. Then the linearized operator $D_u \xi$ will be the derivative of this operation

at the point 0. This is well-defined because of the totally geodesic condition above. This is only when varying u . Varying J as well we get [Weh14, Lecture 9]:

$$D_u \xi + \frac{1}{2} \dot{J} duj$$

Assuming the map u is somewhere injective, this operator is surjective with continuous right inverse, so is regular. The reasoning is as follows. Suppose by contradiction the image is not dense. Take a nonzero linear functional η in the orthogonal complement to the image. Taking $\dot{J} = 0$ we see that η is orthogonal to $\text{im}(D_u)$ as well. So it must be orthogonal to $\dot{J} duj$ for all \dot{J} . However, using bump functions, since $\eta \neq 0$ we can construct a perturbation \dot{J} so η integrated on \dot{J} is nonzero, which gives the contradiction, see [MS12, page 65].

It's still possible to do this construction in the Lagrangian boundary setting because the constructed \dot{J} is supported in a small neighborhood around a somewhere injective point so will be zero near the boundary as required. Somewhere injective points are dense so we can find one close to a given point where η is nonzero. In particular there is a neighborhood of them. Use bump functions to construct a \dot{J} so that the integral of $\int_{\mathbb{D}} \eta(\dot{J} duj) > 0$. This is a contradiction. So η vanishes on the open set of injective points, hence vanishes identically by unique continuation [MS12, Theorem 2.3.2]. This is again a contradiction since $\eta \neq 0$. Thus we find that our original assumption that the image is not dense is false. The image is dense, and since it's closed, the operator is surjective with right inverse.

Sard-Smale: inverse function theorem. Now that we have a Fredholm problem, we can apply the results of [MS12, Appendix A: Fredholm Theory] for Banach spaces. In particular, we have the hypothesis of the [MS12, Theorem A.5.1 (Sard-Smale Theorem)] which relies on the infinite-dimensional inverse function theorem, [MS12, Theorem A.3.1 (Inverse Function Theorem)]. The result of Sard-Smale is that the set of regular J is dense in the set of all J , which is what we were aiming for. So we have existence of regular J .

□

Remark 4.4.8 (Notation). NB: the notation \dot{J} does not mean we can only vary J in one direction as is usually the case with the dot notation. We use the notation as a symbolic way to denote tangent vectors to the space of complex structures; it's denoted Y in [MS12].

Lemma 4.4.9. *The set of parametrized J -holomorphic discs $u : (\mathbb{D}, \partial\mathbb{D}) \rightarrow (Y, \bigcup_i L_i | \gamma_i)$ for $J \in J_{reg}^1(Y, \partial Y)$ is a finite-dimensional manifold.*

Proof from [MS12, Theorem 3.1.6 (i)]. Charts are given using

$$\begin{aligned} \mathcal{F}_u : W^{k,p}(S, \partial S; u^*TY, u^*TL) &\rightarrow W^{k-1,p}(S, \Lambda^{1,0} \otimes_j u^*TY) \\ \xi &\mapsto \bar{\partial}_J(\exp_u \xi) \end{aligned}$$

using the exponential map to obtain a diffeomorphism of an open set around 0 in $\mathcal{F}_u^{-1}(0)$ to a neighborhood of u in the space of parametrized J -holomorphic discs. Regularity of J

implies $d\mathcal{F}_u(0) = D_u$ is surjective. The implicit function theorem [MS12, Theorem A.3.3] implies these are smooth manifold charts after restricting to potentially smaller open sets. This does not depend on k, l because J -holomorphic maps u are smooth by elliptic regularity [MS12, Proposition 3.1.10]. Note that [MS12, Appendix B (Elliptic Regularity)] covers the necessary background with *totally real boundary conditions* e.g. the Lagrangian boundary condition case here. See also [Weh13, Lecture 4–6]. \square

Remark 4.4.10. Even for non-regular J , we can still use the above to construct a Fredholm problem by [MS12, Theorem C.1.10 (Riemann-Roch)], which is proven in the case of Lagrangian boundary condition. How we get the smooth structure will be a different matter though, because J is not regular. This is where abstract perturbations may be necessary.

Example 4.4.11 (Deligne-Mumford moduli space of domains). Recall that limits of holomorphic discs look like unions of discs and spheres, from Gromov compactness, [MS12, §5.5]. They are attached together in a manner that can be encoded by a tree with one vertex for each component and an edge when two components are attached to each other.

A tree encodes information for how to glue, where interior edges are assigned a gluing length, and semi-infinite edges at either end give the resulting marked points of the final glued disc. The idea is that we can have a family of discs, parametrized in the base by possible cyclic configurations. We also have a gluing parameter for each interior edge. More interior edges increases the codimension of the moduli space of that configuration in the moduli space of a disc. We can encode the possible degenerations in an associahedron, see [Sei08, §9].

Deligne-Mumford space $\mathcal{M}_{0,d+1}$ arises from considering degenerations of stable discs with the additional data of $d+1$ boundary marked points. This moduli space of curves is defined by considering maps to a point. A *stable curve* contains enough *marked points* to avoid automorphisms, and is a *stable map* to a point. See [MS12, §5, §6].

In this thesis, we will be concerned with stable maps to Y where the domain is a disc with one boundary marked point, and a disc union sphere with one boundary marked point on the disc and one interior marked point on the disc and sphere each where they meet. These are stable maps (in particular they have finite reparametrization action) but not stable domains.

Claim 4.4.12. Given a Fredholm section, we can compute the expected dimension of the manifold of parametrized curves, and then the moduli space of unparametrized curves will be three less from quotienting by $\text{Aut}(\mathbb{D})$. A spin structure on the Lagrangian determines an orientation on the moduli space of parametrized curves, so quotienting by $\text{Aut}(\mathbb{D})$ induces an orientation on the moduli space of unparametrized curves.

Remark 4.4.13 (Analogue of the Floer differential in Morse theory). With Morse-Smale data we know the dimension of the moduli space by counting eigenvalues. We require

transverse intersection of the unstable manifold of x_- with the stable manifold of x_+ . We have a projection map from the unstable to the perpendicular of the stable. On the other hand, the index of a Fredholm section is computed from the *spectral flow* of a loop of symmetric matrices, see [Wen16, §3.2].

Claim 4.4.14. Aut acts smoothly on the manifold of parametrized curves, hence the moduli space $\hat{\mathcal{M}}/\text{Aut}$ is a smooth manifold.

Claim 4.4.15. We can put a smooth structure on the compactified moduli space using gluing. The configurations we glue are precisely those in Gromov compactness. This allows us to obtain the structure of a smooth compact 0-dimensional manifold, which we can then count.

Sketch proof of Claim 4.4.15. This is covered in [MS12, §3.4, Proposition 6.2.8] and [Weh13]. Gromov compactness implies that the possible limit configurations of discs are: a disc bubble at a boundary point, a sphere bubble, strip-breaking, or in the case of boundary marked points a limit can also be a union of discs when two marked points collide. We will be able to exclude the first three behaviors with regular J for geometric reasons. For example, the intuition for why there are no sphere bubbles is as follows: the union of all points in a zero-dimensional family of spheres is two, and that of discs in a one-dimensional family is three, so generically these two don't intersect in a six dimensional manifold. Here by 'generic J ' we mean that transversality should hold for evaluation maps at marked points on discs and spheres.

Compactifying as topological space. We then consider any disc bubble, sphere bubble, or strip-breaking and show it is the limit of a sequence of J -holomorphic curves. This is done by first pregluing the maps by pasting them together, which may not give something J -holomorphic, and then Newton iterate it to a J -holomorphic map.

The upshot is that the boundary of the unparametrized moduli spaces (namely $\overline{\hat{\mathcal{M}}/\text{Aut}} \setminus \hat{\mathcal{M}}/\text{Aut}$) is a fiber product of moduli spaces which agree at their intersection point. E.g. we will have a component for moduli spaces of discs fiber product with moduli spaces of spheres over their common intersection point, to account for sphere bubbling.

Compactifying as smooth manifold: existence of regular J for limit configurations. So to finish the sketch that the moduli spaces are compact smooth 0-dimensional manifolds, we need to prove the existence of regular J for these additional fiber product configurations. As described above, we can exclude disc bubbling and strip-breaking by the geometry of Y . So we only need to consider sphere bubbling from spheres in the central fiber. The addition of a point where the disc and sphere attach at means we need a notion of additional data to account for these *special points*.

Definition 4.4.16 (Moduli space of stable discs with sphere bubbles). A *stable map* is given by a tree of pseudo-holomorphic maps, where each vertex α is a sphere bubble, except for the

original main disc one. The *stable* refers to the absence of continuous families of nontrivial automorphisms; in particular if we fix three points on every constant component there are no nontrivial automorphisms. The *virtual dimension* is given by the Maslov index minus twice the number of edges in the stable tree. That is, each bubbled off sphere reduces dimension by 2. Thus we expect to have a *pseudocycle*, i.e. the image of the boundary of the moduli space has codimension at least two in the total space. This can be achieved in the *semipositive* case, which means there are no J -holo spheres of negative Chern number for generic J – this is our setting because Y is Calabi-Yau. We define the resulting moduli space by taking a collection of maps, quotient by reparametrization, and then compactify.

Lemma 4.4.17 (Gromov compactness for stable maps, c.f. [MS12, Equation (5.1.5)]). *The compactification of the moduli space of unparametrized curves (i.e. equivalence classes) is a union over possible bubble trees of unparametrized curves.*

Sketch. The reason is that these are the possible limit configurations. Equation (5.1.5) of [MS12] equips the set with a topology and discusses compactness. \square

In particular, we'll need gluing and a discussion of the Fredholm problem for a disc and a sphere. We will then show that the moduli space of a somewhere injective disc union a simple sphere is a manifold of negative dimension, meaning it is empty and can be excluded.

Let Σ be the Riemann surface given by the disc with one fixed boundary point attached to a sphere at the origin. As above, we put a Banach manifold structure on $W^{k,p}(\Sigma, Y)$, via charts modeled off its tangent space, which we know is a Banach manifold. That is, we describe maps “close to” a given map u using the exponential map: given a point u and a tangent direction ξ at that point, we move u along the geodesic (i.e. path where the least action is required) in the tangent direction ξ for time 1 to obtain a new map $W^{k,p}$ map $\exp_u \xi$ that pushes u everywhere slightly in the direction of ξ .

We want to preserve the Lagrangian boundary condition so if ξ is tangent to L and $z \in \partial\mathbb{D}$ then we want $\exp_{u_{\mathbb{D}}} \xi$ to still have boundary on L . This is precisely the definition of *totally geodesic* L . The existence of a metric so that one Lagrangian is totally geodesic is proven by U. Frauenfelder in his diploma thesis, see [MS12, Lemma 4.3.4]. In general we at most have two Lagrangians at an intersection point, and existence of a metric so that both Lagrangians are totally geodesic is proven in [Mil65, Lemma 6.8], which also has a self-contained account in the lecture notes on the Whitney Trick [Fra10, Lemma 0.6, Lec 11], the proof of which is continued in [Fra10, Lec 12].

For the fiber of the Banach bundle, we don't need to worry about boundary conditions c.f. [Sei08, §(8h)].

Lemma 4.4.18 (Excluding bubbling in our setting). *There exists a dense set $\mathcal{J}_{reg}^2(Y, \partial Y; \mathbb{D} \cup \mathbb{P}^1)$ of J regular for the moduli space of a simple sphere union a somewhere injective disk, which is section-like hence must be simple.*

Corollary 4.4.19. *When the expected dimension of the moduli space of disks is zero, the moduli space of stable configurations consisting of a disc and one or more sphere bubbles for the regular J above has negative dimension, which is empty. In particular, the moduli space of any somewhere injective disk passing through the open set U union any configuration of multiply-covered and simple spheres can be excluded.*

Proof of Corollary 4.4.19. The Riemann-Roch theorem [MS12, Appendix] implies the dimension of the manifold cut out by the regular J is of negative dimension, specifically dimension -2 . Lazzarini's result [Laz11] implies any disc can be decomposed into simple discs and his other paper [Laz00] shows that any J -holomorphic disc contains a simple J -holomorphic disc. Thus if we had a nonempty configuration as in the statement of the corollary, we would have a non-constant map in the case of a simple disc union a simple sphere, by factoring through the multiple covers and taking one simple disc that goes through the sphere. But this is a contradiction, so there couldn't have been any such nonempty moduli spaces to begin with. \square

Proof of Lemma 4.4.18. We have dense sets of J regular for each component (the disc and the sphere); the disc was described earlier and the sphere situation is done in [MS12, Chapter 3]. This proof will involve checking that there is still a dense set of J in the intersection of these two dense sets which interact well at the point where the disc and sphere intersect.

Intersect the dense sets of regular J for the sphere and disc separately. Consider $\mathcal{U} \subset \bigcup_{J \in \mathcal{J}(Y, \partial Y)} \mathcal{M}(A_{\mathbb{D}}; J) \times \mathcal{M}(A_{\mathbb{P}^1}; J)$ where A denotes the respective homology classes and $u_{\mathbb{D}}(\mathbb{D}) \not\subseteq u_{\mathbb{P}^1}(\mathbb{P}^1)$ (in contrast with the case of just spheres where we require the images not be equal). Namely, \mathcal{U} is the subset of the products of moduli spaces of parametrized J -holomorphic maps where the disc isn't contained in the \mathbb{CP}^1 . We have the pointwise constraint that the sphere and disc are attached at a point. So we need transversality of the evaluation map $\mathcal{U} \rightarrow Y \times Y$. More specifically, the disc and sphere must intersect at a marked point which we place at 0 in the domain. We also fix a point on the boundary of the disc so there are no nontrivial automorphisms.

Using Sard-Smale we can deduce that \mathcal{U} is a manifold, with an additional check involving annihilators on the multiple components as follows. This is from [MS12, Chapter 6]. To show the evaluation map is transverse, it's enough to construct \dot{J} supported in small balls, one on each component. Each ball should not intersect the other component. Because of the construction of \mathcal{U} inside the product of the moduli spaces for each component, we can find such open sets.

This is possible because: 1) the Lagrangian boundary condition implies \dot{J} is zero near the boundary and so if it's only supported on a small ball in the interior it is of this form and 2) we can extend each \dot{J} by zero and then add them. In order to check transversality, we want the linearized map to be surjective. So we select two tangent vectors in the codomain

at $(0_{\mathbb{D}}, 0_{\mathbb{P}^1})$, and then construct two \dot{J} supported in two disjoint small balls, one on each component, to ensure surjectivity. This construction is described below, and will give us transversality.

We construct the \dot{J} . We follow [MS12, §3.4], then add the additional information from [MS12, §6] for transversality of the evaluation map. Note that the reference considers the case of a sphere, and the argument works for the case of a disc because we have less to test due to more geometric constraints. Suppose by contradiction that there are no \dot{J} for which the linearized operator (with the disc or the sphere) is surjective. So we can construct the following η that locally that lies in a fiber of the Banach bundle; we can find a non-zero L^q form η that annihilates $D_u\xi + \frac{1}{2}\dot{J}duj$ over all $W^{1,p}$ tangent vectors ξ which vanish on the point of intersection of the sphere and disc, and \dot{J} , in particular with $\dot{J} = 0$. So $D_u\xi = 0$ for all ξ . This will imply that η has $W_{loc}^{k,p}$ regularity; recall that the elliptic bootstrapping result of [MS12] is proven for Lagrangian boundary conditions.

Once we have regularity, we can integrate to get $D_u^*\eta = 0$. Via integration by parts we have $D^*\eta = 0$, because taking the adjoint means the boundary term is $d\langle\eta, J\xi\rangle_\omega$. Namely apply Stokes' theorem and the product rule, which is evaluation on the 1-form and inner product on the bundles, and use that the test vectors ξ are tangent to the Lagrangian at the boundary.

However this contradicts that $\eta \neq 0$, using somewhere injectivity to construct a suitable ξ that picks up a nonzero contribution around the point where $\eta \neq 0$, and is zero elsewhere. Then we use Carleman similarity principle to see that if η is zero on an open set it must be identically zero. This allows us to show that the annihilator of a certain space is zero, whence the Hahn-Banach theorem implies that the image of the linearized operator $D_u\xi + \frac{1}{2}\dot{J}duj$ by varying ξ, \dot{J} is dense. So combining that property with the image being closed from the Fredholm property of the operator, we find that the operator surjects onto $W^{k-1,p}$. This will allow us enough freedom to find the vectors \dot{J} .

We are still working on a single component, \mathbb{P}^1 or \mathbb{D} . This surjection tells us that we can find a ξ pointing in a specified direction at a specified point *and* tangent to moduli space. Moreover one can do this in a small neighborhood around a specified point. Hence we can add vectors that work on *different components* using bump functions to extend by zero.

The implicit function theorem puts the structure of a Banach submanifold on

$$\bigcup_{J \in \mathcal{J}(Y, \partial Y)} \mathcal{M}(A_{\mathbb{D}}; J) \times \mathcal{M}(A_{\mathbb{P}^1}; J)$$

at which point we use the evaluation map to ensure transversality. We want the preimage of the diagonal to be a submanifold, and in particular is the desired dense set of regular J of the lemma. Note that elliptic bootstrapping and the implicit function theorem in Appendices of [MS12] apply because they are proven for totally real boundary conditions, such as

Lagrangian boundary conditions. Note also: we have omitted discussion of the asymptotic behavior at strip-like ends in our sketch of the functional analysis setup; the function spaces we consider and their topology need to be appropriately modified in the strip-like ends to enforce the asymptotic conditions, see [Sei08].

Since the linearized evaluation map is surjective on vectors, by Sard-Smale the subset of the universal space where maps respect the pointwise constraint is a manifold and we have existence of a dense set of regular J for the disc and sphere so that the evaluation map at their intersection is transverse. This concludes the proof of Lemma 4.4.18. \square

Limit configurations form smooth manifold. Now that we have a regular J for the limit configuration, we prove that $\bar{\partial}_J$ cuts out $\hat{\mathcal{M}}_{\mathbb{D}}/Aut \times_0 \hat{\mathcal{M}}_{\mathbb{P}^1}/Aut$ transversally so it is a manifold (and our main application is that the manifold will have dimension < 0 so will be empty). To get a manifold structure, we again want a Fredholm section of a Banach bundle where the linearized operator is surjective with right inverse.

We have now excluded all types of bubbling behavior. So the moduli spaces $\hat{\mathcal{M}}/Aut$ are already compact manifolds, and the proof of Claim 4.4.15 is complete. We can now take their zero-dimensional part to use in the construction of the Fukaya category below. \square

Corollary 4.4.20. *The above is valid for a disc with any number of Lagrangians and punctures with strip-like ends, because of the existence of metrics for which two Lagrangians are totally geodesic, [Mil65, Lemma 6.8].*

4.5 $H^0(FS(Y, v_0))$: definition and independence of choices

Now we arrive at the definition of the Fukaya-Seidel category. Because of the linearity of Lagrangians considered, they have a lift that allows for Maslov grading given by their slope, and they have a Spin structure as well.

Definition 4.5.1. The *Fukaya-Seidel category* $FS(Y, v_0)$ is defined as follows, using the *categorical localization method*, instead of Hamiltonian perturbation methods (as in [Sei08]):

- Objects: the Lagrangians in $FS(Y, v_0)$, i.e. in the total space, are allowed to be non-compact. The Lagrangian L_i is obtained by taking ℓ_i over -1 in the base of v_0 and parallel-transporting it around the singular fiber over zero, along U-shapes as in Figure 4.4. We also define L_z to be the parallel transport over the same curve of the fiber Lagrangian t_z , defined by fixing ξ_1, ξ_2 corresponding to a point z and varying the angle coordinates.

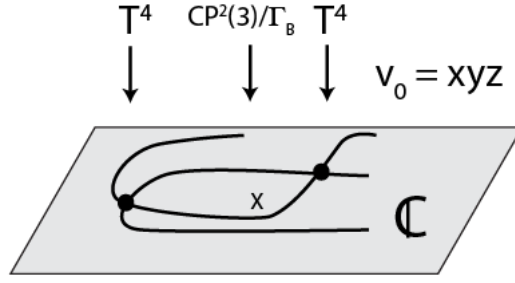


Figure 4.4: L_i = parallel transport ℓ_i around U-shaped curves in base of v_0

Specifically, outside of a compact set around the origin, the Lagrangians must project to rays in the plane, and they are fibered meaning the parallel transport of Lagrangians in the fiber. The directions of the rays over which the Lagrangians project need to stay within an angular sector, e.g. the right half-plane, for morphisms to be well-defined.

- Morphisms: we first define a directed category

$$\text{hom}(K, L) = \begin{cases} CF(K, L), & \text{if } K > L \\ \mathbb{C} \cdot e_L, & \text{if } K = L \\ 0, & \text{else} \end{cases} \quad (4.10)$$

where the ordering $>$ denotes that, outside a compact set, all the rays of K lie above all the rays of L .

- Quasi-units: If $K = L$, then we push the rays of one copy to lie above the rays of the other copy as in Figure 4.4, which we denote by L^ϵ . The quasi-unit $e_L \in CF(L^\epsilon, L)$ is the count of discs with those Lagrangians as boundary conditions. We then localize at these e_L , in other words we set them to be isomorphisms. Recall that formally inverting morphisms involves taking equivalence classes of roofs

$$K \leftarrow K^\epsilon \rightarrow L$$

which is the definition of an arrow $K \rightarrow L$ when $K < L$, namely push up to $K^\epsilon > L$ so that the first arrow of the roof is the quasi-unit e_K , and then $K^\epsilon \rightarrow L$ is defined as above.

- The differential (μ^1), composition (μ^2), and higher order μ^k count bigons, triangles, and $(k+1)$ -gons respectively, with the usual Lagrangian boundary conditions from these L_i , and are J -holomorphic for some regular J , which exists by the above. These moduli spaces can be counted by the theory of the previous section.
- We will also consider in the course of our calculations a Lagrangian obtained by parallel transport of t_z around a circle in the base; however this Lagrangian bounds holomorphic discs and does not define an object of $FS(Y, v_0)$.

Remark 4.5.2. For each Lagrangian in the fiber, there are many different objects of FS obtained by parallel transport along U-shapes that go to infinity in slightly different directions, but these will be isomorphic to each other after localizing.

Lemma 4.5.3. *For Lagrangians in correct position, morphisms and compositions in the localized Fukaya-Seidel category coincide with those in the directed category. Namely, if $K > L$, then $\text{hom}_{FS}(K, L) \simeq CF^*(K, L)$, and if $L_0 > \dots > L_k$, then μ^k in $FS(Y, v_0)$ is the same as in the directed category. Namely it is given by counting J -holomorphic discs.*

Proof references. This is unpublished work of Abouzaid-Seidel, Ganatra’s notes [Gan16b], and Abouzaid-Auroux. \square

Lemma 4.5.4. *The composition of roofs is a roof.*

Proof. This is a consequence of the naturality of quasi-units with respect to continuation maps, see Abouzaid-Seidel and Abouzaid-Auroux. \square

Definition 4.5.5. The *Donaldson-Fukaya category* is obtained by passing to cohomology on the morphism chain complexes.

Lemma 4.5.6. *Let J_1 and J_2 be two regular almost complex structures. Then they define quasi-equivalent Fukaya A_∞ -categories, i.e. isomorphic Donaldson-Fukaya categories.*

Proof outline of lemma. We need to show that the Donaldson-Fukaya categories have isomorphic object and morphism spaces. We also need to show that there exists a functor between them, namely that it respects composition. The Lagrangians depend only on the symplectic form, so remain unchanged upon changing the almost complex structure. Likewise for the Floer complexes, which are generated by their intersection points. Note that Seidel in [Sei08, §(10c)] discusses upgrading this equivalence to the A_∞ -category, in particular for the product or composition map. See [Sei08, §8, §(10c)].

To show the morphism groups are isomorphic, we show that the differential ∂ is the same for each J_1 and J_2 . This will follow from the use of a continuation map. (In general this argument only shows that the Floer complexes with the Floer differentials for J_1 and J_2 are quasi-isomorphic, hence have isomorphic cohomology.) This is the moduli space from solutions of a single PDE that is the usual Cauchy-Riemann equation however instead of J we use J_t where J_t at time 0 is J_1 and J_t at time 1 is J_2 . This defines what the functor does on morphisms. In particular, this will require the existence of a path of regular J in the space of all almost complex structures.

That existence follows from a Sard-Smale argument, as in [MS12, Theorem 3.1.8] in their second edition book. The difference is that our Riemann surface has boundary (a disk with a k punctures on the boundary corresponding to the moduli space in defining the structure map μ^{k-1}). So the base and fiber of the Banach bundle will be the same as in [MS12, pg 55] however the spaces of almost complex structures will restrict to ones that are identically J_0 outside of the open set U around the origin and moduli spaces will consist of maps on disks instead of spheres. The Sard-Smale theorem and elliptic regularity proven in the Appendices of [MS12] already incorporate Lagrangian boundary conditions (called “totally real” there,

which is slightly more general.) We will walk through an example of the existence of regular J for a certain configuration of homology classes later on, and that will serve as the model for constructing a Fredholm problem more generally as needed here and in other cases. \square

Remark 4.5.7 (Other references and theory on invariance). For proving general invariance, the classical approach of FOOO and Floer is to construct a homotopy. See [FOOO09a, p 244] for a discussion of J -invariance; the algebraic background on algebraic homotopy invariance is in section 4.2 and the main theorem is in section 4.6. In between these two they setup the geometrical fundamental chain as an application of the algebraic theory in section 4.2. The theorem is applied to the Fukaya category setting in Corollary 4.6.3 of the book [FOOO09a] or Theorem 15.19 of their 2000 preprint.

Seidel upgrades this system to the A_∞ -setting by packaging all the Fukaya categories for varying choices of J indexed by i into a “total” Fukaya category, and showing that each $\mathcal{F}(Y)^i$ fully faithfully embeds into the total while inducing an isomorphism on cohomology using Salamon-Zehnder’s work [SZ92] and [Sal99] for an actual category. Thus all $\mathcal{F}(Y)^i$ are quasi-isomorphic to the same category, hence to each other.

Corollary 4.5.8. *This category is independent of regular choices of datum so is well-defined. In particular different values of sufficiently small T , so when defining the complex structure we have a proper holomorphic group action of Γ_B that we can quotient by, give quasi-isomorphic Fukaya categories.*

Proof. Invariance under regular J is given above. Invariance under Hamiltonian perturbations in the fiber will be discussed below in the computation section. This completes the proof that we have a well-defined Fukaya category. \square

Chapter 5

The main theorem

5.1 HMS computation

In this chapter we prove that the right vertical arrow of Theorem 1.1.1 is a fully faithful embedding, namely that the arrow is indeed a functor and that the morphism groups between objects and images of those objects are isomorphic.

Remark 5.1.1 (Terminology). We will be concerned with the *Donaldson-Fukaya category* in this thesis, namely passing to H^0 on the morphism cochain complexes. In particular we will need to compute the differential. The full A_∞ -categorical equivalence is a future direction. In physics the functor $(Y, v_0) \mapsto H^0(FS(Y, v_0))$ may be referred to as a *topological quantum field theory* or TQFT. That is, the first part of a TQFT is a functor from certain manifolds to vector spaces. For more background, see Segal's lecture notes [Seg].

Remark 5.1.2 (Outline of proof). To prove a fully faithful HMS embedding on the cohomological level, we need to show morphism groups are isomorphic i.e. $HF^*(L_i, L_j) \cong \text{Ext}^*(\mathcal{L}^i|_H, \mathcal{L}^j|_H)$ for all i, j . Note we already proved it was a functor, i.e. respects composition, in Section 3.3.

- (1) Calculations on the complex side involve theta functions.
- (2) Morphisms on the symplectic side arise from a differential on $CF(L_i, L_j) = CF(\ell_{i+1}, \ell_j)[-1] \oplus CF(\ell_i, \ell_j)$, given the shape of the Lagrangians in Figure 4.4. In Lemma 5.1.5 we use the product rule, one of the A_∞ -relations, to reduce this to something we can calculate.
- (3) Computing the differential is 2-fold: first we use cobordism arguments that allow us to vary the Lagrangian and almost complex structure from a regular J_1 to the non-regular J_0 . Because of non-regularity, there is a jump in dimension on the moduli spaces from one to two at the non-regular J . So the cobordism considers the subset of the two-dimensional space that is a limit of the moduli spaces for regular J .

- (4) Then we cite [KL19] which computes the count of moduli spaces with the new Lagrangian and J_0 . They utilize a result of [Cha11] that the open Gromov-Witten invariants involved have isomorphic Kuranishi structures (see [MTFJ19, Gromov-Witten Theory via Kuranishi Structures] for a discussion of Kuranishi structures) as certain closed Gromov-Witten invariants. Hence [KL19] can use the algebraic theory for computing closed Gromov-Witten invariants. Note: here we use a particular choice of Kähler parameters in the generating series because we've fixed the symplectic form.
- (5) We've only defined the Fukaya category for regular J thus far. In this thesis, we can avoid Fukaya categories with non-regular J because of certain symmetries described below. In general, we may not be able to do this. So another method of proof could be to define it for non-regular choices, that agrees with the previous definition on regular choices, and show the moduli space count there equals that of [KL19], so that we can justify the computation. The definition should again include a cobordism statement on moduli spaces between two different J , so that the corresponding Fukaya categories are quasi-isomorphic. In particular the cohomological categories will be isomorphic, and we could again use the calculation in [KL19]. See Section 5.1.3 for a discussion of this.

Claim 5.1.3. J_0 is not a regular almost complex structure for disc + sphere configurations.

Proof. The standard J_0 is multiplication by i in the toric coordinates. Recall that $H_2(v_0^{-1}(0)) \neq 0$ and v_0 is holomorphic with respect to J_0 , so submanifolds representing classes in H^2 of the central fiber are holomorphic. Then nonzero Dolbeault cohomology implies the spheres are not regular; this follows by the Riemann-Roch theorem and the fact that the cokernel of the $\bar{\partial}_{J_0}$ operator is Dolbeault cohomology. Since the cokernel is nonzero we find that D_u is not surjective for maps u arising from these holomorphic spheres. \square

Figure 5.1 will be used to compute the differential, so we explain the geometry and notation of the picture first.

Remark 5.1.4 (Notation). Capital M^k denotes structure maps on the total space of Y and lowercase μ^k denotes structure maps on the torus fiber, in particular $\partial := \mu^1$. As illustrated in Figure 5.1, $\text{hom}_Y(L_i, L_j)$ decomposes into two hom groups on the fiber, $\text{hom}_{\text{right}}(\ell_{i+1}, \ell_j)[-1] \oplus \text{hom}_{\text{left}}(\ell_i, \ell_j) = CF(\ell_{i+1}, \ell_j)[-1] \oplus CF(\ell_i, \ell_j)$. In particular, M^1 will map from $\text{hom}_{\text{right}}$ to hom_{left} in the Floer differential.

Lemma 5.1.5. $M^1 : CF(\ell_{i+1}, \ell_j) \rightarrow CF(\ell_i, \ell_j)$ can be computed from the data of $M^1 : CF(\ell_{i+1}, t_z) \rightarrow CF(\ell_i, t_z)$ over all z .

Proof. First note that although M^1 is an automorphism of $CF(L_i, L_j) = CF(\ell_{i+1}, \ell_j)[-1] \oplus CF(\ell_i, \ell_j)$, for degree reasons and geometric considerations the only nonzero contribution is from the the first summand to the second summand.

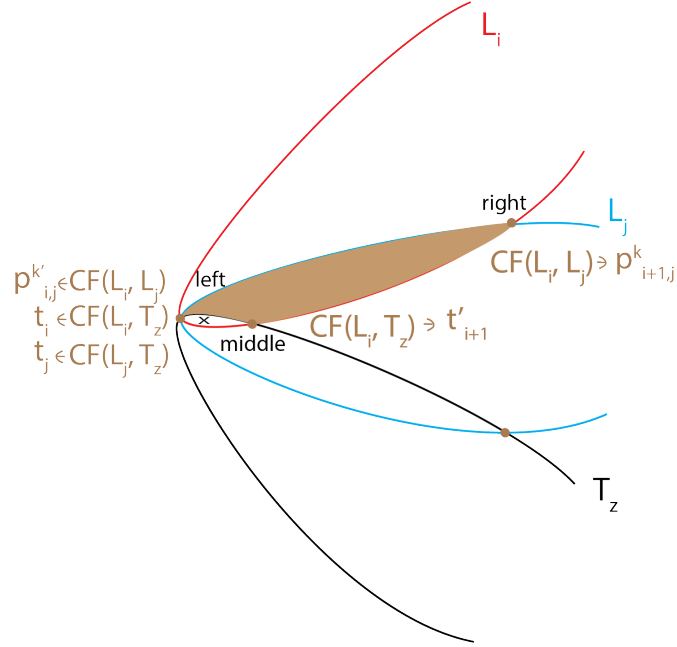


Figure 5.1: Leibniz rule

$$\begin{array}{ccc}
 \mathrm{hom}_Y(L_j, T_z) \otimes \mathrm{hom}_Y(L_i, L_j) & \xrightarrow{M^2} & \mathrm{hom}_Y(L_i, T_z) \\
 \downarrow M^1 \otimes \mathbf{1} + \mathbf{1} \otimes M^1 & & \downarrow M^1 \\
 \mathrm{hom}_Y(L_j, T_z) \otimes \mathrm{hom}_Y(L_i, L_j) & \xrightarrow{M^2} & \mathrm{hom}_Y(L_i, T_z)
 \end{array} \tag{5.1}$$

Figure 5.2: Diagram illustrating Leibniz rule

Let t_j denote the intersection point of ℓ_j and t_z , and let $p^k_{i,j}$ denote the k th intersection point of $\ell_i \cap \ell_j$, where $0 \leq k < (i-j)^2$ as described in the definition of the Fukaya-Seidel category above. We will use the diagram in Diagram 5.1 below. The crux of this argument relies on the Leibniz rule, which is one of the associativity relations in an A_∞ -category. The homs in this diagram are in the total space Y . We can reduce some calculations to the fiber, because each hom on the total space is a direct sum of Floer groups over two fibers, namely over the points of intersection of the curves given by their projection to the base. For the geometric reasoning behind the diagram, see Figure 5.1.

We can simplify this diagram to involving homs only in the fiber, as done in Diagram 5.2 below. The domains for M^1 and M^2 have more terms, but below we only list the ones giving

$$\begin{array}{ccc}
\text{hom}_{\text{left}}(\ell_j, t_z) \otimes \text{hom}_{\text{right}}(\ell_{i+1}, \ell_j) \ni t_j \otimes p_{i+1,j}^k & \xrightarrow{M^2} & \text{hom}_{\text{middle}}(\ell_{i+1}, t_z) \\
\downarrow M^1 \otimes \mathbf{1} + \mathbf{1} \otimes M^1 & & \downarrow M^1 \\
\text{hom}(L_j, T_z) \otimes \text{hom}(L_i, L_j) & \xrightarrow{M^2} & \text{hom}_{\text{left}}(\ell_i, t_z)
\end{array} \tag{5.2}$$

Figure 5.3: Simplified diagram on fibers

the nonzero contributions. The rest are zero because there are no bigons on two Lagrangians in the fiber, hence the only bigons must be over one in the base. Also t_z is invariant under the monodromy hence we don't need to include monodromy of how the fiber Lagrangian changes in these maps.

Subscripts in the simplified diagram indicate which fiber the homs are referring to from the three intersection points of Figure 5.1, which we refer to as left, middle, and right respectively, going from left to right.

Differentiating the product M^2 , the Leibniz rule implies

$$M^1(M^2(t_j, p_{i+1,j}^k)) = M^2(M^1(t_j), p_{i+1,j}^k) + M^2(t_j, M^1(p_{i+1,j}^k)) = M^2(t_j, M^1(p_{i+1,j}^k)) \tag{5.3}$$

because $M^1(t_j) = 0$, since t_j is of degree 0 and there is nothing in degree 1 at the other intersection points of the two Lagrangians; note that t_i is of degree -1 .

- RHS of Equation (5.3): $M^1(p_{i+1,j}^k) := \sum_{k'} T^{\text{area}_{ijkk'}} \alpha_{k'}^{ijk} p_{i,j}^{k'}$ for suitable coefficients $\alpha_{k'}^{ijk}$. This is the differential we want.
- Then: $M^2(t_j, M^1(p_{i+1,j}^k)) = \sum_{k'} \alpha_{k'}^{ijk} M^2(t_j, p_{i,j}^{k'})$ which is in the fiber for degree reasons and equals $\left(\sum_{k'} T^{\text{area}_{ijkk'}} \alpha_{k'}^{ijk} \cdot T^{\omega(\Delta(t_i, p_{i,j}^{k'}, t_j))} n_{k'}^{ij} \right) t_i$ where $n_{k'}^{ij}$ is the count of triangles with vertices at $t_i, p_{i,j}^{k'}$, and t_j . Since it's in the fiber, we can compute $n_{k'}^{ij}$ directly as in Section 3.3.
- LHS of Equation (5.3): $M^2(t_j, p_{i+1,j}^k) = T^{\omega(\Delta(t_{i+1}, p_{i+1,j}^k, t_j))} n_k^{i+1,j} \cdot t'_{i+1} =: D_k^{i+1,j}(z) \cdot t'_{i+1}$ because the fibration is trivializable in the beige region of Figure 5.1.
- Then: $M^1(t'_{i+1}) := C(z)s(z) \cdot t_i$ will be computed by a homotopy argument where $C(z)$ is an infinite series and $s(z)$ is our original theta function in terms of the Novikov parameter T .
- Thus Equation (5.3) becomes

$$C(z)s(z) \cdot D_k^{i+1,j}(z) \cdot t_i = M^2(M^1(p_{i+1,j}^k), t_j) = \left(\sum_{k'} T^{\text{area}_{ijkk'}} \alpha_{k'}^{ijk} D_{k'}^{i+1,j}(z) \right) \cdot t_i$$

which expresses $T^{area_{ijkk'}} \alpha_{k'}^{ijk}$ in terms of $C(z)s(z)$.

To summarize, as seen in Section 3.3 the generators $p_{i,j}^{k'}$ of $CF(\ell_i, \ell_j)$ correspond under homological mirror symmetry for V to a basis of sections $s_{i,j}^{k'} \in \text{hom}_V(\mathcal{L}^i, \mathcal{L}^j)$. Still using HMS for V , the coefficient $D_{i+1,j}^k$ in the expression $D_k^{i+1,j} \cdot t'_{i+1}$ corresponds to the value of $s_{i+1,j}^k$ at the point $z \in V$ in some trivialization of \mathcal{L}^{j-i-1} at z (by considering homs with a skyscraper sheaf). Thus, the expression $C(z)D_k^{i+1,j}(z)$ in the above equation can be written as a linear combination whose coefficients $\alpha_{k'}^{ijk}$ express $M^1(p_{i+1,j}^k)$ in the basis of $\text{hom}_{left}(\ell_i, \ell_j)$ given by the $p_{i,j}^{k'}$.

The reason we would like to use t_z and not some ℓ_j is because this will allow us to count discs with boundary in the preimage of a moment map, as in [CO06]. The Lagrangian T_z obtained by parallel-transporting t_z around U-shaped curves corresponds to evaluation sections at the point z on the mirror side. So what the calculation above says is that once we know the morphisms groups for all t_z , we know homs between any ℓ_i and ℓ_j .

The z subscript in t_z indicates the fiber Lagrangian $\{(\xi_1, \xi_2, \theta_1, \theta_2)\}_{0 \leq \theta_1, \theta_2 < 2\pi}$ where ξ_1 and ξ_2 are fixed (we're on a fiber so η is fixed too) hence $|x|, |y|, |z|$ is a fixed value. So t_z depends only on the norms of the toric coordinates.

□

Now we describe the homotopy argument that allows us to find $C(z)$ in $M^1(t'_{i+1}) = C(z)t_i$. This will use theory developed in [Sei08, §17g] for counting pseudo-holomorphic polygon sections which pass through singular fibers. See Figure 5.4 for a pictorial depiction of the homotopy and Figure 5.5 for an outline of the analytic and algebraic steps involved.

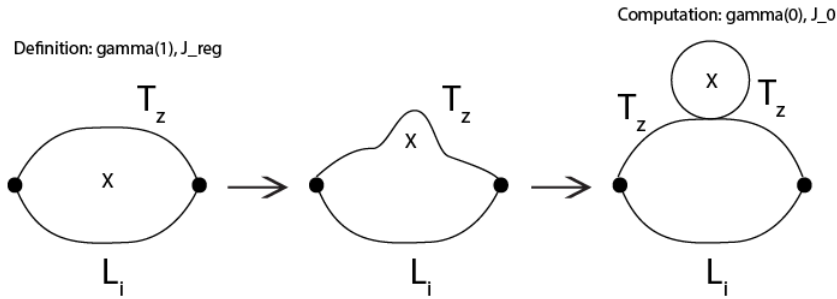


Figure 5.4: The homotopy between ∂ (left) and the count of discs we compute (right)

Remark 5.1.6. This section uses theory developed in [Sei08, §17g] for counting pseudo-holomorphic polygon sections which pass through singular fibers and $\mathbb{Z}/2$ coefficients. In that section, d from Seidel is M^1 here, and \tilde{d} is $M^2(c, -)$. Also L_1 and L_2 from Seidel

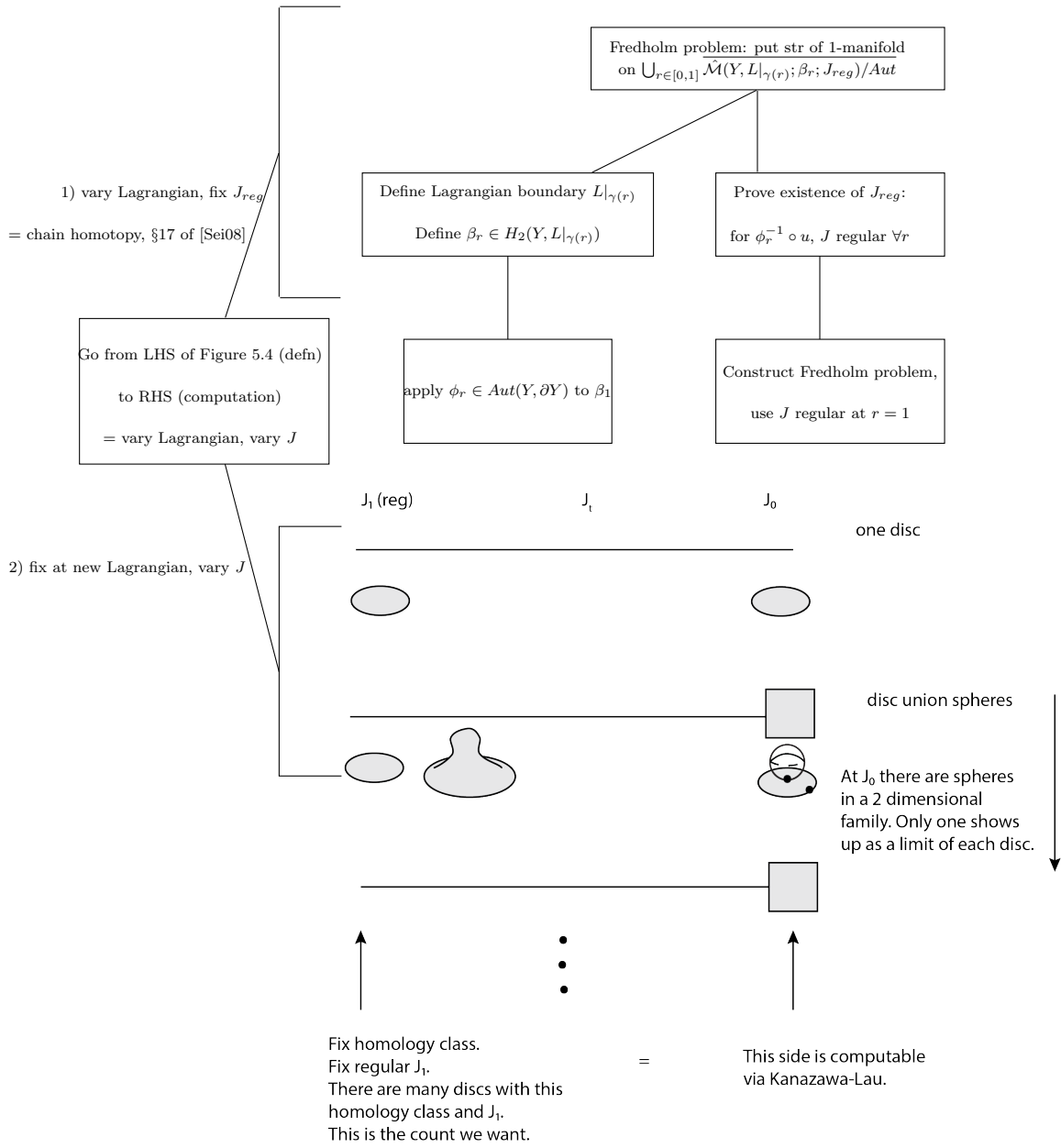


Figure 5.5: Plan for computation

are t_z in this setting and his Q is ℓ_i here. This follows from L_2 being isotopic to $\phi(L_1)$. The symplectic manifold M is the fiber, so that is generically V^\vee in our setting, and the Lefschetz fibration $E \rightarrow S$ considered in Seidel is instead the fibration (with non-Lefschetz singularities) $v_0 : Y \rightarrow \mathbb{C}$ here (in particular our base is fixed). In this setting, the analogue of the vanishing cycle that one Dehn twists from Seidel is three families of T^2 's degenerating to S^1 's which intersect at a point.

Lemma 5.1.7. $M^1 : CF(L_i, T_z) \rightarrow CF(L_i, T_z)$ is homotopic to $M^2(c, -)$, where c is a count of discs times a suitable intersection point p , via a chain homotopy $\xi : CF(\ell_i, t_z) \rightarrow CF(\ell_i, t_z)$ such that:

$$\mu^1 \xi + \xi \mu^1 + M^1 + M^2(c, -) = 0$$

Remark 5.1.8 (Notation). The notation $M^2(c, -)$ suggests a composition in a Fukaya category, involving an element c in $CF(t_z, t_z)$. With a careful setup, c would be a scalar multiple of the identity endomorphism of t_z . Though we are considering a subcategory of the Fukaya category that does not include $T_z|_{\text{circle}}$ as an object, we will adopt the notation $M^2(c, -)$.

In particular, $M^2(c, -)$ will count a configuration of two curves glued together. One curve is a J -holomorphic disc with boundary on $L_i \cup T_z|_{\gamma(0)}$, where $\gamma(0)$ is an arc with two strip-like ends converging to input and output intersections of L_i and $T_z|_{\gamma(0)}$. The other curve is a J -holomorphic disc with boundary on the Lagrangian torus obtained by parallel transport of t_z over a circle centered at the origin. These two components are both section-like with respect to the fibration $v_0 : Y \rightarrow \mathbb{C}$, and we require that, at the point of the base where $\gamma(0)$ and the circle intersect, they evaluate to the same point of t_z . This is depicted in the configuration on the right in Figure 5.4.

The section-like discs with boundary on the parallel transport of t_z over a circle centered at the origin have Maslov index 2, and so we expect that there are a finite number of such discs in any given relative homology class passing through a given fixed point of t_z at the contact point with $T_z|_{\gamma(0)}$. Then c is a weighted count of these discs, times a point which would be the identity element of $CF(t_z, t_z)$ in a set-up of the complete Fukaya category. Deforming the almost-complex structure to a product over the region of the complex plane over which the first components of the configurations described above are sections, the J -holomorphic sections become constant in the fiber and the count of sections with boundary on $L_i \cup T_z|_{\gamma(0)}$ induces the identity map from $CF(\ell_i, t_z)$ to itself. The point of t_z at which these constant sections pass through the point of contact then determines an incidence condition for the disc components, and the outcome is that the count of two-component configurations acts on $CF(\ell_i, t_z)$ by multiplication by the weighted count of Maslov index 2 discs.

Proof of Lemma 5.1.7. First we note that

$$M^1 : CF(\ell_i, t_z) \rightarrow CF(\phi(\ell_i), t_z) \xrightarrow{CF(\phi^{-1})} CF(\ell_i, \phi^{-1}(t_z)) = CF(\ell_i, t_z) \cong \mathbb{C}$$

where ϕ is the monodromy. We've used that applying the diffeomorphism ϕ^{-1} gives a bijection between intersection points, and $t_z = \{(\xi_1, \xi_2, \theta_1, \theta_2)\}_{\theta_1, \theta_2 \in [0, 2\pi]}$ is invariant under parallel transport because it only rotates angles. So we get $CF(\ell_i, t_z)$, which has only one intersection point.

There is existing theory for computing open Gromov-Witten invariants of J_0 -holomorphic discs with boundary on a moment map fiber, one marked point, and passing through the singular fiber of Y once (as is the case here because they are 1-1 in general and v_0 -sections with J_0). However, M^1 as is counts bigons through the singular fiber with boundary on T_z and L_i over a bigon, instead of T_z over a circle. So following [Sei08, §17g] we deform M^1 to $M^2(c \cdot p, \cdot)$ where c counts J_0 -holomorphic discs with boundary on $T_z|_{\text{circle}}$ and marked point p . This deformation constructs the homotopy ξ , which we now define. See Figure 5.4.

The geometry of moduli spaces. We have a composition of maps on one side of the homotopy, namely $M^2(c \cdot p, -)$. As discussed in Remark 5.1.8, we will need to discuss gluing in this particular setting. This is another place where our setting differs from that of Seidel. In the book, he deforms the fibrations. However in this setting, the fibration stays the same, while the Lagrangian boundary conditions are deformed via an automorphism of Y relative to the boundary. So we will need a gluing argument to deduce the following claim.

Claim 5.1.9. There exists a regular $J_{reg} \in \mathcal{J}(Y, \partial Y)$ such that

$$\bigcup_{r \in [0, 1]} \overline{\hat{\mathcal{M}}(Y, L|_{\gamma(r)}; \beta_r; J_{reg}) / Aut}$$

is a topological 1-manifold.

Outline of proof. We use background from [Weh14, Lecture 9], [Weh13, Lecture 14], and [MS12, §10.9]. We first put a smooth structure on $\bigcup_{r \in (0, 1]} \hat{\mathcal{M}}(Y, L|_{\gamma(r)}; \beta_r; J_{reg}) / Aut$, without the component at zero. To prove the existence of such a structure, we construct a Fredholm problem with a particular gluing profile. Different gluing profiles may give different smooth structures. Let γ_r denote the varying path in the base of the fibration indicated in Figure 5.4. Let $\{\phi_r\}_{r \in (0, 1]}$ be an isotopy of diffeomorphisms

$$\phi_r : (Y, L_i \cup T_z|_{\gamma_1}) \xrightarrow{\cong} (Y, L_i \cup T_z|_{\gamma_r})$$

which induces an isomorphism ϕ_{r*} on the corresponding relative second homology groups. There exists a J regular for the set-up at $r = 1$ by a Sard-Smale argument similar to the one in the definition of the Fukaya category above. This J then allows us to define a Banach bundle that will be the base of the bundle which $\bar{\partial}_J$ will be a section of:

$$\tilde{\mathcal{B}}^{k,p} := \{(\phi_r^{-1} \circ u, r) \mid u : \mathbb{R} \times [0, 1] \rightarrow (Y, L_i \cup T_z|_{\gamma_r}) \in W^{k,p}\}$$

Alternatively we can classify the tangent space to a path in \tilde{B} as one where the derivative of the path at the boundary is a vector that is a sum of a vector in the tangent space to the Lagrangian boundary and a vector corresponding to the flow of the isotopy ϕ_r . This will give us a 1-manifold structure on the set of maps u so that $\bar{\partial}_J(\phi_r^{-1} \circ u) = 0$, where J is the regular J defined above.

The next step will be to Gromov compactify at the $r = 0$ end. Note that ϕ_r does not have a limit at $r = 0$, as it becomes very degenerate and is not a diffeomorphism. So instead we consider elements as u in this moduli space instead of $\phi_r^{-1} \circ u$. Then we can modify the gluing argument to glue together two homology classes at $r = 0$ to view the glued curve as a limit of $r > 0$ curves. Conversely by Gromov compactness arguments we can reparametrize to deduce that the limit of $r > 0$ maps will be the triangle glued to the disc as shown in Figure 5.4. More concretely, see below.

Gluing domains and maps. In order to preglue: trivialize the normal bundle in a neighborhood of where we want to glue, and then interpolate linearly between the two maps. See [Weh14, lec 3, 1 hr]. Note that we take the gluing parameter to be $e^{-\ell}$ which goes to zero as the gluing length ℓ goes to infinity, which is the configuration of two discs.

We preglue the domains as follows. We remove a neighborhood of the puncture first. In the (s, t) coordinates on strip-like ends, we glue $(s - \ell, t)$ to (s, t) . That is, we place an amount ℓ in the \mathbb{R} direction on one strip overlapping onto the other strip. The two parts separately give the $r = 0$ case and the two parts glued together is the $r = \epsilon > 0$ case. The embedding that gives the strip-like end embedding is as follows: 1) map $(-\infty, 0] \times [0, 1] \rightarrow (-\infty, 0] \times [0, \pi]$ by $\cdot \pi$. Then map to the lower half of an annulus by e^{-z} , and then lastly to the right half of a disc with a puncture at 1 by $\frac{z+i}{z-i}$. The reason why the preglued map is close to the J -holomorphic glued map is because by continuity $\bar{\partial}_J$ of the glued map is still small; if it were constant on the glued part then it would actually be holomorphic. Since we interpolate slowly, it is indeed close to constant.

Next we apply Newton iteration to the preglued disc to obtain a J -holomorphic curve. The process of gluing is as follows: take the exponential at the preglued map of the pullback of the tangent bundle. The tangent vectors ξ are obtained by Newton iteration (a contraction mapping principle argument), which is applicable on Banach spaces.

The geometry of our setup implies that the moduli spaces of J -holomorphic discs do not limit to disc bubbling, strip breaking, or sphere bubbling for each $0 < r \leq 1$. At $r = 0$, we do have a disc bubble that forms, and we know this happens by Gromov compactness. That is, we compactify to obtain fiber products on the boundary as the zero set of a Fredholm section. Note that we can find a J which is regular at the $r = 0$ configuration as well, following a similar argument as in other cases. We consider the usual $\bar{\partial}$ operator on each disk

component, as well as the difference of the two evaluation maps where they should meet. This also has a Fredholm setup, c.f. [Weh14, Lecture 3, 22 mins].

After this, we then consider gluing maps to the base of $v_0 : Y \rightarrow \mathbb{C}$, versus just the domains as we did above. In other words, we define a new glued map $u^0 \#^R u^\infty$ on this glued domain. Finally we use the moment map coordinates $(\xi_1, \xi_2, \eta, \theta_1, \theta_2, \theta_3)$ to glue maps u to the total space. We know how to interpolate in the base $v_0(z)$ coordinate using $(1 - \rho)u^0 + \rho u^\infty - i$, thus we may apply this same linear interpolation in the ξ and θ coordinates.

This choice of interpolation for the pregluing ensures that, when pregluing a disc and a strip with boundary on $T_z|_{\gamma(0)}$, the resulting preglued map has boundary on $T_z|_{\gamma(r)}$. For in the fiber direction, the values of (ξ_1, ξ_2) on the two components agree along the boundary and the interpolation preserves them. In the base direction, we can choose the family of paths $\gamma(r)$ to be the family of paths obtained from $\gamma(0)$ and the circle centered at the origin by our interpolation procedure.

Thus we have the structure of a compact topological 1-manifold which provides a cobordism between the $r = 0$ and $r = 1$ choices. □

This completes the proof that the homotopy between M^1 and $M^2(c, -)$ is well-defined as the boundary of a 1-dimensional moduli space. □

Claim 5.1.10. The map $d := M^1$ with ℓ_i is chain homotopic to a map \tilde{d} defined with a Lagrangian that is Hamiltonian isotopic to ℓ_i , denoted $\phi_H(\ell_i)$.

$$\begin{aligned} d : CF(\ell_i, t_z) &\rightarrow CF(\ell_i, t_z) \cong CF(\ell_{i-1}, t_z) \\ \tilde{d} : CF(\phi_H(\ell_i), t_z) &\rightarrow CF(\phi_H(\ell_i), t_z) \end{aligned}$$

Remark 5.1.11. The statement that M^1 doesn't depend on choices of conformal structure of \mathbb{D} , the choice of strip-like ends, and regular J was discussed above in the discussion of well-definedness of the Fukaya category. Note that in [Sei08, §17] this is constructed in the chain homotopy called δ .

Proof of claim. We define a continuation map $a : CF(\ell_i, t_z) \rightarrow CF(\phi_H(\ell_i), t_z)$, so that \tilde{d} and $d \circ a$ have the same domain. Next we construct a homotopy α between d and $\tilde{d} \circ a$. This is done by taking a 1-parameter family of fibrations that interpolate between the two choices. Showing the resulting moduli spaces is a topological 1-manifold is analogous to the explanation for interpolating between M^1 and $M^2(c, -)$. □

5.1.1 Computation of discs

In this section we take $J = J_0$ and consider moduli spaces of discs only, for which J_0 is regular. In other words, we only consider homology classes β that arise from disks. Note that since the set of J regular for all configurations (discs and discs union spheres) is nonempty and dense, and the maps are J_0 sections away from a neighborhood of zero we can claim that J_0 is a limit of such J by the denseness of the regular J . I.e. we have a path of J 's limiting to J_0 , so these J 's perturb J_0 near the zero fiber. See the sphere picture in 5.5 for a pictorial depiction of this.

Remark 5.1.12. If we include t_z parallel transported in a circle around the base of $v_0 : Y \rightarrow \mathbb{C}$ as a Lagrangian in the subcategory we are considering, then this Lagrangian bounds nonconstant holomorphic discs. A future direction is to incorporate and define M^0 for the category containing this Lagrangian. Note that M^0 is a degree 2 operation, and the Lagrangian is only $\mathbb{Z}/2$ -graded. In this thesis, we do not include it in the subcategory being considered. We do still want to count the discs and J_0 -spheres, but they will show up only in the c in $M^2(c, -)$ considered as a map on Floer groups.

The following is based on [Aur07] and [CO06].

Definition 5.1.13 (Maslov class of a Lagrangian). Suppose $2c_1(M) = 0$, so the square of the anticanonical bundle is trivializable by some section s . We have a map from LGr to the unit bundle of K^{-2} by taking \det^2 of a basis for each Lagrangian. We can identify that unit bundle with S^1 using the trivializing section s mentioned above. The upshot is that we get a map from $LGr \rightarrow S^1$. The “Maslov class” is the pullback of $[S^1]$, i.e. a homology class in LGr . That is, $\mu(\beta)$ measures the obstruction to extending the square of this normalized section on L to one on a disc representing 2-homology class β .

Lemma 5.1.14 ([Aur07, §3.1]). *Let (X, ω, J) be a smooth, compact and Kähler manifold. Let $\Omega \in \mathcal{M}^0(X, (T^{*(1,0)}X)^n)$ be a global meromorphic n -form, with poles along an anti-canonical divisor D , e.g. using log coordinates. In other words, Ω^{-1} is a nonzero holomorphic section of the anti-canonical bundle on $X \setminus D$.*

Let L be a Lagrangian submanifold in $X \setminus D$ which is special, i.e. $\Omega|_L$ has constant angle in the function in local holomorphic coordinates. Let $\beta \in \pi_2(X, L)$ be nonzero.

Then: for this special Lagrangian L , $\mu(\beta)$ is twice the algebraic intersection number $\beta \cdot [D]$, where $\mu(\beta)$ denotes the Maslov class.

Proof from [Aur07, §3.1]. The tangent space to L is real since being Lagrangian is defined by $(TL)^\perp = JTL$ with respect to $\omega(-, J-)$. Taking a real basis gives a nonvanishing section of $K_X^{-1}|_L$ which we can scale to unit length. Since we've normalized, this section is independent of choice of basis. In particular, its square trivializes the square of the anticanonical bundle over L . And the defining section $s = \Omega^{-1}$ of D trivializes the square of the same

bundle over $X \setminus D$, i.e. $2c_1(X \setminus D) = 0$. So the two agree over L .

That is, recall that $\mu(\beta)$ measures the obstruction to extending the square of this normalized section on L to one on a disc representing β . We can always find a grading μ by [Sei00], because we have a lift to \mathbb{R} for special Lagrangians. We have two nonvanishing unit real sections on TL so they must be the same, one of which is the section (corresponding to divisor D) squared. So the Maslov class of β is, via this squared section, twice the intersection of D and β . \square

Theorem 5.1.15 ([CO06], [Aur07]). *Consider the moduli space of J_0 -holomorphic discs with boundary in L and in the class of β where 1) $L = T_z|_{\text{circle}}$ for a circle around the origin in the base of v_0 , i.e. a product torus in a toric variety, and 2) β is a class of Maslov index 2, i.e. by Lemma 5.1.14, the class of a section over the disc in the base.*

Then for $\mu(\beta) = 2$, the virtual dimension of the moduli space is $n - 3 + \mu(\beta) = n - 1$ and there is exactly one disk in the class β passing through each point of L .

Proof. Dimension. The reason for the dimension claim is that the index theorem in Fredholm theory implies the index of the operator D_u is $n\chi(D^2) + \mu(\beta) = n + \mu(\beta)$ where χ denotes the Euler characteristic, and then we subtract out 3 because of the reparametrization action (3 points determine an automorphism of the disc).

Using the previous result, we can interpret the dimension geometrically from intersection numbers. Since we're considering J_0 -sections u in the moduli space, they pass once through the central fiber at 0, which is also the divisor D in our setting. D is the union of toric divisors in $v_0^{-1}(0)$. They intersect D transversely once, hence they have Maslov index 2 by the above result. There are no nontrivial Maslov zero discs by the fact that Lagrangians in the fiber do not bound discs.

If we require one boundary marked point to map to a given point of L , this cuts down the dimension by n so the expected dimension is then 2 (from the Maslov index) plus 1 for the choice of marked point on the domain, minus 3 from quotienting by reparametrization. This results in an expected dimension of zero. (The collection of discs with boundary on $T_z|_{\text{circle}}$ and a point constraint on the boundary is a zero dimensional family, otherwise we could rotate the disc by the T^3 action and obtain a family of discs. Fixing the image of a marked point cuts the dimension down to zero so we can count the moduli space.)

Moduli space computation. T_z can be thought of as corresponding to the skyscraper sheaf under mirror symmetry. Recall that the definition of ℓ_k involved rotating an amount $2\pi k$ along the two angle directions as we traverse one loop in each of the base ξ_i moment map directions. Rotating only the angle directions and not in the base defines T_z , namely, we fix the moment map coordinates and let the angles vary. This gives the preimage of a moment

map coordinate $A := (a_1, a_2, a_3) = (\xi_1, \xi_2, \eta)$ and we let $|z| := \tau^{2\pi A}$ denote the exponentiated coordinates. The reason for choosing the letter A is that the formula for counting such discs is discussed in a paper of [CLL12] and that notation follows theirs.

Because each disc considered intersects the central fiber only once, its lift to the universal cover \tilde{Y} can intersect only one of the toric divisors of \tilde{Y} . Which divisor it intersects is determined by the class β . The image of the disc is contained in the union of the open stratum of \tilde{Y} and the open stratum of the component of D that the disc intersects, which by standard toric geometry is the image of a toric chart $\mathbb{C}^* \times \mathbb{C}^* \times \mathbb{C}$ inside \tilde{Y} .

Thus we think of the disc as mapping to the chart $\mathbb{C}^* \times \mathbb{C}^* \times \mathbb{C}$. Then a disc with boundary in $S^1(r_1) \times S^1(r_2) \times S^1(r_3)$ implies it is constant in the first two components (by the maximum principle) and we obtain a disc in the last v_0 coordinate. It cannot be multiply covered because it must be Maslov index 2 by the previous paragraph.

So the discs we count correspond to selecting a point A in the moment polytope and drawing a line to a facet in that polytope. Geometrically, fixing A implies each disc has the same $T^3 \cong S^1(r_1) \times S^1(r_2) \times S^1(r_3)$ Lagrangian boundary condition, namely the moment map preimage of A . As we allow $|v_0| \rightarrow 0$, we find that r_1, r_2 remain constant and the third coordinate goes to zero along the disc. (In the moment polytope this corresponds to a path, depending on β , from A to a facet. And ξ_1, ξ_2, η may vary along the path.)

□

Theorem 5.1.16. *The count of discs equals the defining theta function, up to a change of coordinates.*

Proof. The count in this setting of discs in a toric variety is given in [CO06]. Recall that we weight by $\tau^{\int \omega}$ in the count. (Note that τ corresponds to the complex structure on the genus 2 curve, so it corresponds to the symplectic structure on the mirror. The complex structure on the mirror was in terms of T , see Figure 1.8.) If x_i are coordinates on the complex side on V and $|z_i| := \tau^{a_i}$ where the point in the polytope we measure from is (a_1, a_2, a_3) , then from [CO06] the area of the disc intersecting the (m_1, m_2) facet is $2\pi (\langle \underline{a}, \nu(F_{m_1, m_2}) \rangle + \alpha(F_{m_1, m_2}))$.

The facet equations are determined from Equation (1.15). In particular, $(\xi_1, \xi_2, \eta) = (0, 0, 0)$ is a point on the facet in the $\eta = 0$ plane. Denote the facets by F_{m_1, m_2} and let $\nu(F_{m_1, m_2})$ and $\alpha(F_{m_1, m_2})$ denote the normal and constant defining the plane the facet lies in. Recall that $\eta \geq \varphi(\xi)$ where $\varphi(\xi + \gamma) = \varphi(\xi) - \kappa(\gamma) + \langle \lambda(\gamma), \xi \rangle$. Suppose $(\xi_1, \xi_2, \eta) \in F_{m_1, m_2}$. We know from Claim (4.2.13) that Γ_B acts on the moment map coordinates in the following way:

$$\begin{aligned} (-m_1\gamma' - m_2\gamma'') \cdot (\xi_1, \xi_2, \eta) &= (\xi_1 - 2m_1 - m_2, \xi_2 - m_1 - 2m_2, \eta - \kappa(m_1\gamma' + m_2\gamma'') - m \cdot \xi) \\ &= (\xi_1 - 2m_1 - m_2, \xi_2 - m_1 - 2m_2, \eta + m_1^2 + m_1m_2 + m_2^2 - m_1\xi_1 - m_2\xi_2) \end{aligned} \tag{5.4}$$

In particular, this point must be in $F_{0,0}$. We also know $(\xi_1, \xi_2, \eta) \in F_{m_1, m_2}$. Plugging each point into the equation of the corresponding facet, we find that:

$$\begin{aligned}
& \left\langle \nu(F_{m_1, m_2}), \begin{pmatrix} \xi_1 \\ \xi_2 \\ \eta \end{pmatrix} \right\rangle + \alpha(F_{m_1, m_2}) = 0 \\
\Rightarrow & \left\langle \nu(F_{0,0}), \begin{pmatrix} \xi_1 - 2m_1 - m_2 \\ \xi_2 - m_1 - 2m_2 \\ \eta + m_1^2 + m_1m_2 + m_2^2 - m_1\xi_1 - m_2\xi_2 \end{pmatrix} \right\rangle + \alpha(F_{0,0}) \\
& = \eta + m_1^2 + m_1m_2 + m_2^2 - m_1\xi_1 - m_2\xi_2 = 0 \\
\Rightarrow & \nu(F_{m_1, m_2}) = (-m_1, -m_2, 1)^t, \quad \alpha(F_{m_1, m_2}) = m_1^2 + m_1m_2 + m_2^2
\end{aligned} \tag{5.5}$$

So comparing the series from counting discs weighted by area for the differential, and that of the theta function, we find that

$$\begin{aligned}
\theta\text{-function} &= \sum_{n \in \mathbb{Z}^2} x_1^{-n_1} x_2^{-n_2} \tau^{\frac{1}{2}n^t} \begin{pmatrix} 2 & 1 \\ 1 & 2 \end{pmatrix}_n \\
\text{disc count by area} &= z_3 \sum_{n \in \mathbb{Z}^2} z_1^{n_1} z_2^{n_2} \tau^{\frac{1}{2}n^t} \begin{pmatrix} 2 & 1 \\ 1 & 2 \end{pmatrix}_n
\end{aligned}$$

which agree up to a change of coordinates. □

Remark 5.1.17. Note that there are more pseudo-holomorphic discs with J than J_0 . The latter only has one in each homology class. This is because with J some of the discs must converge to a disc union bubbles as $t \rightarrow 0$ for a path from $J_1 := J$ to J_0 . See Figure 5.5.

5.1.2 Gromov-Witten invariants count J_0 -sphere bubbles

Claim 5.1.18. There are spheres that are not regular for J_0 .

Proof. See Claim 5.1.3. For another proof, the index operator implies that moduli spaces of spheres in \tilde{Y} have expected dimension $n - 3 + c_1$ which is $3 - 3 + 0 = 0$. This would be the dimension if they were regular spheres. However, one can obtain holomorphic spheres in \mathbb{CP}^2 which lift to ones in the blowup $\mathbb{CP}^2(3)$ and project to ones in Y under the group quotient map. In particular, we can take arbitrarily many to obtain higher dimensional families. So the spheres cannot be regular. Note that only some configurations may appear as a limit of nonempty moduli spaces while varying J_t as $t \rightarrow 0$. □

Remark 5.1.19 (Terminology). *Closed Gromov-Witten* theory counts spheres, for which we can use the algebraic geometry of stacks. Chapter 10 of [CK99] gives the stack definition of moduli spaces. A reference for an introduction to stacks is [Fan01]. *Open Gromov-Witten* theory involves counting discs with a Lagrangian boundary condition, and this boundary condition is why we introduce analysis into definitions and use Fredholm problems to count the moduli spaces.

We will denote sphere classes in the central fiber by α and the class of the disc passing through the divisor D_{ij} corresponding to the $I := (i, j)$ facet by β_{ij} . Let $n_{\beta_I + \alpha}$ denote the count of the following moduli space:

$$\overline{\mathcal{M}}_{\beta_I + \alpha}(J_0) := \{(u, \underline{v}) : (\mathbb{D}, (S^2)^k) \rightarrow Y \mid u(\partial\mathbb{D}) \subset T_z|_{\text{circle}},$$

$$[u\# \underline{v}] = \beta_I + \alpha, (u, \underline{v}) \in C^\infty, ev_0(u) = ev_0(v_1), \mu([D_I]) = 2, \bar{\partial}_{J_0}(u, \underline{v}) = 0\} \times \{p\} / \text{Aut}(Y, p)$$

Theorem 5.1.20 (Open mirror theorem proved in [KL19, Theorem 3.10]). *\tilde{Y} is a toric Calabi-Yau manifold of infinite-type. Then*

$$\sum_{\alpha} n_{\beta_I + \alpha} q^\alpha(\check{q}) = \exp(g_I(\check{q}))$$

where q denotes the Kähler parameters, \check{q} the complex parameters, $q(\check{q})$ the mirror map and

$$g_I(\check{q}) := \sum_d \frac{(-1)^{(D_I \cdot d)} (-(D_I \cdot d) - 1)!}{\prod_{I' \neq I} (D_{I'} \cdot d)!} \check{q}^d$$

where the summation over d is taken over all $d \in H_2^{\text{eff}}(\tilde{Y}, \mathbb{Z})$ such that $-K_{\tilde{Y}} \cdot d = 0$, $D_I \cdot d < 0$, and $D_{I'} \cdot d \geq 0$ for all $I' \neq I$.

Remark 5.1.21. Note that here we consider particular values of Kähler parameters, because we've fixed the symplectic form so that the three toric divisors $x = 0$, $y = 0$, and $z = 0$ have symplectic area 1 (these form the “banana manifold”). Namely, $|q| = \tau^1$ and $|q|^\alpha$, in our notation, is $\tau^{\omega(\alpha)}$.

Outline. Below in Figure 5.1.2 is a flow chart indicating the necessary background for understanding the sphere count in Kanazawa-Lau [KL19]. Note that they use $J = J_0$ as we are using here.

Flow chart details

Givental: [Giv98]. The Picard-Fuchs differential equation describes the behavior of periods arising from Hodge structures on the complex side. Via mirror symmetry it can compute GW invariants. Givental introduced the I and J functions in solutions of these equations,

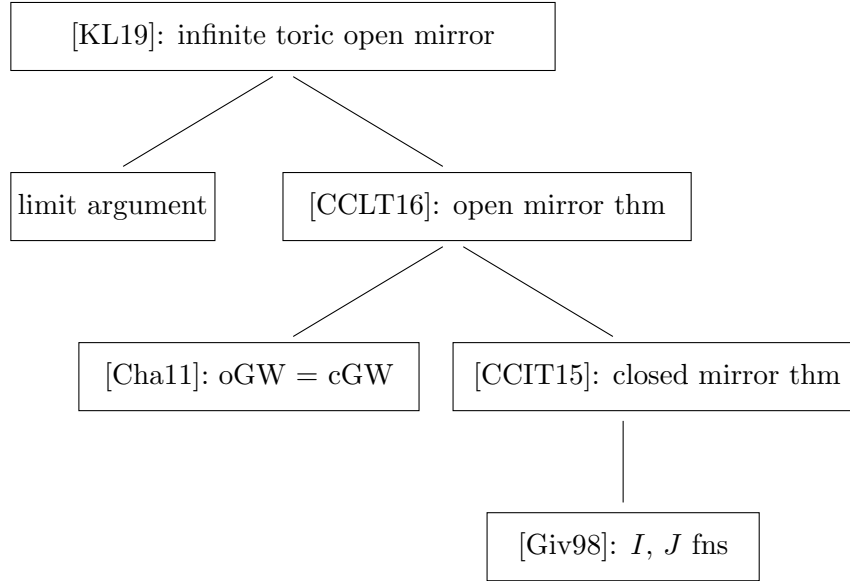


Figure 5.6: Gromov-Witten theory background for mirror symmetry of toric varieties

where I computes the complex invariant and J the Gromov-Witten or symplectic invariant.

Closed mirror theorem: [CCIT15]. The closed mirror theorem relates the I and J function (defined in e.g. [CK99, §2.6.2]) and builds on Givental's paper. Varying the complex moduli gives a variation of the Hodge structure on the complex manifold. The J function on the symplectic manifold corresponds to the I function on the complex manifold. These are functions of the Kähler and complex moduli, which are isomorphic. The mirror map goes between neighborhoods of a Kähler large limit point and a complex large limit point (maximally unipotent monodromy), see [CK99, §6.3, p 151]. Chapter 7 of [CK99] defines GW invariants and Proposition 10.3.4 gives the relation between the J -function and the GW potential.

In particular, [CK99, Equation (10.4)] gives the relation between differentials, intersection theory, and Gromov-Witten theory. The Picard-Fuchs equation [CK99, §5.1.2] is for complex moduli \tilde{q} near maximally unipotent monodromy (denoted y_k in [CK99]). The Kähler moduli q is denoted q_k in the same reference.

Givental's mirror theorem for toric complete intersections is described in [CK99, §11.2.5]. Specific to the toric setting is the GKZ system, see [CK99, §5.5]. An example of the mirror theorem is [CK99, 11.2.1.3]. In the case of toric varieties, we have an equivariance under the toric action of the moduli spaces, discussed in [CCIT15].

The result of [Cha11]. For closed GW invariants, there is a toric mirror theorem based

on Givental's mirror theorem. It can compute GW invariants from solutions to the Picard-Fuchs equation, because the latter gives rise to period integrals (complex side) which fit into the I -function, a function that is related to the J -function which computes closed GW invariants. However in the Fukaya category considered one has open GW invariants, so we would like to be able to count these as well. There is a notion of “capping off” introduced in [Cha11] where, for a toric variety X_Σ , one adds an additional ray to the fan Σ to define a partial compactification \overline{X}_Σ . This is done so the disks in the open GW count are “capped off” to become spheres. See [CCLT16, §6.1] for a construction in the toric CY setting. The result in [Cha11] implying that these open and closed GW invariants are equal is that they have isomorphic Kuranishi structures. The open GW invariants count disks with Lagrangian boundary condition given by the preimage of a moment map from a toric variety, and these can be equipped with Kuranishi structures by [FOOO10]. We are in this setting.

Definition 5.1.22 (Kuranishi chart). A Kuranishi neighborhood of p on moduli space X is the following data:

- V_p smooth finite-dimensional *manifold*, possibly with corners
- $V_p \times E_p \rightarrow V_p$ is the *obstruction bundle*, where E_p is a finite-dimensional real vector space.
- Γ_p is a finite *group* which acts smoothly and effectively (no non-trivial element acts trivially) on V_p , and E_p linearly represents the group.
- Kuranishi map s_p is a smooth *section* of $V_p \times E_p$ (smooth map $V_p \rightarrow \Gamma_p$), and is Γ_p equivariant.
- ψ_p is a *topological chart* which is a homeomorphism from the local model $s_p^{-1}(0)/\Gamma_p$ to a neighborhood of p in X .
- V_p/Γ_p or V_p may also be referred to as a *Kuranishi neighborhood* (rather than the collection of all these pieces of data).
- o_p is a point which the Kuranishi map sends to zero and the chart maps to p .
- For references in the literature on gluing such charts, see [MTFJ19, Fukaya, Tehrani].

Kanazawa-Lau apply [CCLT16] to the infinite toric setting. In [KL19] there is a notion of taking a limit to get to the infinite toric case, which is our setting as well before we quotient by the Γ_B -action. They build on the open mirror theorem of [CCLT16] and compute the sphere count as the coefficient of $1/z$ in the mirror map. This concludes the proof outline for the sphere bubble count of [KL19].

□

Lemma 5.1.23. *Recall our notation above in the second paragraph of Remark 5.1.19. We make the following definitions:*

- Fix $A \in \Delta_{\hat{\gamma}}$.

- Set $z = \tau^A$.
- Lagrangian boundary condition is $T_z|_{\text{circ}}$ over a circle around the origin in the base of v_0 .
- Fix a point $pt_{\text{constraint}}$ on this Lagrangian.
- Fix disk homology class $\beta_{ij} = [D_{ij}]$ in $H^2(\tilde{Y}, T_z|_{\text{circ}})$.

Then we claim that the differential can be computed from the c defined in Lemma 5.1.7, which equals:

$$c = C \cdot \left(\sum_{\gamma} \tau^{\omega(\gamma_* \beta_0)} \right) \quad (5.6)$$

where $C := (\sum_{\alpha} N_{\alpha} \tau^{\omega(\alpha)})$ for N_{α} defined in the proof. Lemma 5.1.5 explains why this suffices to compute the differential, which counts bigons bounded by $L_i \cup L_j$.

Proof. Define a $\Gamma_B \times (\mathbb{C}^*)^3$ -action on \tilde{Y} where (γ, c_{γ}) acts by $c_{\gamma} \circ \gamma$ and c_{γ} is complex multiplication. Specifically, $\gamma \in \Gamma_B$ sends D_{ij} to some $D_{i'j'}$, and c_{γ} is defined by requiring the point $\gamma_*(A)$ in the moment polytope to map back to A via the $(\mathbb{C}^*)^3$ toric action (while fixing the divisors). Thus $\Gamma_B \times (\mathbb{C}^*)^3$ acts on moduli spaces of curves with a fixed Lagrangian boundary condition, varying homology classes, and a marked point pt , by post-composition. Then we have an isomorphism of moduli spaces:

$$\begin{aligned} & \{(u, pt), u : \mathbb{D} \rightarrow Y, pt \in \partial \mathbb{D} \mid u(\partial \mathbb{D}) \subset T_z|_{\text{circ}}, u(pt) = pt_{\text{constraint}}, [u] = \beta_{ij}, \bar{\partial}_{J_{\text{reg}}}(u) = 0\} \cong \\ & \{(u, pt), u : \mathbb{D} \rightarrow Y, pt \in \partial \mathbb{D} \mid u(\partial \mathbb{D}) \subset T_z|_{\text{circ}}, u(pt) = c_{\gamma} \circ \gamma(pt_{\text{constraint}}), [u] = (c_{\gamma} \circ \gamma)_* \beta_{ij}, \bar{\partial}_{(c_{\gamma} \circ \gamma)^* J_{\text{reg}}}(u) = 0\} \end{aligned} \quad (5.7)$$

In particular, for a regular J_{reg} as exists by Lemma 4.4.6, (so moduli spaces are manifolds) and introducing the point constraint (so they are zero dimensional), counting points in these moduli spaces produces an infinite series of discs and no sphere bubbles (because we excluded them). By denseness, we can choose J_{reg} sufficiently close to J_0 so a limit of regular J 's limits to J_0 . The disk will either converge to a disk or to a disk with a sphere bubble configuration. This count of discs for J_{reg} is the differential in the Fukaya category.

By results of [CLL12], we know that the only homology classes that can appear in the compactification are stable trees of the form $\beta_{ij} + \sum_i n_i \alpha_i$ for some integers n_i and spheres α_i . Note that $(c_{\gamma} \circ \gamma)^* J_0 = J_0$ since multiplication by scalars is a holomorphic map.

The claim we want to prove is that the defined moduli spaces are isomorphic as we vary the homology classes. Applying these group actions should produce isomorphic moduli spaces with the same J_0 , and we know that way, whatever the GW count is for a particular homology class $D_{ij} + \alpha$, it will be the same for all others and the counts will be the same so we can pull out a common factor. Namely the counts $n_{\beta+\alpha}$ do not, in fact, depend on the disk class β since there is a 1-1 bijection between moduli spaces of sphere configurations showing up with D_{ij} and with any other $D_{i'j'}$, via the map $c_{\gamma} \circ \gamma$. That is because it has an inverse $(c_{\gamma} \circ \gamma)^{-1}$ given by multiplication by the inverse scalars. Suppose we write for an arbitrary disc and sphere configuration $\beta + \alpha' =: \gamma_*(\beta_0 + \alpha)$ for fixed β_0 with a suitable γ which then determines

α . Then we can denote all $n_{\beta+\alpha'}$ as N_α , independent of β since $n_{\beta+\alpha'} = n_{\gamma_*(\beta_0+\alpha)} =: N_\alpha$. We streamline notation below and use γ to incorporate both actions of γ and c_γ . We choose J_{reg} to also be regular for the homology class $\gamma_*(\beta_I + \alpha)$ so $\gamma^* J_{reg}$ is regular for the class $\beta + \alpha$.

$$\mathcal{M}(\beta_I + \alpha, J_{reg}) \cong \mathcal{M}(\gamma(\beta_I + \alpha), \gamma^* J_{reg})$$

$$\begin{aligned} c &= \sum_{\beta, \alpha} n_{\beta+\alpha'} \tau^{\omega(\beta)+\omega(\alpha')} = \sum_{\alpha, \gamma \in \Gamma_B} n_{\gamma_*(\beta_0+\alpha)} \tau^{\omega(\gamma_*\beta_0)+\omega(\alpha)} \\ &= \sum_{\gamma \in \Gamma_B} \left(\sum_{\alpha} N_\alpha \tau^{\omega(\alpha)} \right) \cdot \tau^{\omega(\gamma_*\beta_0)} \\ &= \left(\sum_{\alpha} N_\alpha \tau^{\omega(\alpha)} \right) \cdot \left(\sum_{\gamma \in \Gamma_B} \tau^{\omega(\gamma_*\beta_0)} \right) \end{aligned}$$

$$\text{Define } C(z) := \left(\sum_{\alpha} N_\alpha \tau^{\omega(\alpha)} \right) \quad (5.8)$$

The first factor we can put in front, and the second is the multi-theta function described above in the computation of J_0 -discs. Note that $N_0 = 1$ by Theorem 5.1.15, hence $C = 1 +$ (higher order terms) and is invertible. \square

5.1.3 Future direction: definition for non-regular J

Remark 5.1.24 (Recap). To summarize what we have done so far: we defined the Fukaya category for regular J and showed it was independent of regular choices, and then we computed the differential in the Fukaya category but with a non-regular J . We got around defining the Fukaya category for non-regular J because of the isomorphism between moduli spaces in this particular setting. If we didn't have that, it would remain to give a definition of the Fukaya category for non-regular J which agrees with the previous definition on regular J , and then show that the count for a particular abstract perturbation Λ_0 agrees with the count in [KL19]. That way we could compute the differential with their formula.

Conjecture 5.1.25. The computation of Gromov-Witten invariants in [KL19] equals the count of the same moduli spaces when abstractly regularized by a particular perturbation Λ_0 in polyfold theory.

Possible ideas. For $J = J_0$ and homology class β' (we use β' to denote what we previously referred to as $\beta + \alpha$, in other words β' is a disk plus sphere classes), the moduli space we want consider to is

$$\begin{aligned} \overline{\mathcal{M}}_{\beta'}(J) &:= \{(u, \underline{v}) : \mathbb{D} \cup (S^2)^k \rightarrow Y \mid u(\partial\mathbb{D}) \subset T_z|_{circle}, [u\#\underline{v}] = \beta', \\ (u, \underline{v}) &\in C^\infty, \text{cond}_{inc}, \bar{\partial}_J(u) = 0 = \bar{\partial}_J(v_i) \forall i\} \times \{p\} / \text{Aut}(\mathbb{D} \cup (S^2)^k, p) \end{aligned}$$

where $cond_{inc}$ denotes the incidence conditions for an arbitrary bubble tree configuration: $ev_0(u) = ev_0(v_1)$ and $\{ev_{p_k}(v_i) = ev_{p_l}(v_j)\}_{i,j,k,l}$ for the collection of points $p_k, p_l \in S^2$ and maps $v_i, v_j : S^2 \rightarrow Y$ describing the configuration. So $\overline{\mathcal{M}}_{\beta'}(J)$ is a set. Define another set $\mathcal{B}_{\beta'}$ to be the Sobolev completion of the set defined by the above with the J -holomorphic condition removed. That is, it's similar to the geometric case of the Banach bundle set-up in [MS12], however the difference here is that we allow varying domains instead of looking at only maps from a disc, or a sphere, or a disc union sphere, etc. This new setup admits a polyfold structure, see J. Li's thesis [WL]. In particular, the base contains the set of smooth maps as a dense subset. We define a bundle \mathcal{E}_J over \mathcal{B}'_{β} by setting the fiber over (u, \underline{v}) to be the codomain of $D_{(u, \underline{v})}$, i.e. $W^{k-1,p}(\mathbb{D} \cup (S^2)^k, \Lambda^{0,1} \otimes (u, \underline{v})^*TY)$.

We consider the following potential action plan. This assumes the existence of full polyfold setups in our setting, which would need to be defined. For now, we label what assumptions are needed for the statements below to hold.

- 1) For all J there exists a polyfold Fredholm section $s_J : \mathcal{B} \rightarrow \mathcal{E}_J$ with $s_J^{-1}(0) = \overline{\mathcal{M}}_{\beta'}(J)$. This requires that \mathcal{B} have no boundary, which holds in the setting here; by [CLL12, Proposition 4.30] there can only be sphere bubbles with the given Lagrangian boundary conditions.
- 2) It is known that when J is regular, s_J is polyfold transverse and $\#\overline{\mathcal{M}}_{\beta'}(J) := \#s_J^{-1}(0)$ is defined, so this definition of the Fukaya category with polyfolds would agree with the previous definition above on regular J .
- 3) For J not regular, such as J_0 , there exists a functor $\Lambda : \mathcal{W}_J \rightarrow \mathbb{Q}^+$ where \mathcal{W}_J is an EP-groupoid with $|\mathcal{W}_J| \cong \mathcal{E}_J$, so that (see [HWZ17] for more details),

$$\#\overline{\mathcal{M}}_{\beta'}(J_0) := \#\text{supp } \Lambda \circ s_{J_0}$$

is defined. Also, by [HWZ17] it is independent of the choice of perturbation Λ , assuming we are in the setting where \mathcal{B} has no boundary.

- 4) We also know that for J_0 and some arbitrary J_1 , then $\#\overline{\mathcal{M}}_{\beta'}(J_0) = \#\overline{\mathcal{M}}_{\beta'}(J_1)$ by [HWZ17], assuming \mathcal{B} has no boundary. So this defines a Fukaya category which is independent of the almost complex structure, as we would like.
- 5) The final step would be to find a particular perturbation Λ_0 such that

$$\#\text{supp } \Lambda_0 \circ s_{J_0} = c$$

for our count c computed in Equation 5.8.

Polyfold theory can abstractly perturb the $\bar{\partial}_J$ -operator and obtain that the resulting zero set is a weighted branched orbifold, which can be counted. If the dimension is zero, there is a “cobordism” between different perturbations, so the result gives equivalent categories under perturbations. There is also a cobordism when varying J , see [HWZ17]. In particular, if we start with a regular J then the perturbation is zero and we get a cobordism between that and the perturbed moduli space which is actually a manifold.

In the setting here where the moduli spaces considered are defined with homology classes that vary under the Γ_B -action, under which the moduli spaces themselves are isomorphic, one potential avenue for showing that the moduli spaces equipped with a polyfold structure are similarly isomorphic is to use [Sch18, Theorem 3.1.4] in Schmaltz’s thesis. It requires that one has a map f between polyfold bundle bases $\mathcal{B}_{\beta'} \rightarrow \mathcal{B}_{\beta''}$ that satisfies a *topological pullback condition* [Sch18, Definition 3.1.2], which looks similar to the notion of continuity on topological spaces.

The theorem states that in this case, one can find a regular perturbation Λ (defined in the theorem, and consists of a transversality and compactness condition) of the defining section s'' of the bundle $\mathcal{E}_{\beta''} \rightarrow \mathcal{B}_{\beta''}$ which pulls back under f to a regular perturbation of the defining section of the bundle $\mathcal{E}_{\beta'} \rightarrow \mathcal{B}_{\beta'}$. We would like to apply this to the map $f = \gamma$.

Specifically, γ acts biholomorphically on Y and so by post-composition it acts as an isomorphism on the sets of curves $\mathcal{B}_{\beta'} \rightarrow \mathcal{B}_{\gamma_*\beta'}$. (Recall we have a map between moduli spaces that realizes the isomorphism $\mathcal{M}(D_I + \alpha, J_0) \cong \mathcal{M}(\gamma_*(\beta_I + \alpha), \gamma^*J_0)$, namely we first take a curve u (in the zero set of the $\bar{\partial}_{J_0}$ operator), and then apply the group action γ , which acts on Y .)

So in the notation of [Sch18, Theorem 3.1.4], we would like to take $\mathcal{Z}_1 := \mathcal{B}_{\beta'}$, $f := \gamma$, $\mathcal{Z}_2 := \mathcal{B}_{\gamma_*\beta'}$, and $\mathcal{W} := \mathcal{E}_{\gamma_*\beta'} := \mathcal{E}_{J_0}$. Then we would obtain the following commutative diagram:

$$\begin{array}{ccc}
 \gamma^*\mathcal{E}_{\gamma_*\beta'} & \xrightarrow{\text{proj}_2} & \mathcal{E}_{\gamma_*\beta'} \\
 \uparrow \gamma^*\bar{\partial}_{J_0} & & \uparrow \bar{\partial}_{J_0} \\
 \mathcal{B}_{\beta'} & \xrightarrow{\gamma} & \mathcal{B}_{\gamma_*\beta'}
 \end{array} \tag{5.9}$$

where $\beta' := \beta_I + \alpha$ and proj_2 is defined on the underlying sets by the projection of $f^*\mathcal{W} \subset \mathcal{Z}_1 \times \mathcal{W}$ onto the second factor. The result of [Sch18] would imply that one may construct an admissible perturbation Λ_0 , so that $\gamma^*\Lambda_0$ is also an admissible perturbation. In particular, the perturbed moduli spaces are isomorphic as weighted branched orbifolds.

We find then that all the moduli spaces for different discs have the same configuration of spheres showing up. (The spheres have non-trivial isotropy so this setup will use the machinery of étale-proper (EP) groupoids in polyfolds.) Note that this is the analogue for J_0 with polyfold-regularized moduli spaces of the result stated above for regular J_{reg} , namely Equation (5.7).

The final step would be to show that the actual counts are equal to that in [KL19]. One should also note that if we want to extend this result to the case when disk bubbling can happen for some J or we want to find more than a single count, the situation will be more complicated than the steps above. □

5.2 Proof: fully-faithful embedding

$$D^b Coh_{\mathcal{L}}(H) \hookrightarrow H^0(FS(Y, v_0))$$

On objects we map $\mathcal{L}|_H^{\otimes i} \mapsto L_i$. If ϕ is the monodromy of the symplectic fibration $v_0 : Y \rightarrow \mathbb{C}$ around the origin, then the symmetry of our definition of ω ensures that $\phi(\ell_i)$ is Hamiltonian isotopic to ℓ_{i+1} . Since Floer cohomology is invariant under Hamiltonian isotopy, we can consider linear Lagrangians in the fibers. This allows us to obtain the bottom row of the following diagram, whenever $j \geq i + 2$. When $j < i + 2$ there are also Ext groups to consider and we get a long exact sequence instead, namely the last horizontal map is not surjective anymore.

$$\begin{array}{ccccccc}
 Hom(\mathcal{L}^{i+1}, \mathcal{L}^j) & \xrightarrow{\otimes s} & Hom(\mathcal{L}^i, \mathcal{L}^j) & \rightarrow & Hom(\mathcal{L}^i, \mathcal{L}^j \otimes \iota_* \mathcal{O}_H) & \rightarrow & 0 \\
 \cong \downarrow \cdot C^{-1} & & \cong \downarrow & & \downarrow & & \\
 CF(\ell_{i+1}, \ell_j) & \xrightarrow{\partial} & CF(\ell_i, \ell_j) & \rightarrow & HF(L_i, L_j) & \rightarrow & 0
 \end{array}$$

The map ∂ is part of the Floer differential on $CF(L_i, L_j) \cong CF(\ell_{i+1}, \ell_j)[-1] \oplus CF(\ell_i, \ell_j)$ and counts pseudo-holomorphic section-like maps (defined in Definition 4.4.3) of $v_0 : Y \rightarrow \mathbb{C}$ with suitable Lagrangian boundary conditions.

Our main result is that the left-side square in the diagram commutes, which then implies that the rightmost vertical arrow is an isomorphism as well. More precisely, we've shown in Lemma 5.1.5 and Lemma 5.1.7 that under the chosen isomorphisms of Section 3.3, the Floer differential ∂ agrees with multiplication by $s \in H^0(V, \mathcal{L})$ up to the multiplicative factor C , the open Gromov-Witten invariant in [KL19] for a particular choice of Kähler parameter. So scaling the first arrow on morphisms by C^{-1} gives a commutative diagram on the left.

The formulas for composition also match because the product structures on the groups in the right-hand vertical arrow of the diagram are those naturally induced on the quotients, and the left two vertical maps are functorial by Claim 3.3.1. So the induced isomorphisms on the cokernels of the horizontal maps should also be functorial (i.e. composition on the complex side versus Floer product on HF match under the constructed isomorphisms).

Hence this provides the desired isomorphism between the morphisms groups for the functor $D_{\mathcal{L}}^b Coh(H) \rightarrow H^0(FS(Y, v_0))$.

Chapter 6

Notation

Section 1.2

- $H = \Sigma_2$ the genus 2 curve
- $V = (\mathbb{C}^*)^2 / \Gamma_B$ abelian variety of which H is a hypersurface
- $\mathcal{L} \rightarrow V$ degree $(1, 1)$ line bundle on V
- $s : V \rightarrow \mathcal{L}$ multi-theta function, section of \mathcal{L}
- λ linear form, determines Chern class of \mathcal{L}
- κ quadratic form, determines holomorphic structure of \mathcal{L}

Section 1.3

- M lattice of characters, or functions on toric variety
- N lattice of cocharacters, or 1-parameter subgroups of toric variety
- $M_{\mathbb{R}} = M \otimes_{\mathbb{Z}} \mathbb{R}$, same for N
- m an element of M or $M_{\mathbb{R}}$
- u a lattice element in N

Section 1.4

- $\Delta_{\tilde{Y}}$ polytope defining \tilde{Y}
- $\Delta_Y = \Delta_{\tilde{Y}} / \Gamma_B$
- $(\xi_1, \xi_2, \eta) \in M_{\mathbb{R}} / \Gamma_B \cong \mathbb{R}^3 / \Gamma_B$ denote coordinates on the polytope
- $v_0 : Y \rightarrow \mathbb{C}$ superpotential

- $V^\vee \cong (\mathbb{C}^*)^2 / \Gamma_B$ fiber of v_0

In calculations, $M := \begin{pmatrix} 2 & 1 \\ 1 & 2 \end{pmatrix}$.

Chapter 5

- α denotes a sphere class in the central fiber
- β_{ij} denotes the class of the disc which passes through the divisor corresponding to the (i, j) facet
- $T_z|_{\text{circ}}$ denotes parallel transport of t_z over a circle centered in the origin in the base of v_0
- $\gamma(r)$, $r \in [0, 1]$ denotes a bigon in the base of v_0 in the homotopy from Seidel

Bibliography

- [AAK16] Mohammed Abouzaid, Denis Auroux, and Ludmil Katzarkov, *Lagrangian fibrations on blowups of toric varieties and mirror symmetry for hypersurfaces*, Publ. Math. Inst. Hautes Études Sci. **123** (2016), 199–282.
- [Abo09] Mohammed Abouzaid, *Morse homology, tropical geometry, and homological mirror symmetry for toric varieties*, Selecta Math. (N.S.) **15** (2009), no. 2, 189–270.
- [ACGK12] Mohammad Akhtar, Tom Coates, Sergey Galkin, and Alexander M. Kasprzyk, *Minkowski polynomials and mutations*, SIGMA Symmetry Integrability Geom. Methods Appl. **8** (2012), Paper 094, 17.
- [APS] Nicolas Addington, Alexander Polishchuk, and Ed Segal, *Summer graduate school, derived categories*, https://www.msri.org/summer_schools/821.
- [AS] Mohammed Abouzaid and Paul Seidel, *Lefschetz fibration methods in wrapped Floer cohomology*, in preparation.
- [AS10] Mohammed Abouzaid and Ivan Smith, *Homological mirror symmetry for the 4-torus*, Duke Math. J. **152** (2010), no. 3, 373–440.
- [Aur07] Denis Auroux, *Mirror symmetry and T-duality in the complement of an anti-canonical divisor*, J. Gökova Geom. Topol. GGT **1** (2007), 51–91.
- [Aur14] ———, *A beginner’s introduction to Fukaya categories*, Contact and symplectic topology, Bolyai Soc. Math. Stud., vol. 26, János Bolyai Math. Soc., Budapest, 2014, pp. 85–136.
- [BD16] Marco Bonatto and Dikran Dikranjan, *Generalize Heisenberg Groups and Self-Duality*, arXiv e-prints (2016), arXiv:1611.02685.
- [Bej18] Dori Bejleri, *The SYZ conjecture via homological mirror symmetry*, Super-school on derived categories and D-branes, Springer Proc. Math. Stat., vol. 240, Springer, Cham, 2018, pp. 163–182.

- [BFW17] Nate Bottman, Joel Fish, and Katrin Wehrheim, *Polyfold theory towards the Fukaya category, June 12-16, 2017 at UC Berkeley*, http://www.polyfolds.org/index.php?title=RTG_workshop_program, 2017.
- [BJ07] B.H. Bransden and Charles Joachain, *Quantum mechanics (second edition)*, Prentice Hall-Pearson, Harlow, England, January 2007.
- [BL04] Christina Birkenhake and Herbert Lange, *Complex abelian varieties*, second ed., Grundlehren der Mathematischen Wissenschaften [Fundamental Principles of Mathematical Sciences], vol. 302, Springer-Verlag, Berlin, 2004.
- [Can19] Catherine Cannizzo, *Homological mirror symmetry for the genus 2 curve in an abelian variety and its generalized Strominger-Yau-Zaslow mirror*, Ph.D. thesis, University of California, Berkeley, 2019, https://math.berkeley.edu/~cannizzo/Cannizzo_thesis.
- [CCIT15] Tom Coates, Alessio Corti, Hiroshi Iritani, and Hsian-Hua Tseng, *A mirror theorem for toric stacks*, Compos. Math. **151** (2015), no. 10, 1878–1912.
- [CCLT16] Kwokwai Chan, Cheol-Hyun Cho, Siu-Cheong Lau, and Hsian-Hua Tseng, *Gross fibrations, SYZ mirror symmetry, and open Gromov-Witten invariants for toric Calabi-Yau orbifolds*, J. Differential Geom. **103** (2016), no. 2, 207–288.
- [CdLOGP91] Philip Candelas, Xenia C. de la Ossa, Paul S. Green, and Linda Parkes, *A pair of Calabi-Yau manifolds as an exactly soluble superconformal theory*, Nuclear Phys. B **359** (1991), no. 1, 21–74.
- [cfFc] Polyfold constructions for Fukaya categories, http://www.polyfolds.org/index.php?title=Polyfold_constructions_for_Fukaya_categories.
- [Cha11] Kwokwai Chan, *A formula equating open and closed Gromov-Witten invariants and its applications to mirror symmetry*, Pacific J. Math. **254** (2011), no. 2, 275–293.
- [CK99] David A. Cox and Sheldon Katz, *Mirror symmetry and algebraic geometry*, Mathematical Surveys and Monographs, vol. 68, American Mathematical Society, Providence, RI, 1999.
- [CLL12] Kwokwai Chan, Siu-Cheong Lau, and Naichung Conan Leung, *SYZ mirror symmetry for toric Calabi-Yau manifolds*, J. Differential Geom. **90** (2012), no. 2, 177–250.
- [CLS11] David A. Cox, John B. Little, and Henry K. Schenck, *Toric varieties*, Graduate Studies in Mathematics, vol. 124, American Mathematical Society, Providence, RI, 2011.

- [CO06] Cheol-Hyun Cho and Yong-Geun Oh, *Floer cohomology and disc instantons of Lagrangian torus fibers in Fano toric manifolds*, Asian J. Math. **10** (2006), no. 4, 773–814.
- [Fan01] Barbara Fantechi, *Stacks for everybody*, European Congress of Mathematics, Vol. I (Barcelona, 2000), Progr. Math., vol. 201, Birkhäuser, Basel, 2001, pp. 349–359.
- [FO97] Kenji Fukaya and Yong-Geun Oh, *Zero-loop open strings in the cotangent bundle and Morse homotopy*, Asian J. Math. **1** (1997), no. 1, 96–180. MR 1480992
- [FOOO09a] Kenji Fukaya, Yong-Geun Oh, Hiroshi Ohta, and Kaoru Ono, *Lagrangian intersection Floer theory: anomaly and obstruction. Part I*, AMS/IP Studies in Advanced Mathematics, vol. 46, American Mathematical Society, Providence, RI; International Press, Somerville, MA, 2009.
- [FOOO09b] ———, *Lagrangian intersection Floer theory: anomaly and obstruction. Part II*, AMS/IP Studies in Advanced Mathematics, vol. 46, American Mathematical Society, Providence, RI; International Press, Somerville, MA, 2009.
- [FOOO10] ———, *Lagrangian Floer theory on compact toric manifolds. I*, Duke Math. J. **151** (2010), no. 1, 23–174. MR 2573826
- [For91] Otto Forster, *Lectures on Riemann surfaces*, Graduate Texts in Mathematics, vol. 81, Springer-Verlag, New York, 1991, Translated from the 1977 German original by Bruce Gilligan, Reprint of the 1981 English translation.
- [Fra10] J. Francis, *Math 465, Spring 2010: Topology of manifolds*, <http://math.northwestern.edu/~jnkf/classes/mflds/>, 2010.
- [Fuk02] Kenji Fukaya, *Mirror symmetry of abelian varieties and multi-theta functions*, J. Algebraic Geom. **11** (2002), no. 3, 393–512.
- [Ful93] William Fulton, *Introduction to toric varieties*, Annals of Mathematics Studies, vol. 131, Princeton University Press, Princeton, NJ, 1993, The William H. Roever Lectures in Geometry.
- [Gan16a] Sheel Ganatra, *Automatically generating Fukaya categories and computing quantum cohomology*, arXiv preprint arXiv:1605.07702 (2016).
- [Gan16b] ———, *Math 257b: Topics in symplectic geometry – aspects of Fukaya categories*, <https://drive.google.com/file/d/1-anqMQbQCxgu01AKCK3rUqmOF95vkhvK/view>, 2016.

- [GH94] Phillip Griffiths and Joseph Harris, *Principles of algebraic geometry*, Wiley Classics Library, John Wiley & Sons, Inc., New York, 1994, Reprint of the 1978 original.
- [Giv98] Alexander Givental, *A mirror theorem for toric complete intersections*, Topological field theory, primitive forms and related topics (Kyoto, 1996), Progr. Math., vol. 160, Birkhäuser Boston, Boston, MA, 1998, pp. 141–175.
- [GP90] B. R. Greene and M. R. Plesser, *Duality in Calabi-Yau moduli space*, Nuclear Phys. B **338** (1990), no. 1, 15–37.
- [Gua17] Roberta Guadagni, *Lagrangian torus fibration for symplectic toric degenerations*, Ph.D. thesis, University of Texas at Austin, 2017, <https://repositories.lib.utexas.edu/handle/2152/63642>.
- [Huy05] Daniel Huybrechts, *Complex geometry*, Universitext, Springer-Verlag, Berlin, 2005, An introduction.
- [HWZ17] Helmut Hofer, Krzysztof Wysocki, and Eduard Zehnder, *Polyfold and Fredholm Theory*, arXiv e-prints (2017), arXiv:1707.08941.
- [KL19] Atsushi Kanazawa and Siu-Cheong Lau, *Local Calabi-Yau manifolds of type \tilde{A} via SYZ mirror symmetry*, J. Geom. Phys. **139** (2019), 103–138.
- [KMS11] Jelena Katić, Darko Milinković, and Tatjana Simčević, *Isomorphism between Morse and Lagrangian Floer cohomology rings*, Rocky Mountain J. Math. **41** (2011), no. 3, 789–811. MR 2824880
- [Kon95] Maxim Kontsevich, *Homological algebra of mirror symmetry*, Proceedings of the International Congress of Mathematicians, Vol. 1, 2 (Zürich, 1994), Birkhäuser, Basel, 1995, pp. 120–139.
- [KS01] Maxim Kontsevich and Yan Soibelman, *Homological mirror symmetry and torus fibrations*, Symplectic geometry and mirror symmetry (Seoul, 2000), World Sci. Publ., River Edge, NJ, 2001, pp. 203–263.
- [Laz00] L. Lazzarini, *Existence of a somewhere injective pseudo-holomorphic disc*, Geom. Funct. Anal. **10** (2000), no. 4, 829–862.
- [Laz11] Laurent Lazzarini, *Relative frames on J -holomorphic curves*, J. Fixed Point Theory Appl. **9** (2011), no. 2, 213–256.
- [Mil65] John Milnor, *Lectures on the h -cobordism theorem*, Notes by L. Siebenmann and J. Sondow, Princeton University Press, Princeton, N.J., 1965.

- [MS12] Dusa McDuff and Dietmar Salamon, *J-holomorphic curves and symplectic topology*, second ed., American Mathematical Society Colloquium Publications, vol. 52, American Mathematical Society, Providence, RI, 2012.
- [MS17] ———, *Introduction to symplectic topology*, third ed., Oxford Graduate Texts in Mathematics, Oxford University Press, Oxford, 2017.
- [MTFJ19] Dusa McDuff, Mohammad Tehrani, Kenji Fukaya, and Dominic Joyce, *Virtual fundamental cycles in symplectic topology*, American Mathematical Society, 2019.
- [Oh93] Yong-Geun Oh, *Floer cohomology of Lagrangian intersections and pseudo-holomorphic disks. I*, Comm. Pure Appl. Math. **46** (1993), no. 7, 949–993.
- [Pas14] James Pascaleff, *M 392c: Lagrangian Floer homology, hw 1*, <https://faculty.math.illinois.edu/~jpascale/courses/2014/m392c/notes/homework1.pdf>, 2014.
- [Pol03] Alexander Polishchuk, *Abelian varieties, theta functions and the Fourier transform*, Cambridge Tracts in Mathematics, vol. 153, Cambridge University Press, Cambridge, 2003.
- [PZ98] Alexander Polishchuk and Eric Zaslow, *Categorical mirror symmetry: The Elliptic curve*, Adv. Theor. Math. Phys. **2** (1998), 443–470.
- [Sal99] Dietmar Salamon, *Lectures on Floer homology*, Symplectic geometry and topology (Park City, UT, 1997), IAS/Park City Math. Ser., vol. 7, Amer. Math. Soc., Providence, RI, 1999, pp. 143–229. MR 1702944
- [Sch18] Wolfgang William Schmaltz, *Gromov-Witten axioms for symplectic manifolds via polyfold theory*, Ph.D. thesis, University of California, Berkeley, 2018, <https://escholarship.org/uc/item/654417s5>.
- [Seg] Graeme Segal, *July-August 1999 ITP workshop on geometry and physics: Topological field theory (‘Stanford notes’)*, <http://web.math.ucsb.edu/~drm/conferences/ITP99/segal/>.
- [Sei00] Paul Seidel, *Graded Lagrangian submanifolds*, Bull. Soc. Math. France **128** (2000), no. 1, 103–149.
- [Sei08] ———, *Fukaya categories and Picard-Lefschetz theory*, Zurich Lectures in Advanced Mathematics, European Mathematical Society (EMS), Zürich, 2008.
- [Sei11] ———, *Homological mirror symmetry for the genus two curve*, J. Algebraic Geom. **20** (2011), no. 4, 727–769.

- [Sym03] Margaret Symington, *Four dimensions from two in symplectic topology*, Topology and geometry of manifolds (Athens, GA, 2001), Proc. Sympos. Pure Math., vol. 71, Amer. Math. Soc., Providence, RI, 2003, pp. 153–208. MR 2024634
- [SYZ96] Andrew Strominger, Shing-Tung Yau, and Eric Zaslow, *Mirror symmetry is T-duality*, Nuclear Phys. B **479** (1996), no. 1-2, 243–259.
- [SZ92] Dietmar Salamon and Eduard Zehnder, *Morse theory for periodic solutions of Hamiltonian systems and the Maslov index*, Comm. Pure Appl. Math. **45** (1992), no. 10, 1303–1360. MR 1181727
- [Weh13] Katrin Wehrheim, *Berkeley math 278: Analysis of pseudoholomorphic curves*, <https://piazza.com/berkeley/fall2013/berkeleymath278/resources>, 2013.
- [Weh14] ———, *Regularization of moduli spaces of pseudoholomorphic curves*, <https://math.berkeley.edu/~katrin/teach/regularization/lectures.shtml>, 2014.
- [Wen16] Chris Wendl, *Lectures on Symplectic Field Theory*, arXiv e-prints (2016), arXiv:1612.01009.
- [WL] Katrin Wehrheim and Jiayong Li, *A_∞ -structures from Morse trees with pseudoholomorphic disks*, <https://math.berkeley.edu/~katrin/papers/disktrees.pdf>.